University of Trento
University of Brescia
University of Padova
University of Trieste
University of Udine
University IUAV of Venezia

Cheng Lan

ON THE PERFORMANCE OF
SUPER-LONG INTEGRAL ABUTMENT BRIDGES
– PARAMETRIC ANALYSES AND DESIGN OPTIMIZATION

Advisor:
Prof. Enzo Siviero
Università IUAV di Venezia, Venice, Italy

Co-Advisors:
Prof. Airong Chen, Prof. Tobia Zordan
Tongji University, Shanghai, China
Prof. Bruno Briseghella
Fuzhou University, Fuzhou, China

UNIVERSITY OF TRENTO

Engineering of Civil and Mechanical Structural Systems

Ph.D. Head: Prof. Davide Bigoni

24 / April / 2012

Board of Examiners

Prof. Enzo Siviero   (Università IUAV di Venezia)
Prof. Antonio Tralli   (Università degli Studi di Ferrara)
Prof. Marina Fumo   (Università degli Studi di Napoli Federico II)

SUMMARY

The concept of "integral abutment bridge" has recently become a topic of remarkable interest among bridge engineers, not only for newly built bridges but also during refurbishment processes. The system constituted by the substructure and the superstructure can achieve a composite action responding as a single structural unit; the elimination of expansion joint and bearings on the abutments, greatly reduce the construction and maintenance costs. To maximize the benefits from integral abutment bridges, the direct way is to achieve the super-long integral abutment bridge. However, as the environment temperature changes, the lengths of superstructure increase and decrease, pushing the abutment against the approach fill and pulling it away. The responses of bridge superstructure, the abutment, the approach system, the foundation/piles and the foundation soil are all different. And it's important to understand their interactions effective design and satisfactory performance of integral abutment bridges.

In order to build longer integral abutment bridges, therefore in this research, the literature survey on the applications of integral abutment bridges in worldwide, especially the current development of super-long integral abutment bridges was carried out firstly. Another literature review on soil-structure interaction was conducted to find out the most suitable methods in considering this kernel issue in design of integral abutment bridge. Through proposing finite element models for integral abutment bridges that could involve the soil-structure interaction, thermal actions, nonlinearity in materials and so on, structural study was performed on an existing super-long integral abutment bridge, including parametric analysis, pushover analysis, and dynamic tests. Then, the performance of integral abutment bridge was better understood, and no critical structural problem was found for integral abutment bridge. Based on that, length limit for this kind of bridge was evaluated and investigated in an analytical way. Considering capacities of abutments and piers, and under the conditions of an existing integral abutment bridge, the length limit was found to be around 540m. With this super length, the piles need to be designed with capacity of large lateral displacement. Therefore, an effective optimization approach, associating the finite element method with global optimization algorithm was presented for pile shape design. At the end, considerations accounted in the design of super-long integral abutment bridges were discussed, making construction of super-long integral abutment bridge of great possibility.

SOMMARIO

Il concetto di "ponte integrale" è recentemente diventato un argomento di notevole interesse tra gli ingegneri di ponti, non solo per i ponti di nuova costruzione, ma anche nel campo del ricondizionamento dei ponti esistenti.

L'azione "integrale" è ottenuta attraverso l'eliminazione di giunti e appoggi e attraverso la solidarizzazione della sovrastruttura al sistema fondale. Ciò consente di migliorare la risposta strutturale del manufatto aumentando il livello di iperstaticità, ma soprattutto di abbattere i costi di manutenzione oltre che quelli di realizzazione.

Tuttavia i vantaggi della soluzione integrale vanno valutati tenendo in debita considerazione l'interazione suolo-struttura, poiché proprio l'assenza dei componenti più vulnerabili ai fini della manutenzione del manufatto comporta una risposta che non può essere analizzata senza valutare tensioni e deformazioni in corrispondenza di elementi quali spalle, diaframmi, pali e solette di transizione.

La tesi presenta i risultati di uno studio teso a valutare il comportamento di ponti integrali di grande lunghezza complessiva e in parte utilizzato per la realizzazione del ponte integrale più lungo al mondo.

Dopo un'analisi dello stato della ricerca e dello stato dell'arte a livello internazionale vengono identificate le azioni dimensionanti, i componenti strutturali chiave atti a descrivere la risposta di questa speciale tipologia di ponti e i legami costitutivi utilizzati nella modellazione agli elementi finiti assieme alle non linearità tipiche del problema in esame.

E' successivamente presentato il caso studio del record del mondo di lunghezza per i ponti integrali, affrontato con analisi di tipo parametrico e di pushover utilizzate per comprendere i meccanismi di rottura al collasso.

La parte finale della tesi è dedicata alla computazione della lunghezza limite teorica per questo tipo di ponti.

DEDICATION

to my parents
and
my sister

ACKNOWLEDGEMENTS

CONTENTS

1. INTRODUCTION

In traditional bridges, there is always a system of expansion joints, roller supports, abutment bearings and other structural releases to account for cyclic thermal expansion and contraction, creep and shrinkage (Arockiasamy et al., 2004). Failure of proper functioning of the expansion joints and abutment bearings due to various reasons leads to highly critical and serious problems. Leakage of water laden with salt, deicing chemicals and contaminants through the joints results in the corrosion of the reinforced concrete, girder ends, bearings and pier caps underneath (Shah, 2007), and other hardware. This problem is magnified in regions subject to heavy snow storms, where sodium chloride and calcium chloride are commonly used in de-icing applications (Krier, 2009). Failure to move properly due to unanticipated movements results in overstress and subsequent structural damage to the bridge elements such as split and rupture of abutment bearings, abutment-rotation and abutment-overturning (Wasserman & Walker, 1996). Besides, the expansion joints are very expensive to design, manufacture and install. The emergence of joint problems came in the 1960s as traffic loads increased in speed, volume, and weight. The continuous maintenance and replacements costs are the considerable portions every year. Joints and bearings in traditional bridges have emerged as major sources of bridge maintenance problems (Wolde-Tinsae et al., 1988a). Integral abutment bridges (IABs) came out to solve these problems and make a definite change in the design of highway bridges.

1.1. The Concept of Integral Abutment Bridges

For generally integral structures, or structures without movable joints, are ages old. The most celebrated are the natural arches carved from bedrock by water and wind. However, when considering man-made integral structures, one cannot go much further back in recorded history than the first arch bridges made of unreinforced concrete constructed by the Romans (Fig. 1a). More recently, most are familiar with the reinforced concrete arch bridges constructed in the early decades of the last century. It began with the substitution of reinforced concrete for stone masonry in the construction of spandrel-filled arch bridges. Although the major supporting elements

of these bridges (abutments, piers, and arch ribs) have no movable joints, they are not what could be classified as true integral abutment bridges because they have such joints in the deck slabs and spandrel walls within each span.

a) roman (masonry) arch bridge

integral joint

flexible pier

expansion joint, bearings on abutment, no soil-structure interaction

b) rigid (portal) frame bridge

integral joint

flexible pier

soil-structure interaction

integral stub-type abutment

c) integral abutment bridge with flexible integral pier

longitudinal fixed or movable

self-supporting pier

soil-structure interaction

d) integral abutment bridge with semi-rigid self-supporting pier

Fig. 1 Scheme of Integral Abutment Bridges Comparing to Other Jointless Bridges

By mid-century, however, many reinforced concrete rigid frame bridges were built. These bridges were a standard type of construction for many countries. The construction of rigid-frame bridges was paralleled by the construction of multiple-span

continuous slab, beam, or girder bridges with embankments and shallow, rigidly supported, stub-type abutments. Movable deck joints were provided but only at the superstructure/abutment interface (Fig. 1b).

Ultimately, the overall economy of multiple-span continuous construction made practical the use of similar bridges but without such joints at abutments. Movable deck joints at the superstructure/abutments interface were eliminated by the use of integral stub-type abutments supported on single rows of vertically driven flexible piles. Although some versions of these bridges are now provided with movable bearings at self-supporting piers, these are no movable deck joints in their super-structures. Thus, although various types of integral abutments in such bridges have been constructed for centuries, the bridges, with single- or multi-span, continuous, deck-type bridges without movable deck joints, are now generally thought to be cat-egorized into the bridge with "integral abutments". They are generally supported by embankments with stub-type abutments on vertically driven flexible piles and by flexible piers constructed integrally with the superstructure (Fig. 1c), or by semi-rigid piers provided with fixed and/or movable bearings (Fig. 1d).

It is still in arguing what the right name for this kind of bridge with integral abutment is. The phrase "integral abutment bridges" is thought to give novice engineers the incorrect impression that it would be proper and acceptable to provide integral abutments for all bridges including multiple-span non-continuous bridges (Burke Jr, 2009). Obviously, such construction is totally inappropriate. And Burke Jr. gave out the designations "integral bridges" and "semi-integral bridges". As defined by him, the former refers to single- or multi-span continuous bridges without movable deck joints at the superstructure/abutment interface. These are generally supported by embankments with stub-type abutments on flexible piles (Waite et al., 2010) (e.g. the integral abutment design detail as shown in Fig. 2a). The second designation refers to single- or multi-span continuous bridges without movable deck joints in their superstructures but with movable longitudinal joints between their superstruc-tures and rigidly supported abutments (e.g. the semi-integral abutment design detail as shown in Fig. 2b). The piers for such structures may be semi-rigid self-supporting structures generally surmounted by movable bearings, or flexible sub-structures constructed integrally with superstructures. These definitions are now widely accepted in engineering practice. For example, Fig. 3 shows the definitions for integral and semi-integral bridges by Swiss guidelines (Kaufmann & Alvarez, 2011).
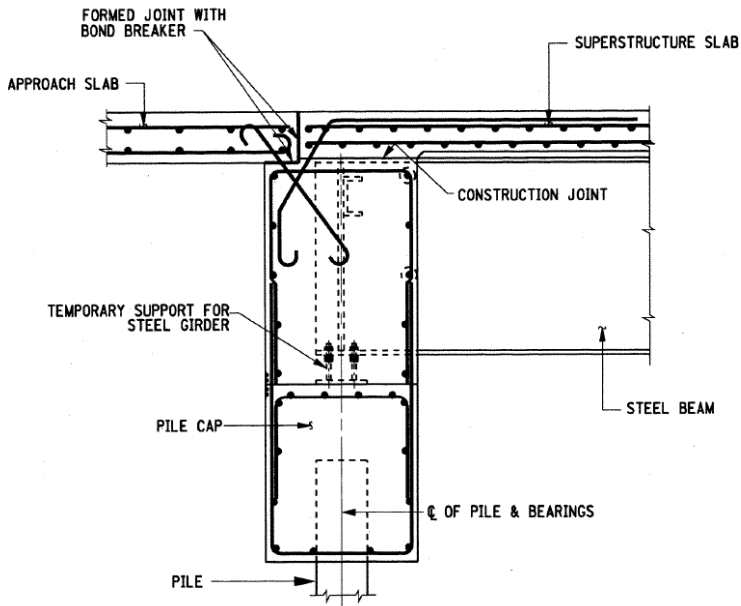
a) integral abutment
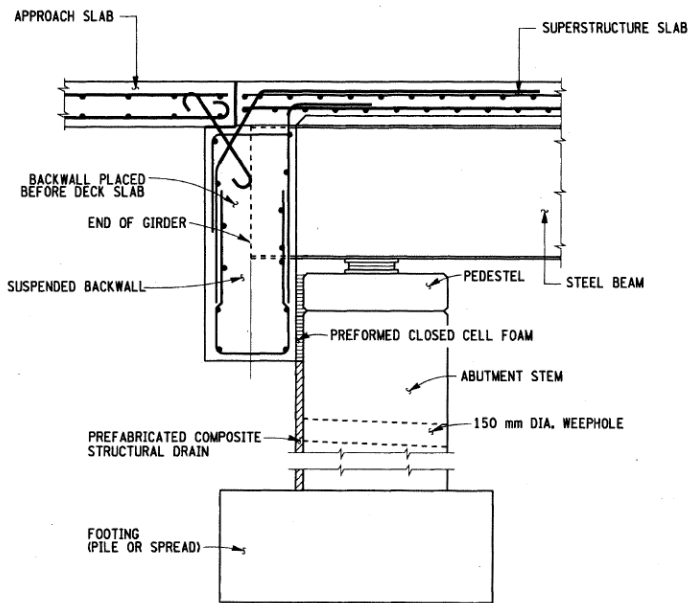
b) semi-integral abutment

Fig. 2 Integral / Semi-Integral Abutment Details of New York State, US (Yannotti et al., 2005)

a) integral bridge ends

d) integral bridge

see a)
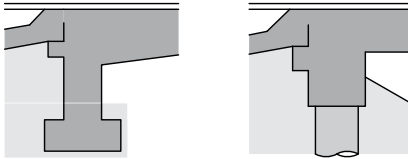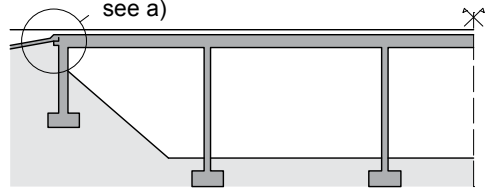
b) semi-integral bridge ends

normal case   exception

flexible
wall
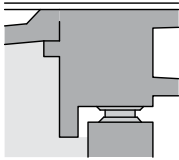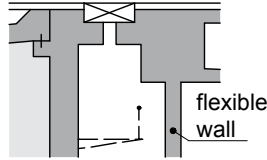
e) semi-integral bridge

see b)
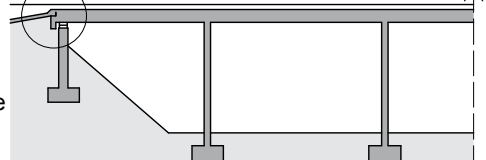
c) jointed bridge ends
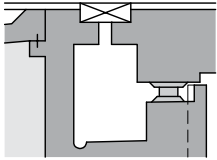
normal case   exception
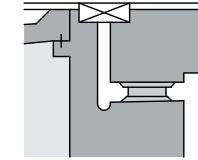
f) bridge with "floating" bearing system

see c)
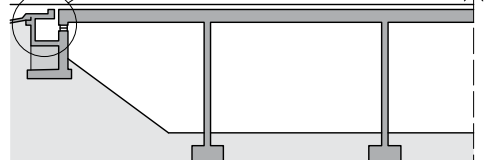
detailing of deck and piers	deck monolithic (jointless)		deck with joint(s)
detailing of bridge ends	all piers monolithic with deck or no piers	pier(s) with bearings or joints (top/bottom)	("gerber"-type joint, joint over piers, ...)
both bridge ends integral	integral bridge		
one bridge end semi-integral, other brdige end integral or semi-integral	semi-integral bridge		
at least one bridge end jointed (= with expansiont joint)	"floating" bearing system (1)		jointed bridge

(1) both bridge ends withe expansion joint and sliding bearings (longitudinally movable).

Fig. 3 Integral Bridge Definitions by (Swiss) Federal Roads Office (FEDRO) (Kaufmann & Alvarez, 2011)

However, the term of "integral bridge" would always be easily confused with others. The other alternative designations referring to integral abutment bridges are including: jointless bridges, integral bent bridges, rigid frame bridges, and so on (Zuk, 1981). Nevertheless, since the phrase "integral abutment bridges" is widely used among the members of the bridge engineering profession, the designations of "integral abutment bridges (IABs)" and "semi-integral abutment bridges (SIABs)" will be used exclusively in this context. The structural elements of an integral abutment bridge are shown in Fig. 4, including the bridge system consisting of continuous deck-type superstructure, abutment, pile/foundation, piers if of multi-span, and the approach system (c.f. Ch.7.2).
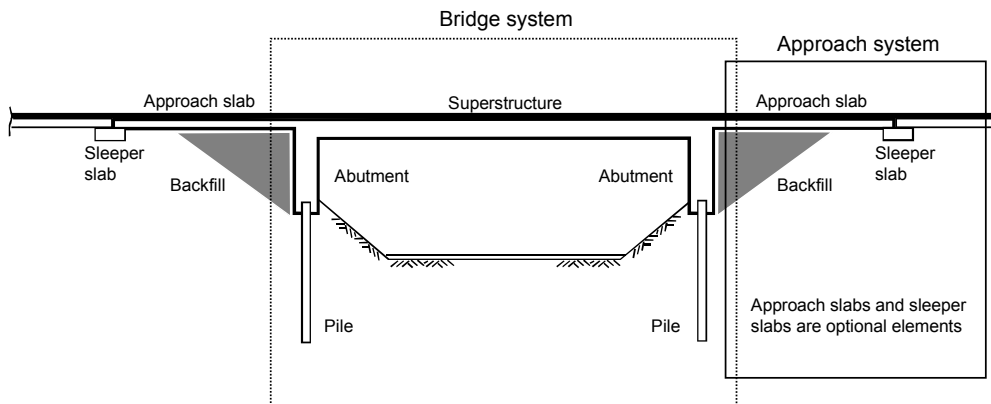
Fig. 4 Simplified Geometry of an Integral Abutment Bridge (Arsoy, 2000)

1.2. The Advantages and Disadvantages

The popularity of integral abutment bridges has grown with their numbers. With thoughtful design and crafting, they are becoming popular structures for rural and urban primary and interstate road systems as well. Originally, as a reaction to the destructive effects of leaking movable deck joints and massive pavement pressures, it soon became evident that these bridges have many more attributes and fewer limitations than their jointed bridge counterparts. Interestingly, the advantages and disadvantages of integral abutment bridges are stated as following.

1.2.1 Advantages

Jointless Construction – Lower Costs of Construction and Maintenance

The primary attribute of integral abutment bridges is their jointless construction, which was investigated and experienced of lower total bridge cost (Fig. 5). As a secondary benefit, the avoidance of damage to movable deck joints also avoids the need for maintenance repair crews to be exposed to the hazards associated with vehicular traffic. In addition it avoids restricted traffic flow and the occasional vehicular accidents that are associated with bridge roadway repair sites. Also the smooth, jointless construction, uninterrupted deck, as characteristics of integral abutment bridge in highway system, improves vehicular riding quality and diminishes vehicular impact and stress levels.

Total bridge cost (Euro/m^2)

A: Bridge founded above ground water level
B: Bridge founded under ground water level, concrete cast in the water
C: Sheet pile wall and unreinforced bottom layer of concrete preventing water intrusion
D: Elevated foundation
E: Integral abutments
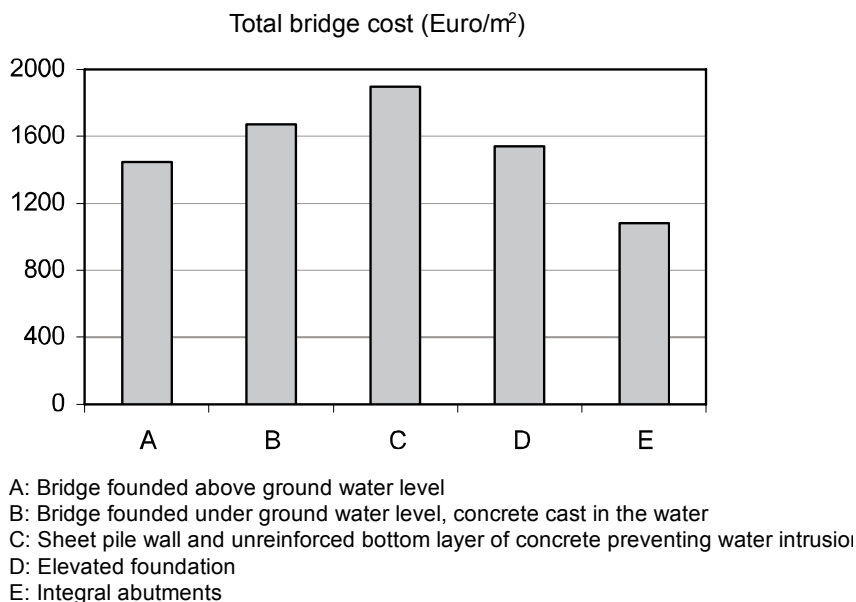
Fig. 5 Investigated Total Cost of Bridges with Different Optional Foundations in Northern Sweden (Nilsson & Torén, 2001)

Pressure Resistance – Fewer Piles

The solid, jointless construction of an integral abutment bridge distributes longitudinal pavement pressures by the pavement G/P phenomenon (Burke Jr, 2009) over a total superstructure area substantially greater than the approach pavement cross-section. Consequently, the smaller more fragile approach pavements are more likely to fail by localized fracturing or instantaneous buckling than the more pressure-resistant integral abutment bridge superstructure. Unless the approaches to an integral abutment bridge are furnished with cycle-control joints that are properly designed – joints that facilitate the thermal cycling of the bridge and approach slabs –

they are more likely to experience early distress because the restrained elongation of the bridge also contributes to the generation of approach pavement pressure.

As integral bridges are capable of sustaining significant longitudinal compression without distress, almost any pavement pressure-relief joint used specifically by maintenance forces to relieve pavement pressure would be suitable to protect them.

Rapid Construction

Numerous features of integral bridges facilitate their rapid construction (Fig. 6), and these features are probably responsible for much of the outstanding economy that has come to be achieved by their construction. Dry construction (most concrete work is done above stream water levels), simple members, broad tolerances, few construction joints, few parts, few materials, avoidance of labor-intensive practices, and many other features combine to make possible the completion of such structures in a single short construction season. Such rapid construction becomes particularly important when collapsed bridges or seriously damaged bridges must be replaced in the shortest possible time. Also, this rapid construction becomes particularly advantageous when bridges carrying high volumes of traffic must be replaced in two or more construction stages. Such rapid construction is possible because of the many simplifying features that are characteristic of most integral abutment bridges. These include but are not limited by the following: small excavations, uniformly spaced piles, few joints, few parts, broad tolerances, reduced removals, simple beam seats, elimination of bearing anchor bars, broad span ratios, and so on.

| Pile | Abutment | Girder erected (temporary seat) | Deck concrete integral with abutment | Backfill, deck slab, approach slab |
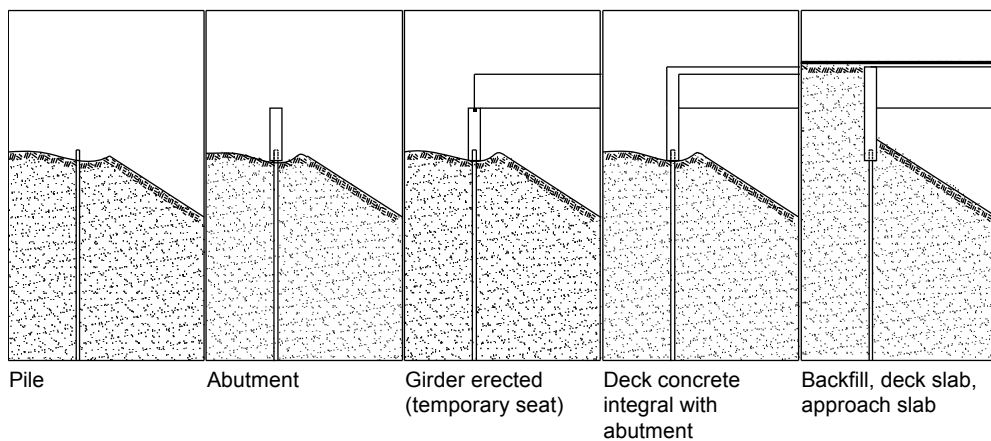
Fig. 6 Typical Construction Phases of Integral Abutment (Collin et al., 2006)

Earthquake Resistant

As the decks of integral abutment bridges are rigidly connected to both abutments and consequently to both embankments, these bridges are in fact part of the earth and will move with the earth during earthquakes. Consequently, when integral abutment bridges are constructed on stable embankments and subsoils, they should have an adequate response to most earthquakes.

Simplified Widening and Replacement

Many bridges in the past were designed for immediate needs without much thought being given to future bridge modifications that would be necessary to accommodate substantially higher traffic volumes and vehicular weights. In general, integral abutment bridges with straight capped-pile substructures are convenient to widen and easy to replace if future demands have not been accurately foreseen. Of particular significance is the fact that their substructures (the piling) can be recapped and re-used or, if necessary, they can be withdrawn or left in place. Such bridges avoid the necessity of building expensive foundations that interfere with the placement of future foundations.

Reduced Superstructure Service Load Stresses

Superstructures that are integrally constructed with capped-pile abutments and piers instead of separated from them by numbers of compressible elastomeric bearings give vehicular wheel loads broader distribution than would otherwise be possible. This arrangement reduces superstructure service load stresses.

1.2.2 Disadvantages

The attributes noted above make integral abutment bridges very desirable structures. However, this desirability has been attained at the expense of a number of limitations, and these limitations should be recognized so that design engineers can evaluate them when considering the use of integral abutment bridges for specific applications.

Piles Stresses

Except for abutment piling and wingwalls, the various members of integral abutment bridges are subjected to essentially the same levels of primary stresses (dead load, live load, impact, etc.) and secondary stresses (shrinkage, creep, thermal gradients, etc.) as their jointed bridge counterparts. But because of their flexural resistance, the vertical piling of integral bridge abutments will resist the lengthening and short-

ening of bridge superstructures responding to temperature changes. Consequently, the piling of long integral abutment bridges can be subjected to flexural stresses considerably greater than those of their jointed bridge counterparts. For long integral abutment bridges, such piling stresses, if they are large enough, will result in the formation of plastic hinges that will limit the flexural resistance of the piling to additional superstructure elongation. For this reason, only steel H-piles or appropriately limited and reinforced prestressed concrete piles should be used to support abutments of the longer (≥ 91 m) integral bridges (Burke Jr, 2009).

Limited Applications

The superior economy of integral abutment bridges is due to their ability, within a limited application range, to satisfy all functional requirements with safety, durability and optimal economy. They are not broadly applicable to most bridge applications, as are their jointed bridge counterparts.

Integral abutment bridges with stub-type abutments supported by single rows of piles should be limited in a number of ways based on the primary design features that have been incorporated into standard designs. In general, their length was limited (a) to minimize passive pressure effects and (b) to limit bridge movements to those that can be accommodated by the movement range of approach-slab/approach-pavement cycle-control joints and standard approach-guardrail connections.

They generally should not be used where beams with horizontal bends, or with extreme skews (> 30°) (Burke Jr, 2009). They should not be used where abutment piles cannot be driven through at least 3~4.5 m of overburden. They should not be used at sites where the stability of subsoils is uncertain or where settlement may be significant (where it cannot effectively be compensated for by added roadway overlays alone).

Buoyancy

As a result of their jointless construction, many types of integral abutment bridges are subject to uplift when they become submerged, especially in many I-beam bridges and box beam bridges. For single spans, abutments should be heavy enough to give the superstructure adequate resistance to uplift. But for multiple-span integral abutment bridges, some positive provisions must be employed to ensure that a structure, which may become submerged, will have an adequate resistance to uplift.

Approach Slabs

Full-width approach slabs should be provided for most integral abutment bridges (c.f. Ch.7.2). Approach slabs tied or linked to integral abutment bridges become part of the bridges. Consequently, they effectively increase overall structure lengths, thereby requiring greater movement ranges for cycle-control joints. To minimize the amount of force necessary to move the approach slabs, they should be cast on smooth, low-friction surfaces (polyethylene sheets, filter fabric, etc.).

Cycle-Control Joints

Integral abutment bridges with attached approach slabs lengthen and shorten in response to temperature and moisture changes. For such structures built adjacent to rigid approach pavements, the joints between approach slabs and approach pavements should be provided with cycle-control joints to facilitate such movements. Otherwise, the longitudinal cycling of both structure and approach slabs can generate pressures sufficient to fracture approach slabs or approach pavement either progressively or abruptly (blow-up) (Burke Jr & Bugler, 2002).

Soil-Structure Interaction

Current integral abutment bridge design mostly depend on idealizations and simplifications on soil-structure interaction relations, which probably do not accurately reflect the true pressure on abutments and piles, especially the effects of long-term pressure together with cyclic temperature changes. Research on passive pressures is needed to describe both the relationship between the amount of backfill compression and the generation of passive pressure, and the effect of alternating cycles of backfill compression and expansion.

1.3. The Problems and Critical Issues

As the above stated, integral abutment bridges have numerous attributes and few limitations. As the current advantages in maintenance and the durability, the concept of the super-long integral abutment bridge comes up. However, integral abutment bridge is a classic example of soil-structure interaction (Faraji et al., 2001; Jayaraman & Merz, 2001). The continuity achieved by this type of construction results in the transfer of thermally induced deformations in the bridge deck to the abutment walls, piles and surrounding soil. A significant and complex non-linear soil-structure interaction that takes place behind the abutment walls and piles has remained largely unknown. Secondary stresses due to thermal and moisture changes of the whole structure and settlements of substructure add to the intrica-

cies of the entire problem. The magnitude and mode of deformation, the overall soil response and the overall structural response are decidedly dominated by the level of compaction in the granular fill behind the abutment walls and adjacent to the piles along with the relative flexural stiffness of the bridge deck, abutment wall, foundation piles, lateral pressure of soil behind the wall and confining stress level in the soil. In return, the stress in the superstructure and piles will change a lot from these interactions.

These unresolved issues have created great uncertainties in the design of integral abutment bridges. Consequently, the current design guidelines are experientially based rather than scientifically based (Bakeer et al., 2005). The limited design and construction guidelines by AASHTO (American Association of State Highway and Transportation Officials, 2002) and a lack of a unified procedure has led to wide variations in analysis, design and construction procedures from one state to another (Arockiasamy et al., 2004). For example, conventionally, the pile for integral abutment bridge was recommended to be flexure enough and not to resist bending moment conducted from abutment. Therefore, there certainly would be variance in designing such piles.

To maximize the benefits from integral abutment bridges, the simple and direct way is to achieve the super-long integral abutment bridge. Before that, the stated structural problems need to be solved.

1.4. The Solution and Objectives

As temperatures change, the superstructure lengths of integral abutment bridges increase and decrease, pushing the abutment against the approach fill and pulling it away. As a result the bridge superstructure, the abutment, the approach fill, the foundation piles and the foundation soil are all subjected to cyclic loading, and understanding their interactions is important for effective design and satisfactory performance of super-long integral abutment bridges. The ability of piles to accommodate large lateral displacements is a significant factor in determining the maximum possible length of integral abutment bridges. In order to build longer integral abutment bridges, the structural components should be kept in serviceable. Therefore, the primary objectives of this research are:

1. Survey on the applications in worldwide, especially the current development of super-long integral abutment bridges;

2. Conduct the literature review on soil-structure interaction, to find the suitable methods in the design, and then propose finite element models for integral abutment bridges that could involve the soil-structure interaction, thermal actions, non-linearity in materials and so on;

3. Perform structural study on super-long integral abutment bridge, through parametric analysis to further understand the performance of integral abutment bridges, pushover analysis to comprehend the formations of plastic hinges due to high stresses, and dynamic tests to compare with finite element analyses and correspondingly update the finite element models;

4. Verify and investigate the length limit for integral abutment bridges in an analytical way, where the limit factors include capacities of abutments and piers, fatigue effects due to cyclic loads, and durability of approach system;

5. Propose an optimization methodology, associating the finite element method with global optimization algorithm, for the pile that imposed by the large thermal-induced displacement due to the super-long superstructure;

6. Discuss the other considerations, which can be made to account in the design of super-long integral abutment bridges.

1.5. Structure of the Thesis

Besides this chapter, in the main body of the thesis, it consists of 6 chapters, from Ch.2 to Ch.7 that introduced as following:

Chapter 2, it states the current applications of integral abutment bridges all around the world, including most developed region of North America, and the other widely used regions of Europe, East Asia, and Oceania. Based on that, the development of the super-long integral abutment bridge is summarized.

Chapter 3, it presents the theory, methodology, and practice of the main critical issues encountered in design, including soil-structure interactions, thermal actions on structure (thermal-induced displacement on the superstructure), and the structural mechanical models for integral abutment bridges. Concerning these issues, a general finite element model for integral abutment bridge is proposed.

Chapter 4, it presents a case study on performance of an existing super-long integral abutment bridge, including the parametric analysis on the soil condition effects on the internal forces in structure, and the pushover analysis to find out the possible failure pattern of the structure under increasing temperature variations. And, the dynamic tests performed on that bridge is introduced and the results are compared with finite element analysis, where the model is updated through this comparison.

Chapter 5, it presents the analytical length limit for integral abutment bridge based on the performance study, which considers the non-linearity correction in the model and the capacities of the pier and abutment. Also, the limit factors on the length limit of fatigue effects due to cyclic loads and durability of approach system are discussed.

Chapter 6, it presents an optimization approach for piles of integral abutment bridges, where the global optimization algorithm is collaborated with finite element models, to design piles that are of capacity of large displacement due to the temperature variation on the superstructure.

Chapter 7, it presents the discussions on the other considerations in the design of super-long integral abutment bridges, including the benefits of integral abutment bridge if retrofitted from other types of structure, the behavior of approach system which is the most important non-structural factor, and the other design details should be involved in design.

At the end, the conclusions drawn from the research and recommendations for future investigation will be presented.

2. STATE-OF-ART: APPLICATIONS

Dating from the late 1930's and early 1940's in United States, Ohio, South Dakota and Oregon were the first states to routinely use continuous construction with integral abutments. California followed suit in the 1950's. With the National Interstate Highway System construction boom in the late 1950's and mid-1960's, Tennessee and other states began moving toward continuous bridges with integral abutments, as standard construction practice. (Greimann et al., 1986; Hong, 2006; Wasserman, 2007).

In the 1970s, Britain started to give effort on the research on jointless and integral abutment bridge. Currently in the UK, the bridges, with the span length less than 65 m, are widely applied with jointless structure; and the displacements of 25 mm for highway and 40 mm for railway are considered to be allowable, which means highway bridges within 100 m, and railway bridges within 120 m.

Other countries or regions, like Europe, China, and Oceania, jointless bridge have been developed rapidly. As early as the 1960s, integral abutment bridge had been used in Australia. The construction method and approach of applying jointless structures in existing bridges had been developed in Japan in 1995 (Road Management Technology Center, 1995). After the applications developed in countries of Iraq, New Zealand, France, Switzerland, Italy, and so on, integral abutment bridges and semi-integral abutment bridge have spread widely and been applied in worldwide, especially in North America.

2.1. Application in North America

2.1.1 United States

The first integral bridge in the United States was the Teens Run Bridge (Burke Jr, 2009). It was built in 1938 near Eureka in Gallia County, Ohio. It consists of five continuous reinforced concrete slab spans supported by capped pile piers and abutments. Integral abutment bridges have been widely built since the 1960s and

are increasingly being used for replacement structures (Comisu, 2005). According to the "integral abutment and jointless bridges" (IAJB) survey conducted in 2004 (Maruri & Petro, 2005), there are approximately 13000 integral abutment bridges, of which approximately 9000 are full integral abutment bridges, approximately 4000 are semi-integral abutment bridges and approximately 3900 deck extension bridges in-service.

As the design guidelines vary from state to state (e.g. the integral abutment details design as shown in Fig. 7), the experiences are different: 11 states reported their overall experience with integral bridges as either very good or excellent; another 21 stated their experience has been good to satisfactory; however, Minnesota reported poor experiences and Arizona has discontinued the use of jointless bridges (Bakeer et al., 2005).
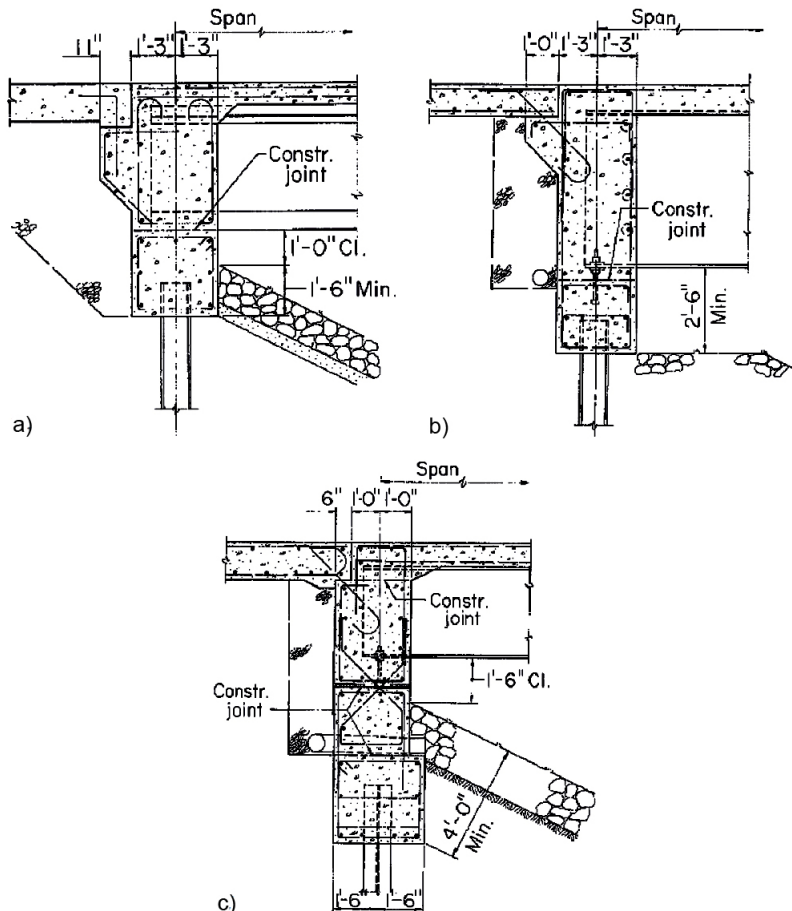
Fig. 7 Details of Integral Abutments: a) Illinois DOT; b) Tennessee DOT; and c) Ohio DOT.

As responses from states, approach slabs are the most common problem reported with integral bridges (Maruri & Petro, 2005). Washington State has reported having problems with their approach slabs on bridges longer than 350 feet (107 m). And the lessons learned from the use experience of integral abutment bridges in United States include (Bakeer et al., 2005):

- Designing the bridge with details that allow sufficient movement,
- Using stub abutment or semi- integral abutments to avoid abutment cracking,
- Limiting span length,
- Limiting skew angle,
- Using a single row of flexible piling (possibly with predrilled holes),
- Using sleeper slabs to reduce the effects of settlement, and
- Using granular backfill with sufficient drainage.

All the states, therefore, have identified the establishment of integral abutment bridge design criteria and guidelines, which are mainly including structural limitations, seismic resistance, approach slab and wingwall design, effects of earth pressure behind the abutments, pile stresses due to the bridge's longitudinal movement, and deck cracking potential. Table 1 lists the maximum bridge length limitations imposed by 31 states. These states have restrictions on skew angles that vary from 0 to 45 degrees, with most states limiting them to about 30 degrees. Tennessee has constructed a super-long curved integral abutment bridge at just over 1175 feet (358 m) in length (Fig. 8). The bridge has 9 spans of precast, prestressed concrete bulb-T girders with no expansion bearings. The spans are ranging from 127 to 138 feet (38.8 to 42.2 m). The two-column pier bents vary in height from 51 to 91 feet (15.5 to 27.7 m). The bridge was constructed in 1997 and has performed satisfactorily (Bakeer et al., 2005; Wasserman, 2007). Table 1 also lists the year each state recorded the construction of its first integral or semi-integral abutment bridge.

Fig. 8 State Route 50 over Happy Hollow Creek, Tennessee, USA

State	First Year Built	Length Limit		Skew Angle Limit
		feet	m	degrees
Arkansas	1996	260	79	33
California	1950	1 inch (25mm) movement		45
Georgia	1975	410/260	(125/79)	0/40
Hawaii	NA	250	76	NA
Illinois	1983	300	92	30
Indiana	NA	300	92	30
Idaho	NA	400	122	30
Iowa	1962	300	92	30
Kansas	1935	450	137	NA
Kentucky	1970	400	122	30
Louisiana	1989	1000	305	0
Maine	1983	150	46	30
Michigan	1990	None		30
Missouri	NA	600	183	NA
Massachusetts	1930	300	92	30
North Dakota	1960	400	122	30
Nevada	1980	200	61	45
New York	1980	300	92	30
Ohio	NA	375	114	30
Oklahoma	1980	210	64	0
Pennsylvania	1946	600	183	20
Oregon	1940	200	61	25
South Dakota	1948	700	214	35
South Carolina	NA	500	153	30
Tennessee	1965	2 inches (50 mm) movement		no limit
Utah	NA	300	92	20
Virginia	1982	500	153	NA
Wyoming	1957	360	110	30
Washington	1965	450	137	40
Wisconsin	NA	300	92	30

Table 1
Maximum Integral Bridge Length and Skew Constraints in USA

2.1.2 Canada

Canada has several provinces with integral experience. Alberta, Quebec, Nova Scotia, and Ontario have jointless bridges, and most have reported "good" to satisfactory experiences with their use. Nova Scotia built its first integral bridge in 1986, and Quebec built its first integral bridge in 1988. Ontario limits its integral bridge span to less than 100 m and a 20-degree skew angle. Ontario's recommendations for their integral bridges are similar to those used by many US states. These include a weak joint between the approach slab and roadway pavement, granular backfill with a 150 mm diameter perforated drain pipe, and a single row of vertical steel H-piles (Kunin & Alampalli, 1999; Bakeer et al., 2005).

The prefabricated bridges using prefabricated wall units and deck elements for integral abutments bridges is developed as a large proportion of bridges built in Ontario (Fig. 9). The completion of the bridge without any significant design, fabrication, transportation or erection problems would be quite encouraging and used in more future projects (Husain et al., 2005).

a) construction before cast-in-place concrete; b) as built
Fig. 9 Moose Greek Bridge, Ontario, Canada

2.2. Application in Europe

European experience with integral abutments is significantly less, but what experience has been gained has been positive. As a result, the trend is towards making integral abutment bridges a larger percentage of all newly constructed bridges across Europe (White II, 2007).

A European survey was conducted in early 2007 to illustrate the design criteria used by each different country for integral abutment bridges, including England, Finland, France, Ireland, Luxembourg, Germany, and Sweden (White II et al., 2010). A unified Eurocode for bridge design has been adopted by most European countries. The old bridge codes are being phased out and should be completely replaced by 2011. However, national rules for items such as bridge detailing will still exist. Since integral abutment bridges are a relatively new concept in Europe, each country represented a slightly different approach to the design of integral abutment bridges. In spite of the different viewpoints, all the survey responding countries and other IAB developing countries, like Switzerland, Italy, Spain, Poland, indicated that their designs were successful (Tlustochowicz, 2005; Collin et al., 2006; Dreier, 2010b; Marx & Seidl, 2011; Rodriguez et al., 2011; Rui-Wamba et al., 2011).

In this section, the applications in UK, Sweden, Germany, and Italy are going to be briefly introduced, as the representatives of the development of integral abutment bridge in European regions.

2.2.1 United Kingdom

A survey of approximately 200 concrete highway bridges in the UK (Lock, 2002), carried out for the Department of Transport, however, revealed that expansion joints are a serious source of costly and disruptive maintenance work. In response to this, the Highways Agency published advice in 1996 (Highways Agency, 2003), promoting the design of integral bridges and stating that all bridges up to 60 m in length and 30 degrees in skew angle should be integral with their supports. The structure schemes of integral abutment are classified into 6 types (Fig. 10). This advice is intended to prevent problems of joint leakage over supports and reinforcement corrosion that typically occur in non-integral forms of bridge construction (Comisu, 2005).

When BA 42/96 first became available, there was little detailed guidance on methods of analysis that were appropriate or on the particular configurations and details that would be effective and economic. SCI (the Steel Construction Institute) produced its first design guide on integral bridges in 1997 and followed this with two publications giving worked examples (Fig. 11). After, the proportion of bridges that are 'integral' has increased significantly in the period of 2000 to 2005 and accounts

for about half of the total bridge construction (Fig. 12). Generally, the bridges being built as 'non-integral' are either long or highly skewed (Iles, 2006).
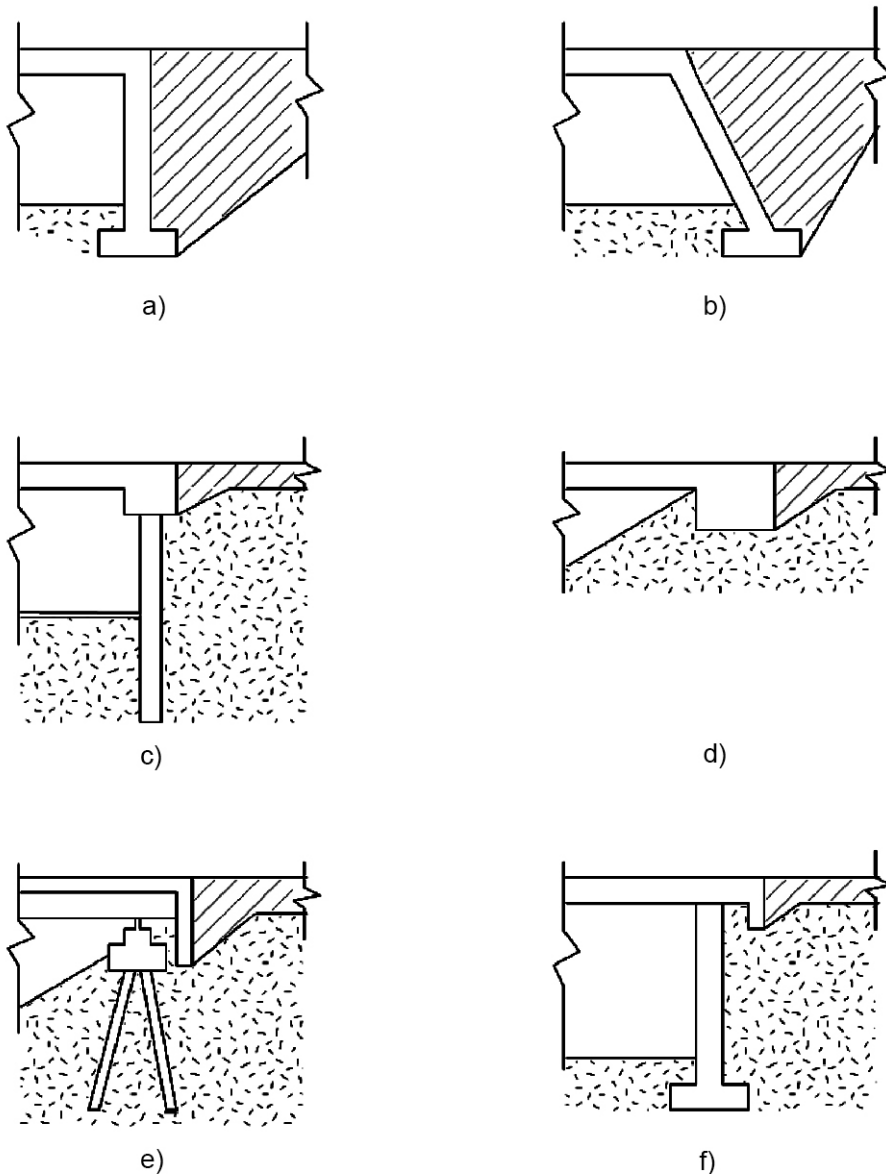

Fig. 10 BA-42 Classification of Integral Bridge Abutments: a) b) frame abutments; c) embedded abutment; d) bank pad abutment; e) f) end screen abutments.

a) steel composite girder

b) end shear connector

c) semi-integral abutment
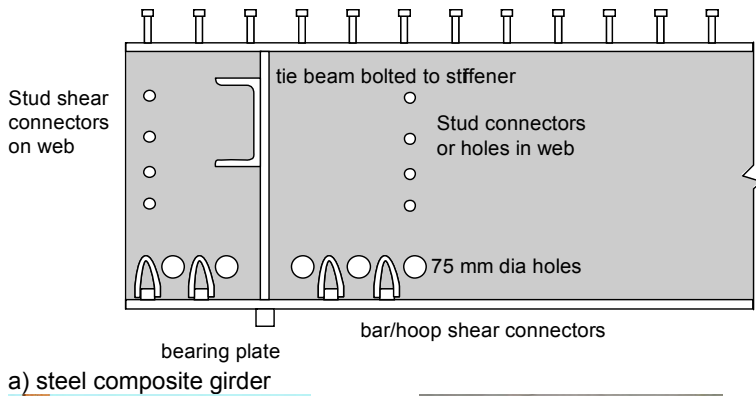
Fig. 11 Examples of Girder End Detail Used in UK (Iles, 2006)
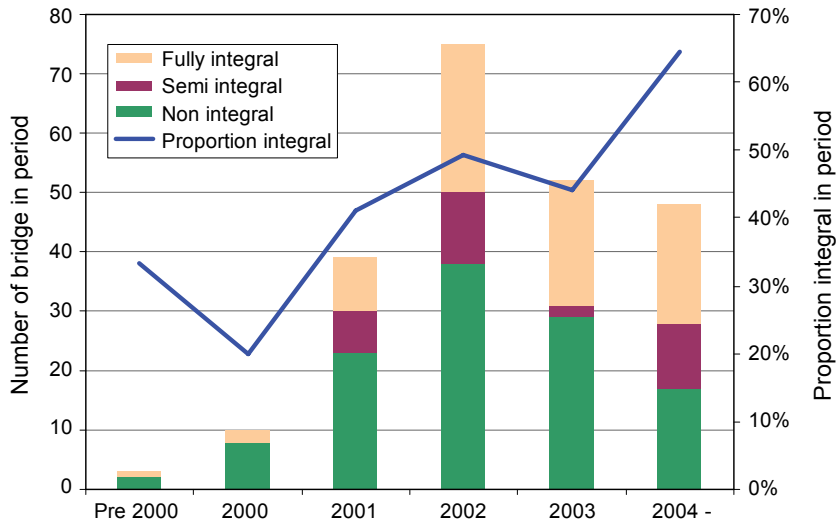
Fig. 12 Summary of Integral Bridge Types in UK by 2005 (Iles, 2006)

2.2.2 Sweden

In Sweden, the integral reinforced concrete slab frame bridge has been very frequent for over 70 years. It has been one of the most common bridge types with 8000 out of 14000 of Swedish Road Administration owned bridges. Bridges with integrated breast walls are also commonly used for medium lengths up to 80 m for reinforced concrete and to 60 m for composite bridges. Some examples of integral bridges in Sweden are presented by Hambly (Hambly, 1997) such as composite bridges in Borlange with screen walls (breast walls) at the abutments, and a 70 m multi-span concrete integral bridge in Leksand. A typical integral abutment reinforcement detail can be seen in Fig. 13.

The recommended maximum bridge length for steel bridges is 40 m to 60 m depending on average low temperatures. For concrete bridges this limit is 60 m to 90 m. According to a damage assessment made on 54-80 m long existing bridges with end screens, 90% of the bridges have been found to have cracks and other damages near the end screen. 52% of the bridges have cracks in the bridge deck (Flener, 2004).

Due to the contributions of researchers and engineers from Luleå University of Technology, Sweden (Pétursson & Collin, 2002; Tlustochowicz, 2005; Hällmark, 2006; Pétursson & Collin, 2006; Nilsson, 2008; Pétursson et al., 2011), the general codes, rules or guidelines for integral abutment bridges have been developed to simplify the conventional design process and applied in practice (e.g. as shown in Fig. 14 and Fig. 15).
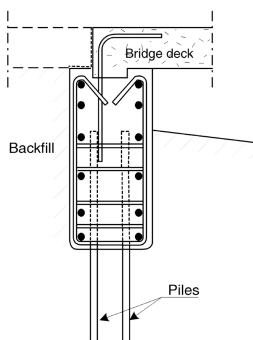
Fig. 13 A Typical Integral Abutment Reinforcement Detail Used in Sweden

Fig. 14 Bridge over Fjällån, Sweden (Pétursson & Collin, 2002)

Fig. 15 Bridge over Leduån, Sweden – Composite Bridge with Single Span of 40 m (Nilsson, 2008)

2.2.3 Germany

Coverage of long span integral abutment bridges in Germany is rather poor. For instance just 2.1% of the large highway bridges which exist in state of Bavaria are integral or semi-integral ones. 78% of them have been built in the last ten years, which at least shows that integral bridges become more and more important. The main application field for integral frame bridges in Germany is the over passing of small side roads. In 1999 the German Federal Ministry of Transport, Building and Urban Development (BMVBS, Bundesministerium für Verkehr, Bau und Stadtentwicklung) published a list of ten single span prototype bridges and recommended their use to the authorities. Eight of these ten bridges were integral ones with a maximum span of up to 45 m (Feldmann et al., 2010).

In 2003 many recommendations from the BMVBS were withdrawn and replaced by the Eurocode based DIN Fachbericht 101 to 104. As no specific rules concerning integral bridges can be found in these standards, there presently isn't any specific standard or guideline for integral road bridges in Germany, as the same for most of the other European countries. A common practice in Germany is the use of vaulted-tapered girders and beams (Fig. 16), which allows for an easier transfer of the bending moments at the frame edge and leads to a very winsome slender shape of the bridge (Weizenegger, 2003). In combination with very rigid foundations quite long single span bridges can be realised, compared to conventional bridges (e.g. Viaduct Rednitztal, as shown in Fig. 17, with 7-span and total length of approximately 170 m).
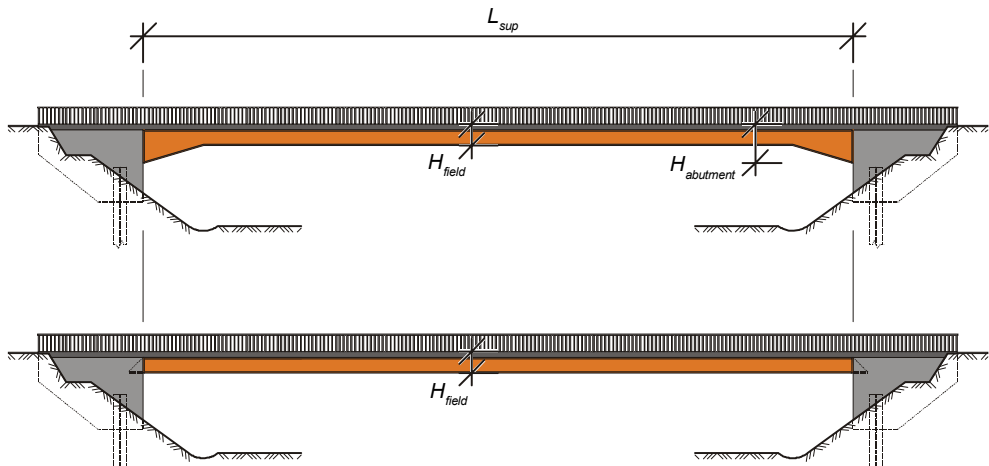
Bridge Type		with haunch		without haunch
		$L_{sup}/H_{abutment}$	L_{sup}/H_{field}	L_{sup}/H_{field}
Road bridges	reinforced concrete	12-18	20-25	18-21
	prestressed concrete	15-19	24-30	20-25
	steel composite	15-19	25-35	21-25
Railway bridges	reinforced concrete	10-15	20-25	16-18
	prestressed concrete	15-20	20-25	-
	steel composite	15-18	25-30	18-21

Fig. 16 Slenderness for Integral Abutment Bridges Used in Germany (Feldmann et al., 2010)

Fig. 17 Viaduct Rednitztal: Monolithically Connected Superstructure with Pier and Abutment (Marx & Seidl, 2011)

2.2.4 Italy

The records of integral abutment bridges in Italy are lack of archives. However, engineers and designers are positive to spread the concept of integral abutment bridges (Briseghella et al., 2004; Briseghella & Zordan, 2004). The retrofitting of an existing short bridge in semi-integral abutment bridge was proposed (Russo et al., 2009). And the integral abutment was applied in a skewed bridge with the width

greater than length (Malerba & Comaita, 2011). In 2007, integral abutment bridge that located at *Isola della Scala* (Fig. 18) in province of Verona was completed (c.f. Ch.4.1). The total length of the structure is approximately 400 m with 13 spans, which is the longest integral abutment bridge in the world up to now (Zordan & Briseghella, 2007). Therefore, it would be of great necessity to have specialty grid-lines for existing and future construction of integral abutment bridges in Italy.

Fig. 18 Isola della Scala Bridge, Verona, Italy

2.3. Application in East Asia and Oceania

2.3.1 China

China began to build integral abutment bridge at the end of 1990's. In 1998, the first jointless bridge was completed connecting the highway in the province of Hunan, with low spans-ratio (11.4 m + 33.2 m + 11.4 m). In 1999, the first integral abutment design was employed in one (east side) of the abutments of a viaduct in the city of Changsha (Hong, 2006; Jin, 2007). The first integral abutment bridge, Sijiu Bridge (Fig. 19), was built in November, 1999, in Qingyuan, Guangdong, with total length of 75.48 m and skew angle of 15-degree. The bridge is a 4-span continuous-frame reinforced concrete bridge (Ma & Jin, 2002). In December of the same year, a bridge in province of Henan was retrofitted to a semi-integral bridge, with total length of 67.96 m and skew angle of 15-degree(Jin et al., 2005). In 2004, the current longest integral abutment bridge, Yongchun Shangban Bridge (Fig. 20), has been completed, with 4 spans of 30 m, and total length of 137.1 m (Hong & Peng, 2004).

The bridges are all reported in excellent service currently have been performing very well with no maintenance problems in the past decade. However, there is still

no any guideline or recommendation for design since the integral abutment bridges campaign in China has been launched.

Bridge	Completed Year	Location	Length (m)	Skew angle (degree)
Yi-Chang Highway Connection	1998	Hunan	56	NA
Changsha City Viaduct	1999	Hunan	171	curved, only one integral abutment
Qingyuan Sijiu Bridge	2000	Guangdong	52	15
Zhoukou Liguanhe Bridge	2000	Henan	67.96	15
Yongchun Shangban Bridge	2004	Fujian	137.1	NA
Nan-You Highway Najiao Bridge	2005	Guangxi	80	NA
Heng-Da Highway Dashuiting Bridge	2005	Hunan	69.46	35
Heng-Da Highway Da-Pu D-Ramp	2005	Hunan	75	curved
Qingyuan Longtang Bridge	2006	Guangdong	109.2	NA

Table 2
Integral / Semi-Integral Abutment Bridges in China

a) elevation (m)

b) plan (m)
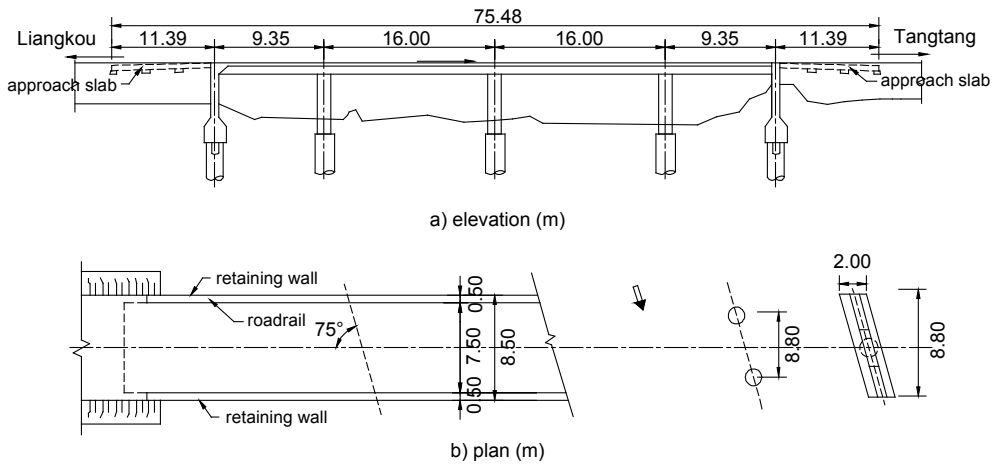
Fig. 19 General Layout of Sijiu Bridge, Guangdong, China
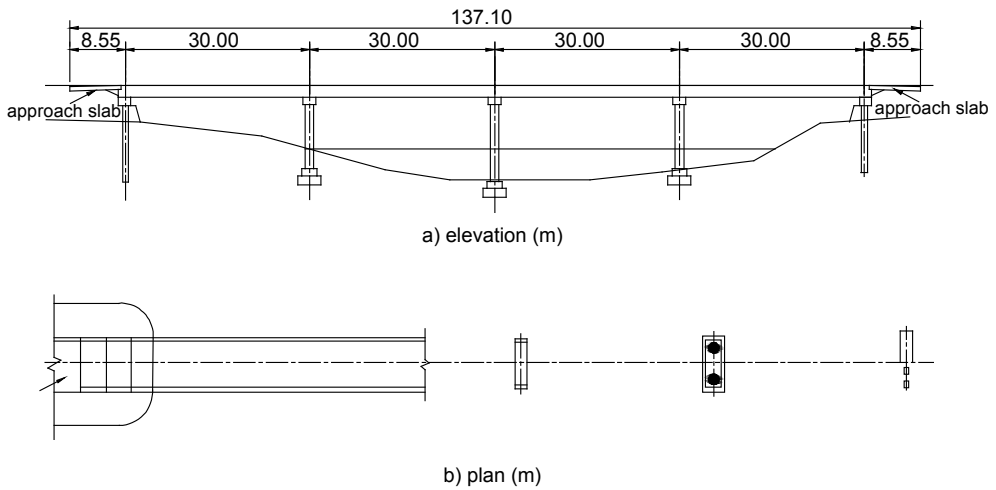

a) elevation (m)

b) plan (m)

Fig. 20 Yongchun Shangban Bridge, Fujian, China

2.3.2 Japan

In Japan, the building method of the integral bridges and composite bridges with eliminating joints were developed after World War II. Research on jointless bridge began in 1983 (Peng, 2001). Based on the surveys on jointless bridges carried out in 1991 and 1993, design and construction manual on the method of existing bridges without expansion joints was published (Road Management Technology Center, 1995). Two approaches were presented for existing bridges without expansion joints (Nippon Dohro Joint Association, 2010). In 1996, the first integral bridge was built (Wasserman & Walker, 1996). In Japan, all the integral bridges and jointless bridges are single-span or multi-span with span length less than 30 m.

However, since 1995, portal frame bridges have been exclusively applied in Japan instead of integral abutment bridges (Iwasaki et al., 2011). The main reasons for replacing integral abutment bridges by portal frame bridges in Japan are:

1) response behavior of IABs during a strong earthquake has not yet been studied thoroughly;
2) there is no suitable design concept for IAB;
3) traditionally two companies share the construction efforts where one company gets the substructure and the other company gets the superstructure.

2.3.3 Australia

The Australian Bridge Design Code contains no particular reference to integral abutment bridges or jointless bridge decks (Connal, 2004). However, the Queensland Main Roads Department (QMRD) of Australia has been constructing one type of precast, prestressed concrete jointless bridge since 1975 (Franco, 1999), and approximately 200 bridges of this type have been constructed according to QMRD survey. The design of the precast, prestressed girders has become standardized in Queensland. Typically, the length of these bridges ranges from 40 to 70 m. The QMRD is considering increasing the allowable length limit to 100 m, based on observed behaviour of older bridges and publications that outline experiences with jointless bridges in the United States.

Since 1963, 49 jointless bridges have been built in New South Wales. Although there are some exceptions, most of the recently built jointless bridges are widenings

or duplications of short concrete bridges built between 1930 and 1960. 41 of these bridges have integral abutments and are built up to the following lengths: 53.6 m (precast, prestressed concrete), 50 m (link slab), 89 m (cast-in-place concrete), and 27 m (steel). The other eight jointless bridges were built using the so-called "abutmentless" bridge concept in lengths up to 88.7 m (Franco, 1999).

As an example, a two span continuous bridge was constructed as part of the Ballarat Bypass project in 1995 (Connal, 2004). The bridge is continuous over a central pier with two spans of 29.5 m and a 10 degree skew. The superstructure comprised T-girders with a cast-in-situ concrete deck slab. The girders were built into the central pier and both abutments giving a jointless deck and integral abutments. The bridge is shown in Fig. 21.

a) elevation view (taken from Google Maps)
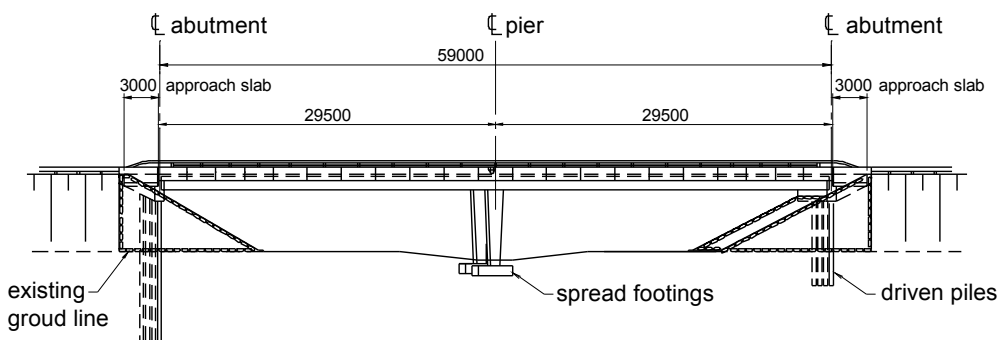
b) general arrangement (Connal, 2004)
Fig. 21 Gillies Street Bridge in Ballarat, Australia

2.3.4 New Zealand

New Zealand's experience with jointless bridges began in the 1930's as well as United States and Australia (Wolde-Tinsae et al., 1988b). At first, relatively short concrete bridges were built with integral-type abutments. By the 1950's, integral abutment bridges were a commonplace in New Zealand, and standardized design drawings for concrete bridges of this type were developed by the New Zealand Ministry of Works and Development (NZMWD) (Franco, 1999). And the NZMWD did note that no reports of any problems with bridges with integral abutments are on file. The NZMWD found it necessary to strengthen several existing concrete integral abutment bridges (by prestressing) for exceptionally heavy loads. For example, the Waiwaka Terrace Bridge (Fig. 22), located in New Plymouth, is a concrete T-beam integral abutment bridge with an overall length of 46.3 m. A few bridges with semi-integral abutments have been built in New Zealand since the 1960's. The length of this bridge type is usually limited to 70 m, although the Kauaeranga Bridge (built in 1986) has an overall length of 136 m. Noting the economical overall cost and simplicity of integral and semi-integral abutments and no problems have been reported with the jointless bridges, the NZMWD length limits of this type of bridge are thought to increase based on the monitoring the performance of the Kauaeranga Bridge (Franco, 1999).
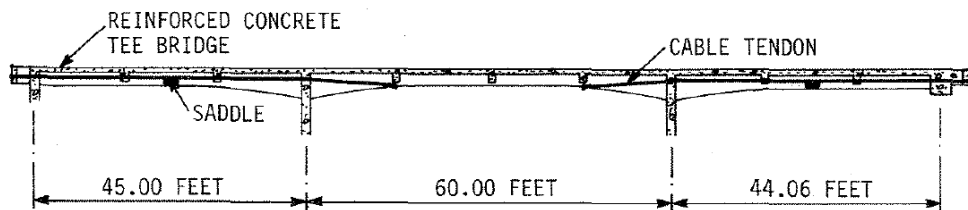
Fig. 22 Strengthening (in 1985) on Waiwaka Terrace Bridge, New Zealand (Dunker et al., 1987)

2.4. Super-Long Integral Abutment Bridges

As known, expansion joints are a nightmare in the maintenance of highway bridges. After a few decades, the junction points between the structure and the road begin to show signs of deterioration. Therefore, the benefits of integral abutment bridges are realized much all over the world. However, according to different geographical and geological conditions, and different temperature variation and construction experience, the length of integral abutment bridge is limited differently in different regions.

As the applications introduced before, In United States, most of the states reported having relatively low maximum span lengths for steel beam bridges within 60 m. Three states (Massachusetts, Tennessee and Virginia) reported steel beam spans over 90 m. Most of the states surveyed stated that their concrete beam bridges were limited to less than 45 m (Baptiste et al., 2011). AASHTO (American Association of State Highway and Transportation Officials, 2002) has also specified strictly the limit displacement of the abutment of 91.4 mm or less, if the integral abutment bridge would be built in seismic area type of D, to avoid severe failure consequence. Although the length (or the movement) is limited, the scientists and engineers are still in motivation to develop longer, super-long integral abutment bridges, which exceed the length limits or displacement limits in specializations.

Table 3 lists the recorded longest integral abutment bridges in the world (length > 200 m) through available survey data. The Isola della Scala Bridge in Italy, with length of 400.8 m (c.f. Ch.4.1), is the longest existing integral abutment bridge; while in United States, the longest precast-concrete-girder integral abutment bridge with length of 358.4 m was built in Tennessee; the longest steel-girder and cast-in-place concrete bridges were both built in Colorado, measuring 318.4 m and 290.4 m, respectively (Kunin & Alampalli, 1999; Frosch et al., 2005; Wasserman, 2007; Kim, 2008; Itani & Pekcan, 2011).

Using the pile-supported stub-type abutment, prestressed girder bridges up to 244 m in length and steel bridges up to 122 m may be routinely constructed

In Switzerland, scientists at EPFL (École Polytechnique Fédérale de Lausanne) are attempting to do away with this costly technique of expansion joints (Evangelista, 2011). The Structural Concrete Laboratory (IBéton) has initiated an innovative research program on abutment and approach slab construction techniques, with the challenge to be able to eliminate expansion joints on future big bridges and modify those of existing bridges, which would become super-long integral / semi-integral abutment bridges that longer than 200 meters. To tolerate very large displacement cycles without damage as the need to build longer integral bridges grows, the role of the semi-integral abutments is expected to become more important (Arsoy et al., 2004).

Some preliminary investigations on design of super-long integral abutment bridges were also carried out through model analyses (Baptiste et al., 2011). From trial design of a 305 m integral abutment bridges with eight 38.1 m spans, and a 457 m long bridge with 12 spans at 38.1 m, integral abutment bridges longer than 305 m

are predicted to develop high pile stress, high stress in the abutment–pile connection, and high stress in the girder at the backwall transverse reinforcing, making these the limiting factors for integral abutment bridges. Therefore, the critical issues in analysis and performance of super-long integral abutment bridges are necessary to investigate.

No.	Name or Location	State / Country	Length	Remarks
1	Isola della Scala, Verona	Veneto, Italy	400.8 m	c.f. Ch.4.1
2	SR 50 (over Happy Hollow Creek)	Tennessee, USA	358.4 m	precast, prestressed concrete bulb-T girders, curved, 9-span (Fig. 8)
3	unkown	Colorado, USA	339.2 m	precast girder
4	unkown	Oregon, USA	335.5 m	precast girder
5	unkown	Colorado, USA	318.4 m	steel girder
6	SR 249 (over US 12)	Indiana, USA	302 m	composite prestressed bulb-tee girder, 10-span (26.4 ~ 35.0 m)
7	unkown	Colorado, USA	290.4 m	cast-in-place
8	SR 34 (over Southern Railway & Whitehorn Creek)	Tennessee, USA	250 m	pile-supported stub-type abutment; 12-span precast/prestressed box beams with composite concrete deck
9	unkown	Virginia, USA	235.5 m	precast girder
10	Bushley Bayou (LA 124)	Louisiana, USA	221 m	9-span, semi-integral abutment
11	unkown	South Dakota, USA	209.2 m	precast girder

Table 3
Super Long Integral Abutment Bridges in the World

3. CRITICAL ISSUES IN ANALYSIS

Although the concept of integral abutment bridge will give a lot benefits and avoid many difficulties in structure, the biggest uncertainty in the analysis and design of an integral abutment bridge is the reaction of the soil behind the abutment walls and next to the foundation piles. The magnitude of these soil forces can become substantial during thermal expansion of the bridge system, and can greatly affect the overall structural design of the bridge-wall-pile system. This lateral soil reaction is inherently nonlinear and depends on the magnitude and nature of the wall displacement, which can both translate and rotate. This is a soil-structure interaction (SSI) problem, where the magnitudes and nature of the soil and structural deformations and stresses are interdependent. (Faraji et al., 2001)

Handling the soil-structure interaction in the analysis and design of integral abutment bridges has always been problematic, usually requiring iterative analysis wherein the soil reactions are manually adjusted depending on the deformation level behind the abutment wall and adjacent to each supporting pile. Such an iterative, equivalent linear approach is time-consuming and approximate, and does not lend itself to dynamic analysis. With the desire to design and construct longer span bridges with skew and non-skew alignments, and to evaluate of the performance of these bridges, the more integrated analysis and design tool is necessary. With the development of numerical computation technique and the application of finite element (FE) method in structural analysis, it has been realized that the complicated non-linear behaviors are implemented well using computer program.

In this chapter, the theories and empirical methods of soil-structure interactions will be summarized, also the thermal actions on bridge, in order to build the reasonable finite-element model for integrated abutment bridges.

3.1. Soil-Abutment Interaction

Although the integral bridge concept has proven to be economical in initial construction for a wide range of span lengths, as well as technically successful in eliminating expansion joint and bearings problems, it is susceptible to different problems that

turn out to be geotechnical in nature. These are potentially due to a complex soil-structure interaction mechanism involving relative movement between the bridge abutments and adjacent retained soil. Because this movement is the result of natural, seasonal thermal variations, it is inherent in all integral bridges (Lock, 2002).

There are two important consequences of this movement: seasonal and daily cycles of expansion and contraction of the bridge deck can lead to an increase in earth pressure behind the abutment; and the soil deformation adjacent to each abutment. Both analytical and numerical modelling undoubtedly are powerful tool for the design and analysis of integral bridges, whose basis have being placed solely on experimental testing and field testing. And these results may also be used to help improve theoretical and numerical modelling techniques. In the section, the analytical and numerical models that widely used for soil-abutment design will be briefly descried.

3.1.1 Classical Theories on Earth Pressure

To describe the pressure a soil will exert, a lateral earth pressure coefficient, K, is used (Coduto, 2001; Shamsabadi, 2011; Wikipedia, 2011a). K is the ratio of lateral (horizontal) pressure to vertical pressure ($K = \sigma_h'/\sigma_v'$). Thus horizontal earth pressure is assumed to be directly proportional to the vertical pressure at any given point in the soil profile. K can depend on the soil properties and the stress history of the soil. Lateral earth pressure coefficients are broken up into three categories: at-rest K_0, active K_a, and passive K_p. There are many theories, empirically based or analytically derived, for predicting lateral earth pressure.
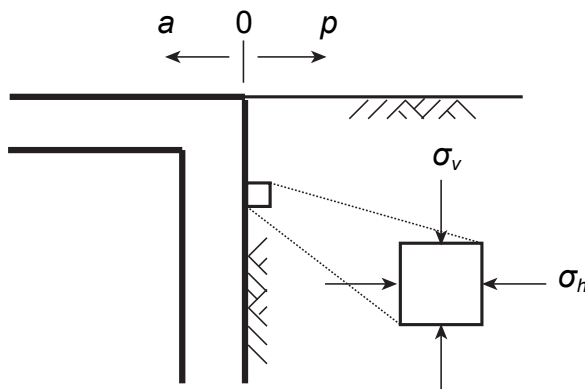

Fig. 23 Stress State of Soil behind the Abutment Wall

Rankine theory

Rankine's theory, developed in 1857, is a stress field solution that predicts active and passive earth pressure. It assumes that the soil is cohesionless, the wall is frictionless, the soil-wall interface is vertical, the failure surface on which the soil moves is planar, and the resultant force is angled parallel to the backfill surface. The equations for active and passive lateral earth pressure coefficients are given below. Note that φ' is the angle of shearing resistance of the soil and the backfill is inclined at angle β to the horizontal.

$$K_a = \cos\beta \frac{\cos\beta - \sqrt{\cos^2\beta - \cos^2\varphi'}}{\cos\beta + \sqrt{\cos^2\beta - \cos^2\varphi'}} \tag{1}$$

$$K_p = \cos\beta \frac{\cos\beta + \sqrt{\cos^2\beta - \cos^2\varphi'}}{\cos\beta - \sqrt{\cos^2\beta - \cos^2\varphi'}} \tag{2}$$

For the case where β is 0, the above equations are simplified to

$$K_a = \tan^2\left(45 - \frac{\varphi'}{2}\right) \tag{3}$$

$$K_p = \tan^2\left(45 + \frac{\varphi'}{2}\right) \tag{4}$$

Coulomb theory

Coulomb (1776) first studied the problem of lateral earth pressures on retaining structures. He used limit equilibrium theory, which considers the failing soil block as a free body in order to determine the limiting horizontal earth pressure. The limiting horizontal pressures at failure in extension or compression are used to determine the K_a and K_p respectively. Since the problem is indeterminate, a number of potential failure surfaces must be analyzed to identify the critical failure surface (i.e. the surface that produces the maximum or minimum thrust on the wall). Mayniel (1808) later extended Coulomb's equations to account for wall friction, symbolized by δ. Müller-Breslau (1906) further generalized Mayniel's equations for a non-horizontal

backfill and a non-vertical soil-wall interface (represented by angle θ from the vertical).

$$K_a = \frac{\cos^2(\varphi' - \theta)}{\cos^2\theta \cos(\delta + \theta)\left(1 + \sqrt{\frac{\sin(\delta + \varphi')\sin(\varphi' - \beta)}{\cos(\delta + \theta)\cos(\beta - \theta)}}\right)^2} \tag{5}$$

$$K_p = \frac{\cos^2(\varphi' + \theta)}{\cos^2\theta \cos(\delta - \theta)\left(1 - \sqrt{\frac{\sin(\delta + \varphi')\sin(\varphi' + \beta)}{\cos(\delta - \theta)\cos(\beta - \theta)}}\right)^2} \tag{6}$$

Caquot and Kerisel theory

In 1948, Albert Caquot and Jean Kerisel developed an advanced theory that modified Muller-Breslau's equations to account for a non-planar rupture surface. They used a logarithmic spiral to represent the rupture surface instead. This modification is extremely important for passive earth pressure where there is soil-wall friction. Mayniel and Muller-Breslau's equations are unconservative in this situation and are dangerous to apply. For the active pressure coefficient, the logarithmic spiral rupture surface provides a negligible difference compared to Muller-Breslau. Since these logarithmic equations are too complex to use, the tables or computers are used instead.

Caquot and Kerisel's log spiral theory is more generally applicable, where the movement of walls are sufficiently large so that the shear strength of the backfill soil is fully mobilized, and where the strength properties of the backfill can be estimated with sufficient accuracy.

These methods of calculation on K_a and K_p are used for practical purposes. Coulomb's trial wedge method can be used for irregular backfill configurations. And Rankine's theory and log spiral analysis can be used for more regular configurations.

Terzaghi and Peck's empirical charts

Terzaghi and Peck, in 1948, developed empirical charts for predicting lateral pressures. Only the soil's classification and backfill slope angle are necessary to use the charts.

Resulting Pressure - Bell's relation

For soils with cohesion, Bell developed an analytical solution that uses the square root of the pressure coefficient to predict the cohesion's contribution to the overall resulting pressure. These equations represent the total lateral earth pressure. The first term represents the non-cohesive contribution and the second term the cohesive contribution. The first equation is for an active situation and the second for passive situations.

$$\sigma_h = K_a \sigma_v - 2c\sqrt{K_a} \tag{7}$$

$$\sigma_h = K_p \sigma_v + 2c\sqrt{K_p} \tag{8}$$

3.1.2 Simplified Method – Modified Coefficients

However, the movement of the abutment into the approach fill develops passive earth pressure that is displacement-dependent. Using full passive pressure regardless of displacement is not conservative because it reduces the flexural effects of dead and live load in the bridge girders.

Some researches were carried out, that proposed modified coefficients based on Rankine' theory. The passive earth pressure coefficients were thought to be reduced by multiplying 2/3 on Rankine's passive coefficients. It recommended to be applied in most of integral abutment bridges with single span, or 2-3 small and medium spans (Burke Jr, 1993; Chen, 1997).

This simplified method is not widely used and has been found difference from others analyses (Hong, 2006).

3.1.3 Continuous Earth Pressure Distribution in Design

Since the lateral pressure on the abutments cannot be determined simply from statically calculations, and the stresses at the soil-abutment interface are governed by a complex soil-structure interaction defined in terms of cyclic thermal movements (ex-

pansion and contraction) of the bridge, many experimental investigations were carried out by bridge engineers and geologists (Lehane et al., 1999; England et al., 2000; Xu, 2010), based on which the numerical studies gave out some empirical relations between the lateral pressure and movement of the wall.

UK

From the experiments on cyclic stress of backfill soil on a concrete wall pinned to a strip footing (England et al., 2000), according to the Highways Agency Design Manual for Roads and Bridges (BA 42), for the lateral earth pressure, whose distribution is derived as a uniform stress ratio K^* from the surface to a depth of one-half the height of the wall and a uniform pressure of $\gamma K^* H/2$ over the bottom half of the wall, the recommended equation to calculate K^* is (Highways Agency, 2003):

$$K^* = K_0 + \left(\frac{d}{0.03H}\right)^{0.6} K_p \tag{9}$$

where, H is the retained height; d is thermal displacement of the top of the abutment; K_0 is the at rest earth pressure coefficient and the passive earth pressure coefficient K_p is based on $\delta = \varphi'/2$ and taken from Eurocode 7.
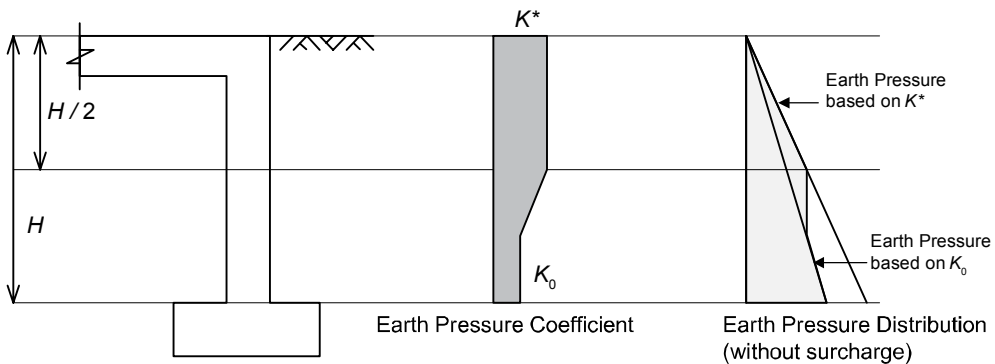

Fig. 24 Earth Pressure Distribution for Frame Abutment (Highways Agency, 2003)

USA

Most bridges in the USA are designed according to the American Association of State Highway and Transportation Officials (AASHTO). It's reported that AASHTO calculates horizontal soil pressures on the bridge abutments according to Rankine active soil pressure (Flener, 2004). The pressure is limited to 4.8 kN/m^2 per meter height of the abutment. K_a is assumed to be equal to 0.3. Uniform triangular and Rankine load distributions are used for the design of soil pressure on integral bridge

abutments, in USA and Canada, and also some of the agencies do not consider soil pressure at all (Kunin & Alampalli, 2000).

Based on obtained the variation of earth pressure coefficient as a function of structure displacement from experimental data and finite-element analyses (Barker et al., 1991), Dicleli proposed, for practical purposes, a linear relationship expressed as (Dicleli, 2000a; Dicleli, 2000b):

$$K = K_0 + \varphi d \leq K_p \tag{10}$$

where, d is the displacement of the integral bridge towards the backfill soil and φ is the slope of the earth pressure variation depicted in Fig. 25. The value of φ varies as a function of the backfill soil type.
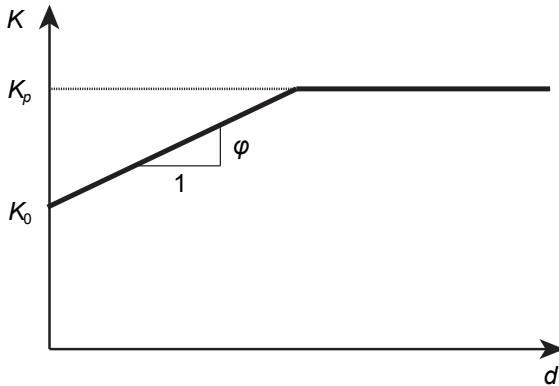

Fig. 25 Variation of passive earth pressure coefficient (Dicleli, 2000a; Dicleli, 2000b)

Results from full scale wall tests performed by University of Massachusetts Amherst (Thompson, 1999) show reasonable agreement between the predicted average passive earth pressure response of standard compacted gravel borrow (Massachusetts Department of Transportation, 2007) and the curves of K versus δ/H for dense sand found in design manuals (Naval Facilities Engineering Command, 1986; Barker et al., 1991). For the design of integral abutments, the coefficient of horizontal earth pressure (K) is dependent on the relative wall displacement, δ/H. When using compacted gravel borrow backfill the pressure coefficient K shall be estimated using the equation (Massachusetts Department of Transportation, 2007):

$$K = 0.43 + 5.7 \left[1 - e^{-190 \left(\frac{\delta}{H} \right)} \right] \tag{11}$$
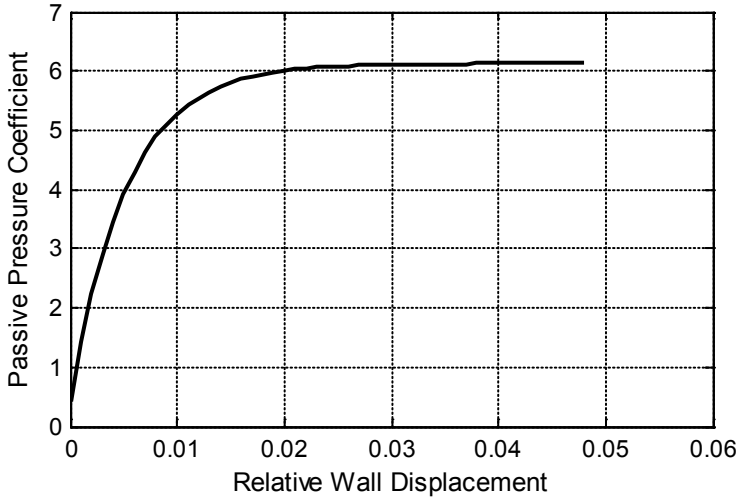

Fig. 26 Passive Presure Coefficient Recommonded by MassHighway

Sweden

According to Swedish design standards (Bro 2002), an additional horizontal earth pressure as a reaction to horizontal movement of the bridge should be taken into account. In Bro 2002, the reaction pressure ΔP on piles, pillars and frame walls can be calculated from Eq.(12), which is valid until the depth of $H_a/2$ and approaches to 0 at the bottom of the wall, and should be used in addition to the existing at rest soil pressure (Fig. 27). The earth pressure coefficients are taken from Table 4. (Flener, 2004), (Vägverket, 2002)

$$\Delta P = C \cdot \gamma_s \cdot z \cdot \frac{\delta}{H_a} \tag{12}$$

where, C = 300 or 600 depending on the forces being advantageous or not; γ_s = soil unit weight; z = depth; δ = horizontal deflection of the abutment; H_a = abutment height.
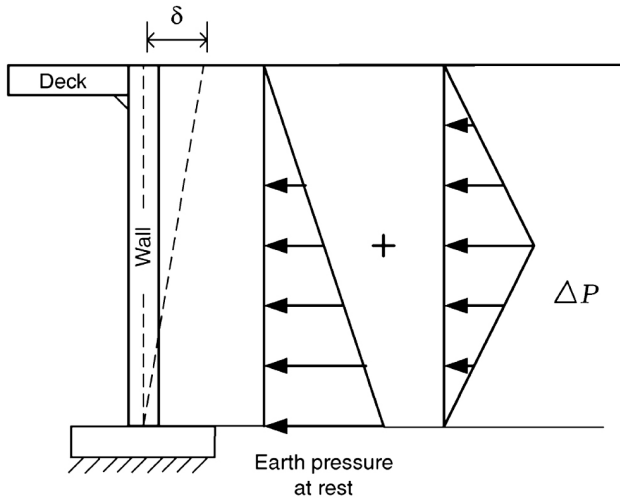
42

Fig. 27 Design Earth Pressures according to Swedish Bridge Code (Bro 2002)

Material	K_0	K_a	K_p
Crushed stone	0.34	0.17	5.83
Subbase material	0.36	0.22	4.60
Clinker	0.43	0.27	3.70
Plastic cell	0.40	0	-

Table 4
Lateral Earth Pressure Coefficients of Different Materials (Bro 2002)

These distributions above are very useful in preliminary design and analytical for-mulations of structural mechanics of integral abutment bridge. However, these sim-plified continuous distributions of lateral pressure could not reflect the real behav-iour of the backfill soil, where, in fact, the coefficient *K* varies non-linearly along the depth from surface. Considering not only the translation movements but also the rotation of abutment and effects of wingwalls, the displacement of the top of the abutment could not represent the other displacements in different depths (Thompson, 1999). Thompson proposes that for a deflection mode of simultaneous rotation and translation, the earth pressure distribution increases from the top to a depth of approximately 38% of the abutment height and from that point on it re-mains constant. Fang's model test results for wall rotation show similar earth pres-sure distribution nonlinearity with the point of application of a passive thrust of 0.55

H_a (Fang et al., 1994). Xu's results also confirm nonlinearity (Xu et al., 2003; Xu et al., 2007).

3.1.4 Discrete Earth Pressure Distribution in Design

As stated, the soil reaction pressure distribution on the wall is inherently nonlinear, and varies with depth, amount, and mode of wall displacement. Depending on the relative flexural stiffness of the composite bridge deck, abutment wall, foundation piles, and lateral stiffness of the soil behind the wall and next to the piles, the amount and mode of deformation of the wall varies. This in turn affects the level and amount of the soil reaction pressure behind the wall.

With the application of finite element method in structural analysis, and the concept of a series of uncoupled "Winkler" springs, where the deflection at one level of the wall is not presumed to affect the value of the reaction force at another level (Faraji et al., 2001), the discrete non-linear springs have been used to simulate the soil-structure interaction behind the abutment wall and next to the pile.

There are some kinds of the non-linear force-deflection relations of the springs applied behind the abutment that widely used in finite element analysis. These curves typically include both active and passive regimes, and are usually used for both pure horizontal translation as well as pure rotation about the base.

In Eurocode 7 (European Committee for Standardization (CEN), 2004b), The limit values of earth pressure on a vertical wall, caused by weight density, are required to be calculated following Bell's relations (Eqs.(7) and (8)). Intermediate values of earth pressure between the rest state and the limit state may be obtained by linear interpolation; and intermediate values of passive earth pressure between the rest state and the limit state may be obtained by parabolic interpolation. While, the limit movement values to reach the limit pressures are different according to types of the movements of the wall.

Besides, one commonly used set of curves, for loose, medium dense and dense cohesionless granular materials, are based on finite element analyses by Clough and Duncan (Faraji et al., 2001), and could be found in several design manuals such as NCHRP report No.343 (Barker et al., 1991) (Fig. 28), and Foundation Engineering Handbook (Clough & Duncan, 1991). A second common set of design curves are found in U.S. Department of the Navy (Naval Facilities Engineering

Command, 1986) (Fig. 30) and the Canadian Foundation Engineering Manual (CGS) (Becker & Moore, 2006) (Fig. 29).

As can be seen, these three families of curves are familiar. They are can be generalized into elasto-plastic nonlinear relations as shown in Fig. 31. For determining K_a and K_p, NCHRP and NAVFAC suggest to apply Rankine's theory or log spiral charts for uniform and regular backfill configurations, while Coulomb's trial failure wedge method for irregular backfill configurations. And CGS considered Rankine's theory to be generally more conservative on active pressure, while logarithmic spiral to be realistically description on passive pressure. Their magnitudes of $\Delta L / H$ that required to reach the minimum active and maximum passive earth pressures are listed in Table 5. From the comparison, the NCHRP values are moderate between these three recommendations and widely used in engineering practices (Arsoy et al., 1999; Faraji et al., 2001; Dicleli, 2004; Dicleli & Albhaisi, 2004b; Erhan & Dicleli, 2009; Ooi et al., 2010; Zordan et al., 2010). Therefore, the NCHRP design curves were used in the following study.
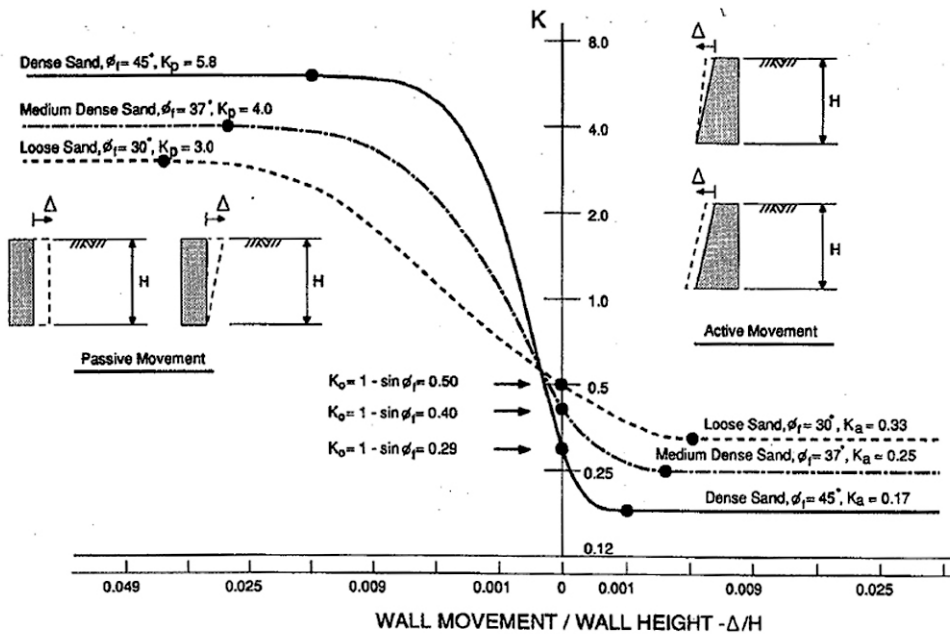
Fig. 28 Relationship between Wall Movement and Earth Pressure (NCHRP, Sand) (Barker et al., 1991)
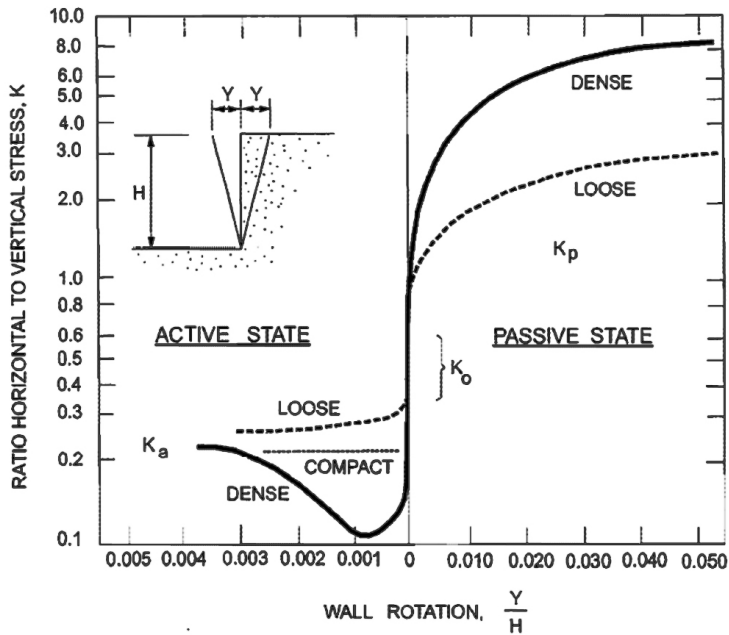
45

Fig. 29 Effect of Deformation on Earth Pressures (CGS, Cohesionless) (Becker & Moore, 2006)
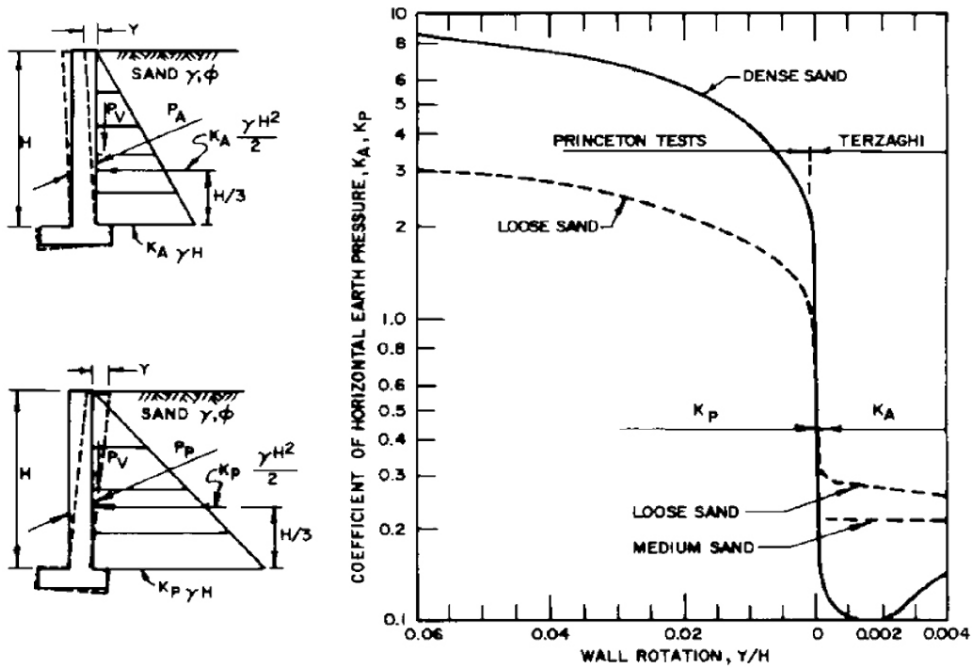

Fig. 30 Effect of Wall Movement on Wall Pressures (NAVFAC, Sand) (Naval Facilities Engineering Command, 1986)
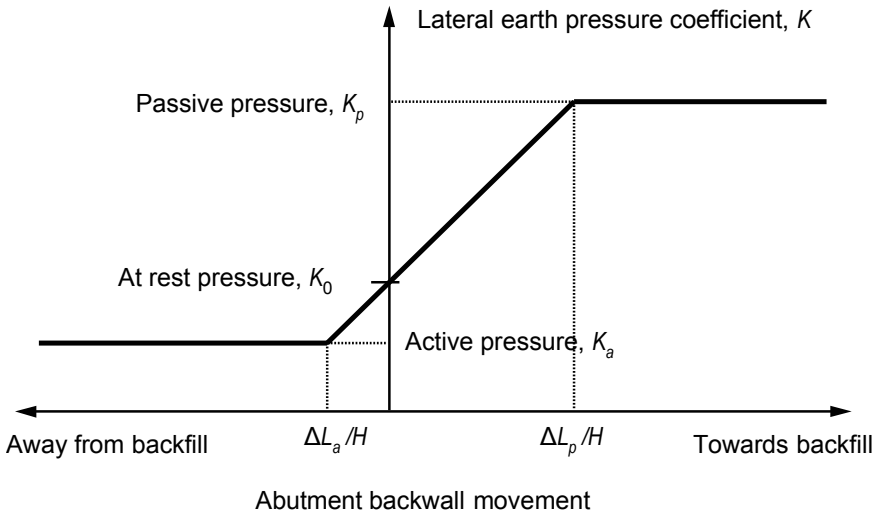
Fig. 31 Elasto-plastic Diagram of Nonlinear Springs Restraining the Abutment Backwall

Type of Backfill	Values of $\Delta L / H$					
	NCHRP		CGS		NAVFAC	
	Active	Passive	Active	Passive	Active	Passive
Dense Sand / Dense Cohesionless	0.001	0.01	0.001	0.02	0.0005	0.002
Loose Sand / Loose Cohesionless	0.004	0.04	0.004	0.06	0.002	0.006
Compacted Clay / Stiff Cohesive	0.01	0.05	0.01	0.02	0.01	0.02
Compacted Clay / Soft Cohesive	0.01	0.05	0.02	0.04	0.02	0.04

Table 5
Approximate Magnitudes of Movements Required to Reach Minimum Active and Maximum Passive Earth Pressure Conditions

3.2. Soil-Pile Interaction

Most bridge abutments utilize either spread footings or pile foundations at the bottom of the wall to support the bridge loads. Piles are often favoured over spread footings because of erosion and vertical deformation considerations. The piles themselves at working loads exhibit essentially elastic behaviour, but the surrounding soil may be in states ranging from elastic to plastic and furthermore may be subject to cyclic degradation. Hence, design of such structural members represents a complex problem of soil-structure interaction.

For integral abutment bridges, it is commonly thought that a foundation that is rotationally and translationally stiff results in larger superstructure loads during thermal loading. In order to increase the lateral and rotational flexibility of the pile head, piles for an integral abutment bridge foundation are often driven into preaugered deep holes which are then backfilled with loose sand (c.f. Ch.6.3.3). Also, the piles are often installed with their weak axis of bending parallel to the bridge centreline (Wasserman, 2007).

The Winkler soil model is used for the analysis of the soil pile interaction. The model assumes that the soil can be represented as a series of vertical and lateral springs along the length of the pile. Also, the model assumes that there is no interaction between the different soil springs as the pile is displaced. The soil characteristics of each of three types of springs can be described by soil resistance and displacement curves (Greimann et al., 1987):

> (1) *p-y* curves, which describe the relationship between the lateral soil pressure (horizontal force per unit length of pile) and the corresponding lateral pile displacement – the main issue going to be discussed in the Chapter;

> (2) *f-z* curves, which describe the relationship between skin friction (vertical force per unit length of pile) and the relative vertical displacement between the pile and the soil; and

> (3) *q-z* curves, which describe the relationship between the bearing stress (vertical force on effective pile tip area) at the pile tip and the pile tip settlement.

All three types of curves assume the soil behaviour to be nonlinear.

Again, the Winkler model assumes that these springs are uncoupled, that is, that motion at one spring does not affect another.
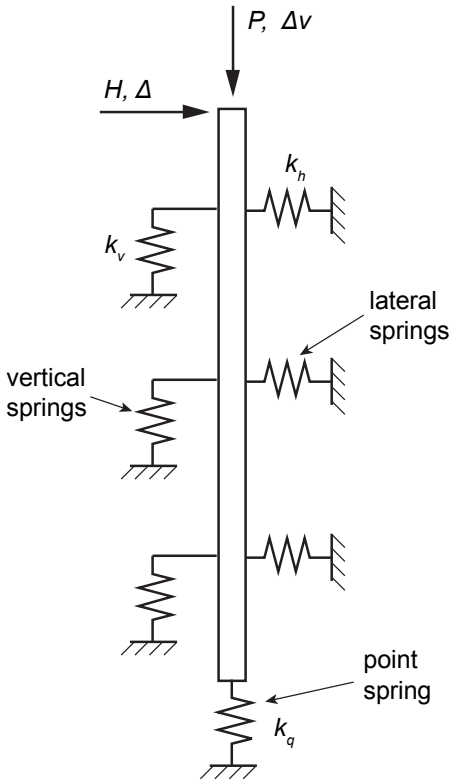

Fig. 32 Design of Soil-Pile System (Greimann et al., 1987)

The different kinds of soil resistance and displacement (p-y) curves methods used in engineering practices and studies are going to be summarized. Besides these methods applied in piles design, an introduction on another useful method in designing piles – equivalent cantilever approach – will be briefly described.

3.2.1 Terzaghi's Theory – Linear Assumption

At the beginning of the study on soil mechanics, Terzaghi and other researchers have made the assumption that the coefficient of horizontal pile reaction, k_h, is a constant (Terzaghi, 1943):

$$\frac{p}{y} = k_h \tag{13}$$

where, p is the pressure on the pile; y is the horizontal displacement of pile. And the coefficient of horizontal reaction k_h is often assumed to be constant (for clay soils) or to vary linearly with depth (for granular soils, sand). The assumption was widely used in analytical study on pile resistances and its preliminary design.

3.2.2 Empirical p-y Curves

The concept of p-y curves was first developed by McClelland and Focht in 1956. Matlock proposed a well-known family of p-y curves (Matlock, 1970) (Fig. 33), which based on the research on laterally loaded piles in soft clay involving extensive field testing with an instrumented pile, experiments with laboratory models, and parallel development of analytical methods and correlations.

Another family of p-y curves for piles in stiff clay was constructed by Reese (Reese et al., 1975) (Fig. 34). As well as a family of p-y curves for sand (Reese et al., 1974) is based on the experimental field testing of piles installed a t a site where the soils consisted of clean fine sand to silty fine sand. And Sullivan (Sullivan et al., 1979; Hong, 2006) made a unified curve both for soft and stiff clays (Fig. 35).
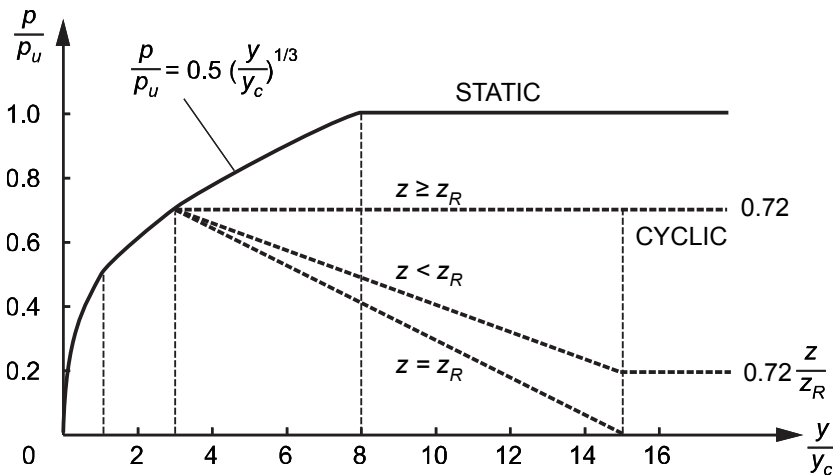

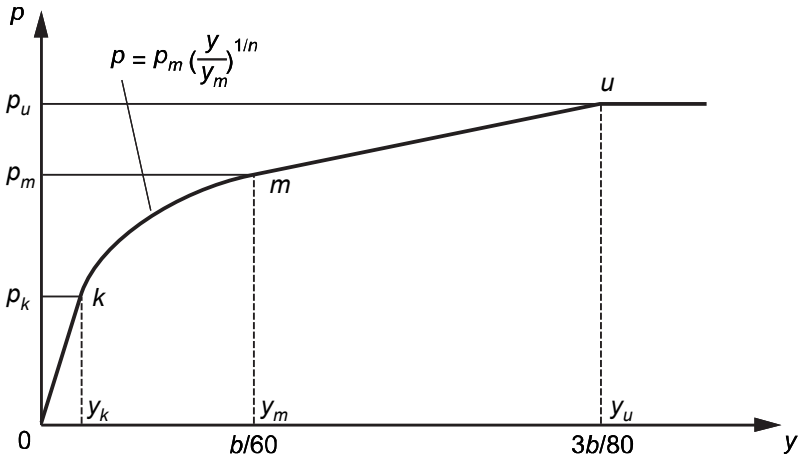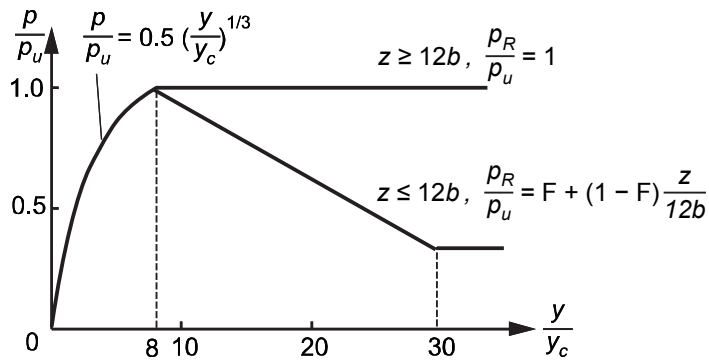Fig. 33 Family of p-y Curves for Laterally Loaded Piles in Soft Clay by Matlock
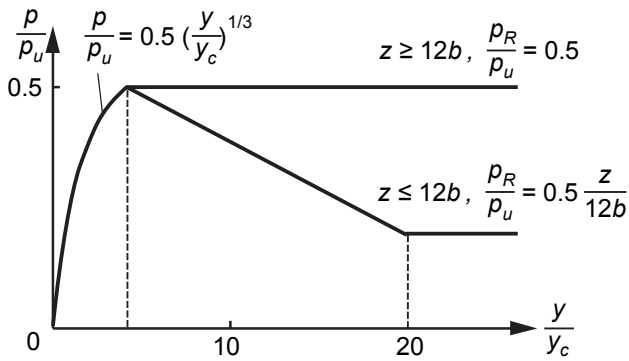
Fig. 34 Family of p-y Curves for Piles in Stiff Clay by Reese

a) static loading

b) cyclic loading

Fig. 35 Family of p-y Curves for Piles in Clay by Sullivan

3.2.3 Elasto-Plasticity Models

To consider the nonlinear behaviour, the simplified elastic and perfectly plastic be-
haviour could be assumed. The only soil spring properties needed for the design
method are the ultimate resistance and the initial stiffness (Greimann et al., 1987).
As well, researchers had developed the modified Ramberg-Osgood model that ac-
commodates loading and unloading of the pile during cyclic loading, which are used
to approximate the *p-y*, *f-z*, and *q-z* soil resistance and displacement curves for use
in the finite element solution (Greimann et al., 1984; Greimann et al., 1987) (Fig. 36).
For example, for *p-y* curves the model could be expressed as:

$$p = \frac{k_h y}{\left[1 + \left|\frac{y}{y_u}\right|^n\right]^{1/n}} \tag{14}$$

$$y_u = \frac{p_u}{k_h} \tag{15}$$

where, k_h is the initial stiffness; p is the generalized soil resistance; p_u is the ultimate
soil resistance; n is the shape parameter of pile; y is the generalized displacement.
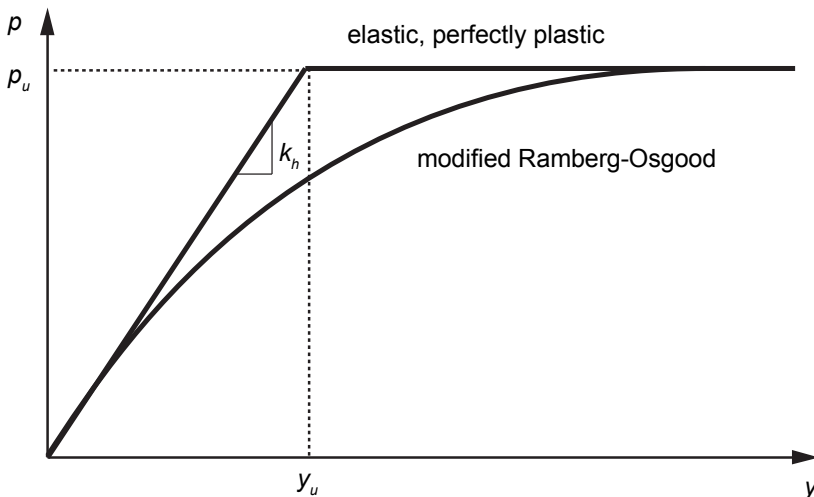The constants can be empirically determined from basic soil properties.

Fig. 36 Typical Elasto-Plasticity p-y Curves

3.2.4 API Design Method

Most current design methods for integral abutment bridges assume that these soil springs exhibit equivalent linear response even though it is widely known to be non-linear and hysteretic. Existing methods for predicting soil resistance, i.e., API methods, Hansen's methods, and Broms methods, give different predictions of soil resistance for the same soil conditions (Fan & Long, 2005; Shia, 2005). Among these methods, the most sophisticated nonlinear soil modelling for lateral pile loading currently done by the oil industry, API methods, are commonly used in engineering practice. Many of the current computer programs for modelling lateral pile behaviour based on the API design guidelines for fixed offshore platforms (American Petroleum Institute, 2000).

The API methods are on the basis of the study of the *p-y* curves that constructed by Matlock for soft clay (Matlock, 1970), Reese for stiff clay (Reese et al., 1975), and O'Neill for sands (O'Neill & Murchison, 1983). This method is going to be described and will be adopted in following study.

For Clay

The non-linear lateral soil resistance-deflection relationships for piles in soft clay, for the short-term static load case and for the case where equilibrium has been reached under cyclic loading, may be generated from the following table:

Static Load		*Cyclic Load*			
		$X > X_R$		$X < X_R$	
p/p_u	y/y_c	p/p_u	y/y_c	p/p_u	y/y_c
0.00	0.0	0.00	0.0	0.00	0.0
0.50	1.0	0.50	1.0	0.50	1.0
0.72	3.0	0.72	3.0	0.72	3.0
1.00	8.0	0.72	∞	$0.72\ X/X_R$	15.0
1.00	∞			$0.72\ X/X_R$	∞

Table 6
API p-y Curves for Soft Clay

where, p is actual lateral resistance (kPa); p_u is ultimate resistance (kPa); y is actual lateral deflection (mm); $y_c = 2.5\ \varepsilon_c\ D$ (mm), and ε_c is strain which occurs at one-half the maximum stress on laboratory undrained compression tests of undisturbed soil samples; X is depth below soil surface (mm); X_R is depth below soil surface to bottom of reduced resistance zone (mm).

For static lateral loads, the ultimate bearing capacity p_u of stiff clay as for would be higher than soft clay. Due to rapid deterioration under cyclic loadings the ultimate resistance will be reduced to something considerably less and should be so considered in cyclic design. While stiff clays also have non-linear stress-strain relationships, they are generally more brittle than soft clays. In developing stress-strain curves and subsequent p-y curves for cyclic loads, good judgment should reflect the rapid deterioration of load capacity at large deflections for stiff clays.
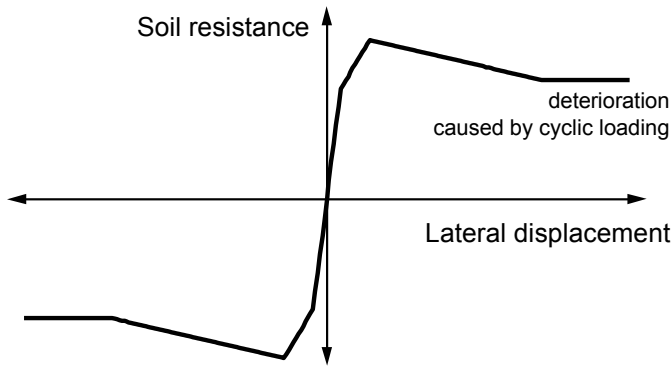
Fig. 37 Soil Resistance of Clay

For Sand
The ultimate lateral bearing capacity for sand can be determined from recommended equations in API guidelines. The p-y curves may be approximated at any specific depth H, by the following expression:

$$P = Ap_u \tanh\left[\frac{kH}{Ap_u}y\right] \tag{16}$$

where, A is factor to account for cyclic or static loading condition; p_u is ultimate bearing capacity at depth H (kN/m); k is initial modulus of subgrade reaction (kN/m^3), which can be determined as function of angle of internal friction (φ').

Soil resistance

$$P = Ap_u \tanh\left[\frac{kH}{Ap_u}y\right]$$

Lateral displacement

Fig. 38 Soil Resistance of Sand

φ', Angle of Internal Friction

| 28° | 29° | 30° | 36° | 40° | 45° |

| Very Loose | Loose | Medium Dense | Dense | Very Dense |

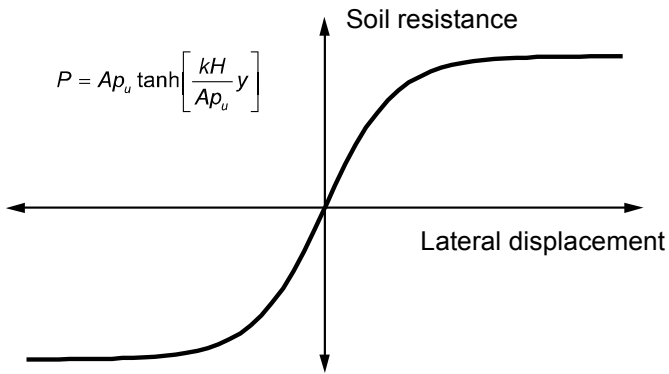Sand above the water table

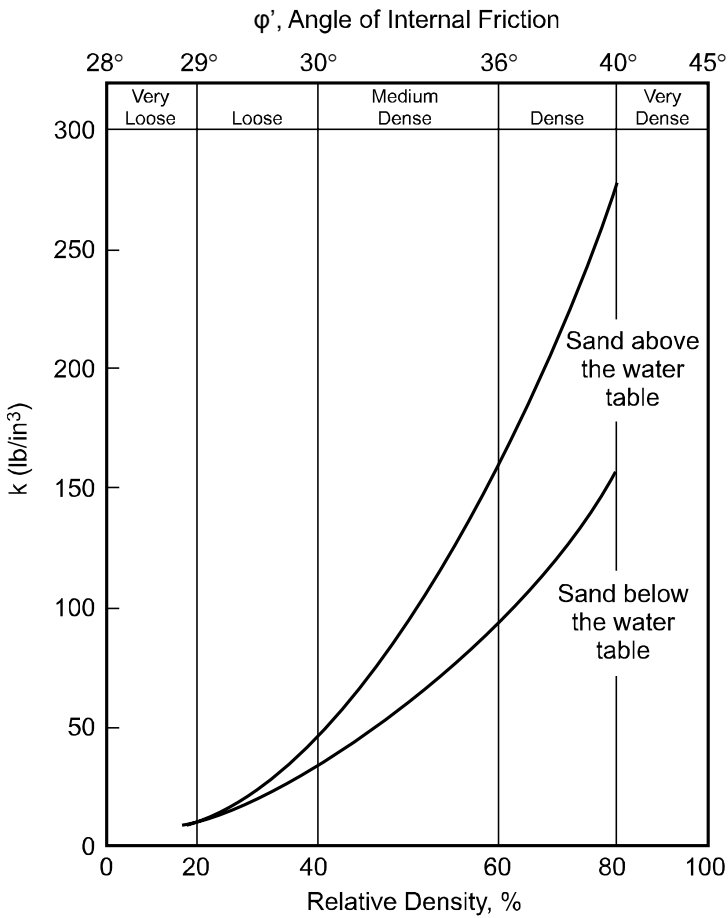Sand below the water table

k (lb/in³)

Relative Density, %

Fig. 39 Initial Modulus of Subgrade Reaction of Different Sands (American Petroleum Institute, 2000)

3.2.5 Equivalent Cantilever Approach

Embedded piles can be represented, using the equivalent cantilever method, as a column with a base fixed at some distant below the ground surface (Fig. 40). The notation is the same for both the fixed and pinned-head conditions. The length of the actual pile embedded in the ground is represented as l, and the length abode the ground is l_u. The equivalent embedded length, le, is the depth from the soil surface to the fixed base of the equivalent cantilever. The total length of the equivalent cantilever is the length l_u plus l_e, represented by L. For a long pile embedded in soil, there is a depth below which the horizontal displacements at the pile head have negligible effects. A critical length, l_c, which represents this depth, can be calculated. Beyond this length, lateral displacements and bending moments are a small percentage (about 4%) of those at the pile head. If a pile is longer than l_c, the pile behaves as if it is infinitely long. For a soil with a uniform subgrade-reaction modulus, the critical length is selected as

$$l_c = 4R \tag{17}$$

in which the relative stiffness factor R is

$$R = \left(\frac{EI}{k_h}\right)^{\frac{1}{4}} \tag{18}$$

Most piles used in practice are longer than their critical length and behave as "flexible" piles. Note that l_c is a parameter of the pile and soil system and is not a physically identifiable length.

Equivalent cantilevers can be used to calculate the forces in the pile and the bridge superstructure. For example, an equivalent cantilever can be determined such that its maximum moment would be equal to the maximum moment in real pile. However, the complete moment diagram below the ground surface could not be determined with the same equivalent cantilever. Three different equivalencies were considered in the development of the design method. They are based on

      (1) the horizontal stiffness of the soil-pile system,
      (2) the maximum moment in the pile, and
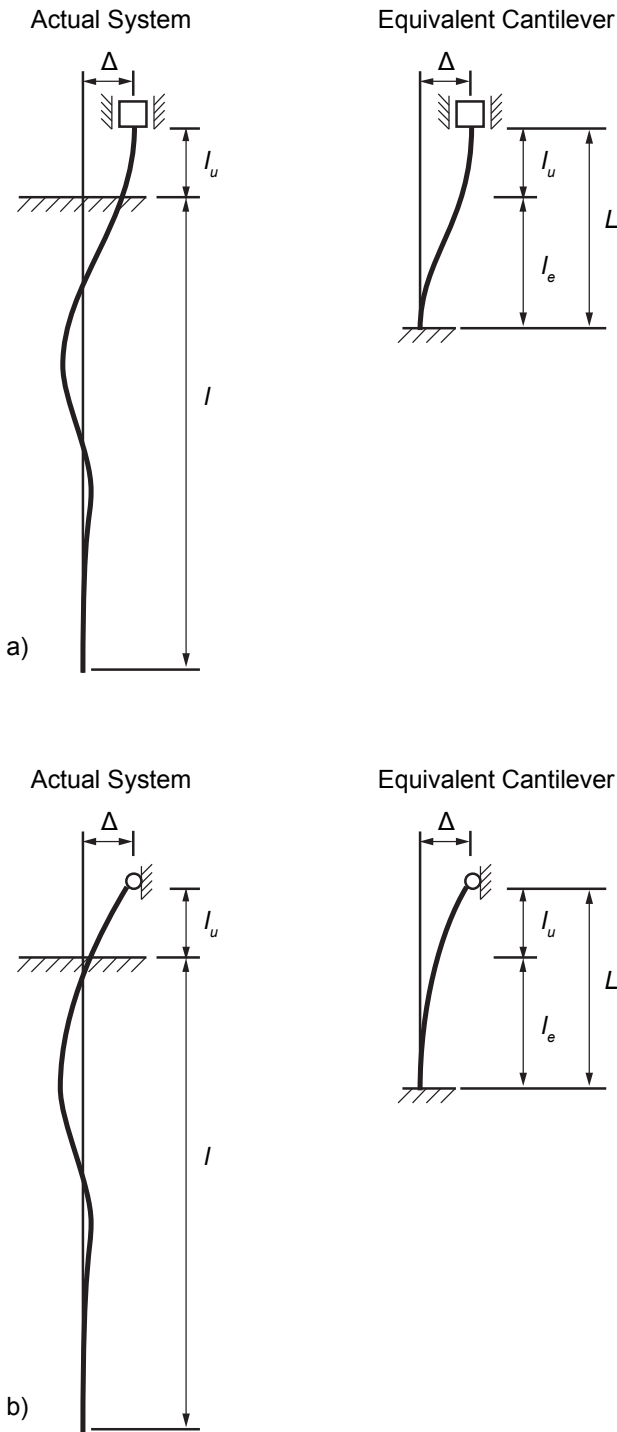   (3) the elastic buckling load of the pile.

Fig. 40 Cantilever Idealization of the Pile: a) Fixed-Head Condition; b) Pinned-Head Condition

For each equivalency, the boundary condition at the pile head was either fixed (no rotation) or pinned (no moment). The horizontal displacement at the top of the equivalent system corresponds to the longitudinal expansion or contraction of the bridge superstructure at the integral abutment. The equations for determining the equivalent embedded lengths are expressed in different equivalencies (Table 7).

Equivalencies	Equivalent Embedded Length
	Fixed-Head Pile
Horizontal stiffness	$\dfrac{l_e}{l_c} = \sqrt[3]{\dfrac{256\left(\dfrac{l_u}{l_c}\right)^4 + 256\sqrt{2}\left(\dfrac{l_u}{l_c}\right)^3 + 192\left(\dfrac{l_u}{l_c}\right)^2 + 48\sqrt{2}\left(\dfrac{l_u}{l_c}\right) + 12}{256\left(\dfrac{l_u}{l_c}\right) + 64\sqrt{2}}} - \dfrac{l_u}{l_c}$
Moment	$\dfrac{l_e}{l_c} = \sqrt{\dfrac{128\left(\dfrac{l_u}{l_c}\right)^4 + 128\sqrt{2}\left(\dfrac{l_u}{l_c}\right)^3 + 96\left(\dfrac{l_u}{l_c}\right)^2 + 24\sqrt{2}\left(\dfrac{l_u}{l_c}\right) + 6}{128\left(\dfrac{l_u}{l_c}\right)^2 + 64\sqrt{2}\left(\dfrac{l_u}{l_c}\right) + 16}} - \dfrac{l_u}{l_c}$
Buckling	$\dfrac{l_e}{l_c} = \left(\dfrac{2\pi}{\beta_e l_u} - 1\right)\dfrac{l_u}{l_c}$
	Pinned-Head Pile
Horizontal stiffness	$\dfrac{l_e}{l_c} = \sqrt[3]{\left(\dfrac{l_u}{l_c}\right)^3 + \dfrac{3\sqrt{2}}{4}\left(\dfrac{l_u}{l_c}\right)^2 + \dfrac{3}{8}\left(\dfrac{l_u}{l_c}\right)} - \dfrac{l_u}{l_c}$
Moment	$\dfrac{l_e}{l_c} = \sqrt{\dfrac{3}{16(Q_M)_{max}}\left[\dfrac{32\sqrt{2}}{3}\left(\dfrac{l_u}{l_c}\right)^3 + 16\left(\dfrac{l_u}{l_c}\right)^2 + 4\sqrt{2}\left(\dfrac{l_u}{l_c}\right) + 1\right]} - \dfrac{l_u}{l_c}$
Buckling	$\dfrac{l_e}{l_c} = \left(\dfrac{\pi}{0.7\beta_e l_u} - 1\right)\dfrac{l_u}{l_c}$

Table 7
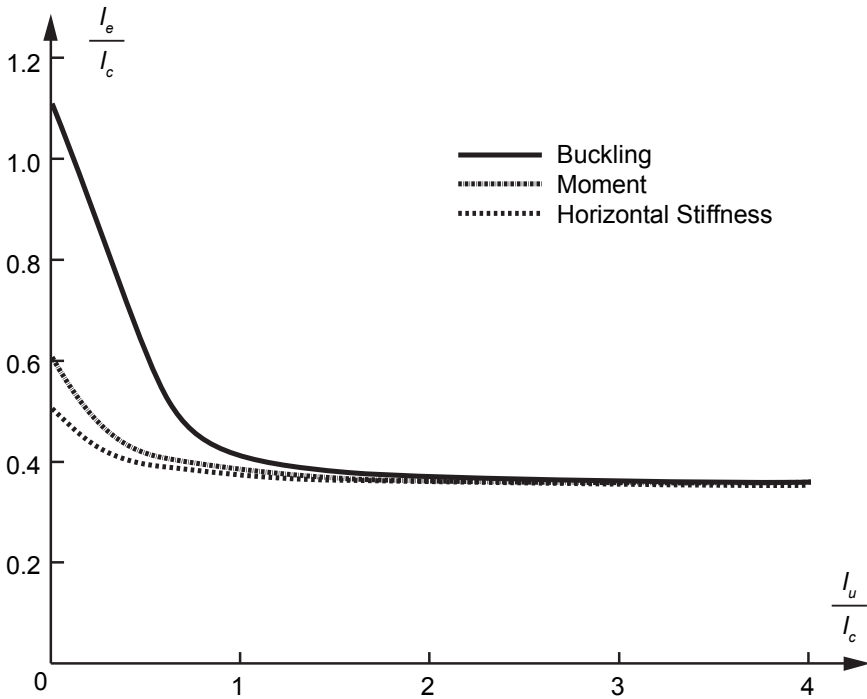*Equations for Equivalent Embedded Length of Piles (Greimann et al., 1987)*

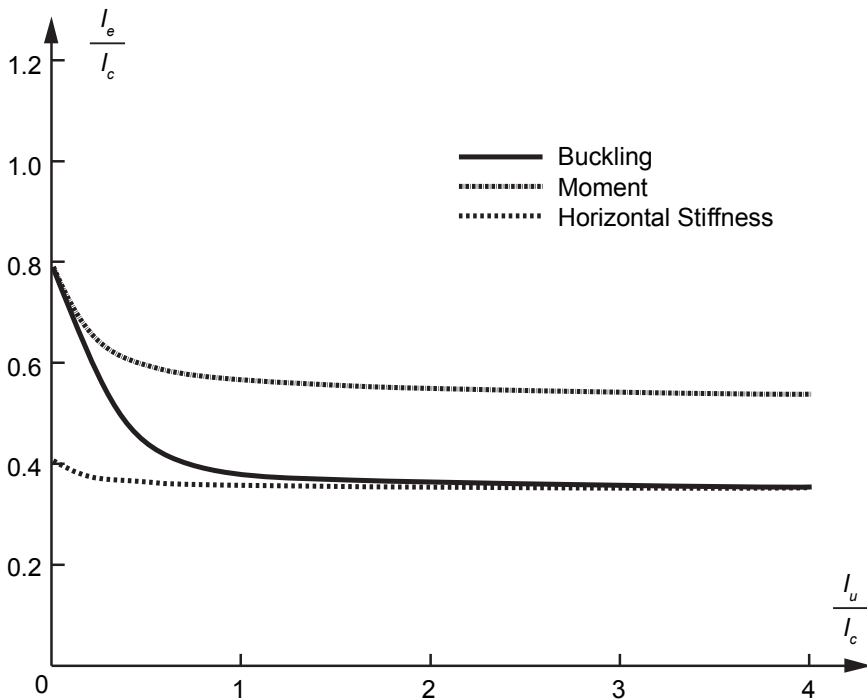Fig. 41 Equivalent Cantilevers for Fixed-Head Piles Embedded in a Uniform Soil

Fig. 42 Equivalent Cantilevers for Pinned-Head Piles Embedded in a Uniform Soil

These equations axe plotted in a non-dimensional form and pinned-head piles embedded in uniform soil in Fig. 41 and Fig. 42, respectively. As can be seen from Fig. 41 and Fig. 42, an unfilled predrilled hole significantly reduces the equivalent embedded length until the hole is approximately l_c deep, that is, l_u / l_c equals approximately one. Below that depth, the effective length remains essentially constant over the range used for most integral abutment bridges.

For piles embedded in a non-uniform soil, the equivalent soil stiffness developed to determine the equivalent cantilevers (Greimann et al., 1987). This equivalent cantilever method currently used in the Massachusetts Highway Department Bridge Design Manual (Massachusetts Department of Transportation, 2007) provided a reasonable approximation to moments in pile in engineering practice (Bonczar et al., 2005).

3.3. Temperature Loads on Superstructure

A change in temperature causes a material to change in length. This fundamental property of materials is responsible for expansion and contraction of bridge superstructures. As the temperature increases, the bridge expands. As the temperature cools down the bridge will contract to shorter. In conventional bridges, expansion joints exist between the superstructure and the abutment to accommodate these displacements. In integral abutment bridges, the expansion joints are eliminated and the superstructure is allowed to freely displace the bridge abutments. Because of the abutment displacements, the pile and the approach fill are subjected to lateral loading and unloading. And the bridge responses to the temperature loads are governed by many factors, such as types of soil adjacent to abutment, abutment displacements including translations and rotations, piles types and arrangements, and so on (Metzger, 1995; Bettinger, 2001; Arsoy et al., 2004; Shah, 2007; Shehu, 2009).

Structure temperatures at a locality are determined by continuously changing meteorological conditions. Although the meteorological conditions are very complex to fully understand, the primary factors that influence the structure temperatures can be summarized as: diurnal temperature, solar radiation, wind speed, precipitation, thermal properties of structural material, and other weather conditions. (Arsoy, 2000; England et al., 2000)

As shown by the survey in United States (Franco, 1999), several states agreed that thermal stresses due to expansion and contraction of the superstructure are very important in the design of an integral abutment bridge. Michigan design practices accommodate thermal stresses with abutment and abutment backwall movement. Kentucky designs for thermal bending moments generated at the abutment / super-structure connection. New York and New Hampshire state that thermal stresses are accommodated by flexible piles and sleeper slab movement. Minnesota and West Virginia design the approach slab joint for thermal movement. West Virginia states that different types of joints accommodate thermal movement when a flexible pavement is used. Approach slabs are required if thermal movement is computed to be more than 0.6 inches (15 mm). Integral abutments are only used for total thermal movement less than 2 inches (50 mm). Other states also limit the use of integral abutments by thermal expansion estimates.

3.3.1 Thermal Induced Displacements

There is a convenient and a simple way to estimate temperature-induced longitudi-nal displacements if no restrictions were imposed at the ends of the bridge deck, as shown:

$$\Delta L = \alpha \cdot \Delta T \cdot L \tag{19}$$

where, α is coefficient of thermal expansion for the superstructure material (as-sumed to be linear and constant along the components when environment tempera-ture changes, in this study, $\alpha = 1.0 \times 10^5$ /°C both for concrete and steel); ΔT is de-sign temperature variation of superstructure; and L is thermal length of bridge, for single-span bridge when ΔL refers to the relative displacement between two abut-ments, L is the span length.

The abutment responds to temperature changes, and its movement can be esti-mated conservatively using Eq.(19). The actual displacement is expected to be slightly less due to backfill restraint, pile resistance and approach slab friction, which will be studied in following chapter (cf. Ch.5.1). The movements will affect the abutment resistance capacities, and be criteria for construction design on super-structure, abutment, bearings and expansion joints if they are used (Roeder, 2002). Besides, the cyclic thermal displacement would cause fatigue problems in the struc-ture or components (c.f. Ch.5.4.1).

3.3.2 Design Temperature Components

The popular design codes for structure engineering, such as AASHTO (American Association of State Highway and Transportation Officials, 2002) and Eurocode (European Committee for Standardization (CEN), 2003a), variation of the temperature through the bridge depth is handled in two parts: the mean bridge temperature, and temperature gradient across the bridge depth, which are called "uniform temperature component" and the "vertical temperature difference component", respectively, in Eurocode.

According to Eurocode, the uniform temperature components of expansion $\Delta T_{N,exp}$ and contraction $\Delta T_{N,con}$ depend on the minimum and maximum temperature which a bridge will achieve.

$$\Delta T_{N,con} = T_0 - T_{e,min} \tag{20}$$

$$\Delta T_{N,exp} = T_{e,max} - T_0 \tag{21}$$

where, $T_{e,max}$ and $T_{e,min}$ are maximum and minimum uniform bridge temperature components, respectively; T_0 is initial temperature when structural element is restrained.

And the effect of vertical temperature differences should be considered by using an equivalent linear temperature difference component with $\Delta T_{M,heat}$ and $\Delta T_{M,cool}$, which should be applied between the top and the bottom of the bridge deck. Moreover, the effect of the vertical temperature differences should be considered by including a non-linear temperature difference component. Fig. 43 shows the factors controlling temperature distribution over the depth of the superstructure and its constituent components, where, a non-linear temperature difference component, ΔT_E, results in a system of self-equilibrated stresses which produce no net load effect on the element.

Therefore, when it is taken into account that both the temperature difference $\Delta T_{M,heat}$ (or $\Delta T_{M,cool}$) and the maximum range of uniform bridge temperature component $\Delta T_{N,exp}$ (or $\Delta T_{N,con}$) assuming simultaneity (e.g. in case of frame structures) one the following combination expressions (Eqs.(22) and (23)) may be used:

$$\Delta T_{M,heat} \left(\text{or } \Delta T_{M,cool} \right) + \omega_N \Delta T_{N,exp} \left(\text{or } \Delta T_{N,con} \right) \tag{22}$$

$$\omega_M \Delta T_{M,heat} \left(\text{or } \Delta T_{M,cool} \right) + \Delta T_{N,exp} \left(\text{or } \Delta T_{N,con} \right) \tag{23}$$

where, the recommended values for ω_N and ω_M are 0.35 and 0.75, respectively.
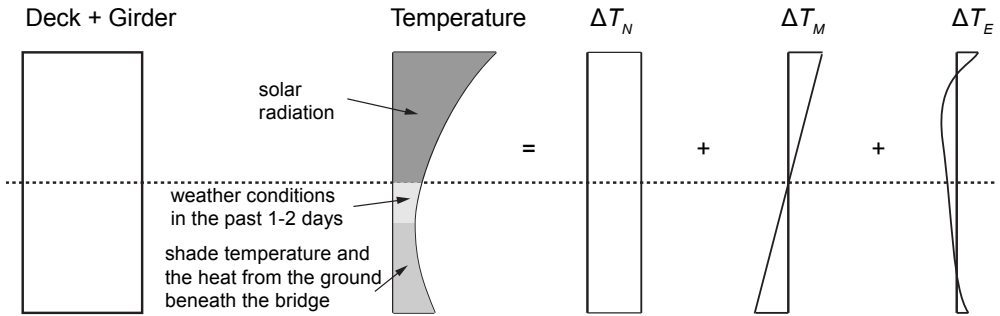

Fig. 43 Diagrammatic Representation of Constituent Components of Vertical Temperature Distribution

3.3.3 Seasonal Temperature Effects

Bridge displacements are affected by both daily and seasonal temperature changes. Each daily variation in temperature completes a cycle of expansion and contraction, and the cycles repeat over time. The greatest expansion takes place during summer days, while the greatest contraction occurs during winter nights. These extreme temperature variations control the extreme displacements of integral abutment bridges (Shah et al., 2008).

In abutments, there could be a build-up of pressure behind the abutment. A steady build-up can be explained by plasticization and flow of granular material during cyclic loading, which is known in the literature as "strain ratcheting", as well as jumps in pressure after the winter months have been found (Hassiotis et al., 2005), which might be explained as: during the spring months, as the temperatures start to increase, the bridge is pushing into frozen or semi-frozen ground and is meeting with high resistance; and during the low temperatures, soil moves in behind the bridge to fill the gap left by the shrinking structure. While in piles, integrally connected with abutment, they would bent in double curvature, where the later displacements in soil directly correspond to temperature changes, especially for skewed bridges (Frosch et al., 2005).

Combined with other time-dependent factors, such as the effects caused by aging creep and shrinkage of concrete, the temperature effects would significantly influence the long-term behaviors and responses of bridges (Pugasap et al., 2009; Kim & Laman, 2010). To predict the long-term behaviors and response, the seasonal temperature data need to be involved in analyses. Researchers also presented magnification factors (Oesterle & Volz, 2005) that were determined from Monte Carlo analyses to account for uncertainty in calculations of bridge movement in order to estimate maximum expected bridge expansion, contraction and re-expansion from full contraction. Besides, further and more researches are still needed to conclude on the possible ramifications caused by temperature, such as low cycle fatigue effect (c.f. Ch.5.4.1), on the integral abutment design.

3.4. Structural Modeling Methods

3.4.1 Conventional Models

Conventionally, an integral abutment bridge is idealized as a continuous beam frame structure if no soil reactions were considered, which could be statically solved manually since moment distribution method (Cross, 1930) had been developed. In this way, the continuous frame is solved out only for the design of deck-abutment joints. But, in the model, the piers are usually idealized as simple roller or hinge supports in most cases. The bridge is designed considering the effect of the loads at the final stage assuming a completed structure. The above approach uses simple structure models for the analysis of integral abutment bridges. Hence, its application is easier and less time consuming when conducted manually.

Consequently, it has been exercised by many structural engineers to design integral abutment bridges for the effects of gravitational loads (Dicleli, 2000b). However, the structure model fails to reflect the actual behavior of the bridge and the effects of several loading conditions and the soil-structure interactions. Until computers began to be widely used in the design and analysis of structures, finite element method has been the most widely practiced method, which could simulate complicated structural behavior under complicated structural loads, such as live load, earth pressure, and effect of temperature variation.
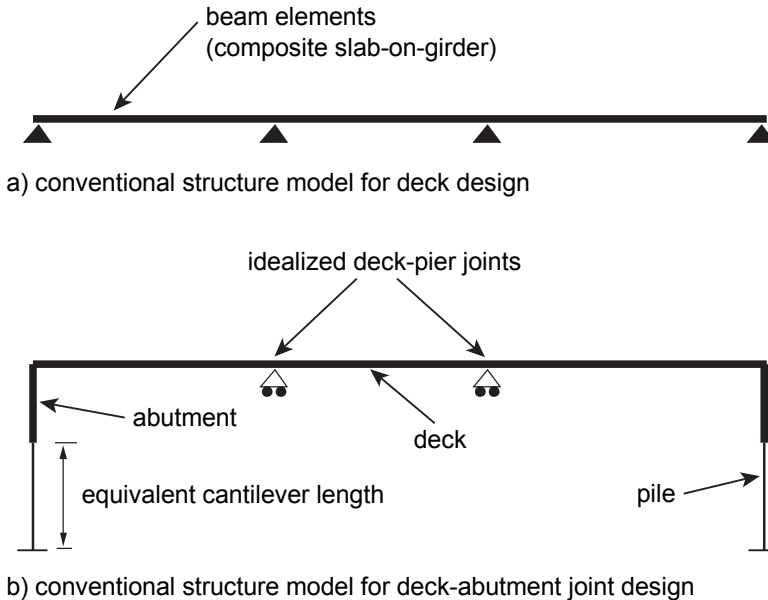
beam elements
(composite slab-on-girder)

a) conventional structure model for deck design

idealized deck-pier joints

abutment

deck

equivalent cantilever length

pile

b) conventional structure model for deck-abutment joint design

Fig. 44 Conventional Structure Models for Integral Abutment Bridges (Dicleli, 2000b)

3.4.2 Finite Element Models

The finite element method is a technique for analyzing complicated structures by notionally cutting up the continuum of the prototype into a number of small elements with different material properties and section characteristics of different structural components, which are connected at discrete joints called nodes. The technique was pioneered for two-dimensional elastic structures during 1950s (Hambly, 1991). Nowadays, most of non-linear structural problems could be simulated in computer programs of finite element method.

There are many finite element model schemes having been developed, both in two-dimensional and three-dimensional, with and without soil springs, piles of full length and equivalent cantilever length (Dicleli, 2000b; Faraji et al., 2001; Hong, 2006; Shah, 2007). For example, the models of integral abutment bridges proposed by Dicleli and Faraji are shown in Fig. 45 and Fig. 46.

An efficient finite element model using nonlinear soil elements at the backwall, abutment, piles, and joints can be implemented using a 3D or 2D model (Dicleli, 2000b; Faraji et al., 2001; Shah, 2007; Kalayci et al., 2009; Pugasap & Laman, 2009; Kim & Laman, 2010). Comparison between the 2D and the more complex 3D

analyses shows the difference within 6% on average (Pugasap et al., 2009). 2D modeling is, therefore, sufficient in analyses and predicting bridge behaviors within the scope of the study.
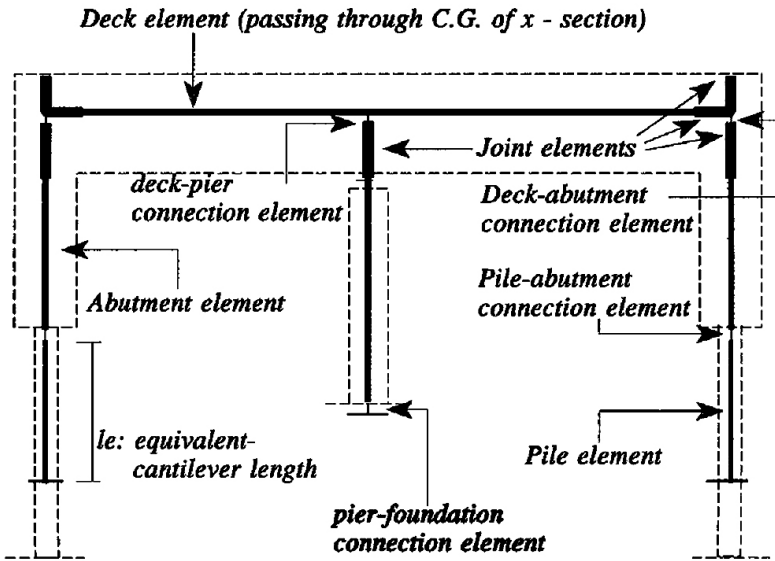

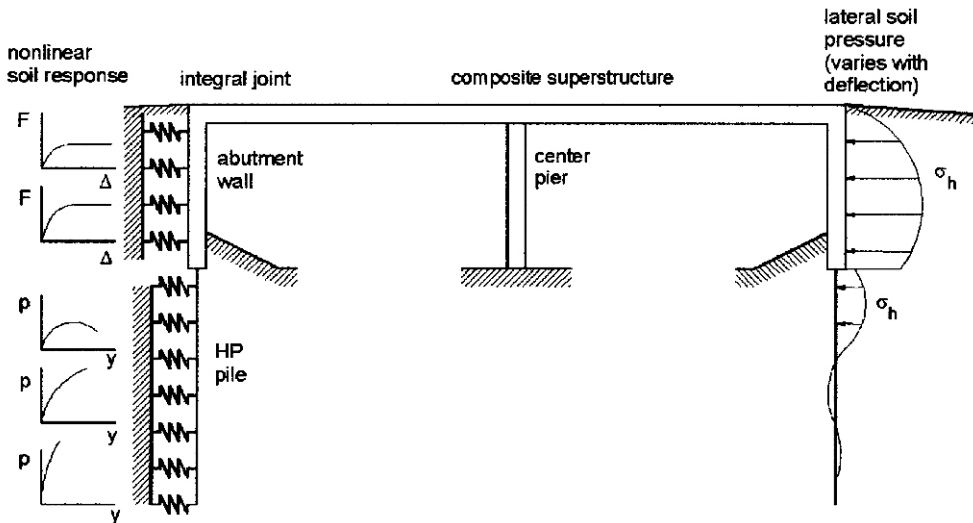Fig. 45 Finite Element Model for Construction Stage Proposed by Dicleli (Dicleli, 2000b)

Fig. 46 Soil Modeling in Finite Element Model (Faraji et al., 2001)

Generally, for a finite element model, it should implement structural elements (beams and plates), an algorithm to account for soil-structure interaction where foundation soil system elements (i.e. driven piles) that could go beyond yielding in some integral abutment bridge systems, and thermal loading capabilities in the finite elements (Krier, 2009). To gain insight into integral abutment bridge's performance and design, in these models, besides the soil-structures interaction and thermal actions, there are still two important issues worth to be discussed: pile length and plastic hinge for nonlinear analyses.

3.4.3 Piles Length in Modeling

In the FE models, some use the full length of piles, while others are using the equivalent length through equivalent cantilever approach mentioned hereinbefore. In fact, because of the assumption of equivalencies in equivalent cantilever approach, the equivalent length of piles could not reflect the real behavior of piles. For example, when the equivalency of the horizontal stiffness of the soil-pile system is made, the horizontal displacement of pile tip and abutment will be the same, rather than the maximum bending moment and its distribution will hardly be the same (Greimann et al., 1987). And the maximum bending moment, usually occurring at a depth above the equivalent depth of fixity, is calculated using the flexural strength of the pile and the ultimate pressure distribution of the soil. It is necessary, therefore, to assume an additional concentrate plastic hinge rotation at the position of maximum bending moment (Chai, 2002), which would make the model more complicated.

Therefore, to completely understanding the pile behavior, different equivalent models should be considered. Moreover, according to Eq.(18), for a multi-layer or non-uniform soil condition, there is also a difficulty in determine equivalent soil stiffness, which need an artificially assumed starting value of equivalent stiffness and calculation iterations. And the convergency has not been verified if the pile consists of different parts of different outer shapes.

Although the equivalent cantilever approach is quite useful in analytical models and suitable for assessing the lateral strength and ductility demand of a yielding soil-pile system, the full length model is going to be used in following finite element model, which is capable in evaluate the pile and the structure behaviors in both ultimate state and service state.

3.4.4 Plastic Hinges in Modeling

As a frame structure, the bending moments are always reaching the materials capabilities in joints when the loadings are intense enough. Therefore, most FE models are using certain kinds of element to simulate the joints. Because of the integral abutment bridges are structures of enough redundancy, the bridge would not failure when one or two plastic hinges are formed. Even in some structures, the plastic hinges are designed to form where the forces can be released.

Since the performance based seismic engineering has placed an emphasis on simulating the nonlinear response of a structural system to seismic excitations, the design of a structural system subjected to earthquake ground motion recognizes that plastic hinges will form in frame members (Priestley et al., 1996). Accurate and computationally efficient numerical models that represent the cyclic loading of plastic hinges in beam-column elements are thus required to simulate the response and evaluate the performance of structural systems.

Finite element models for the nonlinear material response of beam-column members have fallen into two categories: concentrated plasticity (Scott & Fenves, 2006) and distributed plasticity (Chiou et al., 2009). In concentrated plasticity, the nonlinear behavior of a beam-column member is lumped into rotational springs at the ends of one linear-elastic element. The rotational spring is represented by moment-rotation (M-θ) curve. For structural members, the moment-curvature (M-φ) diagrams of sections (Fig. 47a) can be calculated under certain axial-moment interaction by integrating the constitutive models for fragile and ductile materials at sections of the element. Therefore, the lengths of plastic hinges have to be identified for converting M-φ curves to M-θ curves (Fig. 47b).

In girders, using the approach of Coleman and Spacone (Scott & Fenves, 2006), the plastic hinge length l_p can be determined from the concrete properties:

$$l_p = \frac{G_f^c}{0.6 f_c{'}\left(\varepsilon_{20} - \varepsilon_c + 0.8 f_c{'}/E_c\right)} \tag{24}$$

where, $f_c{'}$ = concrete compressive strength; ε_c = peak compressive strain; E_c = elastic modulus; and ε_{20} = strain corresponding to 20% of the compressive strength; G_f^c = concrete fracture energy in compression.

Alternatively, the plastic hinge length can be specified using an empirically validated relationship, such as the Paulay and Priestley (Paulay & Priestley, 1992) equation for reinforced concrete members:

$$l_p = 0.08L + 0.022f_y d_b \tag{25}$$

where, L = length of the member (m); and f_y and d_b = yield strength (MPa) and diameter (m), respectively, of the longitudinal reinforcing bars. The advantage of this approach is that the plastic hinge length includes the effect of strain softening and localization as determined by experiments.
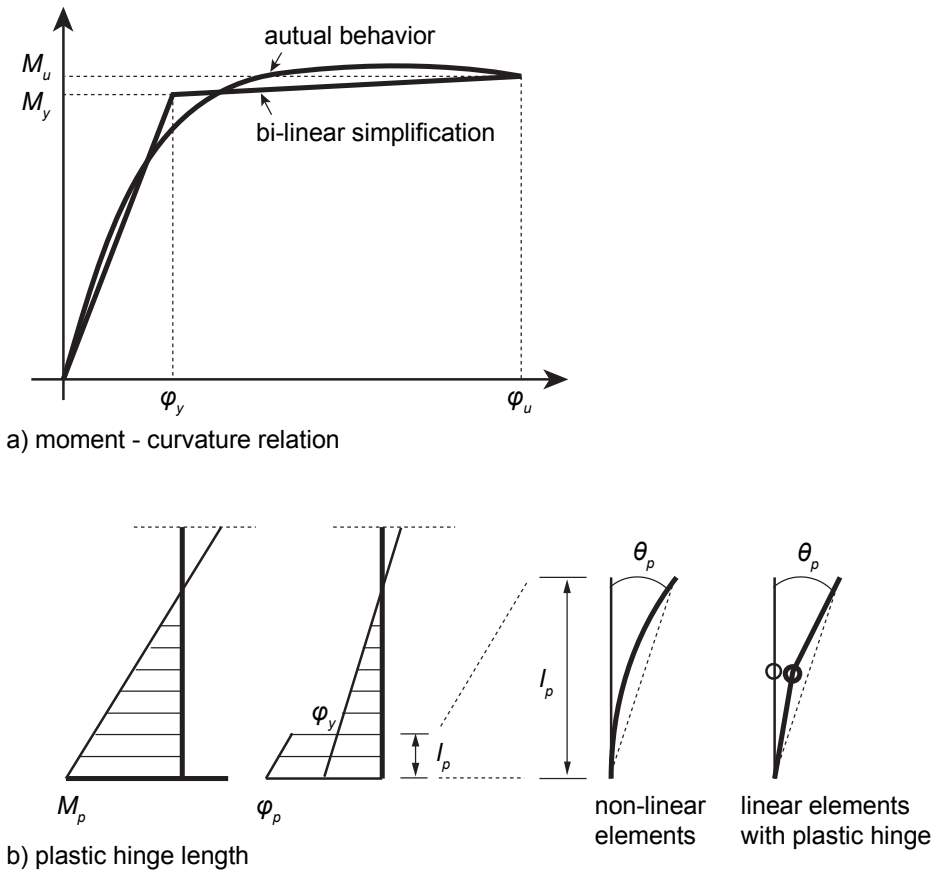

a) moment - curvature relation

b) plastic hinge length

Fig. 47 Plastic Hinge Simulation

In piers, according to Eurocode (European Committee for Standardization (CEN), 2005a), The plastic length can be calculated through Eq.(26), which is similar to Eq.(25).

$$l_p = 0.10H_p + 0.015f_y d_b \qquad (26)$$

where, H_p = the distance from the plastic hinge section to the section of zero moment.

The length of plastic hinges in piles could be estimated also through Eq.(26), since the concentrated hinge model has been adopted to derive analytical models to determine the ductility of piles in several selected limit states (Chai, 2002; Chiou et al., 2009). Besides, in a pile varies with the development of soil plasticity around the pile, the distributed hinge model uses plastic hinges within a possible zone of plasticity in the pile (Chiou et al., 2009). The plastic zone of a pile is considered to form at a certain depth L_p below the ground surface:

$$L_p = \sqrt{\frac{2(M_u - M_y)}{p}} \qquad (27)$$

where, M_y = yield moment of pile section; M_u = ultimate moment of pile section; p = lateral pressure on pile.

Once the range of L_p has been estimated, the plastic hinge length l_p can be set to a fraction of L_p for distributed plastic hinges. Generally, when the fraction is set to about 1/10, the relative error in the ultimate displacement will be acceptably small as below 0.3% based on parametric studies.

3.4.5 Proposed FEM

Consequently, based on these past and current finite element models, the models for integral abutment bridges and piles (implemented in a popular finite element analysis programmes – ANSYS and OpenSees) are proposed as shown in Fig. 48.

Main features of this type of model are:
- Beam elements (2D or 3D);

- Soil-abutment interaction: NCHRP curves;
- Soil-pile interaction: API method;
- Plastic hinges (or potential plastic hinges) in girder-abutment, pier-footing, pile-abutment.
- Pile length: full length.

According to different constructions of bridge, the girder could be supported at piers through hinges or rollers; pile and abutment are connected as hinge for semi-integral abutment bridges. More details will be demonstrated at large in following chapter of case study. Another detailed pile model will be presented in following chapter of pile design optimization.
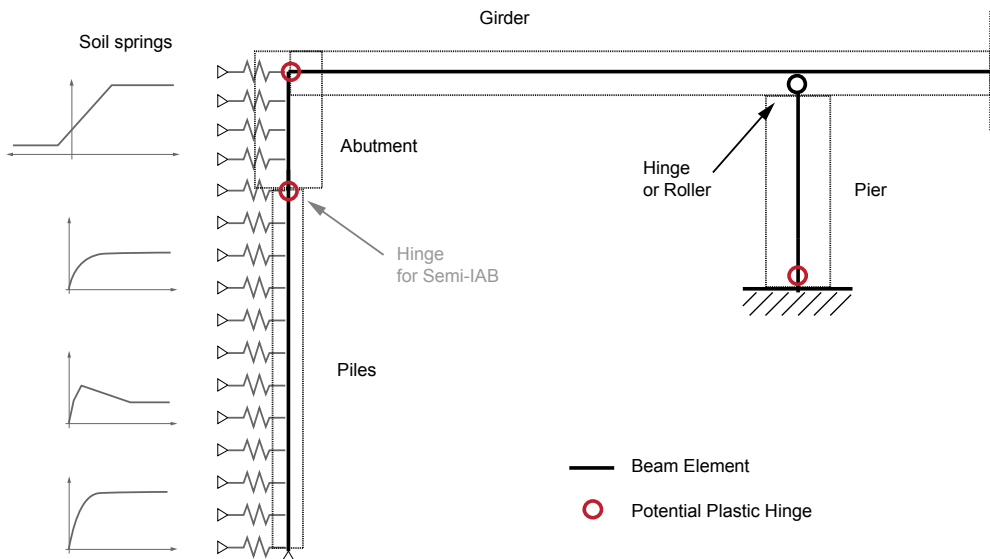
Fig. 48 Proposed Modelling of Integral Abutment Bridges

4. PERFORMANCE OF SUPER-LONG IABS: CASE STUDY

To understand well the performance of integral abutment bridges, especially super-long integral abutment bridges, the case study is going to be presented on an existing structure, including parametric analyses, pushover analyses through finite element method, and dynamic testings carried out on the bridge.

4.1. Isola della Scala Bridge

The case study presented concerns a flyover (Fig. 18), completed in 2007 and located at *Isola della Scala* in Verona, Italy. The total length of the structure, arranged on 13 spans, is approximately 400 m. To the authors' knowledge, this is currently the longest integral abutment bridge ever built.

The construction of the bridge, which began in 2001 as a simple supported flyover, was halted after 2 years because of economic problems affecting to contractor. At that time, all pre-stressed concrete girders and the main pre-fabricated elements were nevertheless purchased. In early 2006, works resumed with a new proposal that aimed to improve the quality of the structure and change the static scheme from "simply supported" to "fully integral" (Fig. 49). This goal should not inolve modifying those parts of the bridge which had already been built (Zordan & Briseghella, 2007), such as the abutments and the piers. Moreover, the new design phase should avoid an increase in the overall cost of the structure.

The main features of the bridge are given in Table 8. The elevation layout is shown in Fig. 51. Details of the typical cross section are given in Fig. 52. During this kind of "refurbishment" process, in order to achieve an IAB, eliminating all bearings and expansion joints, resistance to bending moment was attained at the pier caps with the casting of concrete diaphragms between the beams of adjacent spans at the pier tops. Hogging and sagging moment resistance was also determined with a similar technique at the abutments for the end bays. The connections between the beams of adjacent spans were carried out by casting the concrete of the diaphragms also inside the V-shaped girders for a length of 2 m (Fig. 54) (Briseghella & Zordan, 2007). The connections between the pier-caps and the transverse dia-

phragm were achieved with a segment of steel beam for every beam (Fig. 54). During construction, average air temperature remained approximately 10-15°C. The construction sequence of the transverse diaphragms started from the central part of the bridge (piers 6 and 7) and proceeded symmetrically towards the abutments.

The bridge was opened to traffic in 2007 and no mentionable damages have been noticed until now, except for some uniformly distributed cracks in the approach slabs.

Fig. 49 Isola della Scala Bridge during Construction

Fig. 50 Isola della Scala Bridge after Opening
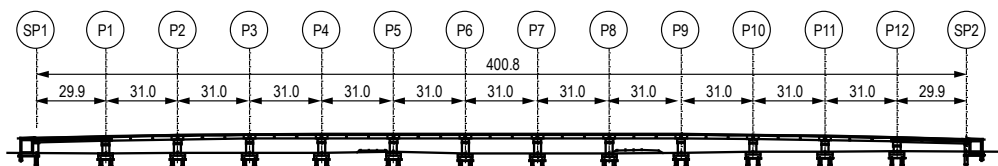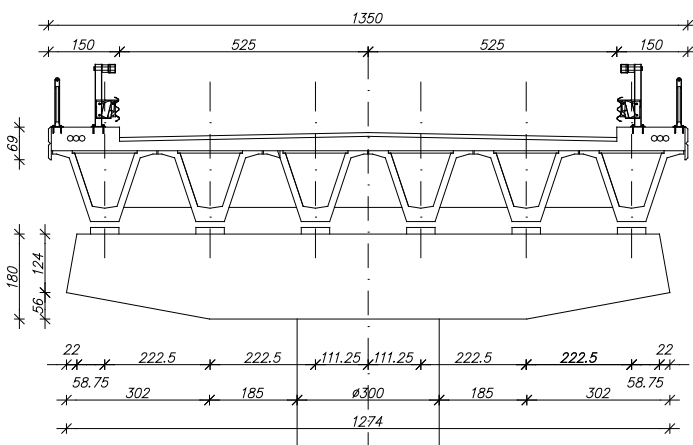

Fig. 51 Elevation Layout of Isola della Scala Bridge

Fig. 52 Typical cross section of Isola della Scala bridge [cm]

Total length	400 m
Number of the spans	13
Single span length	30 m
Static scheme: Pre-refurbishment	Simply supported
Post-refurbishment	Continuous
Number of beams per bay in the cross section	6
Deck width	13.5 m
Beams height	150 + 30 cm
Piers column diameter	3.0 m
Piers height (cap + column + footing): P1	180 cm + 377.5 cm + 250 cm
P2	180 cm + 430.0 cm + 250 cm
P3	180 cm + 461.9 cm + 250 cm
P4	180 cm + 473.5 cm + 250 cm
P5	180 cm + 473.5 cm + 250 cm
P6	180 cm + 538.5 cm + 250 cm

Table 8
Main Features of the Isola della Scala Bridge
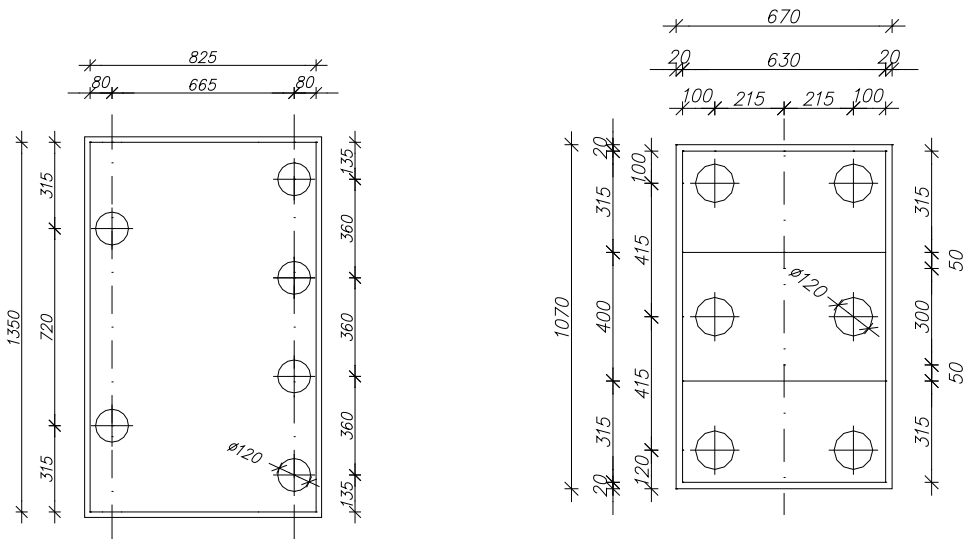
a) south abutment (symmetric in north)   b) pier footings

*Fig. 53 Plan View of Piles Arrangement at Abutments and Pier Footings [cm]*

|	beneath abutments	beneath pier footings
material	concrete C35/40	
reinforcement	30ϕ26 mm with cover of 40 mm	
type	friction	
numbers	4+2	3×2
section shape	circular solid	
diameter (m)	1.20	
length (m)	15	20

Table 9

Piles Properties of the Isola della Scala Bridge

a) existing slab was removed at the end of each girder;
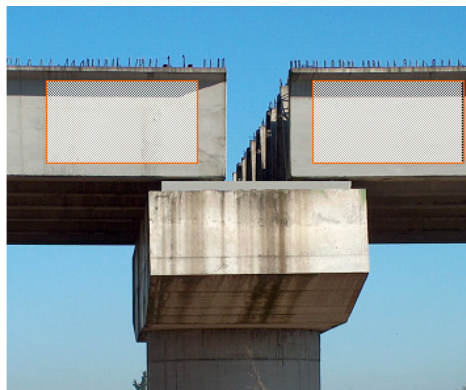
b) internal surface of the girders was prepared, concrete-to-concrete shear connectors were installed and bearings were made inactive;
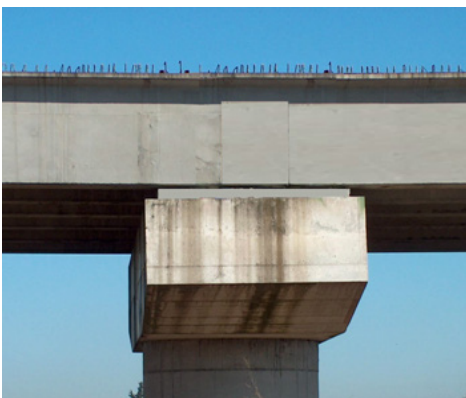
c) transverse diaphragm was poured together with the filling of the extremities of the girders;

d) new slab was concreted.

Fig. 54 Construction Phases at Pier Supports

4.2. Finite Element Model

Applying the model proposed (Fig. 48), the nonlinear finite element models of Isola della Scala Bridge were developed (Fig. 55). The results obtained from a simplified two-dimensional (2D) model, implemented with ANSYS (Fig. 56), are presented, although extensive calibration of the three-dimensional (3D) Strand 7 FEM with field data is reported elsewhere (Briseghella & Zordan, 2007). The 2D modeling is applicable for non-skew and mainly symmetrical bridges such as the one of *Isola della Scala*. The consistency of the results obtained from the 2D and 3D models were checked (Zordan et al., 2010). Further details concerning the basic features of the 2D ANSYS model are given below (Fig. 56). Only half of the bridge was modeled

due to the symmetrical configuration of the structure. The main sections are numbered in Fig. 56.
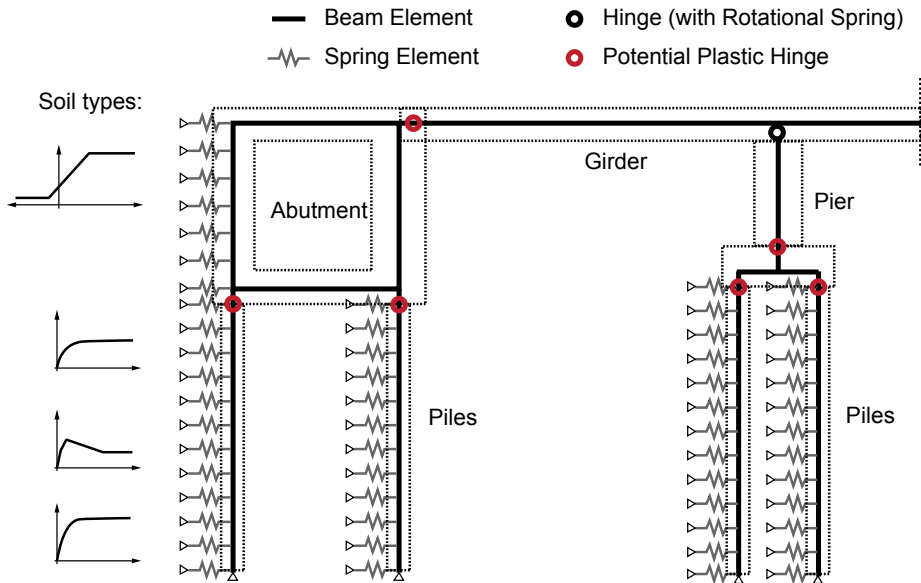

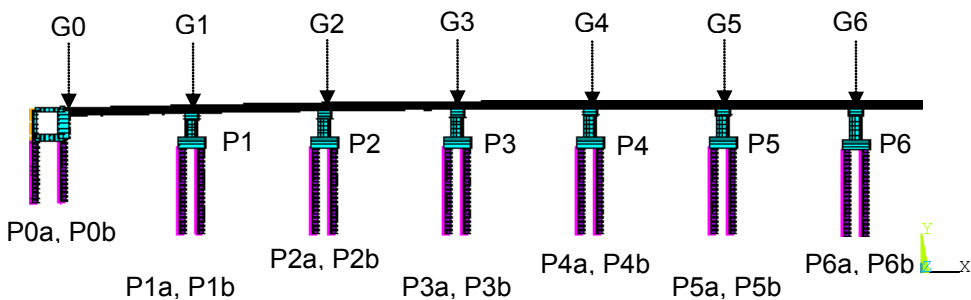Fig. 55 Model Scheme of Isola della Scala Bridge

Fig. 56 The Finite Element Model of Isola della Scala Bridge

4.2.1 Type of Elements

In the FEM implemented in ANSYS, the BEAM188 element type based on Timoshenko beam theory was used for girders, piers and abutments; the BEAM4 element was used for piles; the longitudinal and rotational COMBIN39 spring elements were used to simulate the soil-structure interactions and the plastic hinges respectively.

The potential plastic hinges are applied as rotational springs in the girder sections from G0 to G6, at the bottom of piers from P1 to P6 and at the piles from P0a,b to P6a,b (as numbered in Fig. 56). The M-φ relations of the sections calculated through sectional fiber model (subroutine of "Cumbia", developed and coded in MATLAB) (Philipps, 2010) with the applied materials properties listed in Table 10.

Concrete	C35/45		Steel	B450C
E_c	34,000 N/mm^2		E_s	200,000 N/mm^2
ε_{c2}	2‰		ε_{syd}	1.957‰
ε_{cu}	3.5‰		ε_{su}	67.5‰
f_{ck}	35 N/mm^2		f_{yk}	450 N/mm^2
R_{ck}	45 N/mm^2		f_{tk}	540 N/mm^2
f_{cd}	19.83 N/mm^2		f_{yd}	391.3 N/mm^2

Table 10
Applied Characteristics of Materials

a) girder sections   b) pier column section   c) pile section
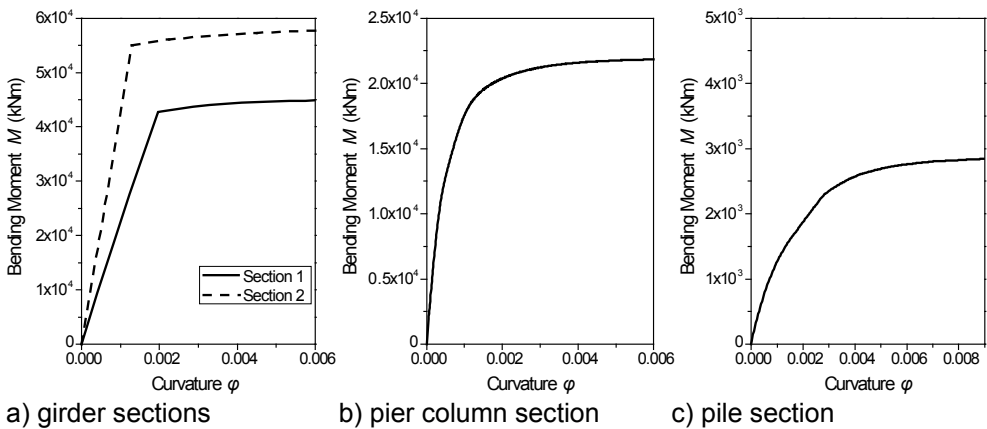*Fig. 57 M-φ Relation Curves of the Sections*

As described in finite element model proposed, the soil-structure interaction is considered in the spring elements on abutments and piles. The nonlinear soil-abutment interaction curves, calculated according to design curves presented in Ch.3.1.4 using values recommended by NCHRP and soil properties of local backfill (Table 11), are shown in Fig. 58 and applied to the nonlinear spring elements on the abutment

backwalls; the relations describing the soil-pile interaction that was composed according to API design method presented in Ch.3.2.4 and local layered soil properties (Table 12), are shown in Fig. 59 and Fig. 60, and used for the horizontal longitudinal spring elements on the piles.

Type	γ (kN/m^3)	ϕ (°)	K_0	K_a	K_p	Δ_a/H	Δ_p/H
Loose	16	30	0.50	0.33	3.0	0.004	0.04
Medium (local condition)	18.5	37	0.40	0.25	4.0	0.002	0.02
Dense	20	45	0.29	0.17	5.8	0.001	0.01

Table 11
Characteristics of Abutment Backfill Soil

Soil layer (m)	Soil properties	Loose			Medium (local soil condition)			Dense		
		γ (kN/m^3)	φ' (°)	c (kN/m^2)	γ (kN/m^3)	φ' (°)	c (kN/m^2)	γ (kN/m^3)	φ' (°)	c (kN/m^2)
0 to -2.0	Soft surface soil	16	-	-	18.5	-	-	20	-	-
-2.0 to -2.8	Sand and gravel w/o free water	16	30	-	18.5	33	-	20	40	-
-2.8 to -4.6	Sand and gravel w/ free water	10	30	-	10	33	-	10	40	-
-4.6 to -6.8	Clay w/ free water	10	-	20	10	-	26	10	-	100
-6.8 to -25.0	Sand w/ free water	10	29	-	10	30	-	10	40	-

Table 12
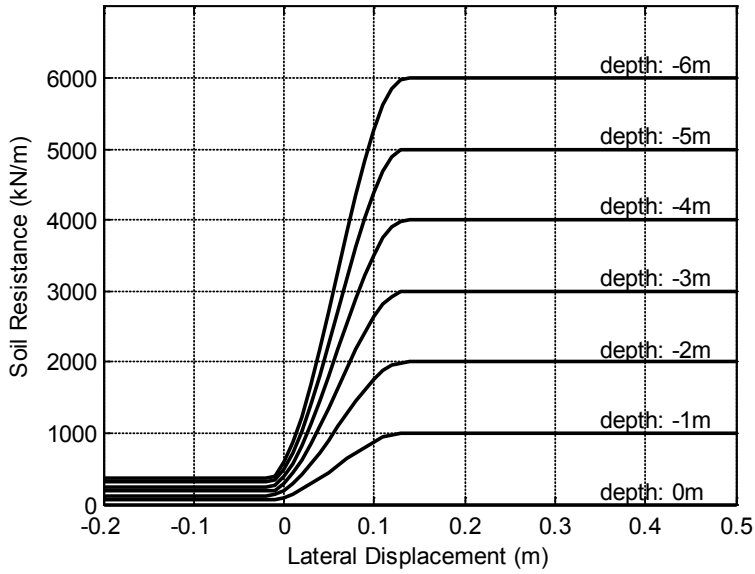Soil Properties next to Piles

Fig. 58 Force-Deflection Relations for Springs Restraining the Abutment Backwall (Medium Backfill)
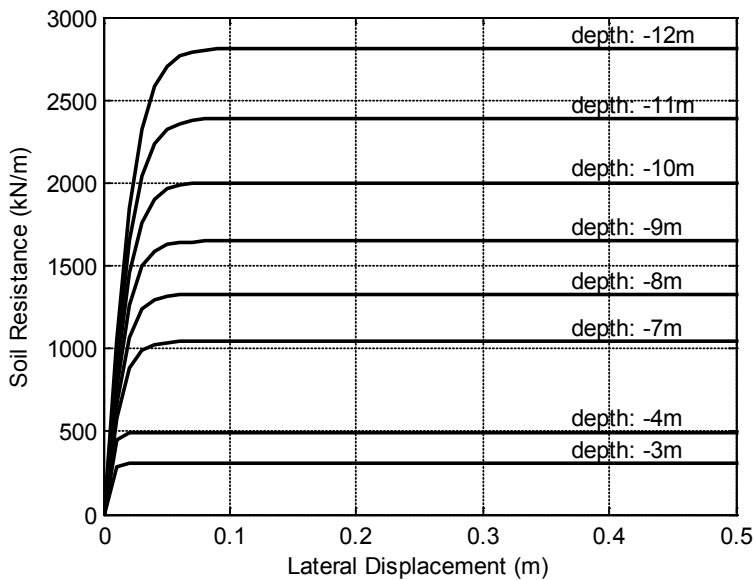

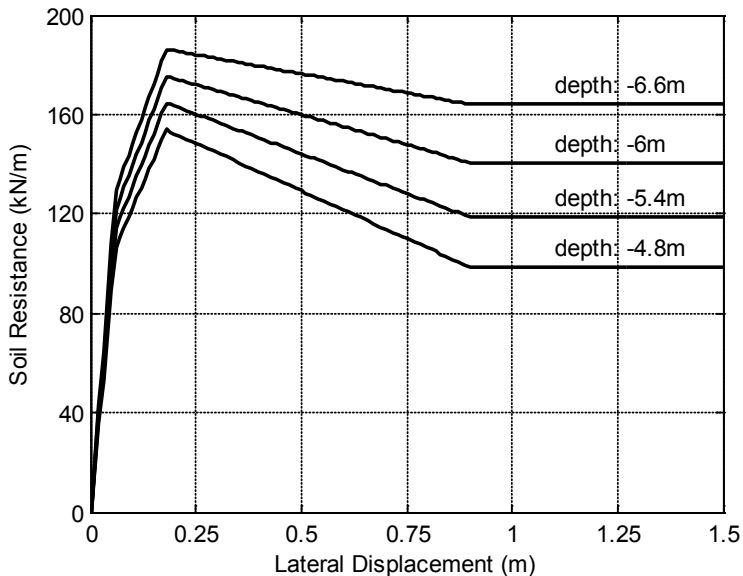Fig. 59 Force-Deflection Relations for Springs Restraining on Piles for Soil Layers of Sand (Medium)

Fig. 60 Force-Deflection Relations for Springs Restraining on Piles for Soil Layer of Clay (Medium)

4.2.2 Degree of Freedom

In order to suitably describe the static scheme of the bridge, the connection between abutment and girder - namely G0 - is considered to provide a certain amount of bending moment resistance while the girder is continuous at supports of every pier (G1-G6). It is assumed firstly that there is a pinned connection between the girder and the piers (Fig. 56), and then it is replaced by a rotational spring with certain stiffness fit through comparing to dynamic tests (c.f. Ch.4.5.5).

4.2.3 Loads and Effects

Loads applied to the FE model include dead loads, live loads and temperature loads, as specified in Eurocodes. With reference to the live loads, model LM1 (European Committee for Standardization (CEN), 2003b) is used (Table 13); uniformly distributed loads *UDL* are considered on every span. A tandem load distribution *TS* was applied to the central span only. According to Eurocodes, dead and live loads are multiplied respectively by a factor of 1.35 and 1.50. The action of temperature variations, including the "uniform temperature component" and the "vertical

temperature difference component" (Table 14), is combined with a multiplying factor of 1.00.

Location	Tandem system TS	UDL system
	Axle loads Q_{ik} (kN)	q_{ik} (kN/m^2)
Lane Number 1	300	9
Lane Number 2	200	2.5
Lane Number 3	100	2.5
Other lanes	0	2.5
Remaining area (q_{rk})	0	2.5

Table 13

Applied Load Model Characteristic Values (according to Eurocode)

	Uniform Temperature Component ΔT_N (°C)	Vertical Temperature Difference Component ΔT_M (°C)	ω_M	Combination
Top warmer than bottom	-20 to +20	10	0.75	$\omega_M \Delta T_M + \Delta T_N$
Bottom warmer than top	-20 to +20	5	0.75	$\omega_M \Delta T_M + \Delta T_N$

Table 14

Applied Simultaneity of Uniform and Temperature Difference Component (according to Eurocode)

Construction phases were carefully planned and checked with reference to the air temperature in order to minimize the horizontal imposed deflection. Joints were cast accordingly to this requirement.

The numerical model should include soil-pile interaction, soil-abutment interaction and construction joint behavior under temperature fluctuation, temperature gradient, time-dependent effects and backfill pressure (Kim & Laman, 2010). The time-dependent effects causing the accumulation of abutment displacements at the ends of the bridge are generally relevant in the first 3 years after the bridge's construc-

tion. They continue for approximately 30 years and thereafter dissipate (Pugasap et al., 2009). The increase in the overall length of the bridge proves to significantly limit this effect already for short span integral abutment bridges; this is shown already when comparing the lengths ranging from approximately 20 to 54 m. Hence, for the purpose of this paper, this kind of effect was neglected and a bridge was considering having an overall length of approximately 400 m.

The shrinkage effect on the bridge deck was not considered because of the construction sequence, which was carefully planned by using a construction that is able to limit this effect. It is known that the older the girders when the bridge is erected, the greater the reduction in long-term abutment displacements. For the case presented, creep effect was neglected in the analysis because the pre-fabricated girders were purchased 5 years before the time of final construction, as specified in Ch.4.1.

## 4.3. Study of Parametric Analysis

4.3.1 Analysis on Temperature Variations

In continuous girder bridges, the presence of large amount of hogging moment at supports can potentially lead to extended cracked areas in the concrete structure. In this study, a reduction of 50% in the elastic modulus of the concrete only in the slab part of the girder was considered in cracked areas. And, considering the local soil conditions of "Medium" properties of the soil (Table 11 and Table 12), the parametric analysis was carried out on temperature variations from -20°C to +20°C at the interval of 5°C for the superstructure (Fig. 61).

For the girder sections, axial forces, bending moments and horizontal displacements caused by temperature variations display a roughly linear behaviour. This is not the case of the bending moment variations in G0 caused by the asymmetrical reaction during expansion and contraction of the soil behind the abutment. Furthermore, P1 section seems to be at the beginning of the plastic region. Sections P0a and P0b of the piles beneath the abutment (Fig. 61) display the largest amount of bending moments and displacements.

Therefore, in the following parametric analyses, only sections G0, G6, P1 and P0a will be considered. The layout of this bridge, with a high concentration of stiffness at
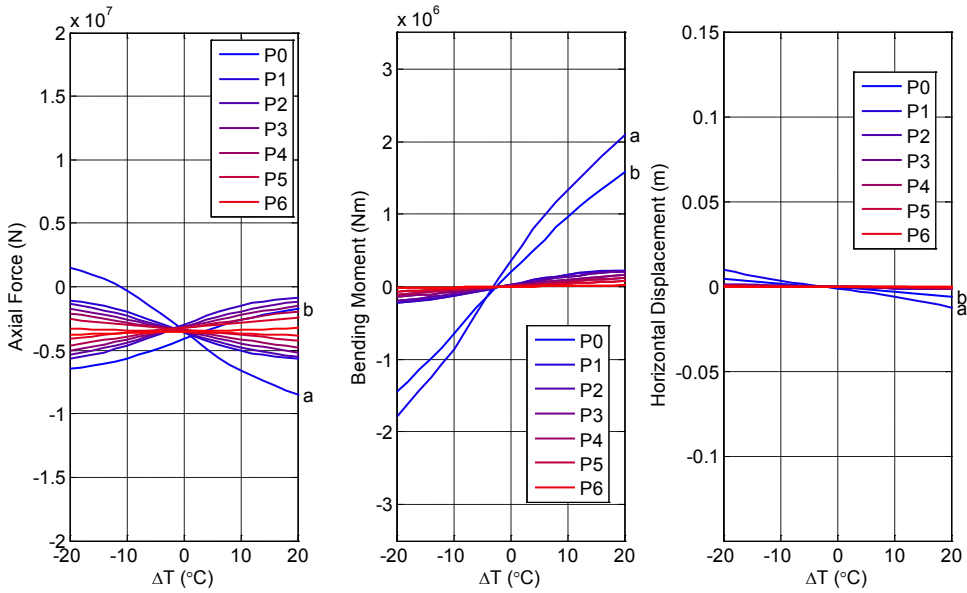
the abutments, is characterized by a remarkable presence of bending moment at the ends of the structure. This aspect needs to be thoroughly investigated and represents one of the key factors influencing the structural response.
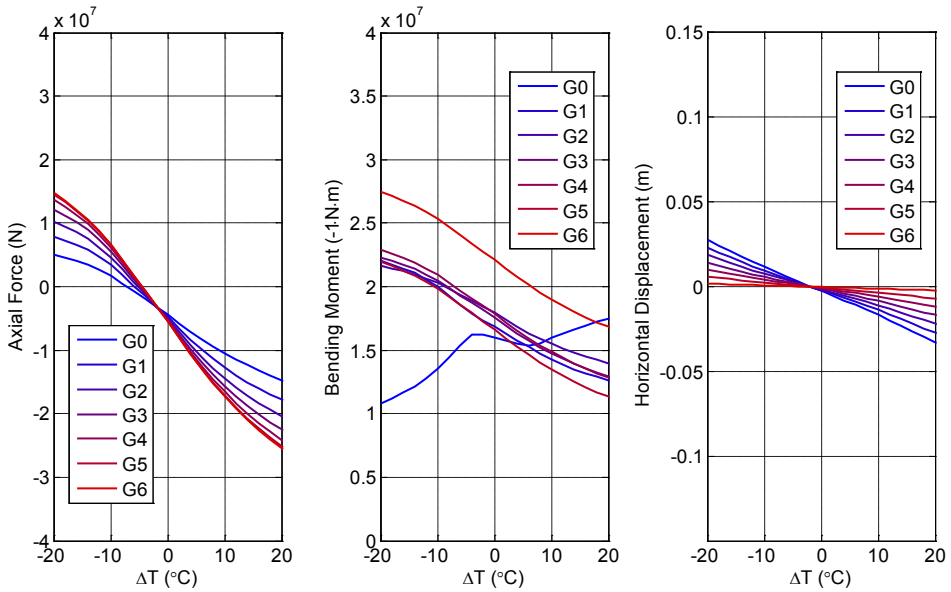
a) girder sections in negative bending areas
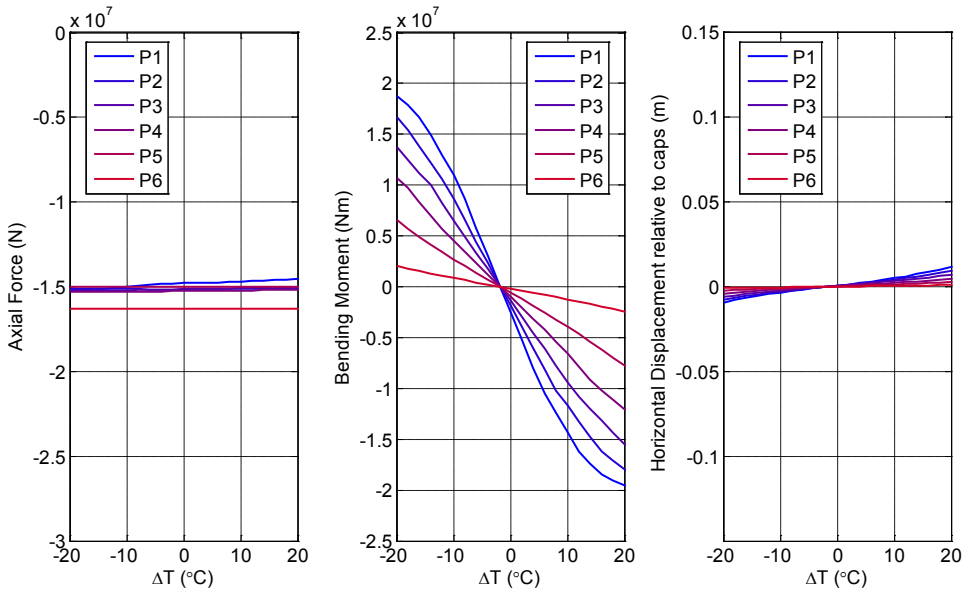
b) bottom sections of piers

c) top sections of piles

Fig. 61 Analysis Results for "Medium" Soil Properties

4.3.2 Variation of Soil Properties

Soil properties were varied behind the abutment backwall and in the zones adjacent to the piles resulting in three combination sets, named "Loose", "Medium" and "Dense".

As already mentioned, the "Medium" soil properties (Table 11) represent the design values derived from on-site soil penetration tests. From this starting point, depending on the range of suggested values presented in the literatures (Evans, 1982; Barker et al., 1991; Bowles, 1996; American Petroleum Institute, 2000), the property sets for "Loose" and "Dense" soils listed in Table 11 and Table 12 were used for the parametric analysis.

4.3.3 Internal Forces and Displacements

For maximum and minimum design temperatures, the results of parametric analyses considering the variation of the soil properties in terms of axial force and bending moment distribution along the girder are plotted in Fig. 62 and Fig. 63. It can be

observed that: 1) the bending moment distribution next to abutments (G0) for upper and lower temperatures displays a remarkable variation while a reduced variability is recorded at the other supports. Hence, in the case of stiff abutments, like the ones characterizing this bridge, the soil properties have a sizeable influence on the bending moment closer to the stiffer zones of the structure while they have a lower influence in the other parts; 2) the distribution of axial force along the girder displays a more regular and smooth variation for different soil properties.

From the results of the critical sections G0, G6, P1 and P0a shown in Fig. 63, we can say that: 1) axial forces, bending moments and horizontal displacements vary regularly and almost linearly with the temperature fluctuations; the axial forces show the most significant changes; 2) the changes of soil properties have almost no effect on the pier response; 3) in the piles beneath the abutment, the axial forces and displacements are greatly affected by varied soil properties while bending moments are affected less.

According to the results found above, the axial forces in girder and piles are remarkably influenced by positive and negative temperature variations which are key-parameters for the assessment of the bridge response. The different soil conditions have a great influence on the bending moment near abutments and axial force along the girder: this is more notable for negative temperature variations than for positive ones and is caused by the different reactions of the soil behind the abutment due to passive and active pressures and according to different load combinations.

In real cases, the temperature variation sometimes could exceed the range imposed by the codes for the structural checks. Therefore, to study the real behavior of the bridge and assess its level of safety together with the failure pattern, a push-over analysis referred to the bending moment-axial force resistance domain of the critical sections was carried out, as presented below.
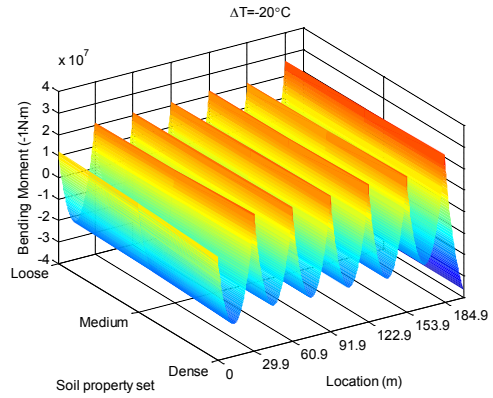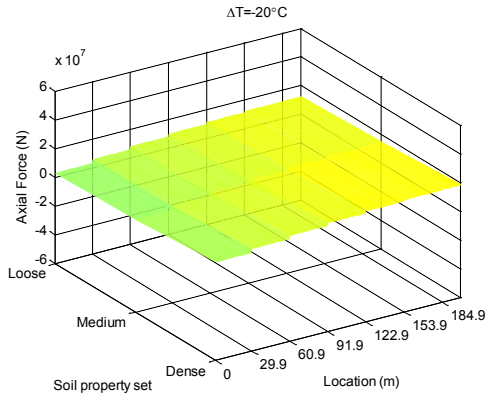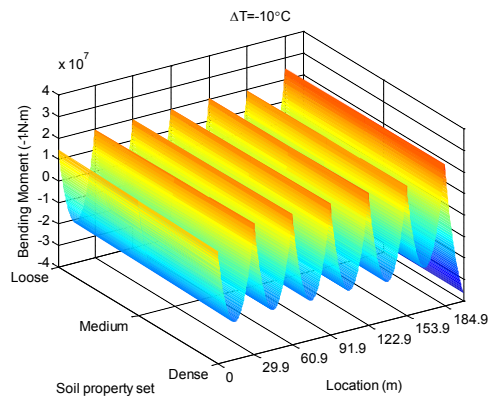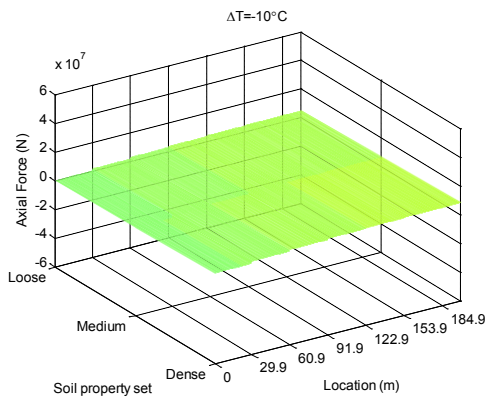
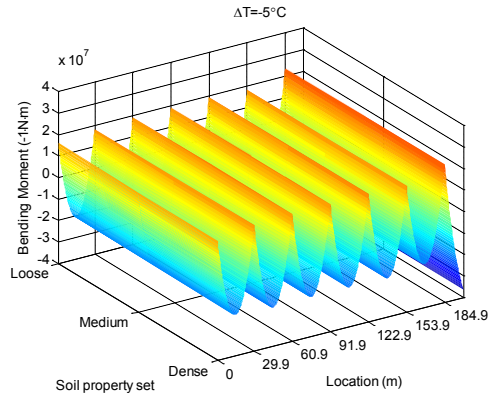a) temperature variation of -20°C
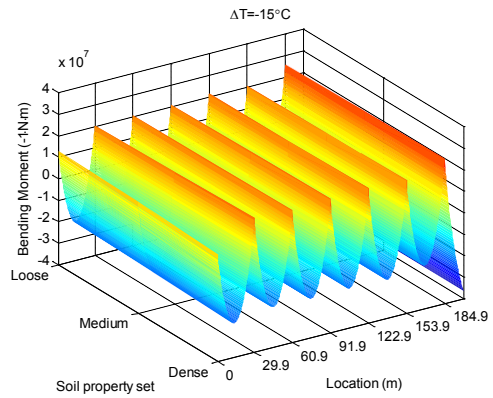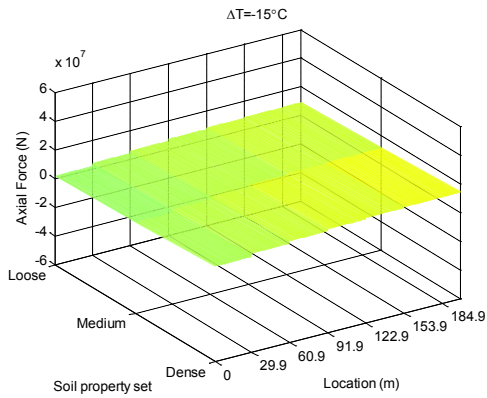
b) temperature variation of -15°C

c) temperature variation of -10°C

d) temperature variation of -5°C
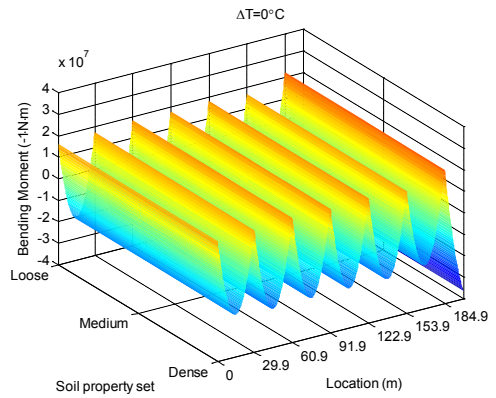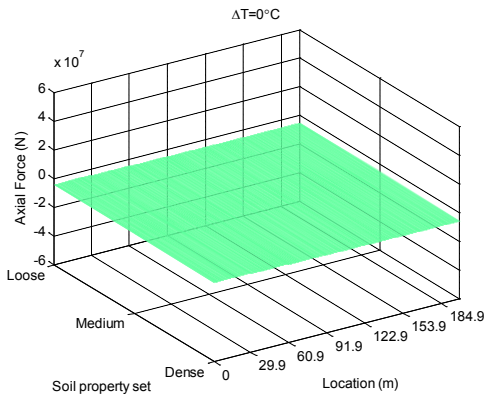
e) temperature variation of 0°C
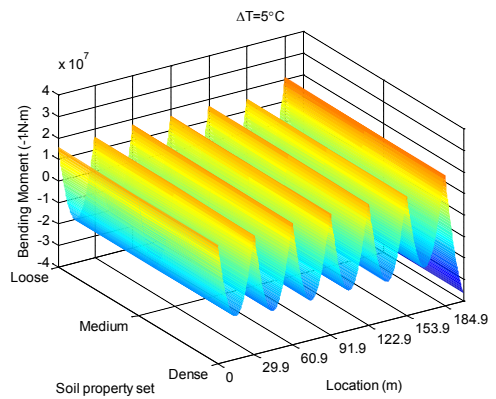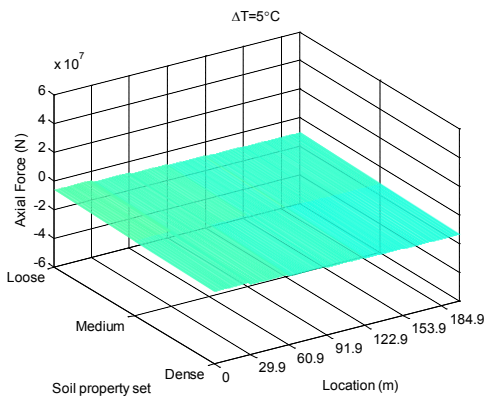
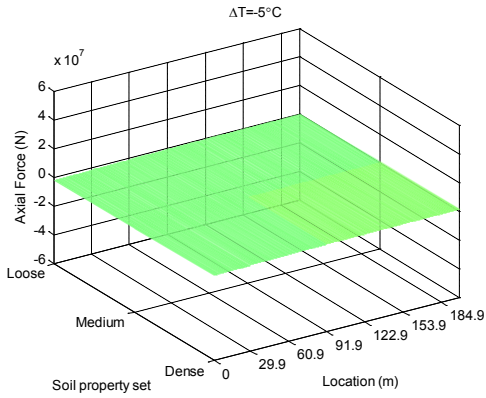f) temperature variation of +5°C
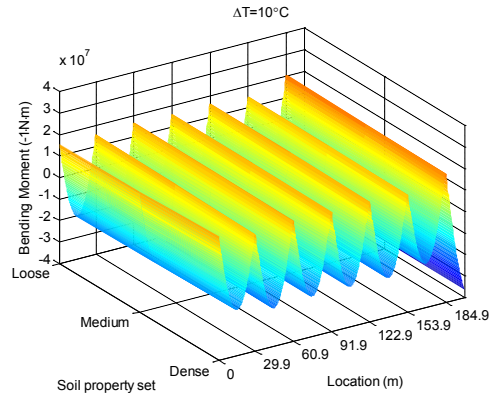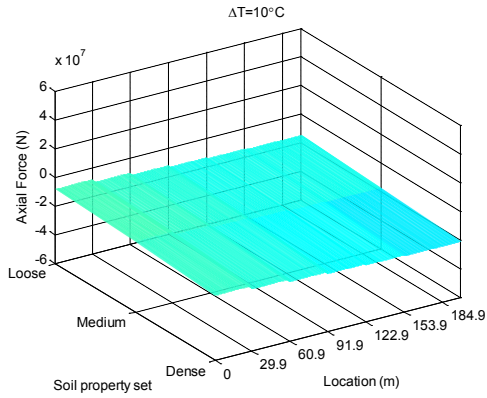
h) temperature variation of +10°C
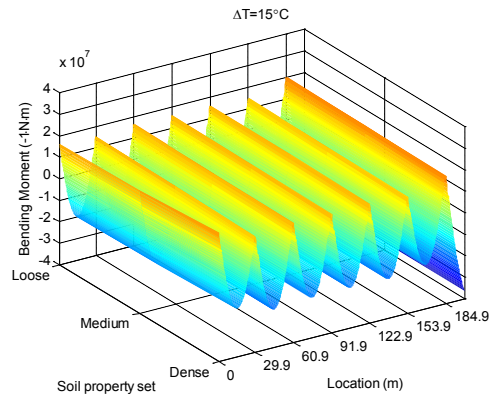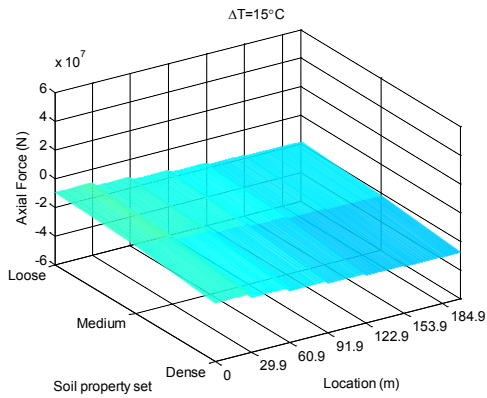
i) temperature variation of +15°C
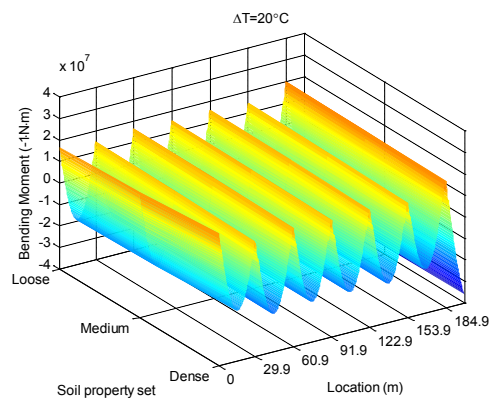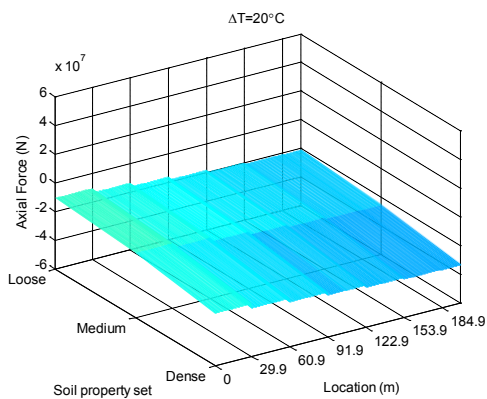
j) temperature variation of +20°C

Fig. 62 Parametric Analysis Results – Axial Forces and Bending Moments of Girder
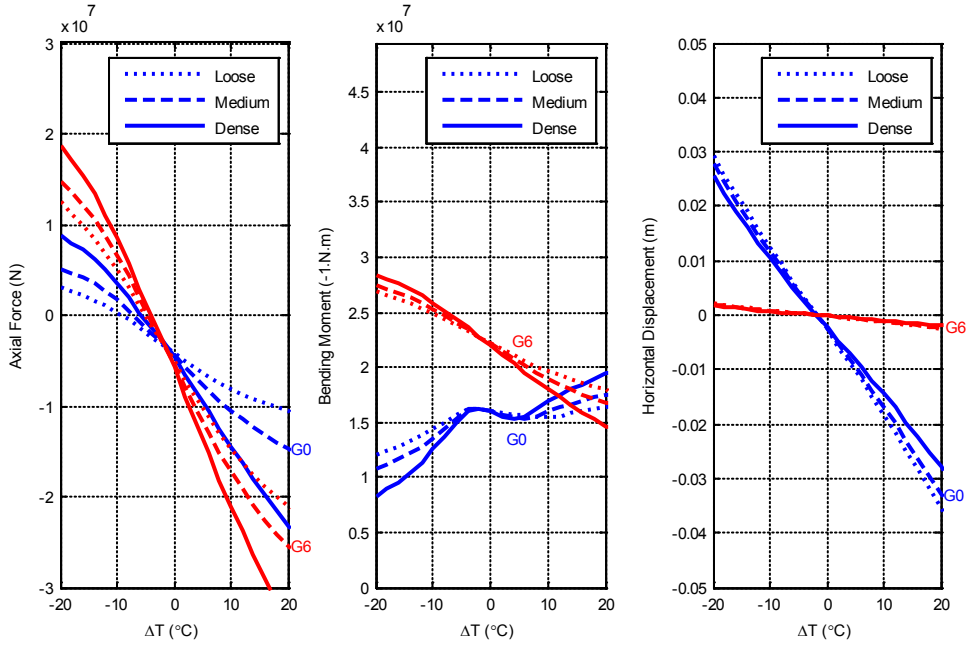
a) sections G0 (blue) and G6 (red) of the girder
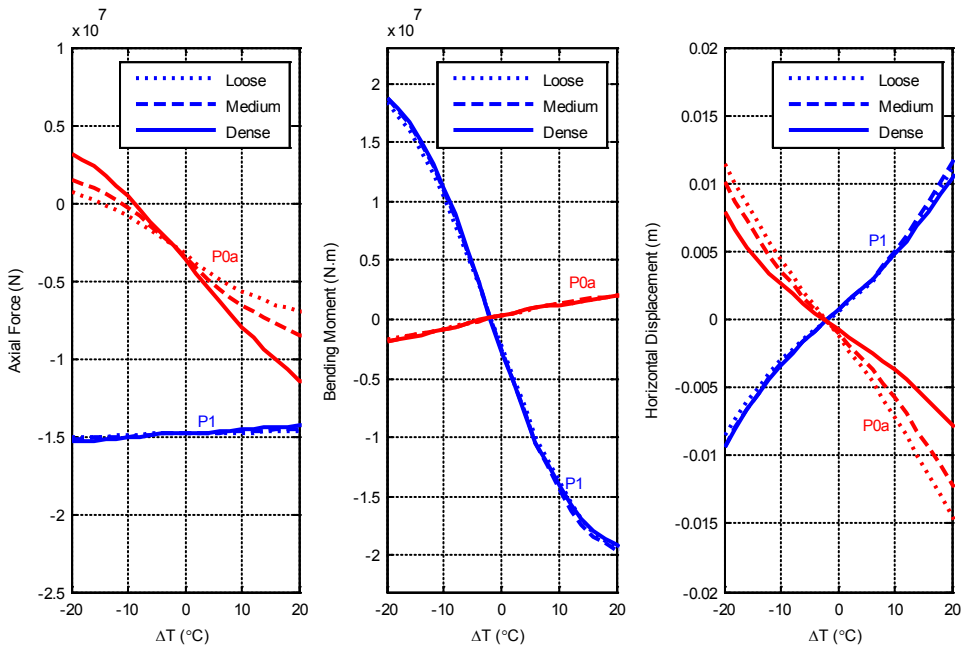
b) sections P1 (blue) of pier and P0a (red) of pile

Fig. 63 Parametric Analysis Results of Concerning Sections

4.4. Study of Pushover Analysis

According to the results presented in Fig. 63, pier section P1 begins to enter the plastic region when the temperature variation exceeds the range of ±20°C. At this stage, the axial forces in the girder and in the piles beneath the abutment start to change remarkably, with potential consequences in the resistance of these elements.

To investigate the failure pattern of the structure caused by temperature variations, a temperature pushover analysis is carried out in the following. The safety of the bridge is assessed with reference to a minimum and a maximum temperature values, and the distance from the critical temperatures causing the failure of the structure is determined both for positive and negative temperature variations.

In order to find the formation sequence of successive plastic hinges, this non-linear incremental temperature analysis was carried out with reference to the M-N domains (axial force N and bending moment M resistances interaction diagram) formerly determined and calculated with the usual hypothesis based on the conditions of equilibrium. The results presented in the following refer to the soil type defined as "Medium", as this soil condition is the real one for the bridge.
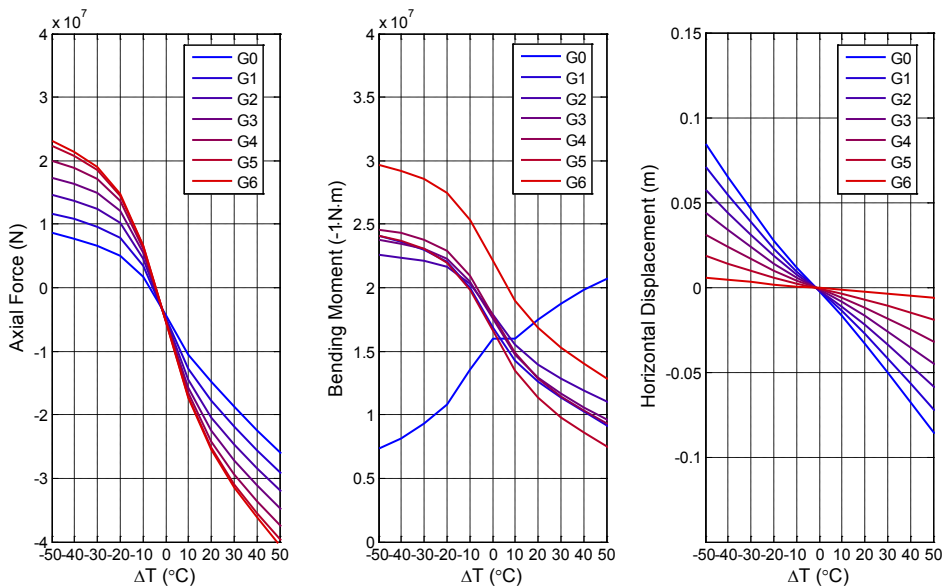
a) girder sections in negative bending areas
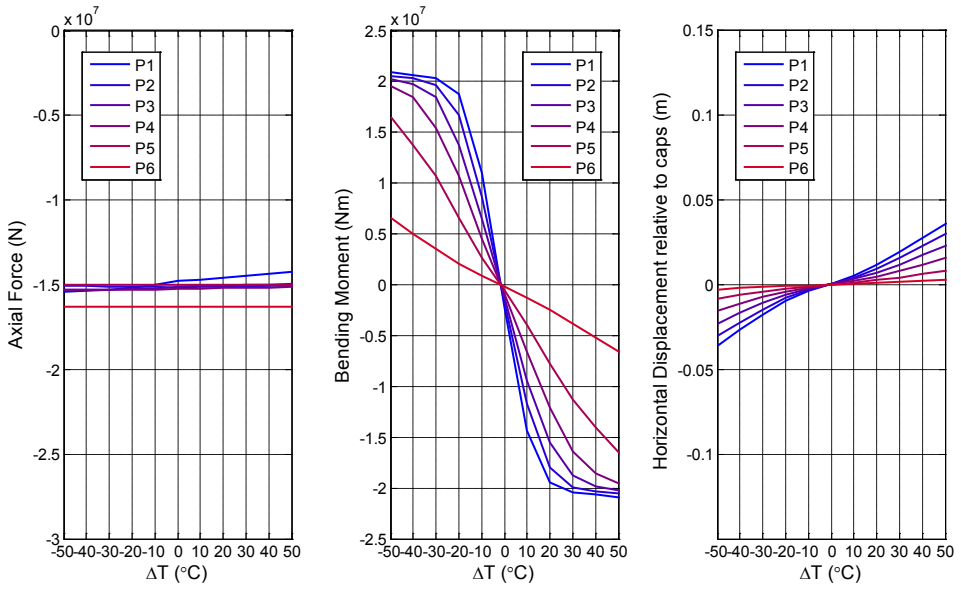
b) bottom sections of piers
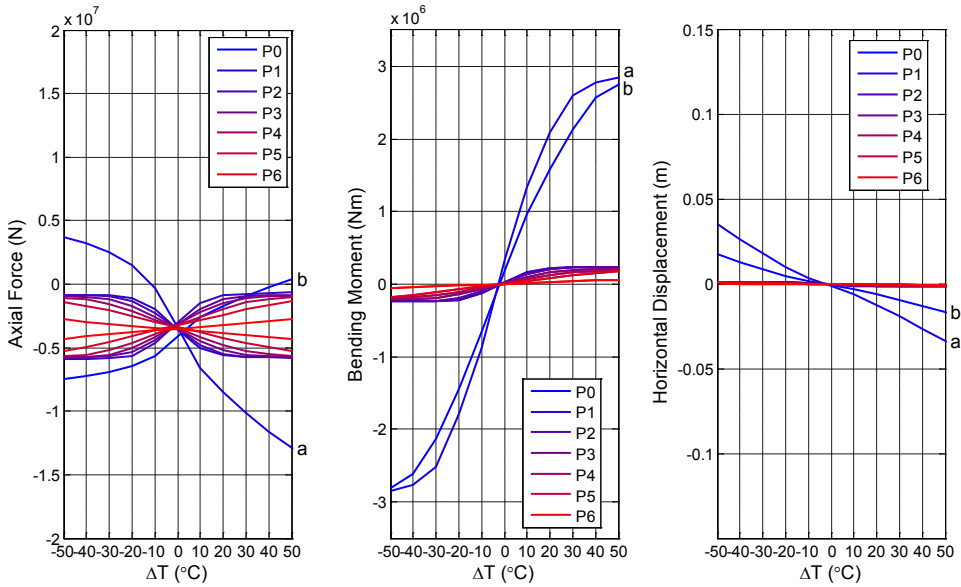
c) top sections of piles

Fig. 64 Pushover Analysis Results of Concerning Sections

The results of the pushover analysis in terms of bending moment for the girder and the piers are shown in Fig. 64. Analyses were carried out for a temperature variation of ±40°C, which is considered already way beyond the limits of real cases. It could be found out that: 1) the bending moment distribution in the girder remains within a limited range without exceeding – not even for section G0 – the cross section resistance (Fig. 65) while the axial force distribution shows a remarkable variation; 2) although the axial forces in piers still change very slightly, from the bending moment curves it can be seen that the critical sections of the piers have entered the plastic regions progressively from P1 to P6 as the temperature reaches higher or lower values; 3) both axial forces and bending moments in the piles beneath the piers display limited changes; on the contrary, the piles beneath the abutment reach their elastic bending resistance at approximately ±40°C.

4.4.1 Moment-Force Interaction Diagram

Since the axial force distribution in the girders and in the piles beneath the abutment is remarkably affected by the temperature variation, these critical sections are checked with reference of their M-N resistance domains in a wider temperature variation than the one prescribed by the codes. It can be observed that (Fig. 65): 1) in the girder, section G6 is the first section to exceed the limits of the M-N domain at a temperature of -60°C; 2) the M-N curves of the piles beneath the abutment exceed the domains respectively at ±20°C. Both values are out of the range prescribed by the codes.
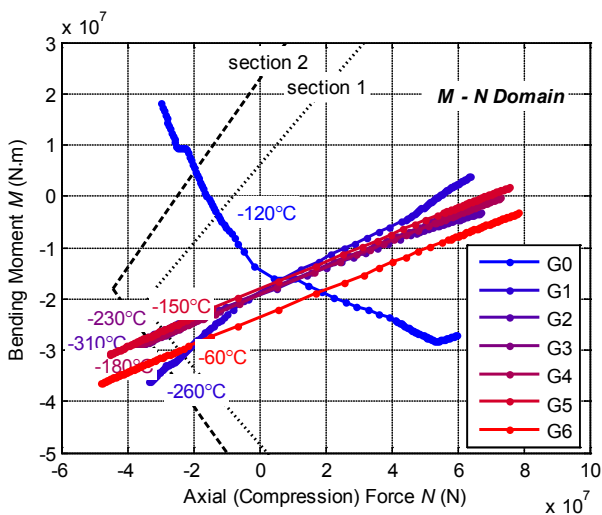
a) girder sections
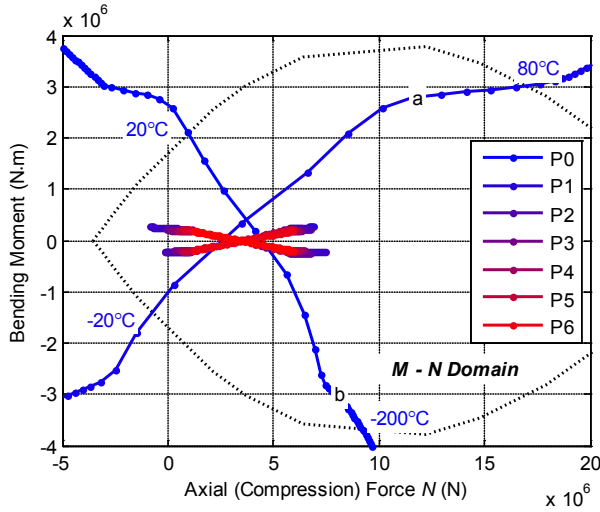
b) pile head sections

Fig. 65 Pushover Analysis Results of Girder and Pile in M-N domain

4.4.2 Failure Patterns

Considering the ultimate rotation capacities of critical sections on the basis of their M-φ relations, in the pushover analysis the rotations of these sections were checked according to the limits prescribed by Eurocodes (European Committee for Standardization (CEN), 2005a; European Committee for Standardization (CEN), 2005b) (Fig. 19).
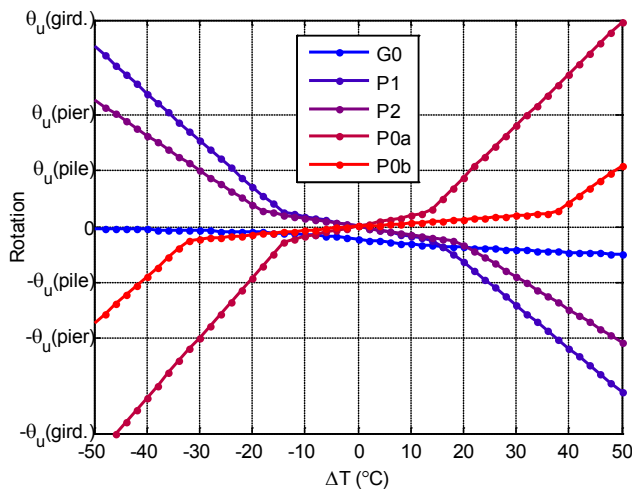
Fig. 66 Ultimate Rotation Checking of the Critical Sections

From the results obtained, assuming that, for the girder and pile sections, the initial M-φ relations are only slightly affected by the variation of the axial force, the sequence of the formation of the plastic hinges for a temperature variation up to ±40°C is shown in Table 15 and Table 16.
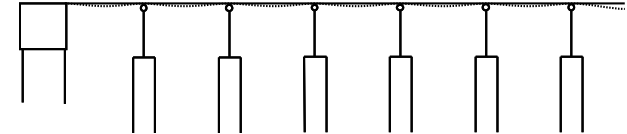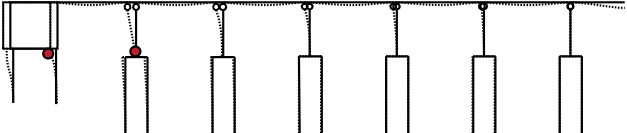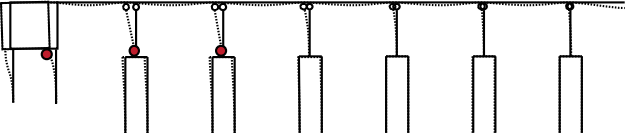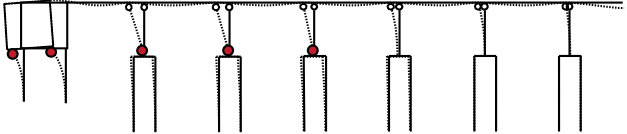
ΔT (°C)	total horizontal expansion (m)	New plastic hinge(s) position	Schematic of deformation
0	0.0025	-	
+20	0.0328	P1, P0b	
+30	0.0499	P2	
+40	0.0675	P3, P0a	

Table 15
Process of Plastic Hinges Formation in Positive Temperature Variations
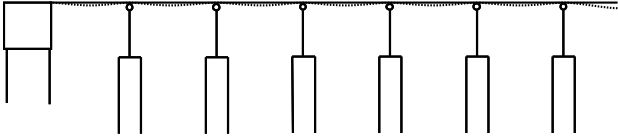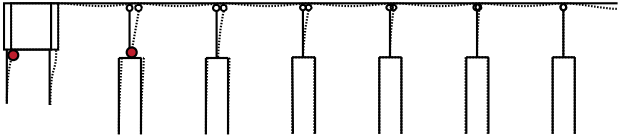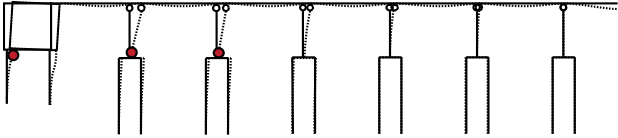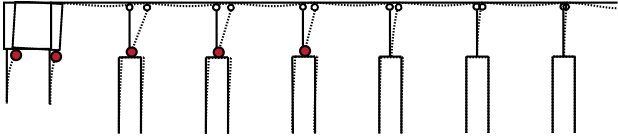
ΔT (°C)	total horizontal contrac- tion (m)	New plastic hinge(s) position	Schematic of deformation
0	0.0025	-	
-20	0.0280	P1, P0a	
-30	0.0462	P2	
-40	0.0645	P3, P0b	

Table 16
Process of Plastic Hinges Formation in Negative Temperature Variations

4.4.3 Effect of Abutment Stiffness

Abutment stiffness has a sizeable effect on the distribution of internal forces and re-actions. The IAB considered in this study is characterized by rigid abutments. Thus, large forces are channeled into these elements, which are not in accordance with the literature for the most suitable design of this kind of structure but derives from the initial condition of the partially built bridge at the beginning of the refurbishment phase that led to its transformation into an IAB.

To assess the effect of the abutment stiffness on the distribution of the reaction forces, a temperature pushover analysis simulating the presence of flexible abut-ments was repeated on the FE model of bridge replacing the real abutments with

abutments characterized by the same stiffness and the same static scheme of the piers. For this case, the results are shown in Fig. 67.

For a positive temperature variation, due to the formation of a plastic hinge in the new slender abutment at a temperature level of about +30°C, force and displacement levels of the piles beneath the abutment maintain almost the same magnitude for higher variations. The same situation could be found for the girder section G0.

For negative temperature variations, the process of plastic hinge formation is similar to that found in the original pushover analysis, except for that which regards the early formation of plastic hinges in girder section G0 and in the piles beneath the abutment for temperatures ranging from -30°C to -40°C.

On the basis of the analyses carried out, it can be said that: 1) bridges characterized by slender and flexible piers respond more uniformly and predictably to temperature variations; 2) flexible abutments or pin connections between girder and abutments should be considered the preferred solution; these options did not apply to the case presented for the reasons outlined on structural converting during construction; and 3) negative temperature variations need to be considered with the utmost attention.
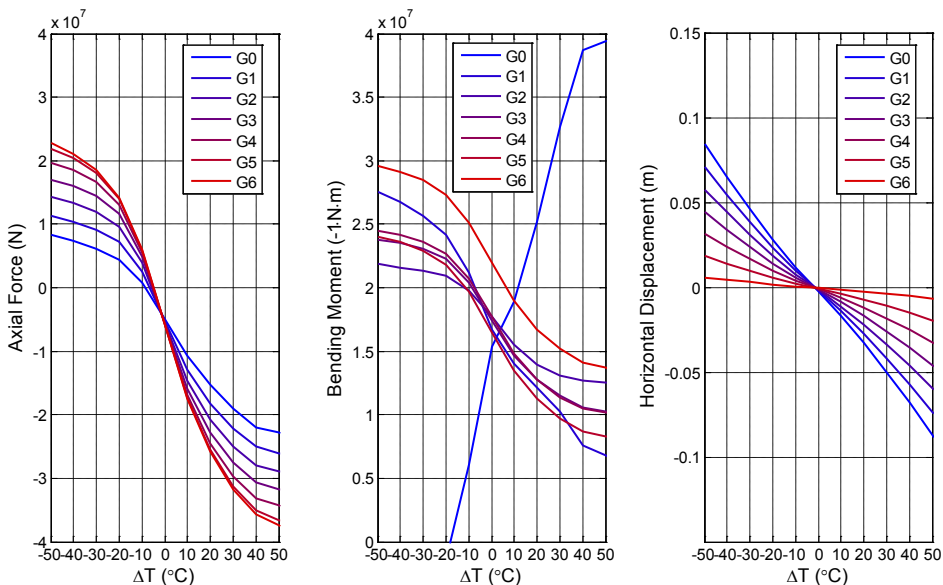
a) girder sections in negative bending areas
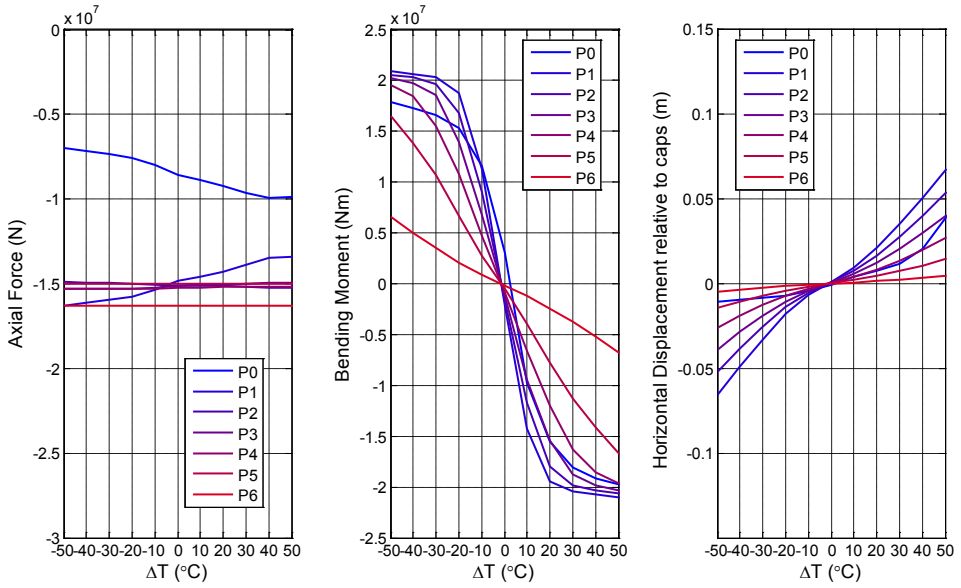
b) sectional forces of piers (P1 to P6) and the flexible abutment (P0)
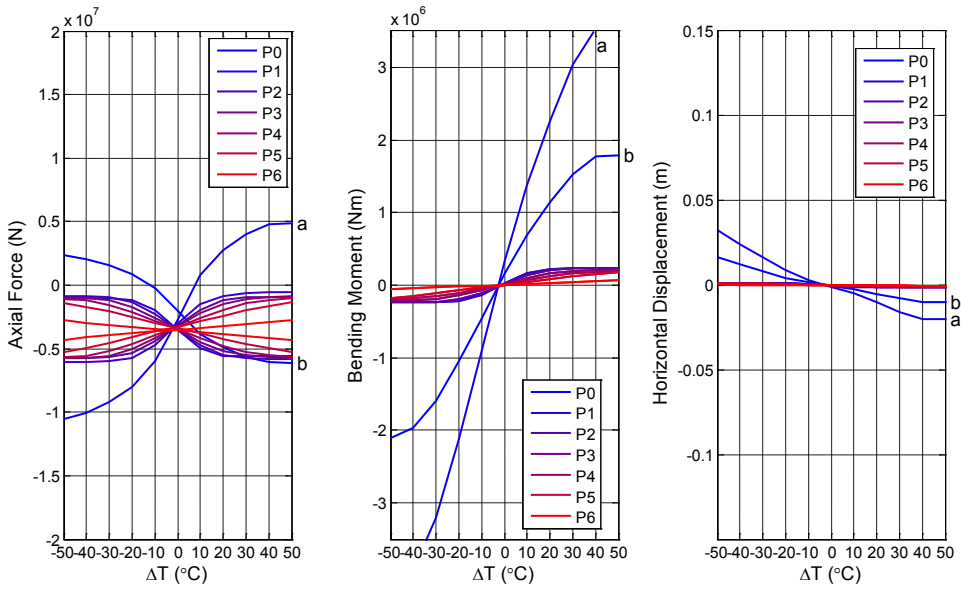
c) top sections of piles
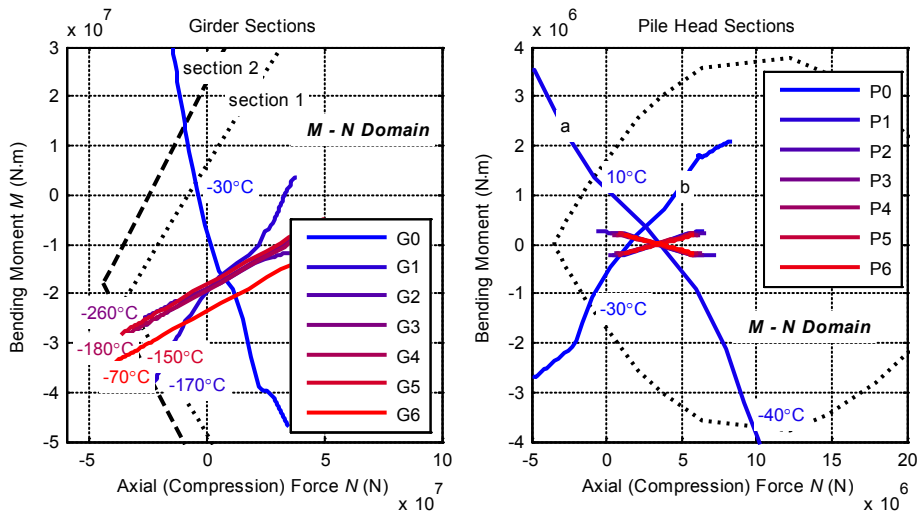
d) results of girder and pile in M-N domains

Fig. 67 Pushover Results of the Model with Flexible Abutment

4.4.4 Conclusions on Analyses

On the basis of the analyses carried out, both parametric and pushover analyses, performance of this integral abutment bridge could be drawn into:

1. The axial forces in the girders and piles are greatly influenced by positive and negative temperature variations, which are key parameters for assessing the bridge's response. The different soil conditions greatly affect the bending moment near abutments and axial force along the girder: this is more evident for negative temperature variations than for positive ones and is caused by the different reactions of the soil behind the abutment due to passive and active pressures and according to different load combinations.

2. The response of the bridge in terms of internal force distribution, at abutments and in the end parts of the structure, is greatly influenced by significant temperature variations. Nevertheless these seem not to remarkably the other parts of the bridge, where a stable situation is recorded.

3. Bridges characterized by slender and flexible piers respond more uniformly and predictably to temperature variations; flexible abutments or pin connections be-

tween girder and abutments should be considered as the preferred solution, even if these options were not applicable to the case presented for the reasons mentioned.

4. Negative temperature variations need to be considered with the utmost attention. The design of an integral abutment bridge should be based on the evaluation of a range of possible solutions instead of being focused on a single result. Therefore, a parametric analysis on a set of starting data should be performed. The case presented demonstrates the feasibility of transforming existing Simply Supported Structures into IABs, thus ensuring extended design life and reducing maintenance costs into the future. To the authors' knowledge, although 400 m is the longest IAB built so far, the results obtained have demonstrated that super-long integral abutment bridges can be constructed.

4.5. Ambient Dynamic Testing

The development of reliable analytical dynamic models is a crucial aspect of major importance in terms of the study of the dynamic response and of the health condition of both new and existing large span bridges under traffic, wind or seismic loads. Although sophisticated finite element codes are currently available for that purpose, the success of their application is strongly dependent on the possibility of experimental verification of the results. An appropriate experimental calibration and validation of such analytical models, so that they can reflect correctly the structural properties and the boundary conditions, involves the experimental identification of the most significant modal parameters of the structure (natural frequencies, mode shapes and modal damping factors), and their correlation with the corresponding calculated values.

4.5.1 Dynamic Testing and Operational Modal Analysis

For bridges that cannot be taken out of service, traffic loading is the primary method for exciting the structure. Many times traffic excitation is coupled with other ambient excitation sources such as wind. With traffic excitation the assumption is often made that the ambient vibration source is a white noise random process. Turner and Pretlove (Turner & Pretlove, 1988) state that this assumption is based on the random arrival times of individual vehicles; the random nature of the vehicles' suspension systems; and the randomly distributed road surface irregularities. Depending on the coupling between torsional and lateral modes, traffic excitation has the

limitation that it may not sufficiently excite the lateral modes of a bridge and these modes are often of interest, particularly in seismic studies.

After tests, the operational modal analysis (i.e. the identification of modal parameters from output-only time-histories data) will be carried out using the Frequency Domain Decomposition (FDD) method (Brincker et al., 2000; Brincker et al., 2001), implemented in the ARTeMIS software. The FDD technique involves the following main steps:

> 1) evaluation of the spectral matrix $\mathbf{G}(f)$, i.e. the matrix where the diagonal terms are the autospectral densities (ASD) while the other terms are the cross-spectral densities (CSD). In the present application, the ASDs and the CSDs are estimated, after decimating the data.

> 2) singular value decomposition (SVD) of the matrix $\mathbf{G}(f)$ at each frequency, according to:

$$\mathbf{G}(f) = \mathbf{U}(f)\mathbf{\Sigma}\mathbf{U}^H(f) \tag{28}$$

> where the diagonal matrix $\mathbf{\Sigma}$ collects the real positive singular values in descending order, $\mathbf{U}$ is a complex matrix containing the singular vectors as columns and the superscript H denotes complex conjugate matrix transpose;

> 3) inspection of the curves representing the singular values to identify the resonant frequencies and estimate the corresponding mode shape using the information contained in the singular vectors of the SVD.

The principle in the FDD techniques is easily understood by recalling that any response can be written in modal co-ordinates and that the spectral matrix of a linear dynamic system subjected to a white-noise random excitation may be expressed as:

$$\mathbf{G}(f) = \phi\mathbf{G}_{qq}\phi^H(f) \tag{29}$$

where Φ is the matrix of mode shapes and $\mathbf{G}_{qq}(f)$ is the spectral matrix of the modal co-ordinates. Since the modal co-ordinates are un-correlated, the matrix $\mathbf{G}_{qq}(f)$ is diagonal; hence, if the mode shapes are orthogonal, it is a SVD of the response spectral matrix. As a consequence, if only one mode is important at a given fre-

quency f_r, as it has to be expected for well-separated modes, the spectral matrix can be approximated by a rank-one matrix:

$$\mathbf{G}(f_r) \approx \sigma_1(f_r)u_1(f_r)u_1^H(f_r) \tag{30}$$

and the first singular vector $u_1(f_r)$ is an estimate of the mode shape. On the other hand, the first singular value $\sigma_1(f)$ at each frequency represents the strength of the dominating vibration mode at that frequency so that the first singular function can be suitably used as a modal indication function (yielding the resonant frequencies as local maxima) whereas the successive singular values contain either noise or modes close to a strong dominating one.

4.5.2 Introduction to Testings

The dynamic testing is going to be described through objectives, method, instruments, configurations, setups, and results.

Objectives of test

The main objective of the dynamic test is to study the vibration characteristics of the bridge on site. The follows would be examined.

    1) Dynamic characteristics (periods, modal shapes, etc.) of the bridge
    2) Equivalent stiffness of key components

Test methods – ambient vibration test (traffics)

Ambient vibration tests are successfully applied to a large variety of civil engineering structures ranging from short to long span bridges, high-rise buildings and dams. This method only requires the measurement of the structural response under ambient excitation, usually due to wind or traffic, and can lead to accurate estimates of the modal parameters quickly and inexpensively. Furthermore, it can provide the benefit of avoiding shut down vehicle traffic during the tests due to the installation of heavy shakers. The usual testing procedure consists of performing several measurements simultaneously at one or more reference points and at different other points along the structure. Assuming that the excitation is relatively smoothly distributed in the frequency band of interest, it is easy to obtain, in the frequency domain, amplitude and phase relations between the structural response at the several

points of measurement, which can lead to accurate estimates of natural frequencies and mode shapes.

The dynamic tests involved:

i). preliminary measurements for evaluation of the levels of acceleration and identification of an appropriate reference section;

ii). the ambient vibration test(s) to identify global natural frequencies and mode shapes of the bridge, measuring the structural response at different points along the girders;

iii). experimental evaluation

Test instruments

Ambient vibration tests were conducted on the bridge using three 4-channel data acquisition systems with 12 piezoelectric accelerometers (model WR-731A, each with a battery power unit WR-P31). Cables connected the accelerometers to a computer workstation with a data acquisition board for A/D and D/A conversion of the transducer signals and storage of digital data. The main instruments are as following.

- PC-based portable data acquisition and storage system.
    1) PC with DAQ (data acquisition) systems; and
    2) The NI 9234 (Fig. 68b) is a four-channel C Series dynamic signal acquisition module for making high-accuracy audio frequency measurements from integrated electronic piezoelectric (IEPE) and non-IEPE sensors with NI CompactDAQ or CompactRIO systems. There are 3 in amount used in test.

- Sensors with power amplifiers
    Wilcoxon WR-731A (Fig. 68a) (sampling frequency range: 0.05~450Hz), seismic accelerometer and power amplifier, There are 12 in amount used in test.

- Cables and misc.
    sensor cables, and other relative electrical instruments.

a)   b)
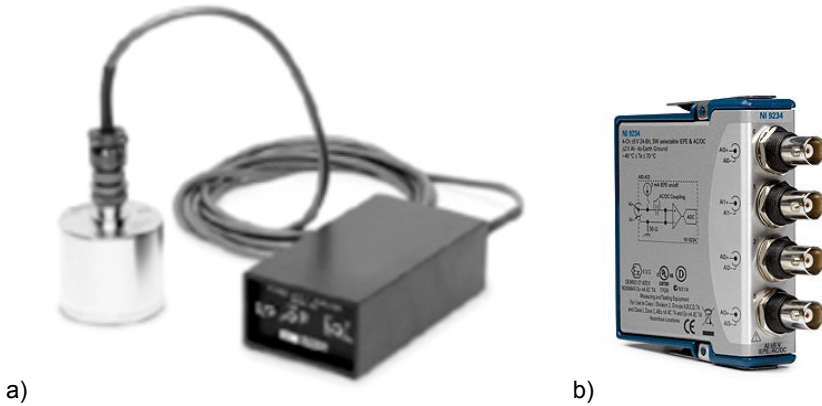
Fig. 68 Test Instruments: a) Sensors of WR-731A / WR-P31; b) NI 9234
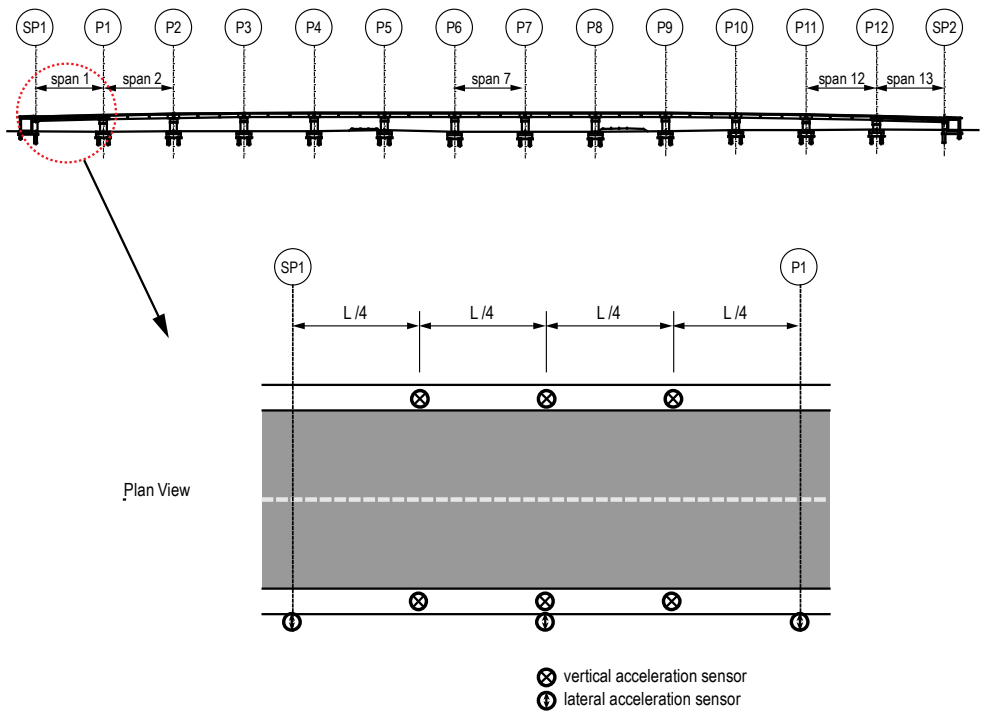
Fig. 69 Setup Arrangement Details (Setup No.2)

Test arrangement and setup

The responses of the bridge was recorded for duration of 3600s (1 hour) with 400 Hz sampling rate. And the amplifiers are set to be 10X during the test.

Both in the tests carried out in Sep. 2010 and Feb. 2011, there are 7 setups, and another additional setup in Feb. 2011. The testing spans including span no.1, 2, 7, 12 and 13, and all spans in two directions: lateral and vertical. The additional setup of Feb. 2011 is to consider the torsional deflection so that both-side channels were placed on some spans. Throughout all the test setups, there are three reference sensors keeping connected all the time, which are placed at the mid-span of span no.2. The locations of sensors in different test setups are shown in Fig. 69, Fig. 70 and Fig. 71, and Table 17. Photos during the tests are shown in Fig. 72.

Setup no.	Test span(s) no.	Direction	Reference span no.	No. of sensors	Reference sensor no.
1	2	Vertical / Horizontal	2	9	5, 7, 3 (1, 2, 3)
2	1	Vertical / Horizontal	2	12	1, 2, 3
3	7	Vertical / Horizontal	2	12	1, 2, 3
4	12	Vertical / Horizontal	2	12	1, 2, 3
5	13	Vertical / Horizontal	2	12	1, 2, 3
6	3, 4, 5, 6, 8, 9, 10, 11	Vertical	2	12	1, 2, 3
7	3, 4, 5, 6, 8, 9, 10, 11	Horizontal	2	12	1, 2, 3
8 (Feb.2011)	3, 4, 5, 6, 8	Vertical	2	12	1, 2, 3

Table 17
Summary of Test Setups
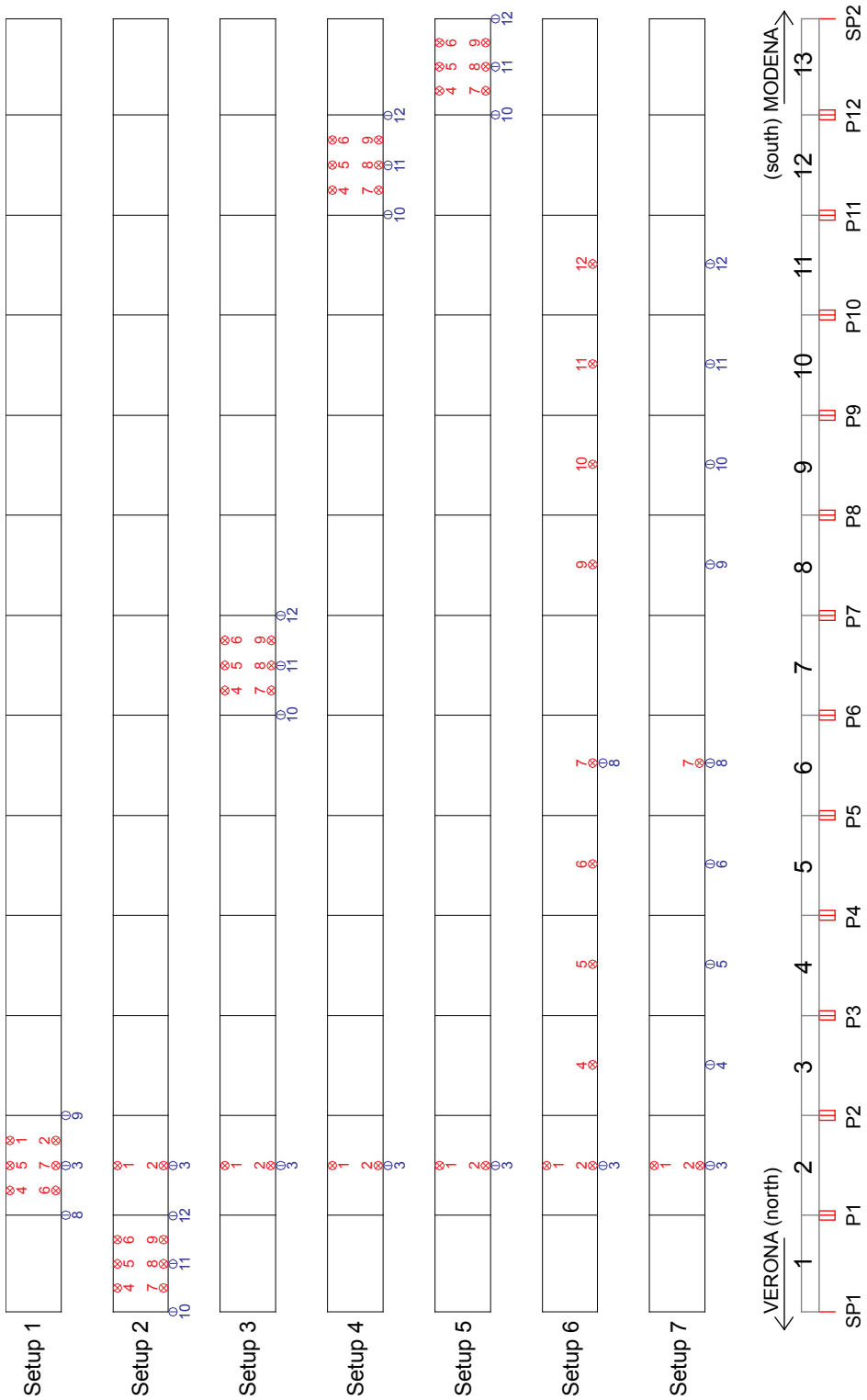
Fig. 70 Test Measurement Setups: Arrangements of Sensors – Sep. 2010
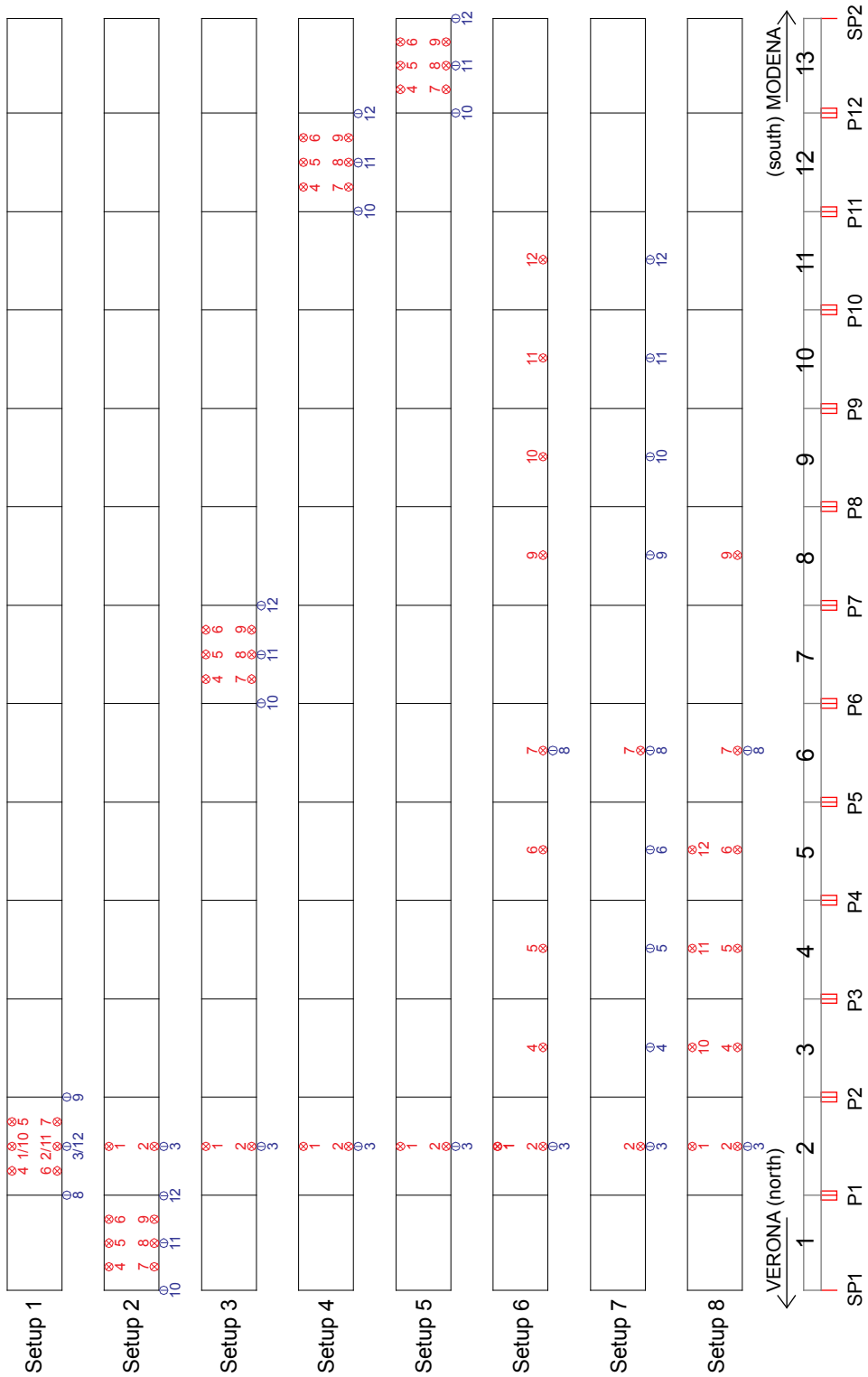
Fig. 71 Test Measurement Setups: Arrangements of Sensors – Feb. 2011
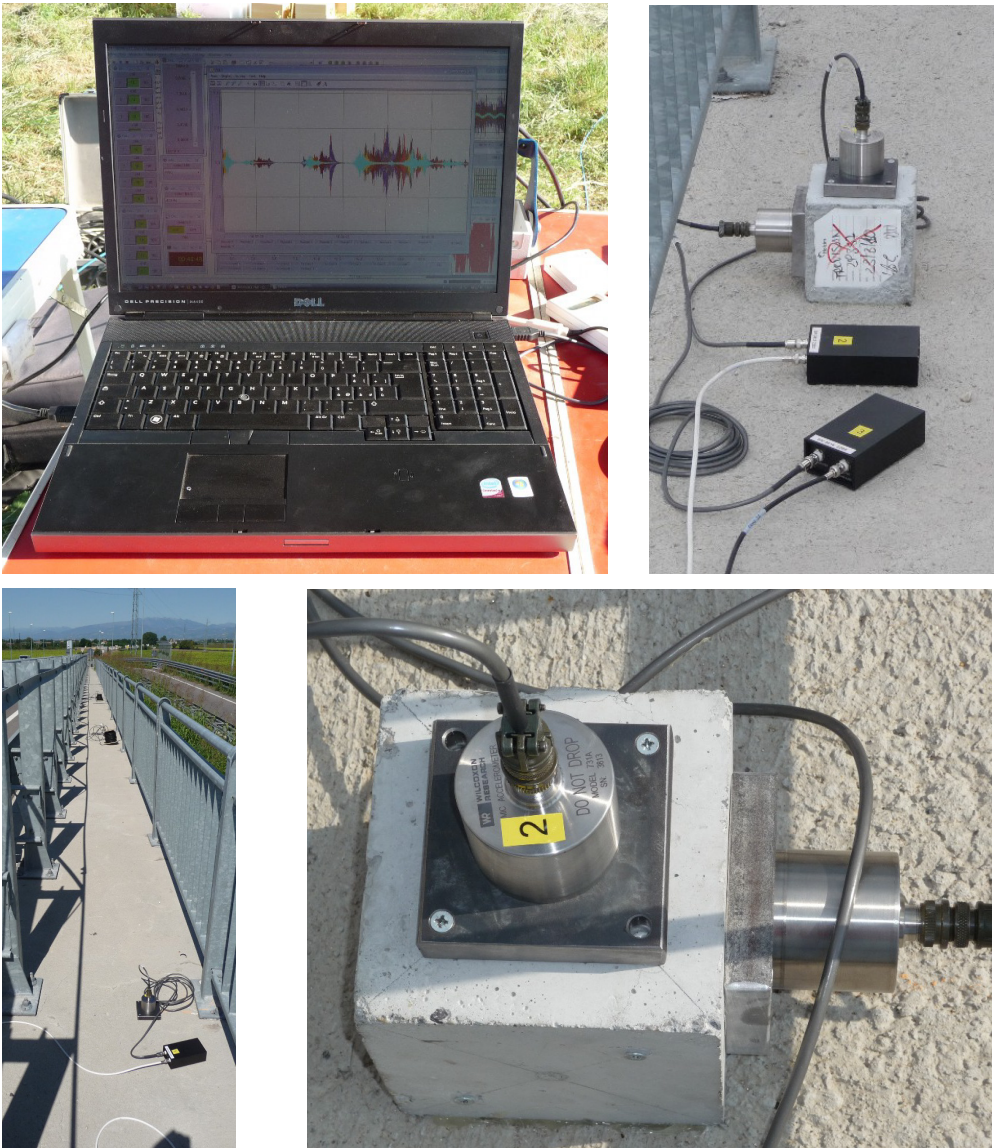
Fig. 72 Photos during Testing

4.5.3 Data Processing and Results

The recorded data of different channels from each set of measurement in the ambient test would be processed through operational modal analysis software ARTeMIS Extractor. Then, the technique of FDD (Frequency Domain Decomposition Identification Techniques) and SSI (Stochastic Subspace Identification) would be applied

to extract the natural modes (frequencies, modal damping ratios, and mode shapes) for the system (Fig. 73).

The data sampling frequency is 400 Hz. In order to identify the fundamental frequency of the structure in low frequency range, decimation of 5th order is applied. Then the sampling frequency turns to 80 Hz (sampling interval 0.0125 s, nyquist frequency 40 Hz). From the preliminary spectral density analysis of all the signal data, in the low frequency range the density is very low and mixed with noises, so that it's hard to identify the fundamental modes. Therefore, the following processes are done in vertical direction and horizontal direction separately (Table 18 and Table 19). However, for the torsional modes, the chart of spectral density appears as same as the vertical-only signals. Therefore, no torsional modes were found. The amplitudes of torsional modes were not evident and can't be identified.
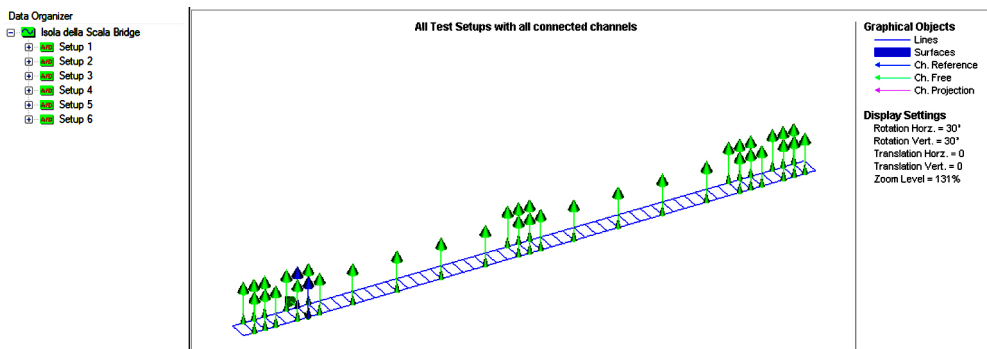
a) data Input in ARTeMIS (all vertical channels)
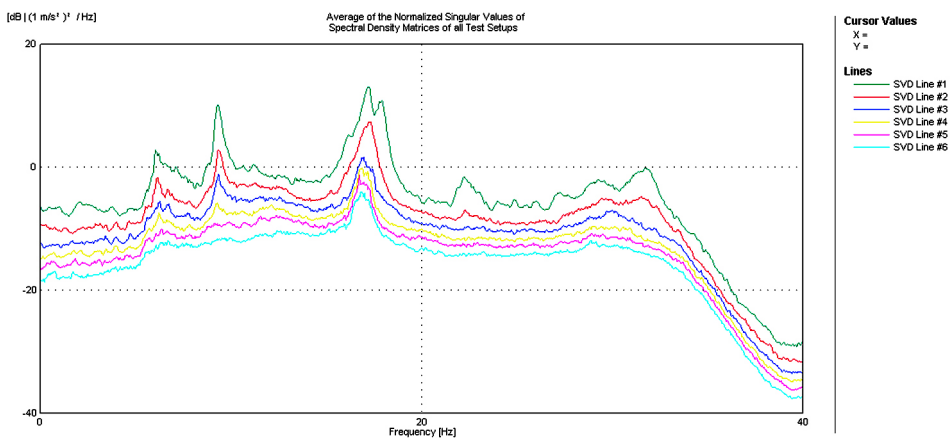
b) spectral density
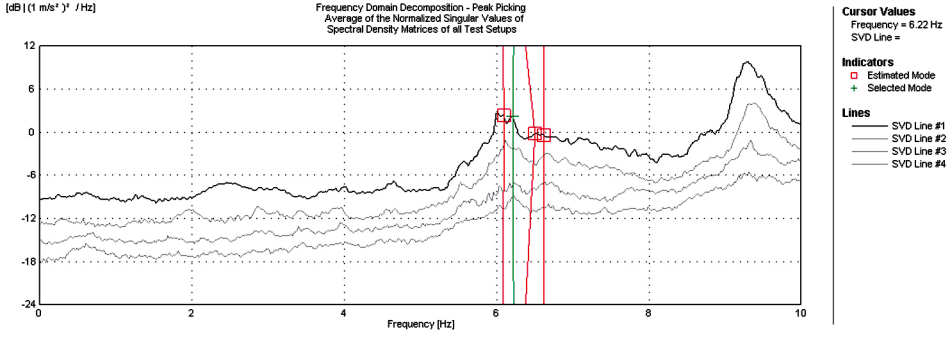
c) FDD modes identification

Fig. 73 Data Processing through ARTeMIS

4.5.4 Comparisons with FEA

With advances in numerical modelling, it is generally expected that FE models based on technical design data, as-built drawings and engineering judgment can reliably simulate both the static and dynamic structural behaviour. However, these FE models often cannot predict natural frequencies and mode shapes with the required level of accuracy, as a consequence of modelling uncertainties. A possible practice to fill the lack between the real structural performance and finite element models is to employ some form of modal analysis on bridges in service. And then the results from test and finite element analysis (FEA) can be compared through the absolute frequency discrepancy D_F and the modal assurance criterion (MAC) (Allemang, 2003).

$$D_F = \frac{\left|f_{FDD} - f_{FEA}\right|}{f_{FDD}} \tag{31}$$

The MAC is probably the most commonly used procedure to correlate two sets of mode shape vectors and is defined as:

$$MAC(\Phi_{A,k},\Phi_{B,j}) = \frac{(\Phi_{A,k}^T \Phi_{B,j})^2}{(\Phi_{A,k}^T \Phi_{A,k})(\Phi_{B,j}^T \Phi_{B,j})} \tag{32}$$

where $\Phi_{A,k}$ is the *k*-th mode of data set *A* and $\Phi_{B,j}$ the *j*-th mode of the data set *B*. The *MAC* is a coefficient analogous to the correlation coefficient in statistics and

111

ranges from 0 to 1; a *MAC* value of 0 indicates that the two mode shapes are completely uncorrelated, while a *MAC* value of 1 indicates perfect correlation between them. In general, a *MAC* value greater than 0.80 ~ 0.85 is considered a very good match while a *MAC* value less than 0.40 is considered a poor match.

Therefore, comparisons were carried out between of testings and finite element analysis (FEA) results. The both frequencies and mode shapes of modes that identified were compared to corresponding mode from FEA (Table 18 and Table 19).
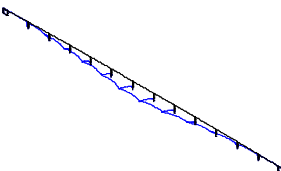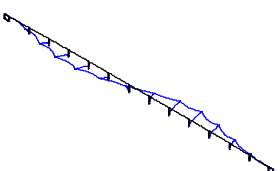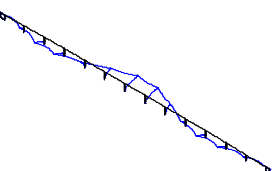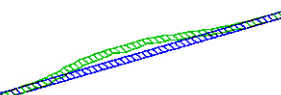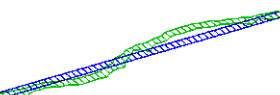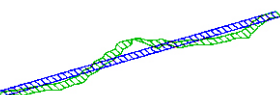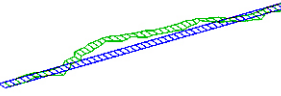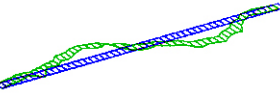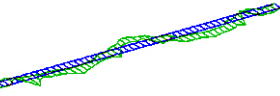
	Mode 1	Mode 2	Mode 3
	Corresponding Modes from FEA		
Freq. (Hz)	2.893	3.028	3.206
Mode shape	Twisting / Lateral bending	Twisting / Lateral bending	Twisting / Lateral bending
	Modes Identified from Test – Sep. 2010		
Freq. (Hz)	2.832	3.118	3.444
Mode shape			
D_F	2.15%	2.89%	6.91%
MAC	0.9098	0.7330	0.7824
	Modes Identified from Test – Feb. 2011		
Freq. (Hz)	2.930	3.122	3.460
Mode shape			
D_F	1.26%	3.01%	7.34%
MAC	0.8992	0.9059	0.7373

Table 18
Horizontal Modes Comparison
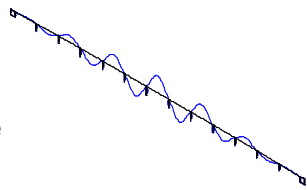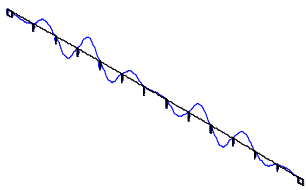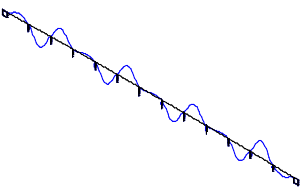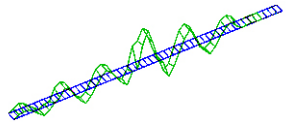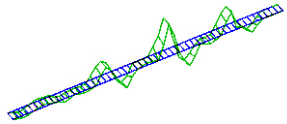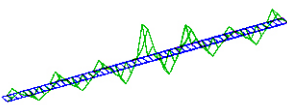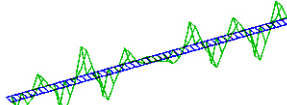
	Mode 1 (17)	Mode 2 (19)	Mode 3 (21)
Corresponding Modes from FEA			
Freq. (Hz)	6.172	6.262	6.504
Mode shape			
	Vertical bending	Vertical bending	Vertical bending
Modes Identified from Test – Sep. 2010			
Freq. (Hz)	6.185	N/A	6.634
Mode shape			
D_F	0.21%		1.96%
MAC	0.7714		0.5947
Modes Identified from Test – Feb. 2011			
Freq. (Hz)	6.086	6.223	N/A
Mode shape			
D_F	1.40%	0.63%	
MAC	0.8797	0.7635	

Table 19
Vertical Modes Comparison

4.5.5 Finite Element Model Updating

Table 18 and Table 19 are showing the FEA results from the FE models that have already been corrected through the preliminary comparisons. From the preliminary comparisons, the modifications were tried to apply on different parts of the model to

fit the frequencies and mode shapes. Finally, it is found that the girder-pier connection stiffness is of the most influencing uncertain factor. Due to the girder-pier construction (Fig. 54 and Fig. 74), the girder-pier connections were considered to be hinges in the finite element models. However, in fact, the connection is not a pure hinge, where the vertical pressures and horizontal frictions could provide certain rotational resistances.
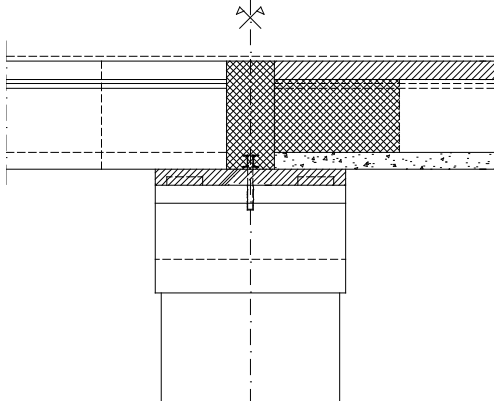
a) construction details
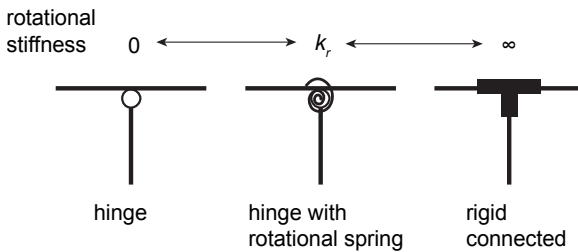
b) mechanical models

Fig. 74 Girder-Pier Connection of Isola della Scala Bridge

Generally, the uncertain structural parameters were approximated by minimizing the difference between theoretical and experimental natural frequencies through the approach of least square (Douglas & Reid, 1982; Gentile, 2006). Once the model updating was performed, a complete correlation analysis was carried out between theoretical and experimental modal parameters.

Here, firstly assume the reasonable rotation stiffnesses in three directions are k_{rx}, k_{ry}, and k_{rz}, with reasonable ranges of values. Then perform the finite element analyses by applying these values of parameters. A function table, frequencies $f_{i,FEA}$ to

stiffnesses k_{rx}, k_{ry}, and k_{rz}, was created. Then the differences between $f_{i,FEA}$ and the experimental frequencies $f_{i,2010}$ and $f_{i,2011}$ were calculated. At the end, the solution of "least square" was found by summing the squares of the differences.

Rotation Direction	Rotation Stiffness k_r (MN.m/rad)
X (longitudinal)	4.8×10^3
Y (vertical)	0
Z (lateral)	1.0×10^5

Table 20

Modified Rotation Stiffnesses of Girder-Pier Connection in FE Model

5. LENGTH LIMIT FOR INTEGRAL ABUTMENT BRIDGES

The design of wide and relatively short integral abutment bridges with flexible piers built integral with superstructures with concrete deck slabs is further simplified because piers and abutments generally need not be designed to resist either lateral or longitudinal loads. This is possible because the laterally and longitudinally rigid concrete deck slabs are rigidly attached to abutments and to one or more piers, and abutments are rigidly restrained by confining embankments (Burke Jr, 2009). Consequently, essentially all lateral and longitudinal loads applied to the superstructures of such bridges are transmitted directly to abutment embankments. Therefore, the abutment's design could affect a lot on the performance of the integral abutment bridges.

In the design of piers, essentially, since all horizontal superstructure loads are transmitted to approach embankments, the moments associated with pier-superstructure continuity connections are usually negligible (Snedeker et al., 2011). Therefore, piers of integral bridges (capped-pile or self-supporting types with movable bearings) need be designed only for vertical superstructure and pier loads and for lateral loads that may be applied directly to the piers (stream flow, stream debris, earth pressure, wind). Where these lateral pier loads are small, and this is usually the case, most piers, like abutments, can be designed essentially for vertical loads alone. However, the connections could not be ideally hinges or pulleys, Isola della Scala Bridge as an example, so the piers may have taken the moments induced longitudinal bending, which might be the factor, especially if the length of the bridge is too long.

On the basis of Isola della Scala Bridge, and the finite element analyses, considering the abutment strengths and piers capabilities, therefore, the analytical length limit for integral abutment bridge is investigated as following. Meanwhile, the other factors affecting the possible super-long integral abutment bridges, such as fatigue problem and long-term cyclic loadings, will be discussed.

5.1. Analytical Formulation

As the vertical loadings would not affect a lot on the total length of the integral abutment bridge, only the horizontal loading – the temperature load – was considered in the following analytical formulation (Zordan et al., 2011).

5.1.1 Thermal Displacements Relations of Each Span

For a general case, the following parameters are considered: E = elastic modulus of the girder concrete; A = area of the cross section of girder, the same L = span length for all spans; K_i = stiffness of i-th pier top.

Firstly, the case of an odd number of spans is considered. The results obtained will be then extended to the case of an even number of spans.

For an odd number of spans, namely $n_s = 2n - 1$, considering the symmetry of the bridge and starting from the central span , the forces and the deformations involved in the equilibrium and compatibility conditions for all the spans are listed in Fig. 75.
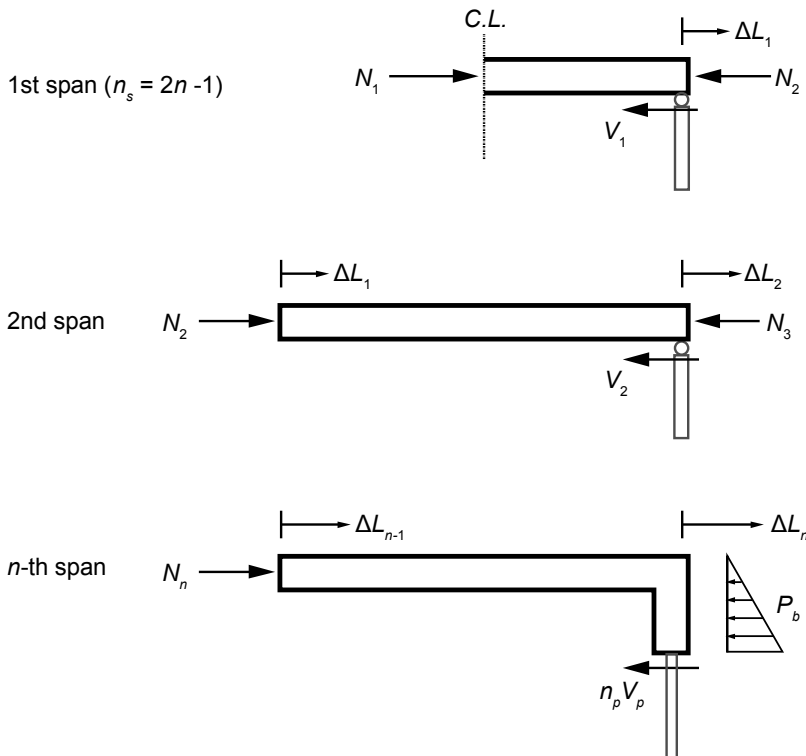
Fig. 75 Horizontal Forces of Each Span

For the 1st central half span, from compatibility equation and horizontal force equilibrium the following equations can be derived:

$$N_1 = EA\left(\alpha\Delta T - \frac{2\Delta L_1}{L}\right) \tag{33}$$

$$N_2 = N_1 - V_1 = EA\left(\alpha\Delta T - \frac{2\Delta L_1}{L}\right) - K_1\Delta L_1 \tag{34}$$

Similarly for the 2nd span:

$$N_2 = EA\left(\alpha\Delta T - \frac{\Delta L_2 - \Delta L_1}{L}\right) \tag{35}$$

$$N_3 = N_2 - V_2 = EA\left(\alpha\Delta T - \frac{\Delta L_2 - \Delta L_1}{L}\right) - K_2\Delta L_2 \tag{36}$$

From Eqs. (34) and (35), the relation between the displacements of 2nd and 1st pier tops can be expressed as:

$$\Delta L_2 = \left(3 + \frac{K_1 L}{EA}\right)\Delta L_1 \tag{37}$$

And for *i*-th span $(3 \le i \le n)$, similarly it is found:

$$\Delta L_i = \left(2 + \frac{K_{i-1}L}{EA}\right)\Delta L_{i-1} - \Delta L_{i-2} \tag{38}$$

Therefore, for span number $n_s = 2n - 1$:

$$\Delta L_i = \begin{cases} \Delta L_1 & i = 1 \\ \left(3 + \dfrac{K_1 L}{EA}\right)\Delta L_1 & i = 2 \\ \left(2 + \dfrac{K_{i-1}L}{EA}\right)\Delta L_{i-1} - \Delta L_{i-2} & 3 \le i \le n \end{cases} \tag{39}$$

119

For an even number of spans, namely $n_s = 2n$, similarly it is found:

$$\Delta L_i = \begin{cases} \Delta L_1 & i = 1 \\ \left(2 + \dfrac{K_1 L}{EA}\right)\Delta L_1 & i = 2 \\ \left(2 + \dfrac{K_{i-1} L}{EA}\right)\Delta L_{i-1} - \Delta L_{i-2} & 3 \le i \le n \end{cases}$$ (40)

Equations (39) and (40) can be generalized as:

$$\Delta L_i = c_i \Delta L_1$$ (41)

where, c_i is the constant function of K_{i-1}, L, EA: $c_i = f_i (K_{i-1} L / EA)$ for different i and n_s. Creep and shrinkage can be considered modifying elastic modulus E as well as concrete cracking can be taken into account locally acting on the same parameter; and the parameter expressing the longitudinal horizontal stiffness of the piers K_i needs to be considered properly as described in Ch.5.1.2.

And, from the compatibility condition on the n-th span, it is obtained:

$$N_n = EA\left(\alpha\Delta T - \frac{\Delta L_n - \Delta L_{n-1}}{L}\right) = EA\left(\alpha\Delta T - (c_n - c_{n-1})\frac{\Delta L_1}{L}\right)$$ (42)

5.1.2 Pier's Horizontal Stiffness

For different types of piers (Dreier, 2010a), the horizontal stiffnesses at the top of the pier are different as shown in Fig. 76, where $E_p I_p$ = sectional modulus of pier, and H_p = height of pier. However, the horizontal displacement will cause not only the flexure bending of the pier but also the deformation on the foundation that the pier connected to.

For a pier-foundation system, usually, the rotational rigidity is approximately linearly proportional to soil modulus, proportional to the square root of depth of the soil foundation and proportional to the square of the width of foundation; While these parameters have an important effect on the translational behavior too (Dreier, 2008).

Contrary to the rotational behavior, generally, it is more difficult to find a direct relationship between the variations of parameters and the translational stiffness. However, an equivalent pier-foundation (pier and substructure) horizontal stiffness can be approximately estimated through Eq.(43) (European Committee for Standardization (CEN), 2005a).

$$\frac{1}{K} = \frac{1}{K_p} + \frac{1}{K_{Fu}} + \frac{H_p^2}{K_{F\theta}} \tag{43}$$

where, K_p = horizontal stiffness of pier flexure (Fig. 76); K_{Fu} = foundation horizontal translation stiffness; $K_{F\theta}$ = foundation rotational stiffness.
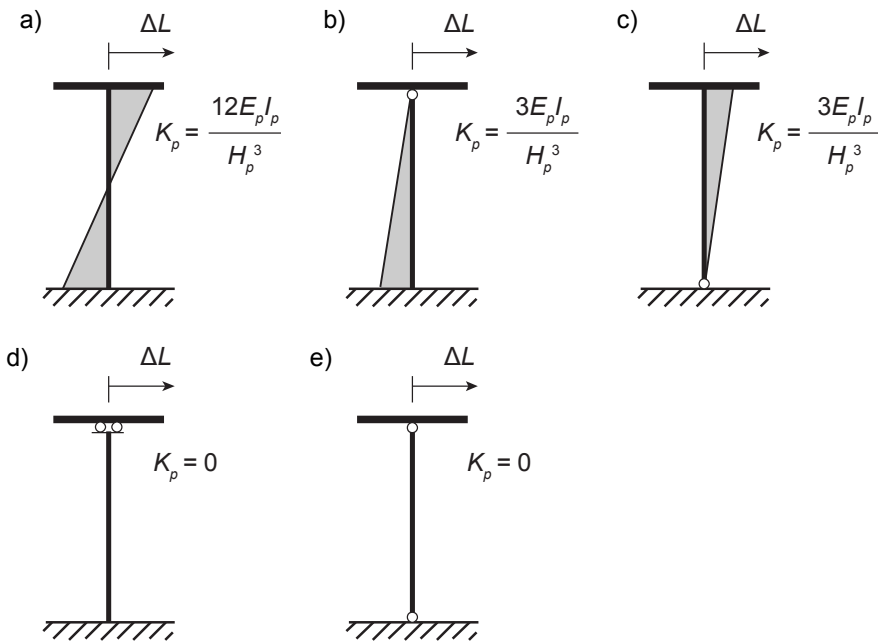
Fig. 76 Horizontal Stiffnesses of Piers

5.1.3 Earth Pressure on Abutment

Due to the restraining effect of the pile-soil system underneath the abutment, preventing the abutment from fully pushing against the backfill soil, and the backfill yielding under the large displacement of the abutment, the backfill pressure distribution usually is not of a classical triangular shape (Fig. 77), which is reflected in abutment design as shown in Fig. 24 and Fig. 27. It is also observed that the shape

of the backfill pressure distribution is nearly similar regardless of the foundation soil stiffness (Dicleli & Erhan, 2011).
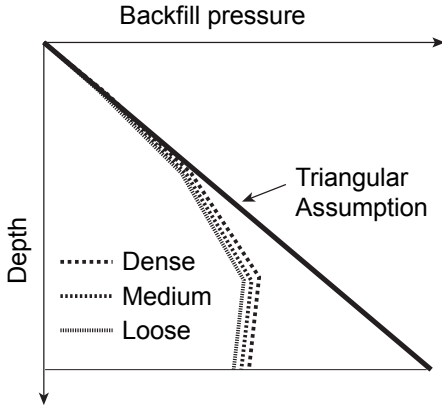
Fig. 77 Earth Pressure Distribution along the Abutment Height

However, for conservative consideration of the higher internal forces under higher earth pressure, and on the basis of observations from the static pushover analysis, the shape of the backfill pressure could be conservatively approximated as triangular (Dicleli & Albhaisi, 2003) for practical purposes and analytical derivation, and can be expressed as:

$$P_b = \frac{1}{2} K_s \gamma H_b{}^2 w_b \tag{44}$$

Where: γ = unit weight of backfill soil; H_b = height of abutment; w_b = width of abutment; and K_s = backfill soil pressure coefficient obtained from $K_s - (\Delta L / H_b)$ limit points from NCHRP report (Barker et al., 1991). In order to simplify the problem, bilinear $K_s - (\Delta L / H_b)$ curves were used (as shown in Fig. 31), with slope k_p for passive pressure before reaching K_p, as well as k_a for active pressure. Taking the example of positive temperature variation, the backfill pressure can be written as:

$$P_b = \frac{1}{2} \left(K_0 + k_p \frac{\Delta L_n}{H_b} \right) \gamma H_b{}^2 w_b \tag{45}$$

5.1.4 Pile Head Reactions

On the other hand, the plastic moment capacity of the piles may be reached for small thermal displacements caused by the combined effects of superimposed dead loads, live loads and temperature expansion or contraction, as experimentally sup-ported by field measurements (Arsoy, 2000; Dicleli & Albhaisi, 2003; Dicleli & Albhaisi, 2004a; Dicleli, 2005; Civjan et al., 2007; Pugasap et al., 2009). Therefore, when determining the maximum shear and bending moment in the abutment, the piles may conservatively be assumed to have reached their plastic moment capaci-ty. Therefore, horizontal force equilibrium of the *n*-th span can be written as:

$$N_n = P_b + n_p V_p \tag{46}$$

Where: n_p = number of piles and V_p = critical shear of pile; P_b = earth pressure on the abutment backwall. Therefore, to determine the displacements, the earth pres-sure P_b and pile head reaction V_p are needed to be identified firstly. V_p can be de-termined from the plastic bending moment capacity of piles using equivalent shear length method with an average constant (Dicleli, 2005), or could be obtained from pushover analyses on the piles (c.f. Ch.6).

5.1.5 Analytical Displacement Formulation

Therefore, given a certain temperature load ΔT and span number n_s, using Eqs.(42) to (45) and substituting, the displacement ΔL_1 can be obtained as for Eq.(47) and ΔL_n then can be calculated as Eq.(48) by substituting Eq.(41).

$$\Delta L_1 = \frac{EA\alpha\Delta T - n_p V_p - \dfrac{1}{2}K_0\gamma H_b^2 w_b}{EA\left(c_n - c_{n-1}\right) + \dfrac{1}{2}k_p c_n \gamma H_b L w_b} \cdot L \tag{47}$$

$$\Delta L_n = \frac{EA\alpha\Delta T - n_p V_p - \dfrac{1}{2}K_0\gamma H_b^2 w_b}{EA\left(c_n - c_{n-1}\right) + \dfrac{1}{2}k_p c_n \gamma H_b L w_b} \cdot c_n L \tag{48}$$

The relation curves between displacements and the total number of spans are cal-culated and shown in a qualitative way in Fig. 78.
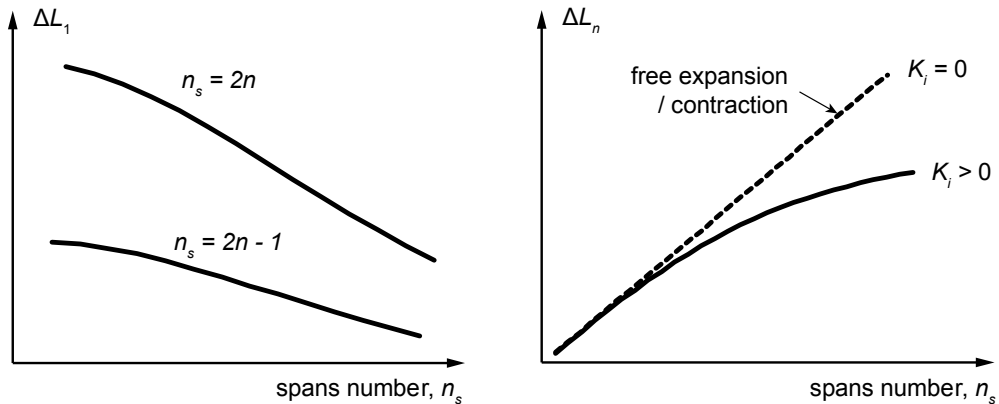
a) ΔL_1 v.s. n_s b) ΔL_n v.s. n_s

Fig. 78 Relations between Displacements and Number of Spans

5.2. Non-Linearity Correction

5.2.1 Non Linear Response

The derived formulation is used to calculate the displacement of each span of a general bridge model with 13 spans (n_s = 13). And at the same time, different solutions of finite element models both based on the general model (Fig. 48) and Isola della Scala Bridge (Fig. 55), are carried out. All the solutions are compared in Fig. 79: the analytical formulation, the FEM of Isola della Scala Bridge (FEM IdS), FEM of general model without plastic hinges (FEM GM w/o PH) and general model with plastic hinges (FEM GM w/ PH). As shown in Fig. 79, the results supplied by the analytical formulation and elastic FE analysis are in good agreement.

The expected difference between the curves might mainly be caused by bending moment in girder due to vertical temperature distribution and different distributions of the backfill pressure due to rotation of abutment, and the other non-linear features of the structural components considered in finite element models. In order to achieve a more reliable and conservative analytical formulation, and to take into account the non-linear effects deriving from that such as variation of girder section properties, backfill failure under large displacement, and especially the presence of plastic hinges in piers, where stiffness are considered to have reductions according to different displacements or rotations, as shown in Fig. 80.

124
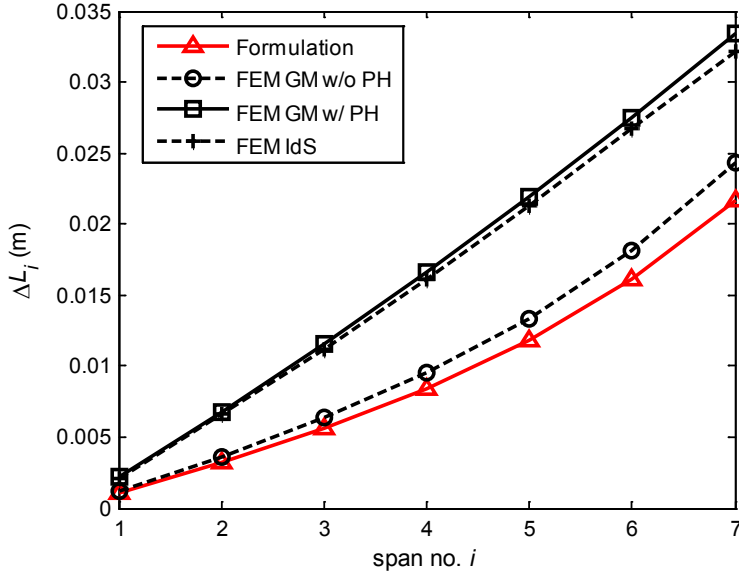
Fig. 79 Displacement of i-th Span

5.2.2 Correction through Modifying Piers Stiffness

In the simplified formulation presented above, only the linear and elastic properties are considered. there are several possible ways to take into account the non-linearity in the formulations:

1) to modify modulus *EA* for each span as a function of span number *i* for different temperatures, $EA = f_{EA} (i, \Delta T)$;

2) to modify pier horizontal stiffness K_i varying along the bridge length due to the different bending condition (rotation) of the piers of different horizontal displacement (Fig. 80); and

3) to modify the backfill earth resistance and pile resistance as a non-linear function to the displacement.

From the FEA in the performance of Isola della Scala Bridge in Ch.4, the piers behaved in great non-linearity and differed from pier to pier. Therefore, through comparison to FEA, the formulations could be modified by correcting the pier horizontal stiffness K_i. Besides, considering the simplification on formulae, the other non-linear are considered as constant multipliers and already affecting the modification of K_i,

which means only reductions applied on K_i, and the other effects are thought to be involved in these reductions.
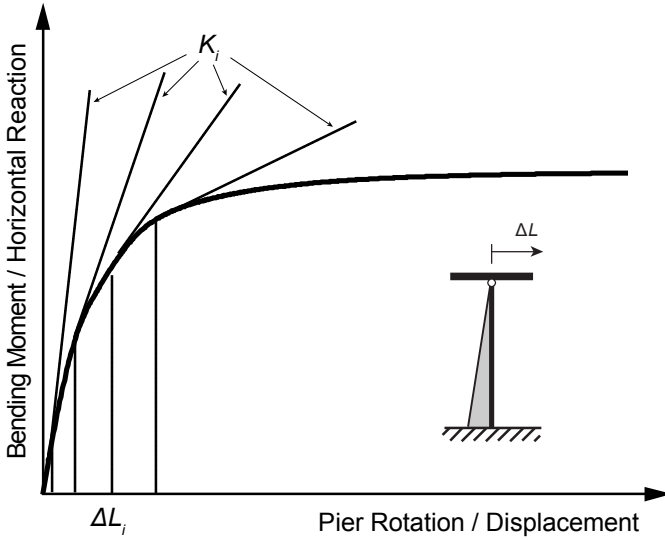
Fig. 80 Non-Linear Behavior of Pier

Therefore, a reduced stiffness coefficient is applied in Eq.(49), which is obtained through a conservative approach that interpolates the FEM results.

$$K_{i,m} = \frac{K_i}{i^{3/2}} \tag{49}$$

where $K_{i,m}$ = modified shear stiffness of i-th pier top, to be used instead of K_i in the calculation of c_i as expressed in Eq.(41). The modified formulation solution is shown in Fig. 81, where the modified formulation results could envelop all the finite element results.

For different condition of a specified bridge, the modification coefficients would apparently different. The modification like Eq.(49) should be obtained from comparison to the finite element analysis involving nonlinear effects or the other numerical or experimental results. In this study, the condition of the super-long integral abutment bridge is considered to be based on Isola della Scala Bridge. Thus, the modification of Eq.(49) is going to be applied on longer bridges that might reach the length limit based on the conditions of Isola della Scala Bridge.
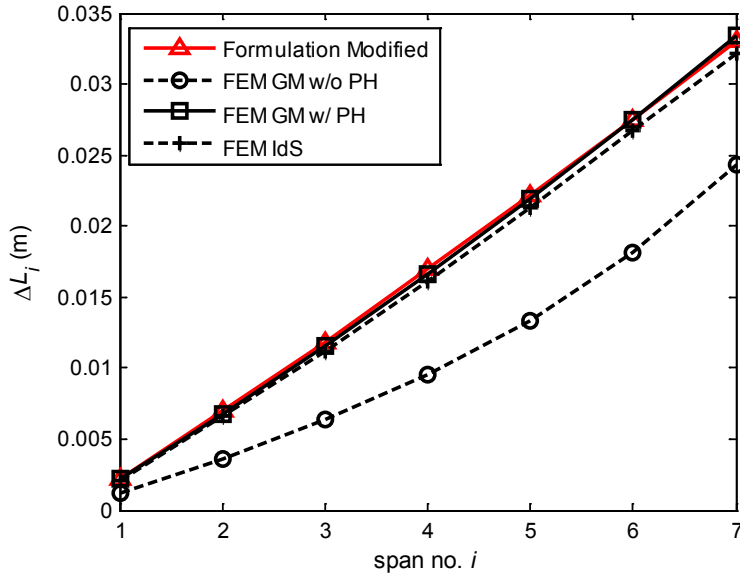
Fig. 81 Modified Displacements Curves

5.3. Overall Length Limit

To know the limit of overall length of an integral abutment bridge has to consider many possible factors. From the structural perspective, however, the structural capabilities of the components are the main effective factors. Instead of the yielding and interaction of the soil, the pier rotation capability and abutment flexure and shear capabilities are taken into account, while the pile is considered to be well designed as stated in Ch.5.1.4.

5.3.1 Pier Rotation Capacity

In evaluating the allowable imposed displacement at the top of piers, the importance of soil-structure interaction accounting for the cracking limit state is revealed (Dreier, 2008): the influence of the stiffness of the foundation is very significant; a low stiffness leads to a static system with a hinge at the base of the pier; on the contrary, a large stiffness leads to a static system clamped at the base; the pier height is also significant.

However, to simplify the problem, only plastic hinge is thought to be form at the bottom of the pier and the pier rotates about the position of plastic hinge, and neglecting the influence of the structural stiffness of the foundation, of second order effects, of the time-dependent behavior of concrete, of soil compaction with cyclic rotation of the foundation, and so on. Therefore, it has to be considered that, the (n-1)-th pier displacement should satisfy the rotation capability of the pier:

$$\Delta L_{n-1} = c_{n-1}\Delta L_1 \le \theta_{pr}H_p \tag{50}$$

where: θ_{pr} = rotation capability of piers; H_p = height of piers. Eq.(50) can be expressed for ΔL_n as:

$$\Delta L_n \le \frac{c_n}{c_{n-1}}\theta_{pr}H_p \tag{51}$$

The allowable rotation of the pier, θ_{pr}, can be calculated from the modeling of plastic hinge (c.f. Ch.3.4.4) (Fig. 57).

5.3.2 Abutment Strength Capacities

However, for large displacements in abutments, although the plastic hinges have formed in piles in earlier stages they still can channel remarkable internal forces, especially for the case of integral abutment bridges. It's possible that the critical shear or bending moment in abutments would be reached under the movement of abutments and earth pressure on them (Bozorgzadeh, 2007), before piers reach their rotation capability. From the force equilibrium in the abutment, assuming the section positions of maximum shear and bending moment as shown in Fig. 82 (Erhan & Dicleli, 2009), the critical internal forces can be obtained as:

$$V_{a,cr} \ge V_{a,max} = \frac{1}{2}K_s\gamma\left[H_b^2 - (h_D + d)^2\right]w_b + n_pV_p \tag{52}$$

$$M_{a,cr} \ge M_{a,max} = K_s\gamma\left[\frac{(H_b - h_D)^3}{3} + \frac{h_D(H - h_D)^2}{2}\right]w_b + n_p\left[M_p + V_p(H - h_D)\right] \tag{53}$$
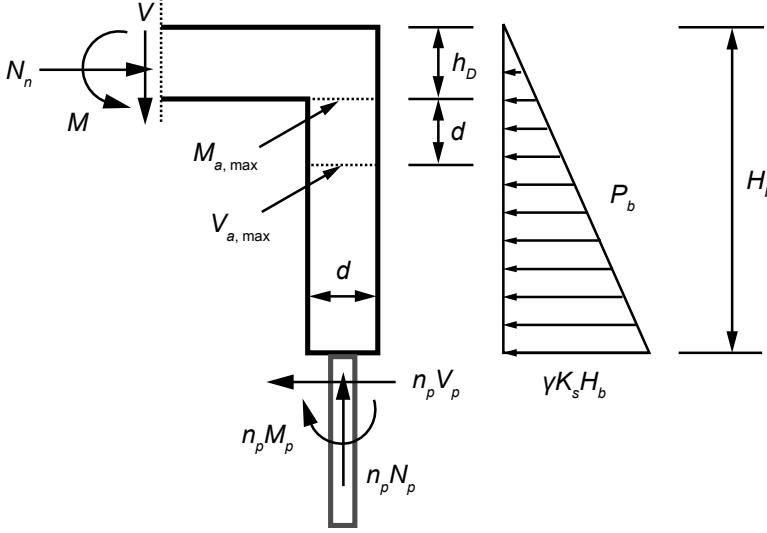
Fig. 82 Forces on the Abutment

From Eqs.(52) and (53), taking the example of positive temperature variation before the backfill passive pressure would reach the plastic phase, the limits of ΔL_n, on the basis of abutment strength capability, are expressed as follows:

$$\Delta L_n \leq \frac{2\left(V_{a,cr} - n_p V_p\right)H_b}{k_p \gamma \left[H_b^2 - \left(h_D + d\right)^2\right]w_b} - \frac{K_0 H_b}{k_p} \tag{54}$$

$$\Delta L_n \leq \frac{M_{a,cr} H_b - n_p H_b \left[M_p + V_p\left(H_b - h_D\right)\right]}{k_p \gamma \left[\dfrac{\left(H_b - h_D\right)^3}{3} + \dfrac{h_D\left(H_b - h_D\right)^2}{2}\right]w_b} - \frac{K_0 H_b}{k_p} \tag{55}$$

Therefore, controlling the limits of ΔL_n through Eqs.(51), (54) and (55), the corresponding n_s can be found from the curves in Fig. 78b. Hence, the overall length could be easily obtained as: $L_s = n_s L$.

5.3.3 Length Limit under Condition of Isola della Scala

The search for the limit length of an integral abutment bridge has to be referred to the boundary conditions and the geometrical and mechanical properties of the

structure considered. In the present study the parameters affecting the design of the 400 meters long Isola della Scala Bridge were taken as a reference being this bridge, as for the knowledge of the authors, the longest integral abutment bridge ever built.

Therefore, besides the parameters of Isola della Scala Bridge, the following reference parameters were considered: pier rotation capacity of θ_{pr} = 0.0050 rad, abutment flexural capacity of $M_{a, cr}$ = 50 MNm, and shear capacity of $V_{a, cr}$ = 10 MN. The mentioned values were used in Eqs.(51), (54) and (55) as limit values. And the temperature variation of +20°C as ultimate load condition was considered (passive earth pressure on the abutment); the modification of Eq.(49) was applied. The solution obtained from the modified analytical formulation is presented in Fig. 83 and compared to the case of free expansion.

It can be seen that, due to the boundary conditions affecting the analysis, the maximum number of spans would have been limited to n_s = 18 due to the pier rotation capacity. Hence, under the assumptions and the approximations introduced, the overall length limit of this type of bridge would be L = 540 m.
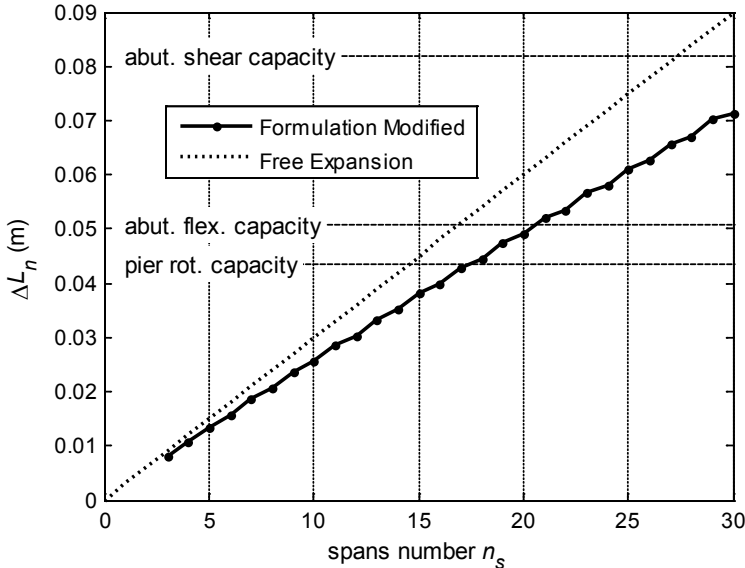
Fig. 83 Thermal Displacements of Different Span Numbers Based on Isola della Scala Bridge

5.4. Other Limit Factors

Despite the common practice to design integral abutment bridges to cover rather limited lengths, it is proved that this kind of structures are suitable also for longer bridges. Integral abutment bridges must be nevertheless still considered as it has always been done, as low-cost bridges built with common building materials and possibly with the use of pre-fabricated elements: with reference to these character-istics, super-long IABs are defined as those close to the limits deriving from the use of conventional building materials under the design boundary conditions given by the mechanical properties of the soil.

The introduction of parametric analyses in the design practice to take into account for the presence of uncertainties related to the thorough understanding of the soil-structure interaction leads to more reliable solutions with positive effects in terms of overall maintenance costs during the lifespan of the bridge.

An analytical formulation suitable to assess the overall limit length for an integral abutment bridge given the single span length and the general boundary conditions was proposed for the case of positive temperature variation. Similar results can be obtained in case of negative temperature variations. The solution is highly affected by the characteristics of the bridge and the method proposed is still under develop-ment: the exact definition of the coefficients $c_i = f_i (K_{i-1}L / EA)$ for different i and n_s needs to be thoroughly investigated for different cross sections, abutment and pier layouts, type of piles, soil properties and other factors.

Nevertheless it is proved that for a very conventional and low-cost bridge such Isola della Scala bridge in Verona-Italy, built with pre-fabricated pre-stressed beams and common construction materials, and overall limit length of more that 500m can be theoretically reached. And for this kind of super-long integral abutment bridges, there are still important considerations as followed.

5.4.1 Fatigue Effects due to Thermal-Induced Displacement

As the ultimate horizontal load (temperature variation) has been considered for length limit analysis, while vertical load being neglected, however, the important re-sistance of structure to fatigue should be verified in special cases.

In the steel piles, for example, the thermal-induced longitudinal movement of the integral bridge deck results in one dominant cyclic lateral displacement of piles at the abutments each year due to seasonal (summer and winter) temperature changes and numerous smaller cyclic lateral displacements due to daily and/or weekly temperature fluctuations (Girton et al., 1989; England et al., 2000; Dicleli, 2004).

Commonly observed strain cycles corresponding to the summer and winter times as shown in Fig. 84. The field-test records demonstrated that the amplitude of the small strain cycles ($\beta 2\varepsilon_a$) in the steel piles fall within 20 to 40% range of the amplitude of the large (seasonal) strain cycles ($2\varepsilon_a$). The above observations are assumed to be generally applicable to integral abutment bridges in North America in lieu of extensive field test data. The amplitudes of the positive and negative strain cycles corresponding to the summer and winter times usually may not be equal as observed. However, as the range of strain amplitudes rather than the strain amplitude itself defines the extent of fatigue damage, the positive and negative strain amplitudes are assumed to be equal for fatigue assessment.
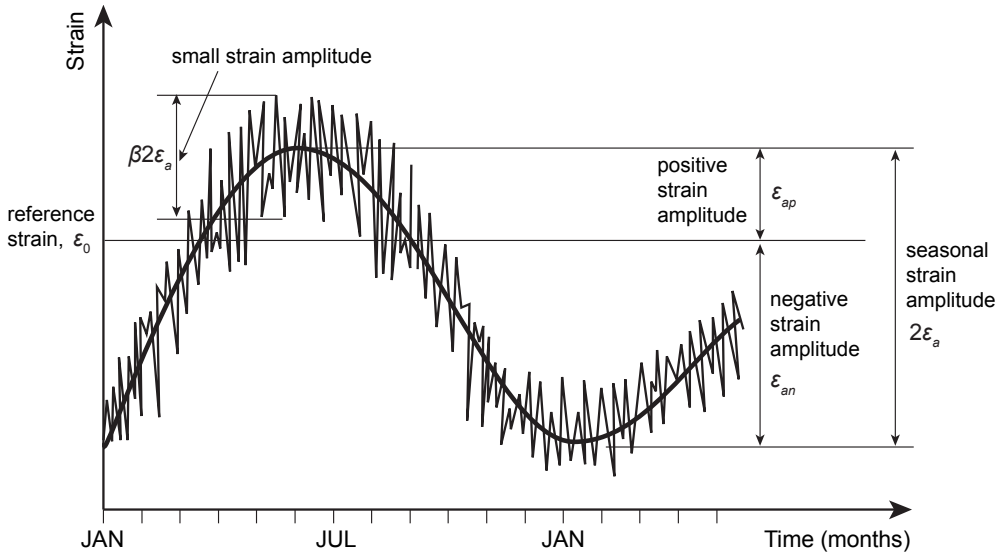
Fig. 84 Pile Strain Variation as a Function of Time in Integral Abutment Bridge

Therefore, both thermal induced small cycles and large low-cycle fatigue effects need to be considered (Huang et al., 2011). Low-cycle fatigue failure of structural components is caused by cyclic loads or displacements of relatively larger magnitude that may produce significant amounts of plastic strains in the structural component (Dicleli, 2004). There are three common methods to predict the low-cycle

fatigue life or evaluate the fatigue effect: general strain-life equation, Manson's universal slope equation, and extrapolated S-N curves (Huang, 2004). Generally, the number of displacement cycles that leads to failure of a component is determined as a function of the equivalent fatigue stresses or plastic strains in the localized region of the concerning component.

The displacement of the pile under the thermal expansion and contraction of the superstructure, thus, should be within the pile's displacement capacity, which could be obtained through pushover analysis of the pile. In the purpose of satisfying the steel pile's thermal-induced fatigue displacement capacity, from the curvature diagram about the free end of the equivalent cantilever for pile, and ignoring the earth resistance on stub-type abutment, the length limits for integral abutment bridges with steel H-pile fixed connected to abutment were derived as listed in Table 21 (Dicleli, 2004) (assuming a construction temperature of 15°C, and using the average temperature ranges for steel and concrete bridges are respectively calculated as 34°C and 20°C for moderate climates and as 43°C and 23°C for cold climates; and pile embedded in a medium-stiff clay soil condition). However, the resistance to force action on the abutment is consisted of earth pressure on abutment and shear force on the top of pile, where earth pressure takes 74%~88% proportion of the applied load (Arsoy et al., 1999). So the length limits are conservative without considering the earth resistance.

Pile size	Steel bridges		Concrete bridges	
	Moderate climate	Cold climate	Moderate climate	Cold climate
HP310×125	220m	145m	320m	265m
HP310×110	205m	135m	300m	250m
HP250×85	160m	110m	240m	195m
HP200×63	125m	80m	180m	150m

Table 21
Maximum Length Limits Based on Pile's Displacement Capacity (in Medium-Stiff Clay)

Obviously, the length limit for integral abutment bridge not only depends on the environments such as climates and soil conditions, but also a lot on the materials applied in the bridge components. For integral abutment bridges with steel piles, the fatigue effects might greatly affect the displacement of the piles. While with concrete piles or concrete piers fixed connected to girder, the assessment becomes compli-

cated, and both the materials of concrete and reinforcing or prestressing steel bars need to be verified.

For concrete piles, it is of more concerning on daily thermal induced displacements. In Eurocode, the fatigue assessment are required to be performed separately for concrete and reinforcing steel (European Committee for Standardization (CEN), 2004a). Under the cyclic loadings, the performance of components will be reduced as the cycling number increases. As shown in Fig. 85, Eurocode 1992-1-1 characterizes the S-N curve for reinforcing steel: for straight bars, $k_1 = 5$, $k_2 = 9$, and the fatigue resisting stress range $\Delta\sigma_{Rsk}$ (N^*) = 162.5 MPa at cyclic number of $N^* = 10^6$.
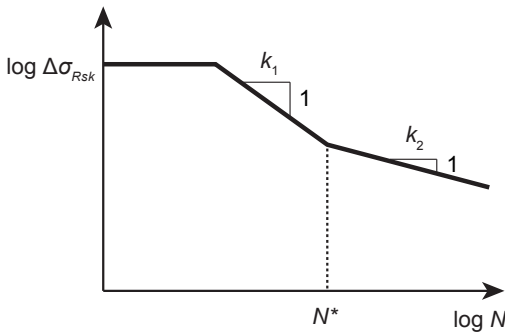
Fig. 85 Characteristic Fatigue Strength Curve (S-N Curve) for Reinforcing Steel

And for concrete, the design fatigue strength:

$$f_{cd,fat} = k_1\beta_{cc}\left(t_0\right)f_{cd}\left(1-\frac{f_{ck}}{250}\right)$$

(56)

where, k_1 = 0.85 (recommended value for N = 10^6 cycles), β_{cc} = 1 (the time of the first cyclic load application is usually set to 28 days in analyses, which is the usual time of demoulding and therefore the first time of load application).

The fatigue stress strengths both for steel and concrete then need to be compared to the stress amplitudes in the components due to the cyclic loadings in certain combinations with partial factors. Taking the materials in Table 10 as example, and if considering the daily temperature variation of 10°C, according to Eurocode, the stress in concrete would not be allowed to be over 15 MPa, and 141 MPa for stress in reinforcement. Therefore the daily pier rotation capacity and abutment strength capacities in Fig. 83 will be much lower. However, the daily fatigue loads are lower too, and with daily temperature variation about a quarter of seasonal variation

(Arsoy, 2000) (0.25 ΔT_N, and assessed under a special ultimate limit state combination that similar to service limit state). Simply and conservatively, therefore, assuming the daily factors of 0.5 are applied both for temperature variation of ultimate state (20°C) and materials strengths for Isola della Scala Bridge, while the other conditions and formulations are the same. The length limit factor turns out to be abutment flexure capacity (Fig. 86), as the length is limited to 450 m (30 m × 15 spans).
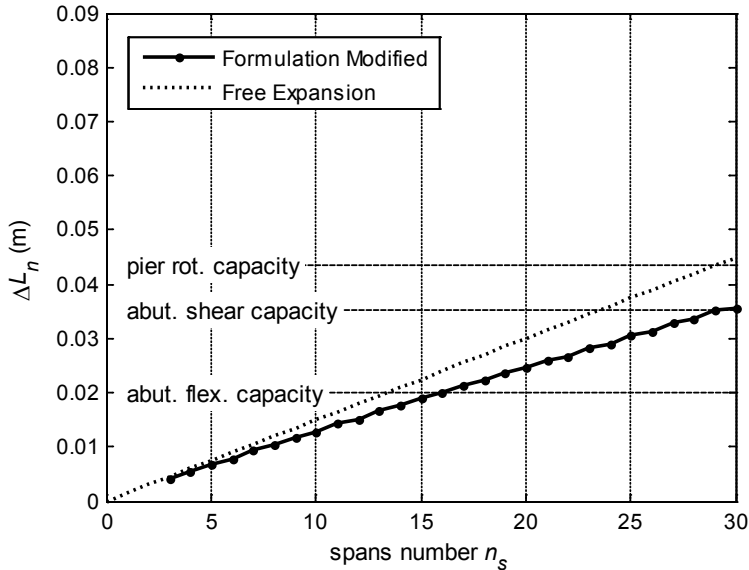
Fig. 86 Thermal Displacements with Consideration of Fatigue Effects

5.4.2 Durability of Approach System

Since integral abutment bridge eliminates the bearings and joints, it reduces a lot the maintenance cost. And from the performance of the bridge, the structure itself would not have structural problem under thermal expansion and contraction as the bridge becomes super longer. However, thermal-induced displacement at the end of the bridge will become larger too, which would cause the large deformation on the approach pavements.

The maintenance of bridge approach pavements needs special attention. This is particularly important with pavement having deteriorated or failed (Burke Jr & Bugler, 2002). This also is the main reason that most of the states in USA limit the length of

the bridge by displacements (Table 1). As the bridge length increases, the approach slab (or sleeper) in approach system is required to apply, to mitigate the "bump at the end of bridge" (Arsoy et al., 1999) and the possible crackings on pavement or G/P phenomenon of jointed rigid pavement (Burke Jr, 2009).

It is reported that in the case of conventional bridges, much of the cost of maintenance is related to repair of damage at joints because such joints require periodic cleaning and replacement (Arsoy et al., 1999; Puppala et al., 2009). Other times, pavement patching at the ends of the bridge represents most of the maintenance costs. For longer bridges, the pavement patching lengths are longer due to problems experienced by the temperature induced cyclic movements. However, integral abutment bridges with approach slabs are reported to perform well with fewer maintenance problems than conventional bridges (Fig. 87). The development and construction details are discussed in Ch.7.2.
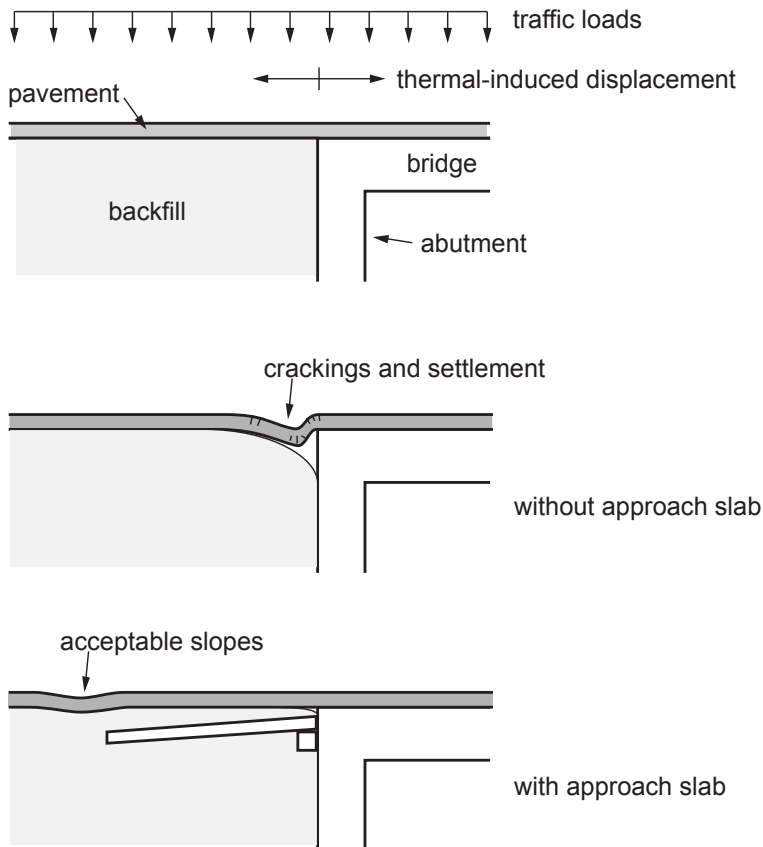
Fig. 87 Typical Consequences of Bridge – Approach System under Loads and Actions

Recently, to ensure that integral or semi-integral abutments will be durable and perform satisfactorily at the serviceability limit state, the thermal-induced displacement of more than 43mm at the end of the bridge with proper approach slab is numerically and experimentally verified as acceptable for Swiss standard (Dreier, 2010a; Dreier et al., 2011). Therefore, considering the durability of approach system, the corresponding length limit for integral abutment bridge could be more than 430m (assuming imposed temperature variation of 20°C).

6. OPTIMIZATION ON PILE DESIGN

In integral abutment bridge, piers and abutments generally need not be designed to resist horizontal loads applied to superstructures (Burke Jr, 2009). In fact, the horizontal loads are distributed complicatedly due to the interactions of soil-abutment and soil-pile, where the backfill earth pressure may take the larger proportion of 74%~88% of the applied load while shear force at the top of pile may take the small proportion of 12%~26% (Arsoy et al., 1999). This distribution might be caused by the geo-phenomenon of "ratcheting" (Horvath, 2004). Meanwhile, the displacement at the top of the pile nearly equals to the displacement at the top of stub-type abutment. Therefore, the piles should be designed to have the ability to accommodate the certain (lateral) shear force and large thermal-induced displacement. The current design optimization on piles shows that lateral loaded pile could be optimized for better performance with less material. With this purpose, the piles of integral abutment bridge, especially concrete piles, with fixed or pinned connection to the abutment, are going to be optimized with less material without failure in materials through a proposed design optimization approach.

6.1. Design of Pile

6.1.1 Pile Shape Design Optimization

For the laterally loaded piles, the beams surrounded by soil and laterally loaded at the top, are used as foundation structures usually with no or negligible axial loads, like, for example, in bridge abutments, retaining walls, off-shore wharfs, and the foundation piles of wind generators (Bowles, 1996). One of the simplified models in technical fields is to consider the laterally loaded beams surrounded by different materials to behave as beams in a Winkler medium, where earth pressure can be expressed as Terzaghi's equation Eq.(13) when k_h is constant.

Through fully stressed design (FSD) method with finite element method (FEM), the iterations of structural analysis and mass distribution would found out the optimum solution with minimum weight. And this kind of heuristic method has been used to

optimize the beam length and section dimension as shown in Fig. 88 (Fenu, 2005; Fenu, 2010).
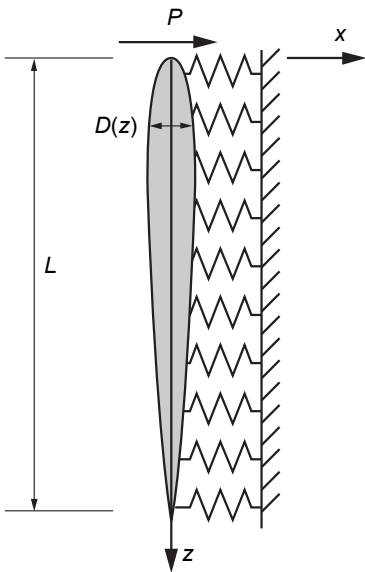
Fig. 88 Shape of Fully Stressed Beam with Optimum Length
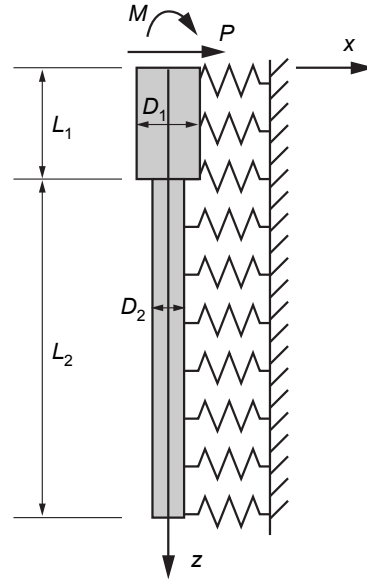
Fig. 89 Model of the R/C Bored Pile Made Up of Two Parts

However, in fact, the best mass distribution of laterally loaded piles is not achievable for real piles due to the difficulties in fabrication and shape casting as such a distribution should continuously change along the pile. Thus, for R/C bored piles, for example, the best mass distribution that can be achieved, by realizing bored piles with two parts with two different diameters (Fig. 89). The problem to be solved is then how to design it, that is which diameter and length chose for the upper and lower part respectively.

Besides, piles in different conditions and different structures, the design principles or objectives would be different. Most of the piles are required to have less displacement of pile head under the same loading (or saying stiffer) with the same or less pile length or volume, in purpose of making better use of materials.

6.1.2 Pile Design for Integral Abutment Bridge

Traditionally, a system of expansion joints, roller supports, and other structural releases has been provided on bridges to prevent damage caused by thermal expan-

sion and contraction of the superstructure with annual temperature variations. Expansion joints within the superstructure increase the initial cost of a bridge and often do not function properly after years of service unless they are extensively maintained. Thus, integral abutment bridges, which have no expansion joints within the span or at supports, provide a design alternative that potentially offers lower initial costs and lower maintenance costs. However, the piles in an integral abutment bridge are subjected to horizontal movements as the bridge expands and contracts.

Piles have been designed to be flexible under forces and moments acting on the abutment, in order to subject to horizontal movements as the bridge expands and contracts that caused by temperature variations. That is the reason that the piles are often installed with their weak axis of bending parallel to the bridge centreline in integral abutment bridges (Greimann et al., 1987; Wasserman, 2007).

Design details are offered on integral abutment piles in Recommendations (Franco, 1999). New York and Pennsylvania mention that piles should be designed for vertical and lateral loads and fixity between superstructure and pile top is ignored. Pennsylvania also states that piles should be analyzed for bending induced by superstructure movements. Maine provided a step-by-step design procedure for piles. Typically steel H-piles have been used in the substructure mainly in North America. Concrete and wooden piles are seldom used because of flexibility requirements. Some states (Virginia, Pennsylvania and New York) allow use of concrete encased-steel piles. Pennsylvania and New York specify that concrete encased piles are not to be used with spans greater than 150 feet (45.7 m). Virginia specifies only using concrete piles with a shelf abutment, similar to a spread footing on a set of piles. And, the majority of the states specified orienting piles on their weak axis, perpendicular to the direction of movement. Two states specified using strong axis orientation, and other states had specific criteria for which orientation to use. For instance, New York relates use of axis to length of span (weak axis for spans less than 90 feet / 27.4 m, strong axis for spans greater than 90 feet / 27.4 m).

For integral and semi-integral abutment bridges, the design optimization objectives of these types of pile are obviously different; the different abutment-pile connections would affect a lot on the design results. However, all of them could be dealt with through the same approach of design optimization proposed as following by different problem description.

6.2. Design Optimization Approach

In structural design, there are many parameters should be decided, such the materials types, components dimensions, sectional shapes, and so on. As a designer or engineer, it's necessary to find an optimum solution under the required conditions, in the purpose of economy and safety. Based on FEM discretization, the structural optimization is generalized as a nonlinear large-scale optimization problem. And the system will change when the meshing of model change due to the different design parameters.

The methods for solving the nonlinearly constrained optimization problem was developed from unconstrained optimization calculations with the fast convergence of Newton's method (Powell, 1978). And, the methods and algorithms, like interior point method, sequential quadratic programming, barrier method, trust region method, were introduced for the treatment of inequality constraints (Byrd et al., 1999; Gill et al., 2002; Waltz et al., 2006).

6.2.1 Optimization Problem Description

Generally, the independent variables in an optimization problem are the design variables (DV). The vector of design variables is indicated by:

$$\mathbf{x} = \begin{bmatrix} x_1 & x_2 & \cdots & x_n \end{bmatrix} \tag{57}$$

Design variables are subject to *n* constraints with upper and lower limits, that is,

$$\underline{x}_i \le x_i \le \overline{x}_i \quad \left(i = 1, \, 2, \cdots, n \right) \tag{58}$$

where: *n* = number of design variables. The design variable constraints are often referred to as side constraints and define what is commonly called feasible design space. Now, minimize

$$f = f\left(\mathbf{x} \right) \tag{59}$$

subject to

$$g_i(\mathbf{x}) \le \bar{g}_i \qquad (i = 1,\, 2, \cdots, m_1)$$
$$\underline{h}_i \le h_i(\mathbf{x}) \qquad (i = 1,\, 2, \cdots, m_2) \qquad\qquad (60)$$
$$\underline{w}_i \le w_i(\mathbf{x}) \le \bar{w}_i \qquad (i = 1,\, 2, \cdots, m_3)$$

where: f = objective function (OBJ); g_i, h_i, w_i = state variables containing the design, with under-bars and over-bars representing lower and upper bounds respectively, called constraints function (CON); $m_1 + m_2 + m_3$ = number of state variables constraints with various upper and lower limit values. The state variables can also be referred to as dependent variables in that they vary with the vector $\mathbf{x}$ of design variables, in forms of equality and inequality equations. The objective function in structural optimization is usually considered as the total volume (or weight) of the components or certain material (like steel); and deflection and stress are usually chosen as state variables to control the behavior of the structure after optimized.

Design configurations with certain values of design variables that satisfy all constraints are referred to as feasible designs. Design configurations with one or more violations are termed infeasible. In defining feasible design space, a tolerance is added to each state variable limit.

As design sets are generated by methods or tools (e.g. subproblem approximation method) and if an objective function is defined, the best design set is computed and its number is stored. The best set is determined if one or more feasible sets exist the best design set is the feasible one with the lowest objective function value. In other words, it is the set that most closely agrees with the mathematical goals expressed.

For example, the pile to be optimized consists of two different parts with circular solid section of reinforced concrete as shown in Fig. 89, with the design purpose of minimizing the displacement using better the structural materials. Then this optimization problem can be described as:

Design Variables (DV): section diameter D_1, D_2, and length L_1, L_2;
Constraints Function (CON): bending moment in pile, $M < M_R$, or stresses in concrete and reinforcement $\sigma_c < f_{ck}$, $\sigma_s < f_{yd}$; and keeping the same total volume V_{tot} = const.
Objective Function (OBJ): pile head displacement v_0.

6.2.2 Programs Implemented for Optimization

In the optimization module of ANSYS ("Design Optimization" tool integrated in ANSYS (ANSYS Inc., 2007), two methods are available. In the Subproblem Approximation method (SA), the objective function is replaced by an approximation based on the function values calculated in previous iterations. This method makes no use of derivative information. The First Order Optimization method (FOO) is a line search method in which gradient information is used to determine a decent search direction. The ANSYS program converts the constrained problem to an unconstrained optimization problem because minimization techniques for the latter are more efficient. The conversion is done by adding penalties to the objective function approximation to account for the imposed constraints. The search for a minimum of the unconstrained objective function approximation is then carried out by applying a Sequential Unconstrained Minimization Technique (SUMT) at each iteration.

These methods are rather limited for realistic problems. Instead, tool of MATLAB is established to extend the possibilities and to have better control on the process. There are two methods in the "Optimization" toolbox of MATLAB (MathWorks Inc., 2011). The first, *fmincon*, is a trust region method in which derivative information is used to compute a good approximation of the objective function in a small trust region. The second, *lsqnonlin*, uses specific least squares techniques. From the comparison of these 4 methods (Arnout et al., 2008), only the SA-method of ANSYS is apparently less efficient, the other methods are competitive.

However, the mentioned methods above are all local, so there is uncertainty about the nature of the optimum and strong dependence on the initial starting values. If the starting point is too near a local minimum, it may find that point instead of the global minimum.

Therefore, the method of the Coupled Local Minimizers (CLM) is implemented. CLM is a recently developed global optimization technique (Suykens et al., 2001; Teughels et al., 2003; MathWorks Inc., 2011). In this method, the information of several local optimizers is combined to avoid local optima. The local optimizations are started from random points over the domain, and constraints are imposed to force the search points to end up in the same point. In a successful run, this point has the lowest function value, and is the global minimum. The reliability of this method is due to the evaluation of a lot of points, spread over the domain. The advantage compared to other global methods is the use of first order information, which enforces faster convergence. To reduce calculation time, this method is used

to identify the global minimum with a limited precision. When the search points have located the valley of the global minimum, the CLM-method is stopped and a local method is used until the necessary precision is reached.
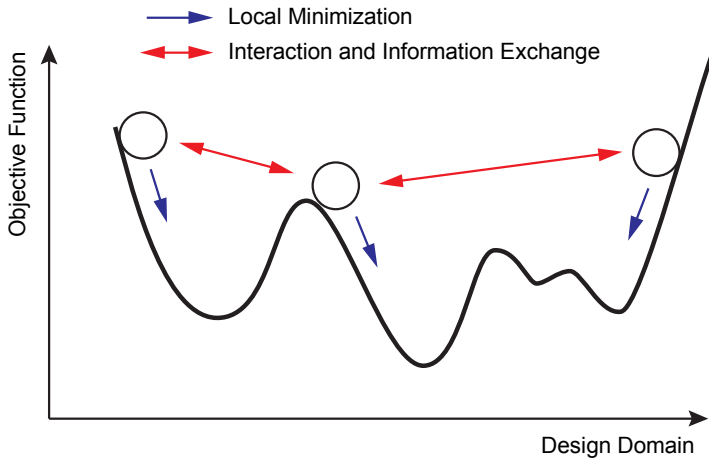
Fig. 90 Illustration of Coupled Local Minimizers

6.2.3 Optimization Procedure

Based on the global optimization algorithm, the frame of optimization approach is illustrated as following flowchart in Fig. 91. In the presented procedure, it is collaborated with main coding program of MATLAB and finite element modeler and solver of OpenSees. The finite element modeling in OpenSees and its advantage in saving computation time will be introduced in next section.

In this procedure, based on the optimization description, firstly, the design variables were assigned. Then their values were wrote to file and passed to subroutines that computes the objective function and constraint function, where, the finite element modelling and solving part might be called according objective and constraint required.

Based on these loops of creating design variables (DV) then calculating constraints (SV/CON) and objectives (OBJ), the sampling of the optimization problem was passed to the "Global Optimization" setup. Then, by setting some control parameters of global search, such as variables tolerances, maximum iteration number and search step size, coupled local minimizers would be launched, until the converged

145

optimal solution was found, or an unconverged results if tolerances or maximum iteration numbers were reached.
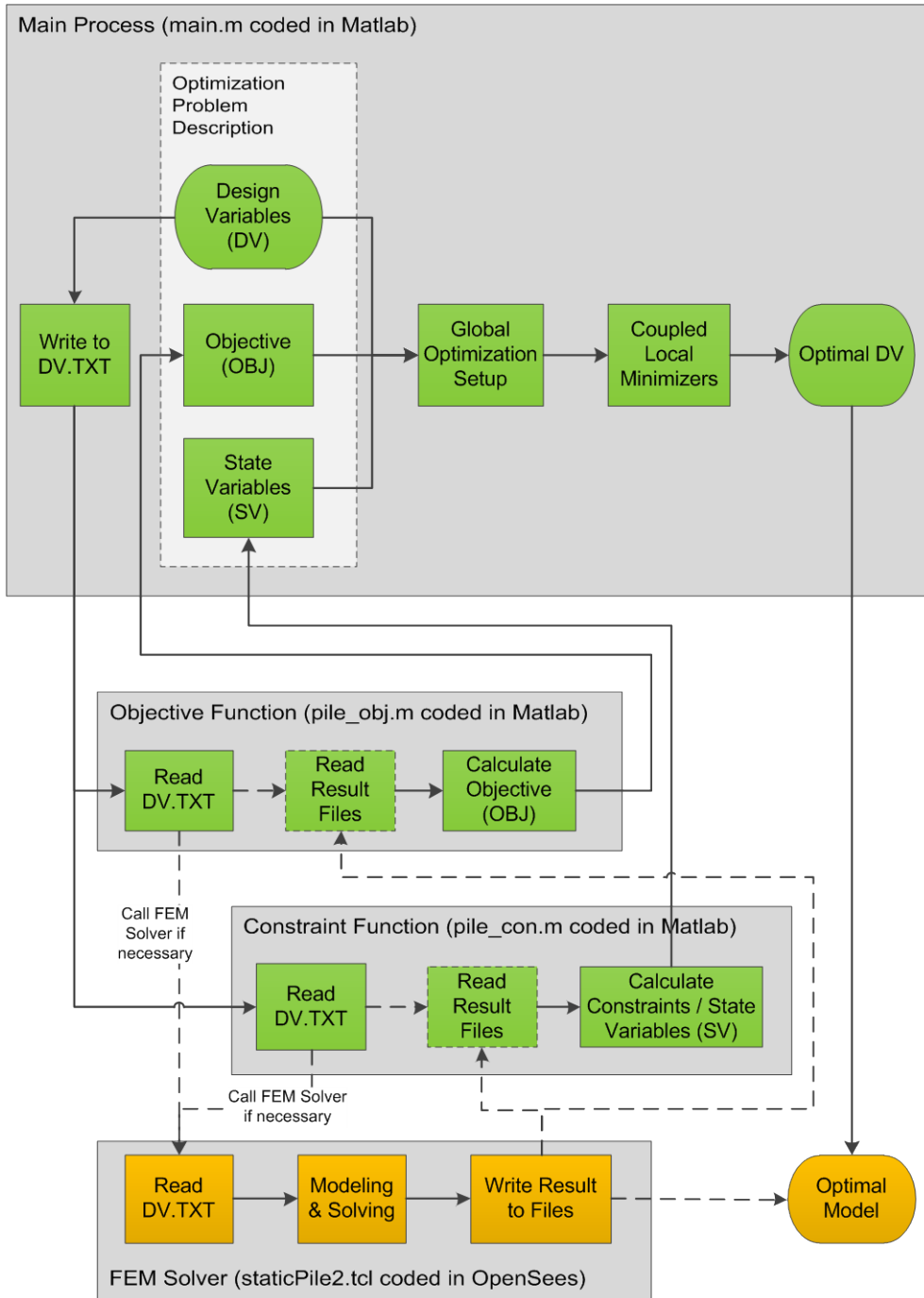
Fig. 91 Frame of the Optimization Programming

6.2.4 Finite Element Modeling of Pile

As stated and studied above, the most common method employed for the numerical analysis of piles under lateral loads is the *p-y* method. In this method, the three-dimensional (3D) laterally loaded pile problem is analysed by using a beam on non-linear Winkler foundation (BNWF) approach in which uncoupled one-dimensional (1D) springs are used to describe the soil-pile interaction. Therefore, despite known shortcomings inherent to the method, the *p-y* approach can be used successfully in many types of lateral pile analysis. To this purpose, Finite element simulations were conducted using the open-source FE framework of OpenSees (The Open System for Earthquake Engineering Simulation) (OpenSees, 2011). Embedded in this open-source software, the soils materials models are based on API recommendation and fiber section are available for building pile concrete sections. Besides, the important advantage of OpenSees is that it can easily interact and exchange the data with MATLAB through file operations during the process of optimization.

The model was adapted from a simple example of OpenSees - a beam on a nonlinear Winkler foundation (BNWF) (McGann & Arduino, 2011; McGann et al., 2011), and then developed by applying fibre section and non-linear materials properties. Besides, in the example of optimization of integral abutment bridge pile design, the pile of Isola della Scala Bridge was taken from the global model: the forces obtained on the pile head were applied as the loads on pile; the same soils condition was considered; the geometry and section properties were all taken as starting values for optimization.

Model Description
In the model of the laterally-loaded pile problem, displacement-based beam elements are used to represent the pile and a series of nonlinear springs to represent the soil. The soil springs are generated using zero-length elements assigned separate uniaxial material objects in the lateral and vertical directions. An idealized schematic of the laterally-loaded pile model is provided in Fig. 92.
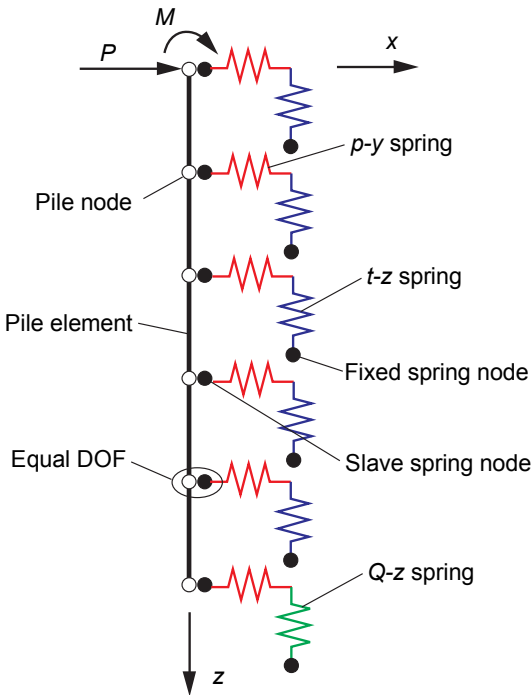
Fig. 92 Pile Modeling in OpenSees

Spring Constitutive Behavior

The constitutive behavior of the springs is defined such that the springs oriented in the lateral direction represent *p-y* springs, and the vertically-oriented springs represent *t-z* and *Q-z* springs for the pile shaft and tip, respectively. Zero-length elements are used for the soil springs using the element zeroLength. These elements connect the fixed and slave spring nodes. The PySimple1 material objects are incorporated in the x-direction (direction of loading), while the TzSimple1, and at the pile tip, the QzSimple1, material objects are incorporated in the z-direction (vertical direction).

The equations describing PySimple1 behavior are described as backbone of *p-y* curve approximates Matlock (1970) soft clay relation (when soilType = 1) and backbone of *p-y* curve approximates API (1993) sand relation (when soilType = 2) (Boulanger et al., 1999). Similarly, TzSimple1 material are defined as backbone of *t-z* curve approximates Reese and O'Neill (1987) (when soilType = 1) and backbone of *t-z* curve approximates Mosher (1984) relation (when soilType = 2). And QzSimple1 implemented as the backbone of q-z curve approximates Reese and O'Neill's (1987) relation for drilled shafts in clay (when qzType = 1) and backbone of q-z

curve approximates Vijayvergiya's (1977) relation for piles in sand (when qzType = 2). (Jeremić, 2001; OpenSees, 2011)

The constitutive behaviors of these uniaxial material objects are set up to automatically generate the required spring material objects based upon the input geometry and soil properties in the modeling input file.

Pile Constitutive Behavior and Elements

Displacement-based beam element, element dispBeamColumn, which is based on the displacement formulation and considers the spread of plasticity along the element, was used to facilitate incorporation of elastoplastic pile section behavior using fiber section models. A fiber section has a general geometric configuration formed by subregions of simpler, regular shapes (e.g. quadrilateral, circular and triangular regions). In addition, layers of reinforcement bars can be specified. Individual fibers, however, can also be defined and associated with uniaxialMaterial objects, which enforce Bernoulli beam assumptions. In this model, uniaxialMaterial Steel02, uniaxial Giuffre-Menegotto-Pinto steel material object with isotropic strain hardening, was used for reinforcement; uniaxialMaterial Concrete02, uniaxial concrete material object with tensile strength and linear tension softening (a Fedeas Material), was used for confined and unconfined concrete. The geometric parameters are defined with respect to a planar local coordinate system (y, z) as shown in Fig. 93.
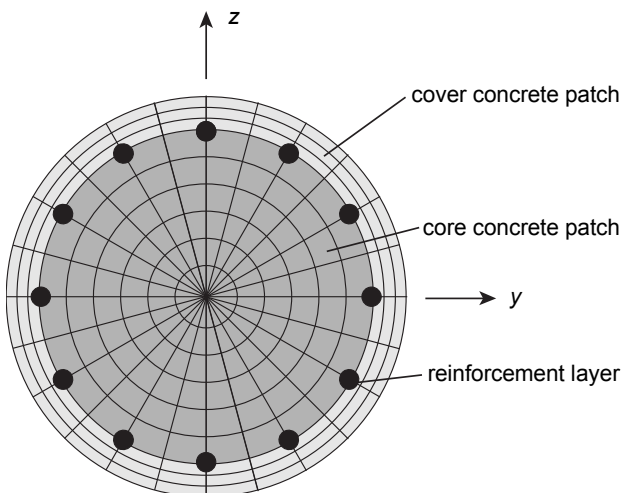
Fig. 93 Example of Fiber Section of Reinforced Concrete

The pile nodes over the embedded length of the pile are use linked with the slave spring nodes (using equalDOF command). The pile nodes are the master nodes in

this example. These two sets of nodes share equal degrees-of-freedom in the x- and z- translational directions only.

6.2.5 Verification with Lateral Loaded Pile

The lateral loaded pile, usually considered as surrounded by Winkler soil, is widely designed and used in many structures (Fenu & Serra, 1995). Therefore, as a design optimization problem, the pile with changing diameter is implemented through finite element method, where its top displacement is minimized by varying the design variables that are the dimensions of each of the two pile parts needed to describe it.

For example, consider an R/C bored pile laterally loaded at the top by a force P = 100 kN (M = 0, considering pile-abutment is pin connection). The unitary coefficient of subgrade reaction of the earth is k_h = 11.1 MPa, that is referred to a cohesive soil with undrained cohesion c_u=0.166 MPa. The Young's modulus of the concrete is E_c=25000 MPa. The parameters values (linear materials) were the same as a design example presented by Fenu (Fenu & Madama, 2006), where, the exhaustive enumeration search were used to find out the optimal solution, instead of using algorithm of global optimization.

This optimization problem can be described through defining design variables, state variables (constraints) and objective, and their initial values and optimization ranges are listed in Table 22. The procedure is starting from a pile with total volume of 2 m^3 and uniform section of diameter of 0.6 m.

The converged result obtained through the optimization procedure are shown in Fig. 95, where the pile is made up of two diameters has the upper part with D_1 = 1.305 m and L_1 = 0.79 m, and the lower part with D_2 = 0.500 m and L_2 = 4.79 m, which was the verified as the same optimum solution found out by Fenu's exhaustive enumeration search (optimal discrete variables L_1 = 0.8 m, L_2 = 4.8 m, D_1 = 1.3 m, D_2 = 0.5 m). This optimization procedure is also verified with the solutions with different type to sections, like hollow circular section, and more different parts of pile, as the optimum solutions obtained already (Fenu & Madama, 2006).

Therefore, for a pile in integral abutment bridge, in the following text, the same optimization procedure would be applied with different problem description and different modeling conditions, in order to find out the optimal pile profile for an integral abutment bridge.

Problem Description	Parameters		Initial	Limits	Optimal
Design Variables	length of part 1	L_1 (m)	1.0	0.5 ~ 2.0	0.790
	length of part 2	L_2 (m)	5.6	5.0 ~ 8.0	4.790
	diameter of part 1	D_1 (m)	0.6	0.5 ~ 1.5	1.305
	diameter of part 2	D_2 (m)	0.6	0.5 ~ 1.0	0.500
State Variables / Constraints	total volume	V_{tot} (m^3)	2.0	difference < 0.5%	1.997
Objective	displacement of pile head	d_0 (mm)	10.3	minimum	8.3

Table 22
Optimization Problem of Lateral Loaded Pile
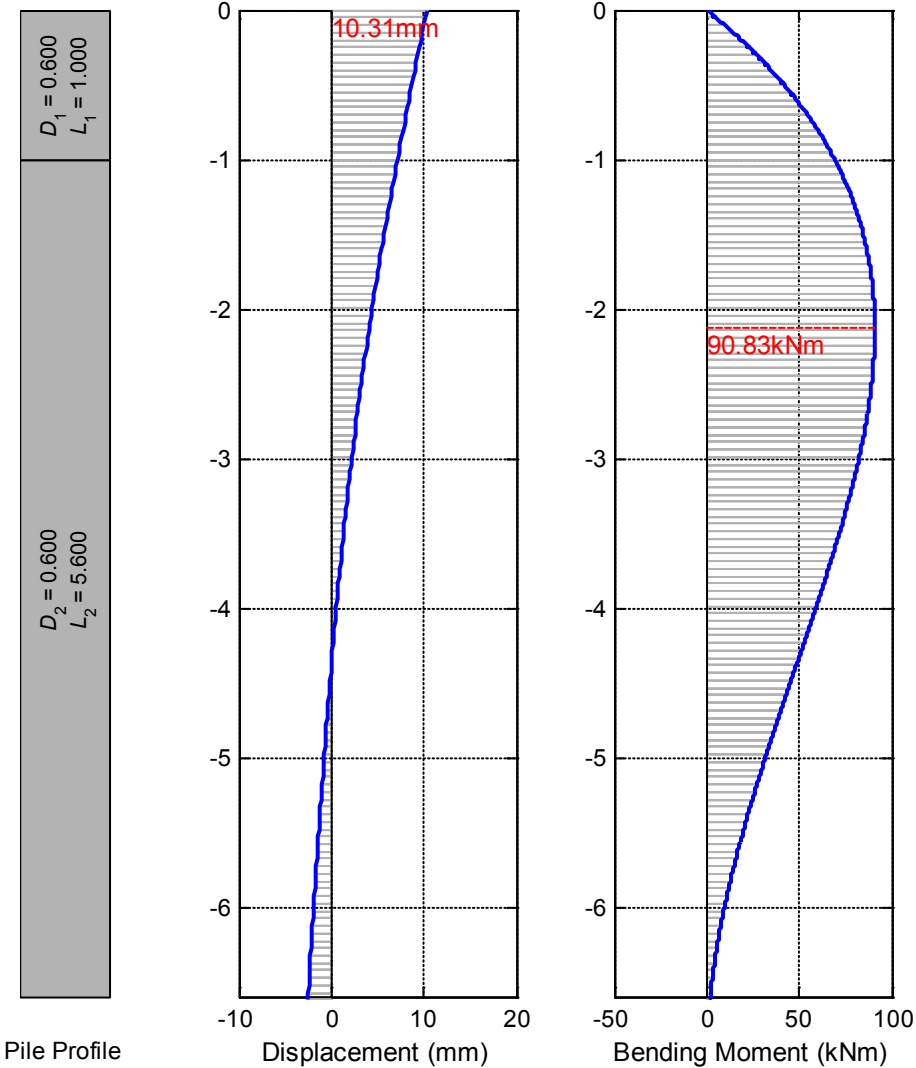
Fig. 94 Stating Profile of Lateral Loaded Pile
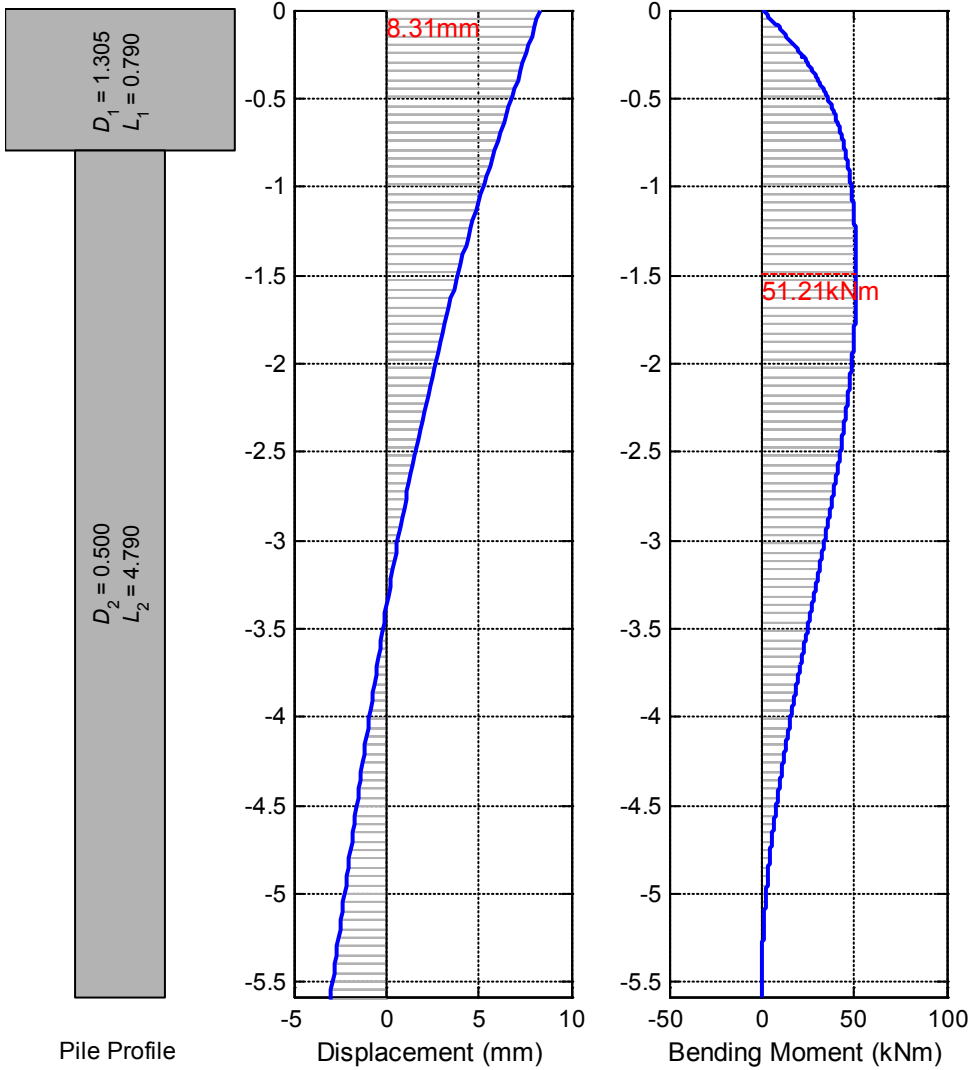
Fig. 95 Optimized Profile of Lateral Loaded R/C Pile

6.3. Optimized Design of Pile Shape

Although this surrounded Winkler's soil is precise enough comparing to continuous elastic semi-space model, in many cases, the length of the piles are long that would usually penetrate several layers of soil underground. Also, the reaction of the soil would vary significantly with depth in deep layers. Moreover, in integral abutment bridges, the large thermal induced displacement would come up and lead to the yielding of soils, of which the behaviors are non-linear in soil springs and sections of pile. Therefore, a real soil condition and non-linear material properties are going to be considered along the pile as described in pile model for integral abutment bridge implemented in OpenSees.

6.3.1 Pile Size Limits Considering Ultimate Axial Load

To perform the optimization on pile design, the conditions of Isola della Scala Bridge for piles were taken as example. Considered as a friction pile, in order to have enough friction length for pile (Greimann et al., 1987), the total length of the pile is constrained to original length of 15 m. And from the analyses of full bridge model, the maximum axial load on the pile is about 2000 kN. Therefore, a lower bound of size of the pile with respect to this length and axial load need to be found. According to the Rankine equation and circular concrete section resistances (Greimann et al., 1987; Tlustochowicz, 2005; MOHURD, 2010), the ultimate load N_u can be expressed as Eq.(61).

$$\frac{1}{N_u} = \frac{1}{N_{cr}} + \frac{1}{N_{pl}} \tag{61}$$

where, N_{cr} = elastic buckling load, and N_{pl} = plastic capacity, could be calculated according to Table 23. In Table 23, where, k_h = the initial stiffness of the soil; n_h = constant of subgrade reaction ($n_h = k_h/z$); N_p, M_p = section resistance, which could be estimated through Eqs.(62) and (63); d_0 = displacement of pile head (assuming a large displacement of d_0 = 50 mm).

$$N_p = \alpha f_{cd} A \left(1 - \frac{\sin 2\pi\alpha}{2\pi\alpha} \right) + (\alpha - \alpha_t) f_{yd} A_s \tag{62}$$

$$M_p \approx \frac{1}{3} f_{cd} AD \frac{\sin^3 \pi\alpha}{\pi} + f_{yd} A_s \left(\frac{D}{2} - a \right) \frac{\sin \pi\alpha + \sin \pi\alpha_t}{\pi} \tag{63}$$

where, α = compression concrete central angle ratio (assuming compression area of half section, α = 0.5); α_t = tension reinforcement ratio (α_t = 1.25 - 2α, when $\alpha <$ 0.625); a = concrete cover thickness (a = 0.04 m); A = section area; A_s = reinforcement area (assuming A_s/A = 1.5%); D = section diameter; f_{cd} = concrete design strength (Table 10); f_{yd} = reinforcement design strength (Table 10). By this assumed values, and the conservative buckling consideration of soft clay soil with k_h = 1.742 MPa, it's found that the governing factor for this pile is plastic capacity N_p. And the resulting ultimate loads are plotted in Fig. 96.

Capacities		Pinned pile head	Fixed pile head
Elastic buckling load N_{cr}	constant soil stiffness	$2.0\sqrt{k_h EI}$	$2.5\sqrt{k_h EI}$
	linearly varying soil stiffness	$2.3(EI)^{\frac{3}{5}}(n_h)^{\frac{2}{5}}$	$4.2(EI)^{\frac{3}{7}}(n_h)^{\frac{2}{5}}$
Plastic capacity N_{pl}	lateral deflection effect	$\frac{2M_p}{d_0}$ ($\leq N_p$)	$\frac{4M_p}{d_0}$ ($\leq N_p$)

Table 23
Calculation Formulae for Axial Capacity of Pile
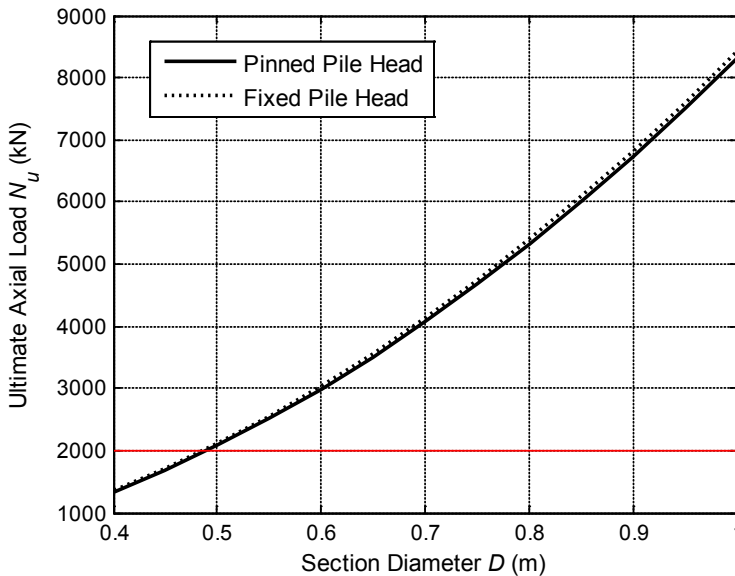
Fig. 96 Ultimate Loads Referring to Different Section Diameter

Therefore, for the considerations of axial plastic capability and stability for the length of 15 m under the maximum equivalent axial load of about 2000 kN, the lower bound of pile diameter is set as 0.5 m, and the vertical load thus will be ignored during the following optimization calculations.

6.3.2 Pile Optimization for Isola della Scala Bridge

The pile is modeled as the substructure of previous model of Isola della Scala Bridge, where the loads are considered as a lateral force load of 857 kN (in the x-direction) and a bending moment of 358 kNm (in the y-direction), applied at the head of the pile (uppermost pile node); since the axial compression will increase the section resistance, the axial load was neglected. The surrounding soil properties are listed in Table 24. The pile to be optimized is with circular solid sections of concrete with reinforcement ratio of 1.5%, cover thickness of 40 mm, and the initial sections diameter $D_1 = D_2 = 1.2$ m; initial length of pile $L_1 = 5$ m, $L_2 = 10$ m, as shown in Table 25 and Fig. 97.

The converged result was obtained through optimization procedure. The optimal pile profile is shown in Fig. 98. Under the same loads the optimized pile is of more flexibility, large displacement, with volume reduction from 16.965 m^3 to 8.503 m^3, nearly 50%. And the stresses both in concrete and reinforcement are well controlled as setting limits. Considering the long-term effects, these limits might be set with a reduction factor and resulting a conservative solution for service state. However, in this case study, the loads were taken from ultimate state condition, which could be thought as more conservative.

Besides fixing the reinforcement ratio, some pile designers prefer to vary the reinforcement ratio instead of section diameter. However, the problem would be essentially the same. Through the optimization procedure presented, the optimal reinforcement ratio distribution would be found out for guiding the design. However, to realize these kinds of multi-section piles, efficient connections between different parts are necessary, which would make the construction complicated. This could cause more cost in time, technical, and economy. Since the filling piles and prefabricated piles of uniform section are quite widely used in engineering practice, it's of more worth to optimize the uniform section pile. In that case, it reduces the number of design variables, the optimization procedure would be more effective, which will be discussed in next section.

Depth (m)	Soil type	γ (kN/m^3)	φ (°)	c_u (kN/m^3)	with free water
0.0 to -2.8	Sand	18.5	33	-	no
-2.8 to -4.6	Sand	18.5	33	-	yes
-4.6 to -6.8	Clay	18.5	-	26	yes
-6.8 to -25.0	Sand	18.5	30	-	yes

Table 24
Soil Properties for Piles in Integral Abutment Bridge

Problem Description	Parameters		Initial	Limits	Optimal
Design Variables	length of part 1	L_1 (m)	5.0	1.0 ~ 5.0	7.169
	length of part 2	L_2 (m)	10.0	5.0 ~ 15	7.831
	diameter of part 1	D_1 (m)	1.2	1.0 ~ 2.0	1.088
	diameter of part 2	D_2 (m)	1.2	0.5 ~ 1.5	0.501
State Variables / Constraints	total length	$L_1 + L_2$ (m)	15.0	difference < 5%	15.0
	stress in concrete	σ_c (MPa)	13.09	< 30	19.42
	stress in rein-forcement	σ_s (MPa)	195.56	< 330	329.94
Objective	total volume	V_{tot} (m^3)	16.965	minimum	8.209

Table 25
Optimization Problem of Pile in Integral Abutment Bridge
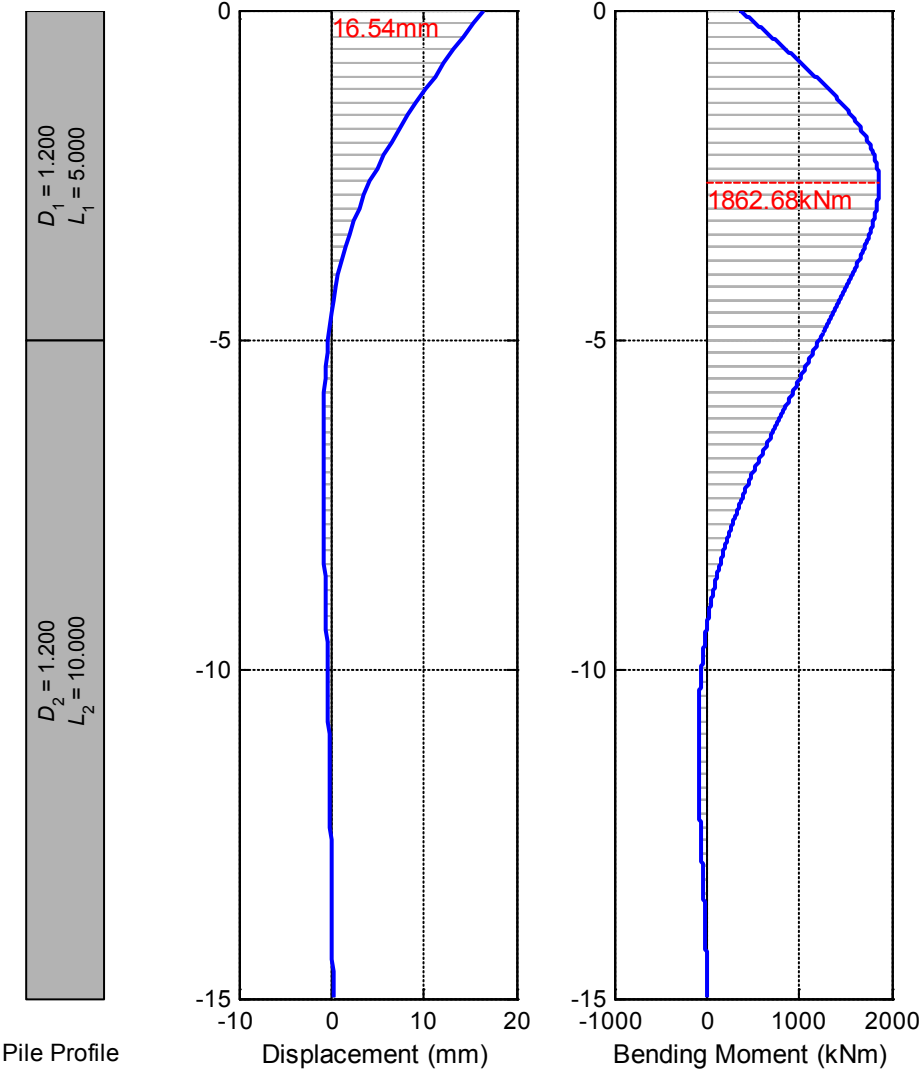
a) displacement and bending moment
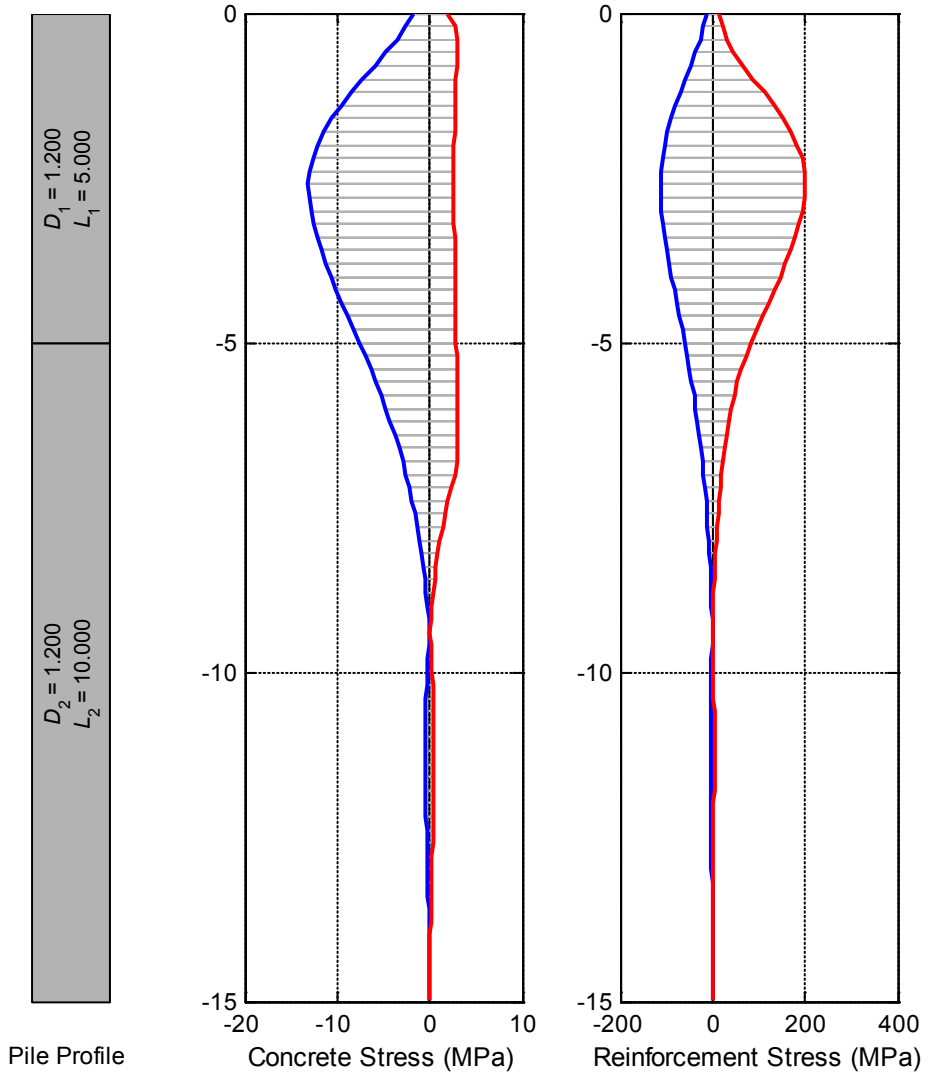
b) stresss in concrete and reinforcement

Fig. 97 Original Profile of R/C Pile in Integral Abutment Bridge
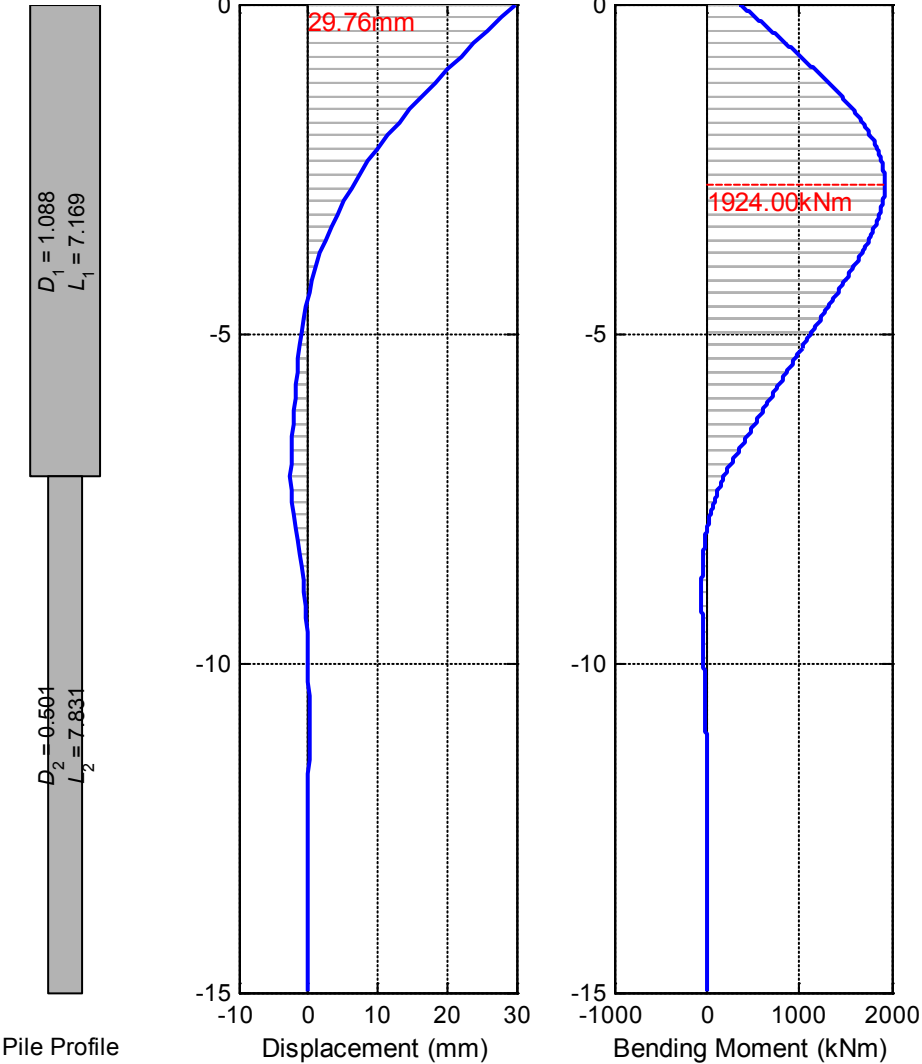
a) displacement and bending moment
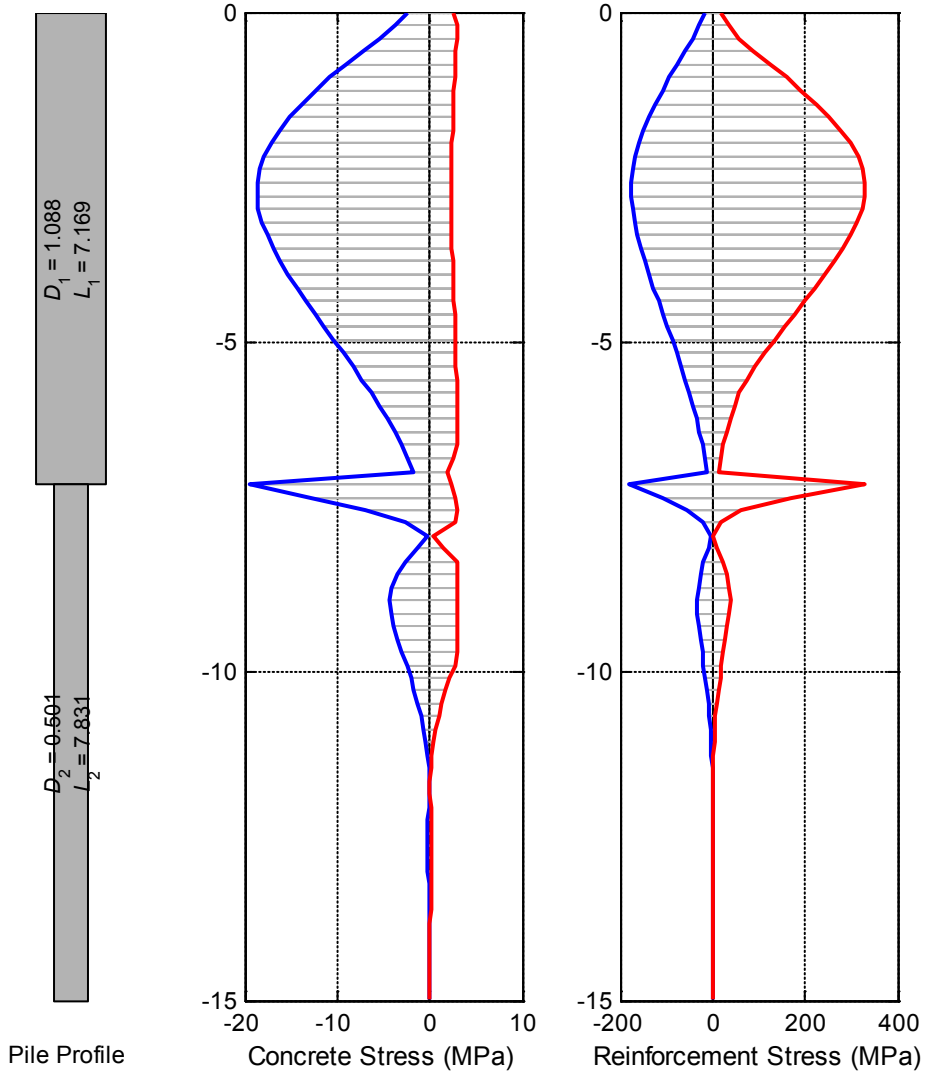
b) stress in concrete and reinforcement

Fig. 98 Optimized Profile of R/C Pile in Integral Abutment Bridge

6.3.3 Pre-Hole Effects on Pile Design

For integral abutment bridges, it is commonly thought that a foundation that is rotationally and translationally stiff results in larger superstructure loads during thermal loading. In order to increase the lateral and rotational flexibility of the pile head, piles for an integral abutment bridge foundation are often driven into pre-augered (or pre-drilled) deep holes which are then backfilled with loose sand (Wasserman, 2007). Drilling a pilot hole for some top portion of the pile and then backfilling the hole with some type of loose backfill material creates a hinge-effect in the substructure. This increases the flexibility of the piles and the substructure. Massachusetts specifies pre-augering to a depth of 5 feet (1.5 m), New York to 8 feet (2.4 m), Pennsylvania, and Maine to 10 feet (3.0 m). New York backfills this hole with sand, Massachusetts fills with pea stone gravel, and Maine uses dense gravel. It has been shown from the analyses (Thanasattayawibul, 2006) that piles in 9 feet (2.7 m) deep predrilled holes filled with loose sand have a significant reduction in the equivalent stress and the displacements in the piles.

Since this treatment increases deformability of pile head, and reduce stress concentration on pile head, and the durability of pile will be improved, the shape optimization with depth of the pre-hole is going to be performed. Considering the same optimization problem as stated above, and taking into account convenience in fabrication and casting, pile is with uniform section along the length, with the section of circular solid diameter of 1.2 m, reinforcement ratio of 1.5% and cover concrete of 40 mm. The starting profile is shown in Fig. 99. Then the optimization problem can be described as listed in Table 26.

The resulting optimal solution through optimization is shown in Fig. 100. Comparing to the starting profile as shown in Fig. 99, the optimized solution is with smaller diameter and shallow pre-hole depth, while with few increment in flexibility (the limited displacement increment). And, compared with the optimized profile as shown in Fig. 98, it can be found that the flexibilities of these three solutions are in the same level; the optimal profile without pre-hole could reach the least volume expense (reduction of 50%); and the pile of uniform section with less volume reduction (reduction of 25%) and a shallow pre-hole. Therefore, in the purpose of economical pile, the designers need to balance the saving between volume reduction and multi-section casting, according to the specified field conditions.

Problem Description	Parameters		Initial	Limits	Optimal
Design Variables	length of part 1 (pre-hole depth)	L_1 (m)	2.0	0.2 ~ 5.0	0.225
	length of part 2 (embedded part)	L_2 (m)	13.0	5.0 ~ 15	14.775
	diameter of pile	D (m)	1.2	0.8 ~ 1.2	1.031
State Variables / Constraints	total length	$L_1 + L_2$ (m)	15.0	difference < 5%	15.0
	stress in concrete	σ_c (MPa)	18.34	< 30	21.31
	stress in reinforcement	σ_s (MPa)	249.67	< 330	329.02
Objective	total volume	V_{tot} (m^3)	16.965	minimum	12.523

Table 26
Optimization Problem of Pile with Pre-Hole

a) displacement and bending moment

Diameter = 1.200
Pre-Hole Depth = 2.000

Pile Profile

Concrete Stress (MPa)
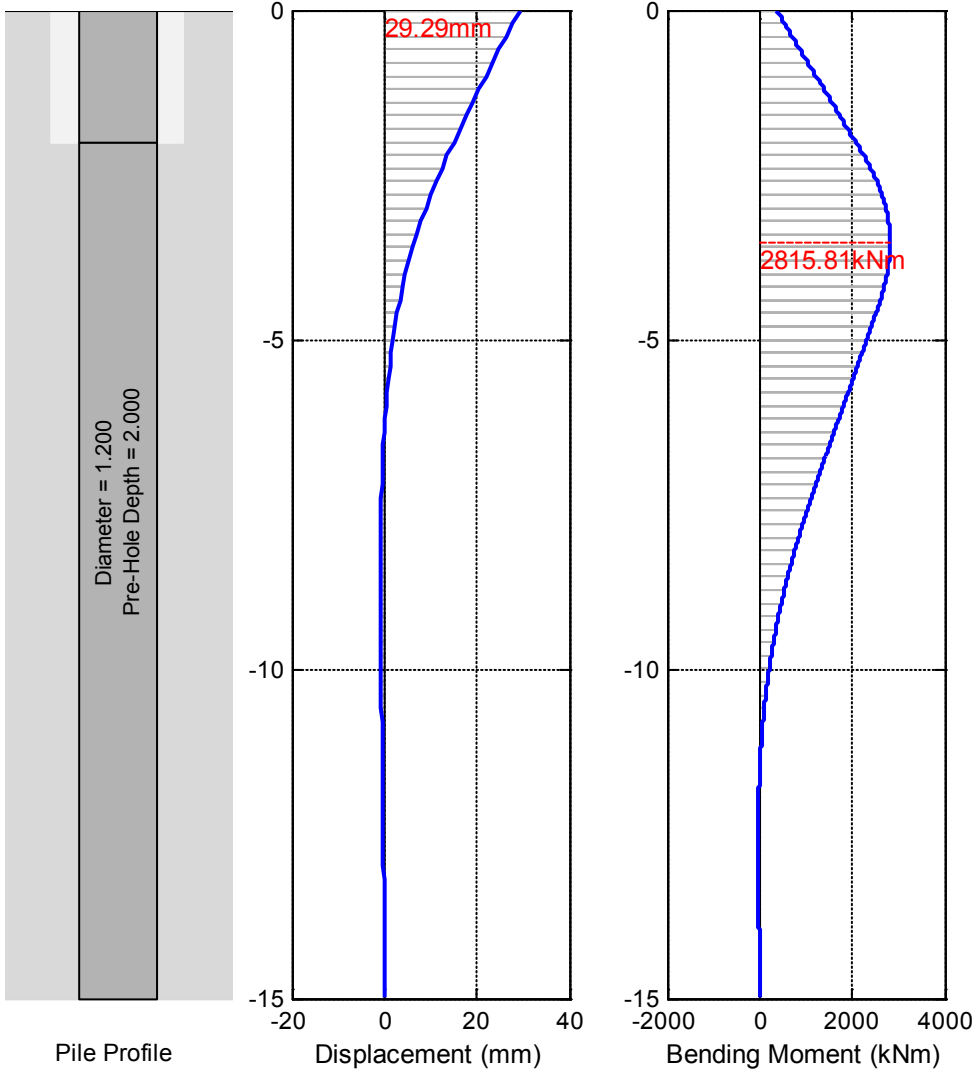
Reinforcement Stress (MPa)
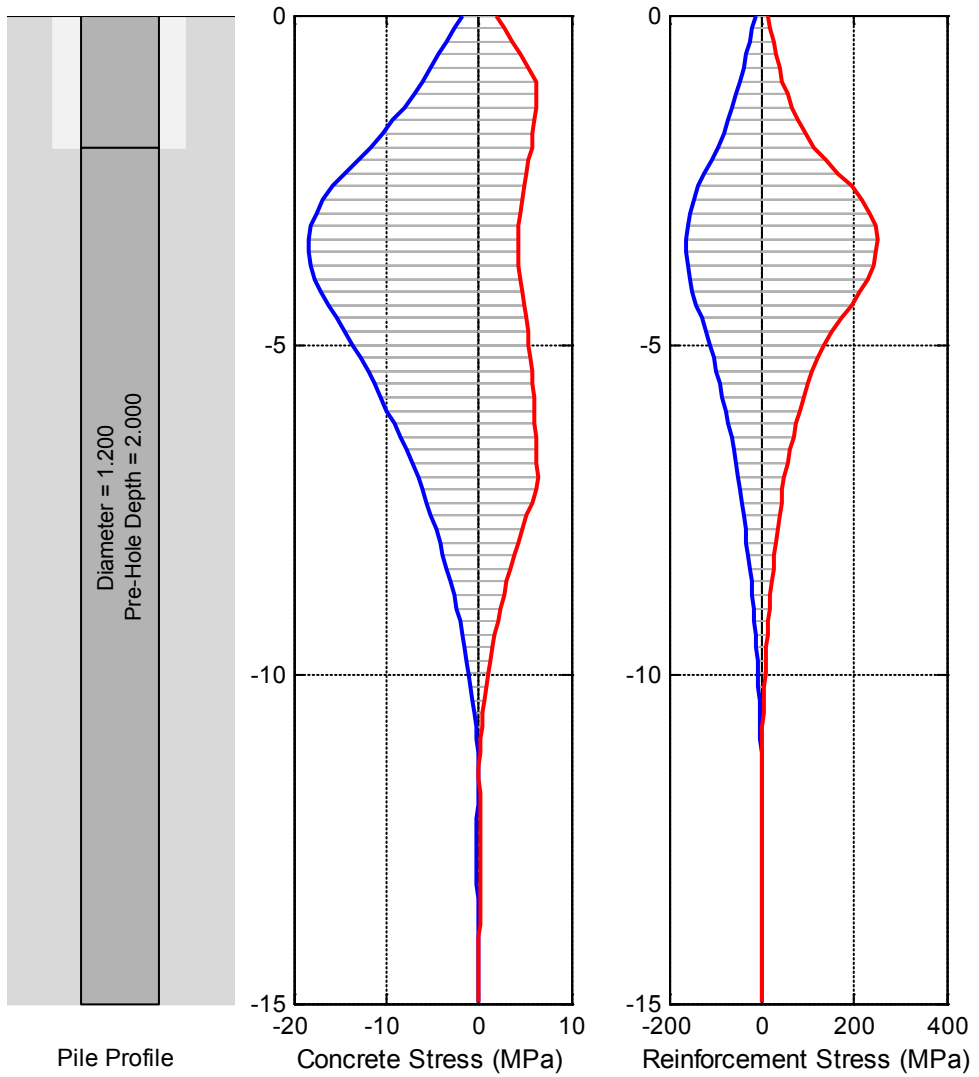
b) stress of concrete and reinforcement

Fig. 99 Starting Profile of R/C Pile with Pre-Hole

a) displacement and bending moment

Diameter = 1.031
Pre-Hole Depth = 0.225

Pile Profile

Concrete Stress (MPa)
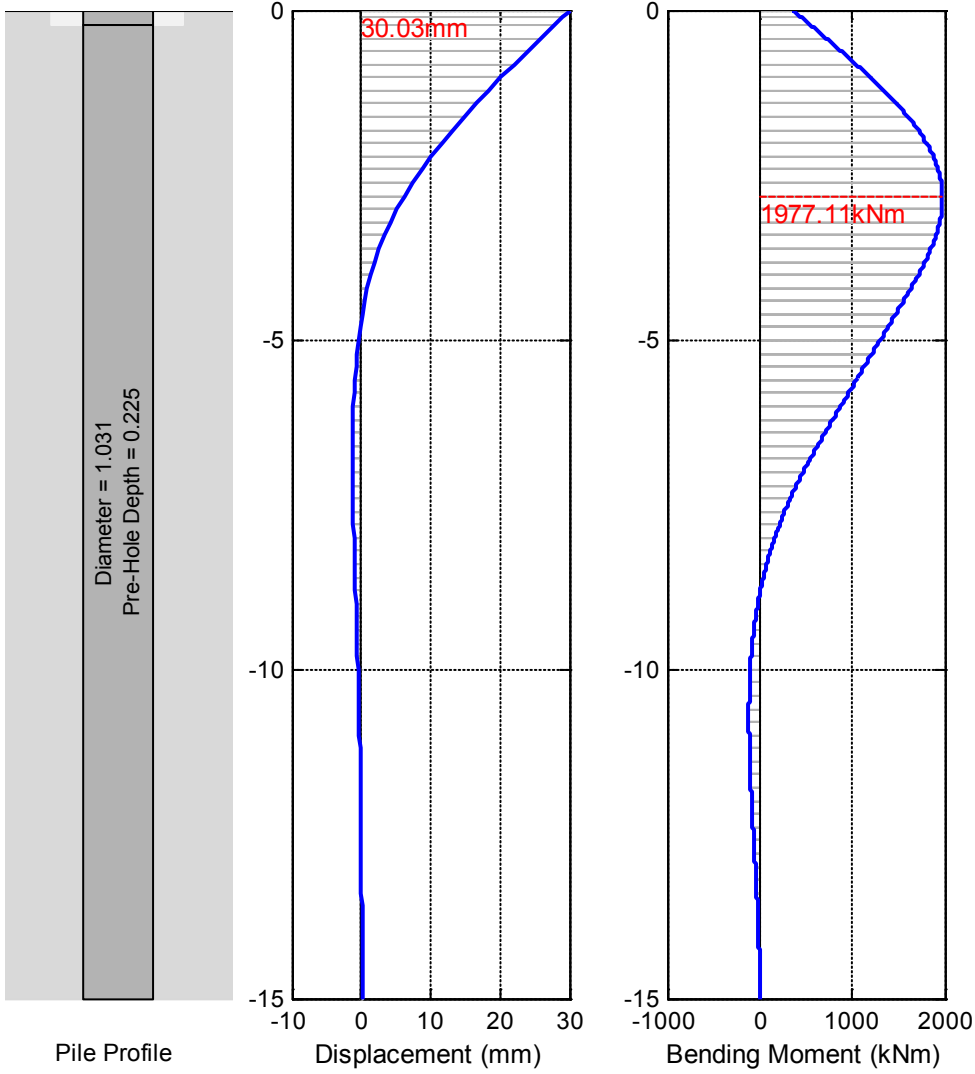
Reinforcement Stress (MPa)
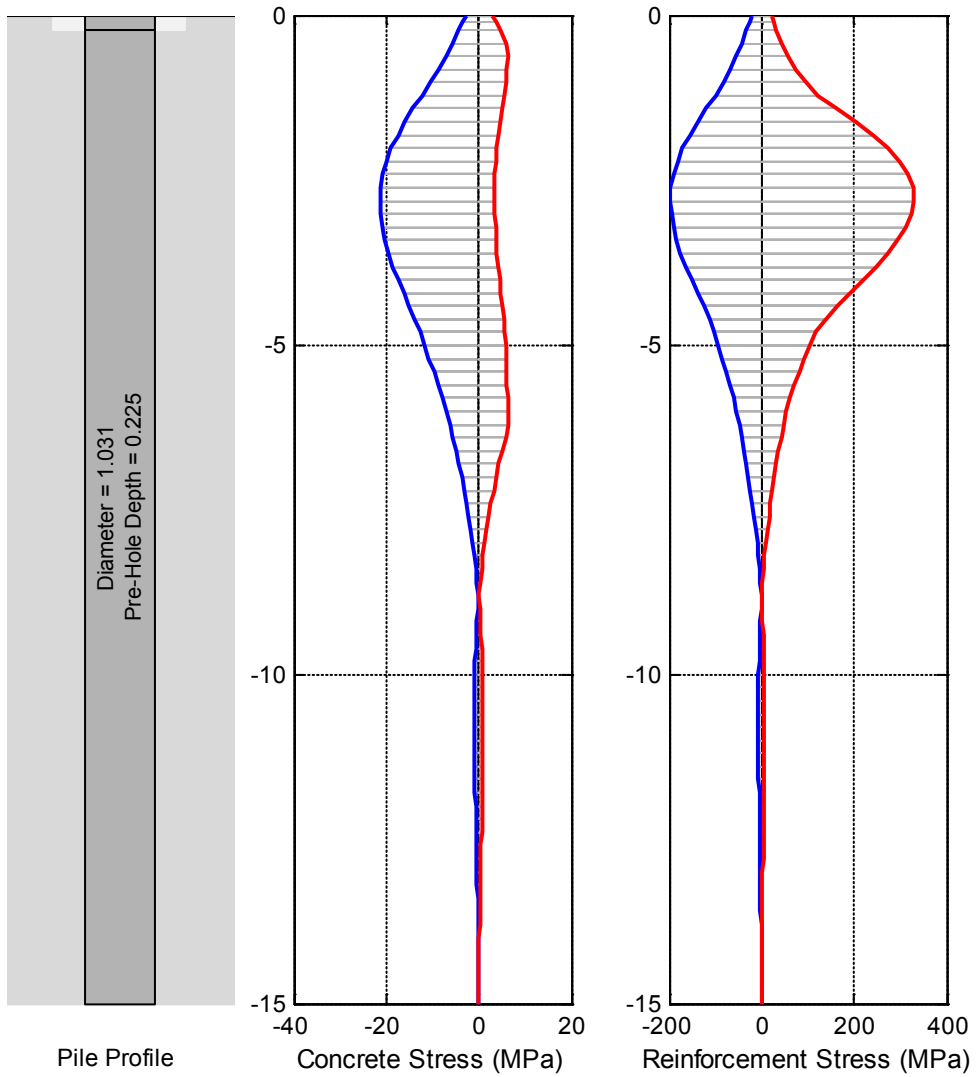
b) stress of concrete and reinforcement

Fig. 100 Optimized Profile of R/C Pile with Pre-Hole

6.3.4 Comparison of Optimized Piles

The optimized piles profiles, the profile with two varying sections and the profile with uniform section and pre-hole treatment, and their behaviors from above procedures are listed in Table 27. Under the ultimate conditions for Isola dell Scala Bridge, through the design optimization procedure proposed, the piles could be designed with less materials and more capacity to displacement. Although the stresses level increase, they are in absolutely reasonable and acceptable range considering the ultimate conditions. Certainly, for service conditions, the profiles need to be verified under different load combinations.

The two different treatments for pile construction, reach nearly the same pile head flexibility to lateral displacements, stresses level in concrete and reinforcement. Although the profile with varying sections has a higher reduction in volume, the construction technique for piles of varying sections is surely of more difficulty. The continuous connection in the point of section change needs more attention in construction, while for uniform section pile with pre-hole the amount of work seems to be much smaller. However, an arguing about the maintenance and durability problem on the material that filling into the pre-hole around the pile is still among the engineers

Overall, the proposed design optimization shows the competitive approach and optimized solutions for pile design, which not only assures the pile displacement capacity for possible super-long integral abutment bridges, but also the application example of this design optimization procedure in general structural analysis and design.

	Parameters		Original	Optimal with two sections	Optimal with pre-hole
Profile	length of part 1	L_1 (m)	5.0*	7.169	0.225
	length of part 2	L_2 (m)	10.0*	7.831	14.775
	diameter of part 1	D_1 (m)	1.2	1.088	1.031
	diameter of part 2	D_2 (m)	1.2	0.501	1.031
	total length	$L_1 + L_2$ (m)	15.0	15.0	15.0
	total volume	V_{tot} (m^3)	16.965	8.209	12.523
		Δ		-51.61%	-25.18%
Structural behaviour	pile head displacement	d_0 (mm)	16.48	29.78	30.03
		Δ		+75.85%	+82.22%
	maximum bending moment	M_{max} (kNm)	1862.72	1924.00	1977.11
		Δ		+3.29%	+6.14%
	maximum stress in concrete	σ_c (MPa)	13.09	19.42	21.31
		Δ		+48.36%	+62.80%
	maximum stress in reinforcement	σ_s (MPa)	195.56	329.94	329.02
		Δ		+68.72%	+68.25%

Table 27
Comparison of Optimized Piles

6.3.5 Pile Optimized Design for Large Displacement

From the optimizations above, the optimized piles could reach the displacement capacity around 30 mm for Isola della Scala Bridge. However, for super-long integral abutment bridges that might be longer than Isola della Scala Bridge proved in Ch.5, the thermal induced displacement would larger. According to Eq.(19) and common design guidelines for bridges, it is assumed that the thermal induced strains ($\varepsilon = \Delta L / L = \alpha \, \Delta T$) on superstructure would exceed 20×10^{-5}. Then if superstructure length reaches 500 m the corresponding displacement on one bridge end would be 50 mm.

Therefore, optimal (RC) pile shapes are tried to be found out through the optimization procedure, under the imposed lateral displacement of 50 mm on pile head. Considering abutment-pile connections, even if the pile is not required to design to resist bending moment, the connections should be of sufficient lateral stiffness, rotational stiffness and bearing strength (Ahn et al., 2011). Besides, if semi-integral abutment is applied, the pinned abutment-pile connection would dramatically increase the displacement capacity of the piles as both observed and analyzed (Dicleli, 2004). In this purpose, with the same condition of Isola della Scala Bridge, there are 4 pile design optimization cases being performed:

1) pinned pile head for semi-integral abutment;
2) fixed pile head without pre-hole;
3) fixed pile head with pre-hole of any depth; and
4) fixed pile head with pre-hole of limit depth (< 2 m) in consideration of enough embedded length for friction pile.

With the same objective of total pile volume, constraints of total pile length of 15 m and minimum section diameter of 0.5 m (pre-hole depth limit of 2 m for case.4), material ultimate strains of 0.35% for concrete and 6.75% for steel, the obtained optimized pile profiles are listed in Table 28 and shown as from Fig. 101 to Fig. 104.

As could be seen from the optimization results, the pinned head pile is the only one that material hasn't reached the ultimate strains, which proves the higher displacement capacity of pile in semi-integral abutment than that of integral abutment. Also the pre-hole would evidently increase the displacement capacity of fixed-head pile. If the pre-hole depth is not limited, the lateral displacement capacity would not be the principal for design; if the pre-hole depth is limited due to construction technique or pile embedment length requirements, the large displacement capacity still could be reached with an optimized pile profile. However, in this case, the pile volume

would be even greater than the same fixed-head pile without pre-hole, because of the pile part 1 would conduct the bending moment from the top to part 2, which requires a certain length of part 1 that embedded in soil to reduce the magnitude of moment with a faster rate.

	Parameters		Pinned-Head (no pre-hole)	Fixed Head		
				no pre-hole	pre-hole any dep.	pre-hole limit dep. (< 2m)
Profile	length of part 1	L_1 (m)	5.0*	1.693	5.0*	3.415
	length of part 2	L_2 (m)	10.0*	13.307	10.0*	11.585
	diameter of part 1	D_1 (m)	0.5	1.349	0.5	1.632
	diameter of part 2	D_2 (m)	0.5	0.932	0.5	0.846
	pre-hole depth	H_{pre} (m)	-	-	2.150	1.260
	total length	$L_1 + L_2$ (m)	15.0	15.0	15.0	15.0
	total volume	V_{tot} (m³)	2.945	11.498	2.945	13.656
Structural behaviour	shear force at d_0 = 50 mm	Q_{max} (kN)	168.5	2021.1	162.1	2740.3
	bend moment at d_0 = 50 mm	M_{max} (kNm)	-	4732.7	232.0	8363.5
	max. stress in concrete	σ_c (MPa)	16.02	19.83	19.83	19.83
	max. strain in concrete	ε_c	0.11%	0.35%	0.35%	0.35%
	max. stress in reinforcement	σ_s (MPa)	396.37	413.87	416.24	414.62
	max. strain in reinforcement	ε_s	0.62%	2.09%	2.28%	2.15%

Table 28

Optimized Piles for Imposed Lateral Displacement of 50 mm
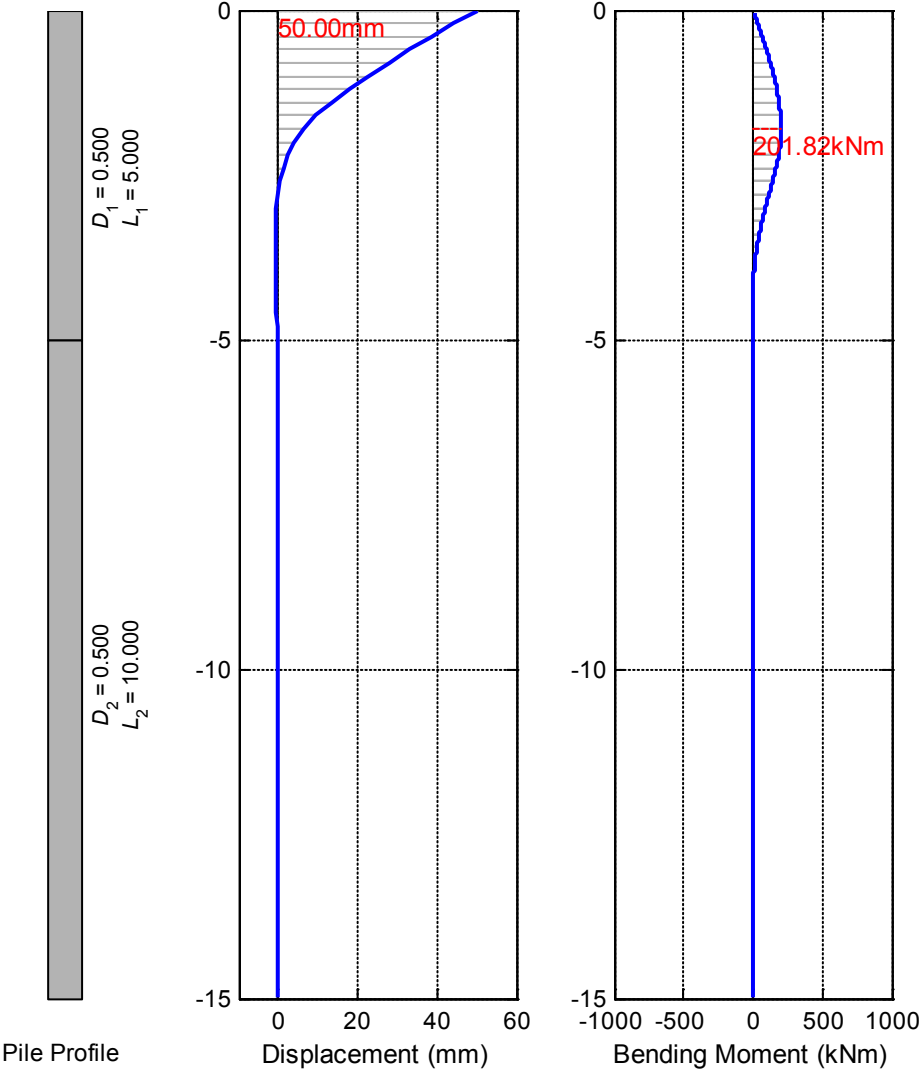
Fig. 101 Optimized Profile of R/C Pile (Pinned Head, without Pre-Hole) for Imposed Lateral Displacement of 50 mm
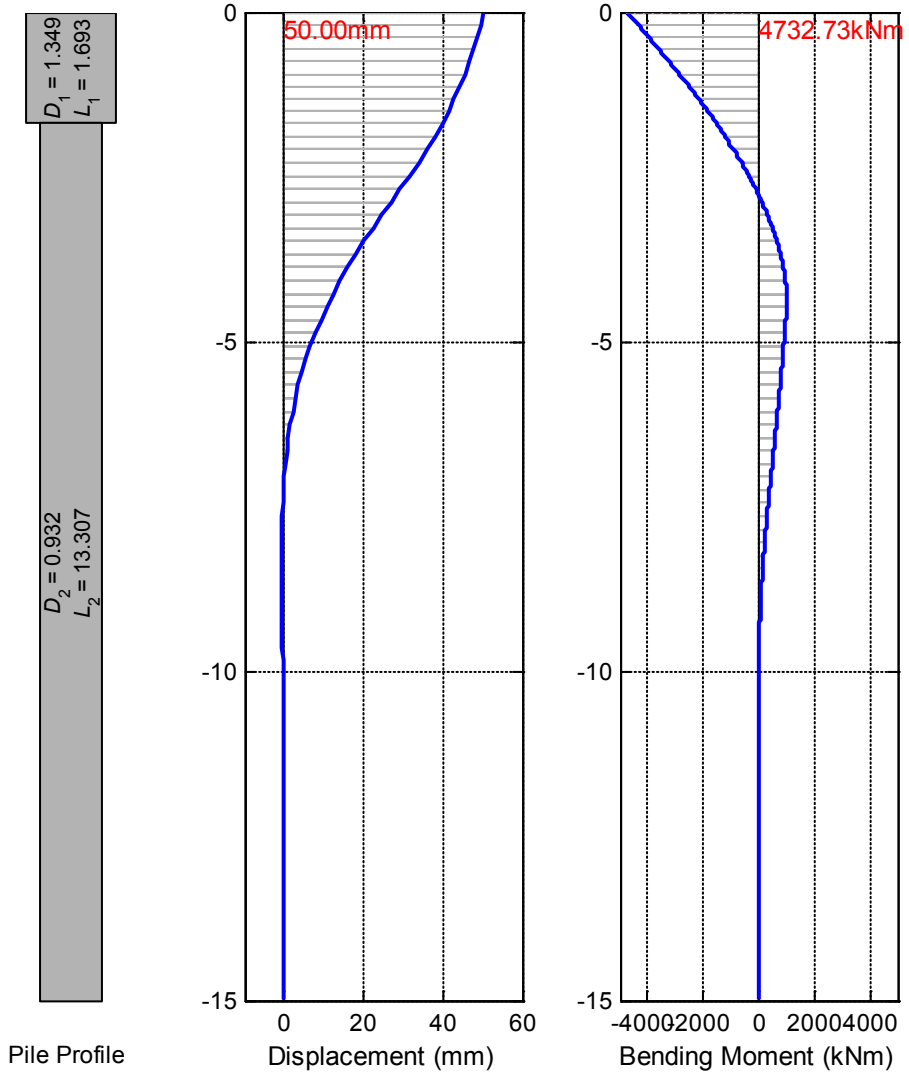
Fig. 102 Optimized Profile of R/C Pile (Fixed Head, without Pre-Hole) for Imposed Lateral Displacement of 50 mm
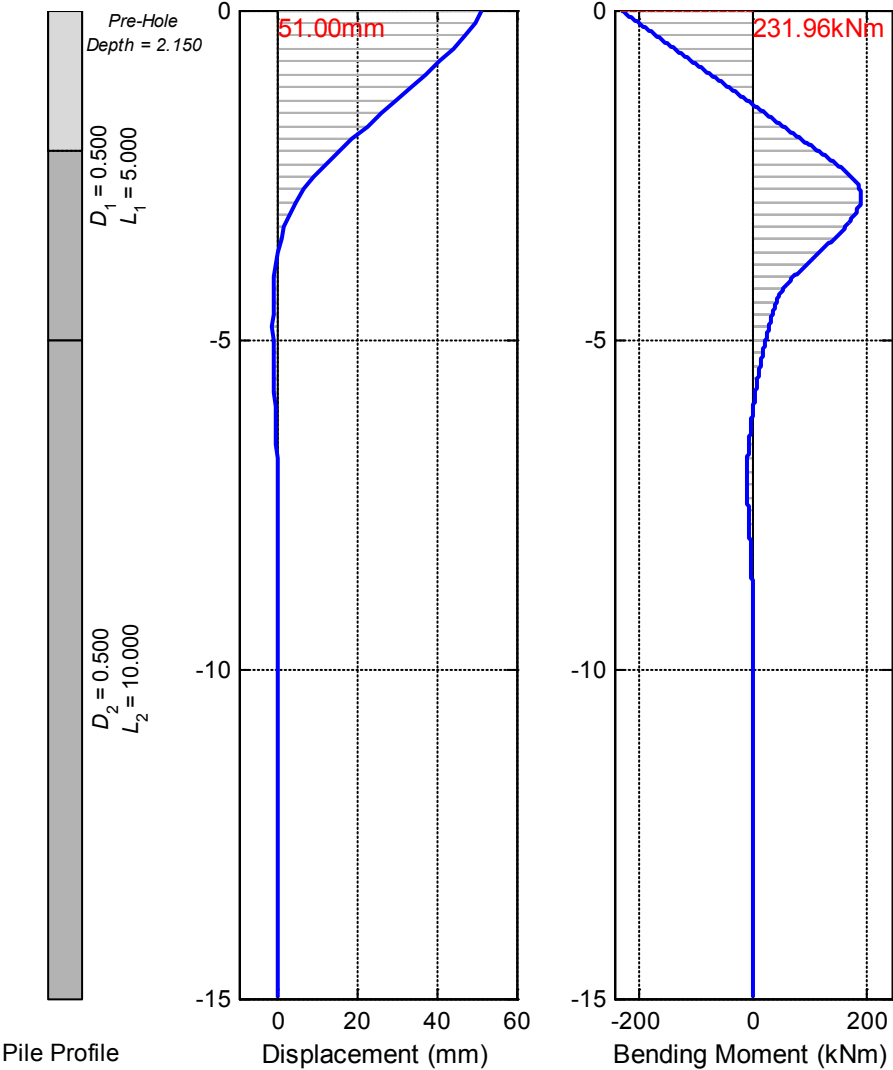
Fig. 103 Optimized Profile of R/C Pile (Fixed Head, with Pre-Hole of Any Depth) for Imposed Lateral Displacement of 50 mm
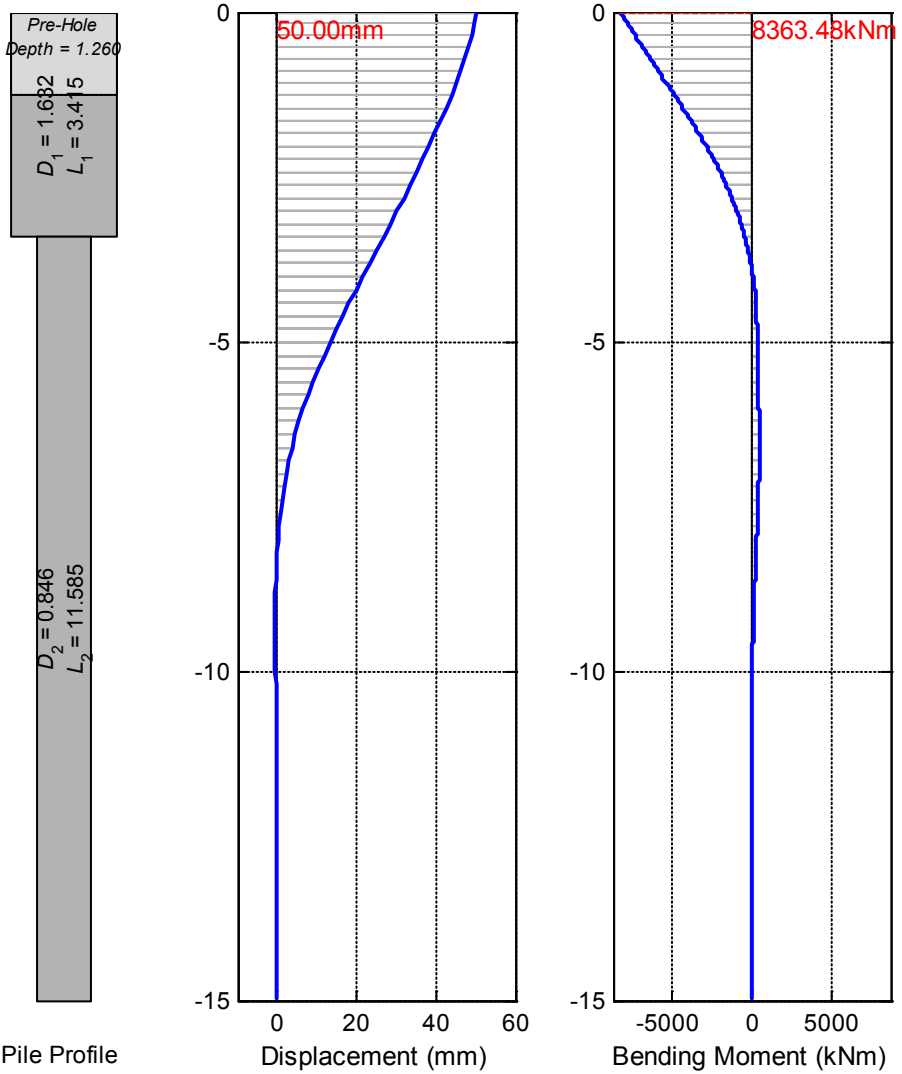
Fig. 104 Optimized Profile of R/C Pile (Fixed Head, with Pre-Hole of Limit Depth) for Imposed Lateral Displacement of 50 mm

6.3.6 Discrete Optimization Design

Practical engineering design sometimes requires that some design variables belong to an ordered set of values - discrete variables. This makes it a discrete optimization problem. This is also common for pre-fabricated piles to select the pile from a list provided by the producer. It is worth to recognize that the reason for discrete optimization is to choose an off-the-shelf pre-fabricated pile which will obviously keep the cost and production time down. In this case there are no more dimensional constraints but integer number associated design sets.

Discrete optimization problems are implied when the design variables are not continuous. If the set is made up only of integers, then the problem in characterized as an integer optimization problem, where each integer will be represented by its binary equivalent. The methods to solve this kind of integer optimization includes, exhaustive enumeration, branch and bound (partial or selective enumeration), and dynamic programming (Venkataraman, 2002). In this case, the design variables, as geometric parameters of pile profile, are reduced to one integer variable. This, in some sense, would simplify the optimization problem. For a limited products list, this could be simply solved through enumeration method.

7. CONSIDERATIONS FOR SUPER-LONG IABS

In previous chapters, for super-long integral abutment bridges, the performance was studied through numerical and experimental analyses on the existing longest integral abutment bridge; and the length limit for such super-long bridge was verified based on structural behavior and the optimized pile design. However, there are still important issues in design and construction considerations for super-long integral abutment bridges, which will be discussed in this chapter.

7.1. Retrofitting with Integral Abutment Bridge

Concept of integral bridge could be advantageously used in many situations, not only for the construction of new bridges, but also for the strengthening or retrofitting of existing bridges. Some states reported that the problems associated with leaking expansion joints were eliminated when bridges were retrofitted. Massachusetts reported modifications to bearings and seismic retrofitting that was performed at the same time as the joint retrofit. It was estimated from the responding states that between 95 to 210 retrofits will be performed in these states by the year 2000. However, conversion of non-integral abutment bridges to integral or semi-integral abutment bridges is not widely used, and only 39% of the American states was found that have a policy to investigate the feasibility of transforming non-integral to integral abutment bridges during retrofitting phases (Maruri & Petro, 2005). Some thought is is very common retrofit and that the selection of bearings is critical and tried to incorporate this retrofit with major superstructure replacement projects since there are severe problems at the abutment; while some consider retrofitting only on short spans and small skew.

The integral abutment tendency also could be found in European project INTAB (Economic and Durable Design of Composite Bridges with Integral Abutments) started from 2005 (Collin et al., 2006; Feldmann et al., 2010). The retrofitting work of simply supported bridges by using the concept of integral abutment bridge has been conducted in some real projects, including the studied bridge – Isola dell Scala Bridge (c.f. Ch.4.1).

The retrofitting with integral or semi-integral abutment bridge on existing bridges, are analyzed and reported to be of significantly improved deck and slab behavior, bridge seismic behavior, and with lower retrofitting cost (Jayaraman & Merz, 2001; Jayakumaran et al., 2005; Russo et al., 2009).
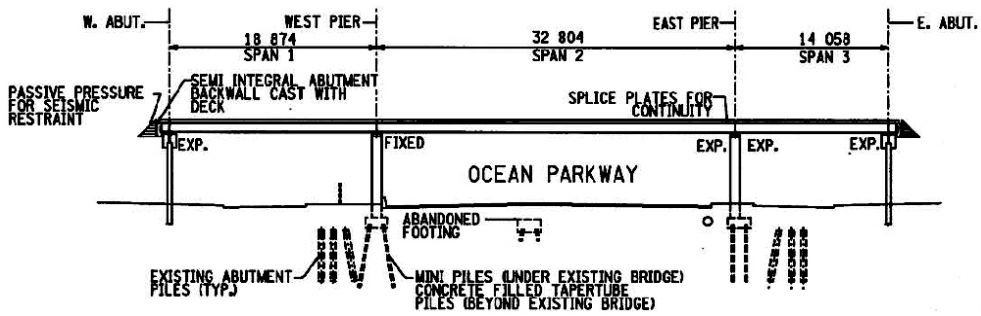
Fig. 105 Replacement Proposed to Rapidly Deteriorating Belt Parkway Bridge over Ocean Parkway in Brooklyn, New York (Jayakumaran et al., 2005)
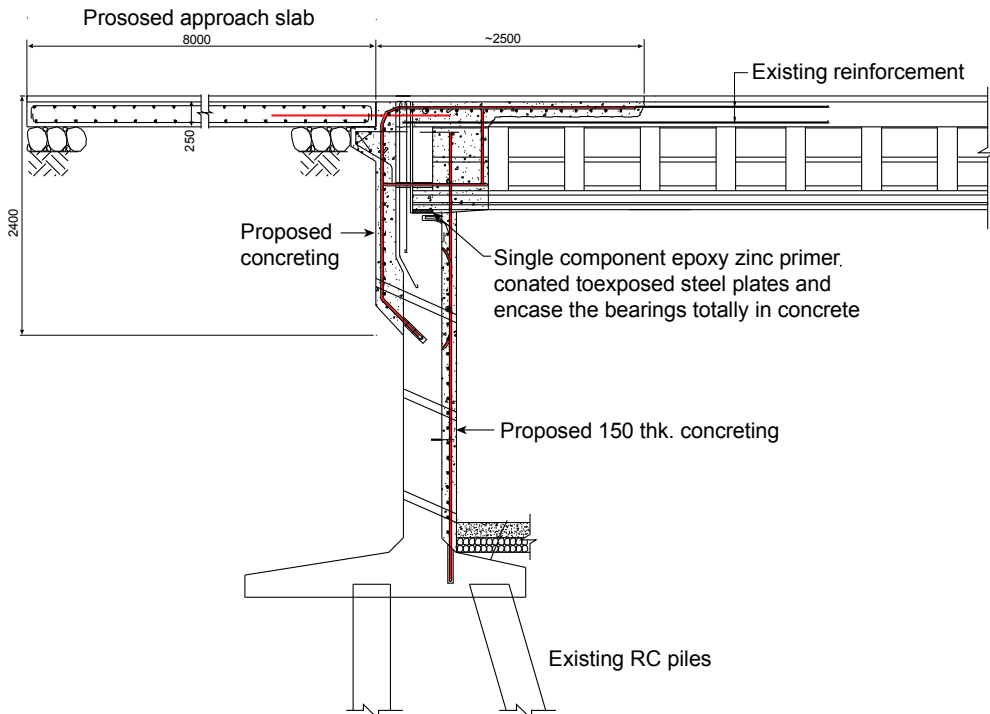
Fig. 106 Conversion of an Existing Simply Supported Deck to be Integral with the Abutments (Jayaraman & Merz, 2001)

178
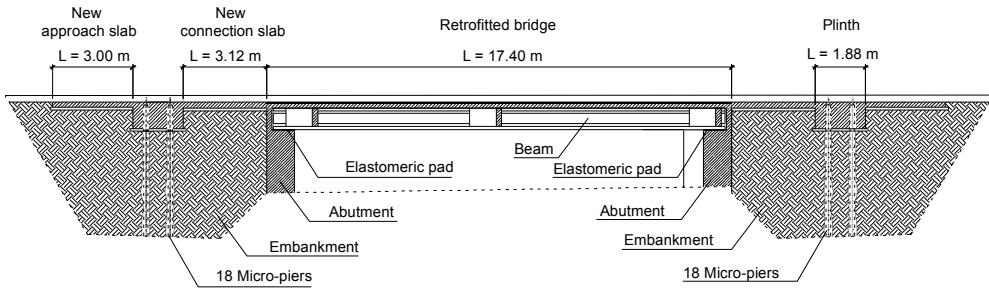
Fig. 107 Retrofitting a Short Span Bridge with a Semi-Integral Abutment Bridge (Russo et al., 2009)

During the deck slab connection construction in the retrofitting, in negative moment regions of deck slab over piers in continuous bridges, would not be subjected to flexural tensile stresses due to deck slab dead load if retrofitted from simply supported bridge. However, in the abutment-superstructure connections, occasionally, tensile stressing of fresh deck slabs resulted in slab cracking. With the advent of self-propelled finishing machines and set-retarding admixtures, it became more cost-effective on any bridges to help compensate for the probability of such cracks, crack sealers were developed that could be applied to deck surfaces after curing. For longer, more significant structures, set retarders, placement sequences, night placement, and crack sealers can all be used to help achieve acceptable results (Burke Jr, 2009).

However, the design of converting abutment/superstructure to continuity connections and other standards like transverse wingwalls haven't been established, which could be used for a wide range of bridge applications. Once these standard details have been established, each bridge abutment can then be configured and reinforced for the vertical reactions associated with various roadway widths and span lengths with even low retrofitting costs. With the development on the retrofitting technique and better understanding on the performance of integral abutment bridges, the possibility grows for existing multi-span simply supported bridges to be retrofitted with integral or semi-integral abutment bridge, which will lead more super-long integral abutment bridges to come up. Then, the thermal induced displacement will accumulate up on bridge ends, so besides the behaviour of structure system, the approach system at the bridge ends needs certain attention for the super-long integral abutment bridges both retrofitted from existing bridges or newly built.

7.2. Design and Behavior of Approach System

The approach system of a bridge consists of the backfill, the approach fill, and the foundation soil. In conventional approach system of bridges, at the transition between the surfacing on the bridge deck and the pavement beyond the bridge, expansion/contraction is usually accommodated by an asphaltic plug joint. The joint prevents the movement and any force on the abutment and the embankment caused by displacement of the bridge deck. However, abutments with joints have some serviceability and durability problems. Indeed, the degradation of the mechanical elements comprising the expansion joints and bearings occurs over time. These degradations are significant, especially in countries where deicing salt is intensely used, as in Switzerland (Dreier et al., 2011), and in bridges exposed to sea water. Consequently, these mechanical elements must be replaced, which leads to costly and complicated maintenance operations. And, the maximum total movement range for such joints, for example, is stated in British design manual as 40 mm (Highways Agency, 1994), which effectively limits the length of a continuous bridge to 80 m (the design thermal strain given in BA 42 is ±0.0005), where, however, approach slabs are not currently favored by most of the highway authorities due to difficulties in designing satisfactory approach slabs (Iles, 2006).

The use of approach slabs would eliminate the joint or move the location of the joint away from the abutment backwall. This kind of approach slab (or called link slab, transition slab, or drag plate), if used, are also part of the approach system for an integral abutment bridge (Arsoy et al., 1999). Although, due to their jointless construction avoiding the degradations related to expansion joints and bearings, integral abutment bridges are considerably more resistant to longitudinal pressures than the approach pavements. When properly designed both on bridge and approach system, these bridges can usually withstand without visible distress the pressures generated by both pavements and bridges (Arsoy et al., 1999; Burke Jr, 2009; Puppala et al., 2009). This is also the primary reason why aware and pragmatic bridge engineers favor the use of integral or semi-integral abutment bridges where jointed concrete pavements are used.

With the introduction of integral abutment bridges, the impact of superstructure on approach slab has become an area of greater concern. The approach slab, at first, was intended to provide the functions (Briaud et al., 1997) that: 1) to span the void that may develop below the slab; 2) to provide a ramp for the differential settlement between the abutment and embankment (Fig. 87); and 3) to provide a better seal against water percolation and erosion of the backfill material.

Most states in United States require to construct approach slabs as part of integral abutment bridges, with the expectation that they will mitigate the settlement of the backfill near the abutment, as almost half (46%) of those states reported the maintenance problem in settlement (Maruri & Petro, 2005). Some states require approach slabs in all of their integral abutment bridges. For example, Pennsylvania specifies 25 feet (7.3 m) and New York requires from 10 to 20 feet (3 to 6 m). West Virginia requires an approach slab when thermal movement is anticipated to be greater than 0.6 inches (15 mm). Maine requires approach slabs for steel integral abutment bridges greater than 80 feet (24.4 m) long and greater than 140 feet (42.7 m) for concrete structures. However, there is still no unified standardization and guidelines to provide the detailing of approach slabs, including the connection to the abutment backwall and the interface between the approach slab and approach fills. Many states indicated that they have or are using corbels on the abutment backwall for the support of the approach slab, while other states indicated that they use reinforcing projecting from the abutment backwall to tie the approach slab to the abutment backwall, and other states are using a combination (Fig. 7). Approach slab design examples are shown in Fig. 108 and Fig. 109.

While in Europe, according to the European survey (White II et al., 2010), approach slabs are not required for bridges with integral abutments. However, most countries indicated that approach slabs were desirable and that their length range from 3.0 to 8.0m. European approach slabs are most commonly buried beneath the roadway surface. One end is connected to the back of the abutment stem and moves horizontally along with the bridge abutment. The other end of the slab is buried at least 500mm under the road surface (Fig. 110 and Fig. 110). Although this kind of typical approach slabs are seldom used in Sweden, similar link slabs are more common (Flener, 2004). Link slabs are buried under the backfill soil to some level and linked to the end screen (Fig. 111). In Switzerland, the connections between bridge and approach slab are differently recommended (Fig. 113).
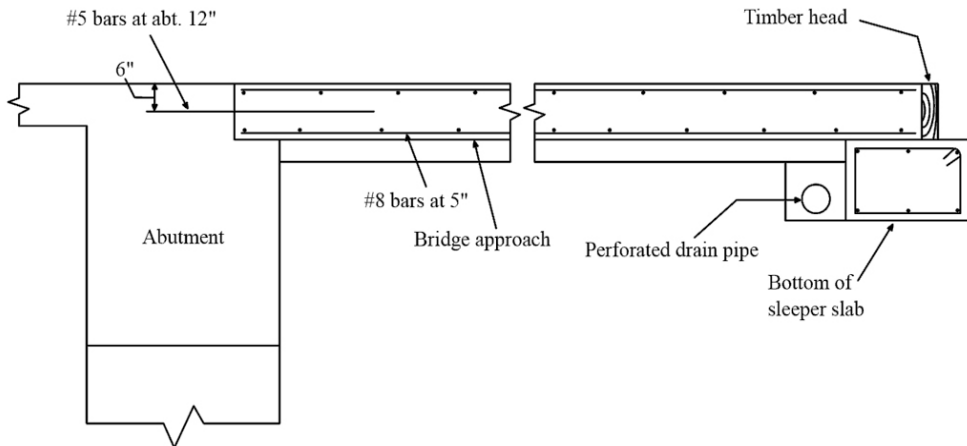
Fig. 108 Bridge Approach Connected to Bridge –Missouri DOT (Puppala et al., 2009)
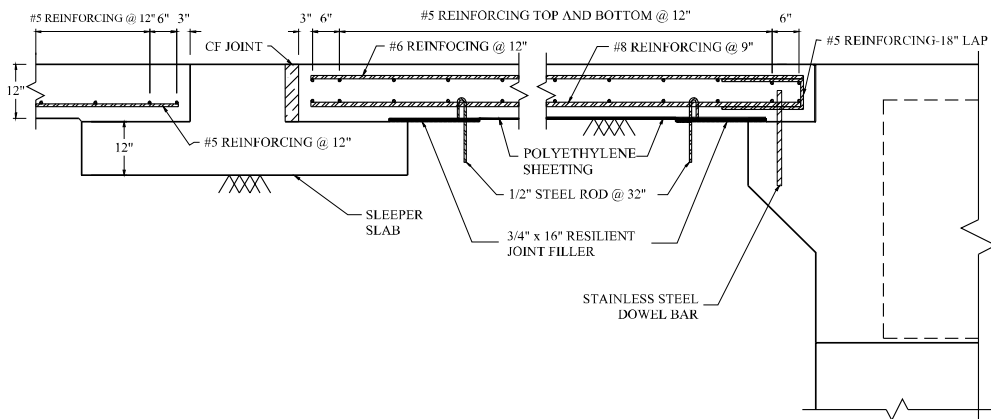
Fig. 109 Connection Detail for the Cast-in-place Approach Slab to Abutment – Iowa DOT (Greimann et al., 2008)
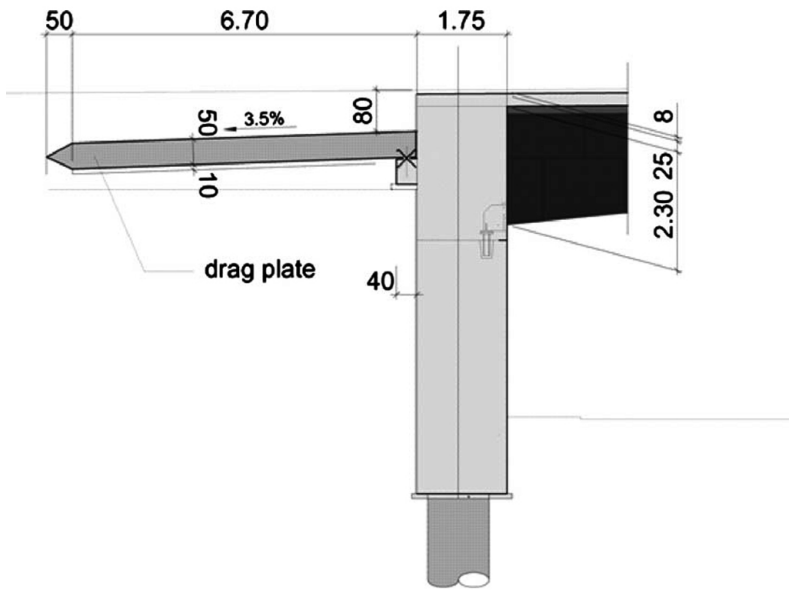
Fig. 110 Example of a German Drag Plate Approach Slab (White II et al., 2010)
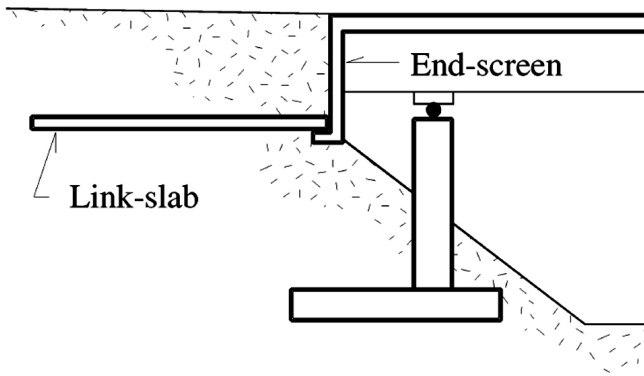
Fig. 111 A Typical Link Slab Application together with an End-Screen Used in Sweden (Flener, 2004)
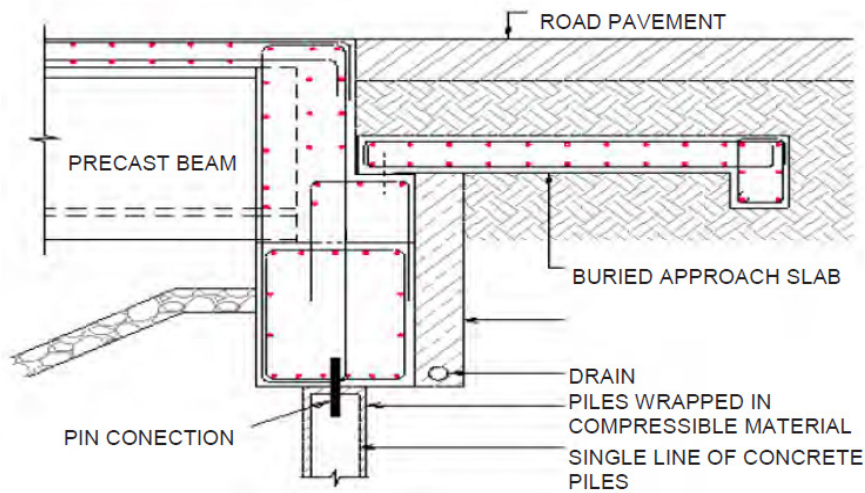
Fig. 112 Buried Approach Slab and Integral Abutment (Connal, 2004)

1: surface layer
2: support layer
3: additional support layer
4: mass concrete
5: first water sealing layer
6: second water sealing layer
7: bituminous layer
8: steel stud
9: synthetic foam
10: connection reinforcement
    (other reinforcement not shown)
11: sliding bituminous layer
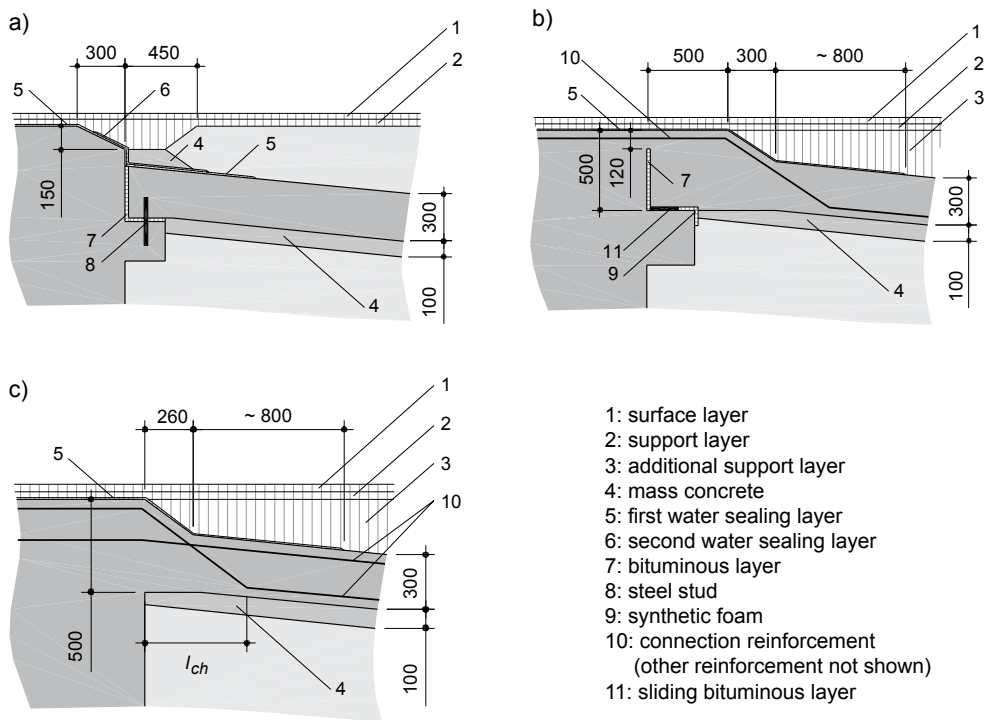
Fig. 113 Details of Connection between Abutment and Approach Slab in Switzerland (units in mm): a) detail for standard abutment with joints according to the Graubünden/CH Department of Civil Engineering; b) detail for integral abutment according to Swiss recommendations; (c) improved detail for standard and integral abutments (Dreier, 2010a).

For the length/size of the approach slab, recommendations are different based on experience, finite element simulation, and approximate calculation methods (Arsoy et al., 1999; Dreier, 2010a; Dreier et al., 2011). In the experimental studies of the settlement in the vicinity of the abutment wall due to imposed displacement, have shown that the settlement comes from the repeated active failure of the embankment subsequent to the cyclic displacement of the abutment wall. And this settlement can be reasonably estimated based on an active plastic mechanism (Dreier, 2010a). In fact, displacing an abutment causes movement of a wedge of the backfill with a height equal to the height of the abutment, and a length equal to $\tan(45+\Phi/2)$ times the height of the abutment (Fig. 114), which is about twice the abutment height.
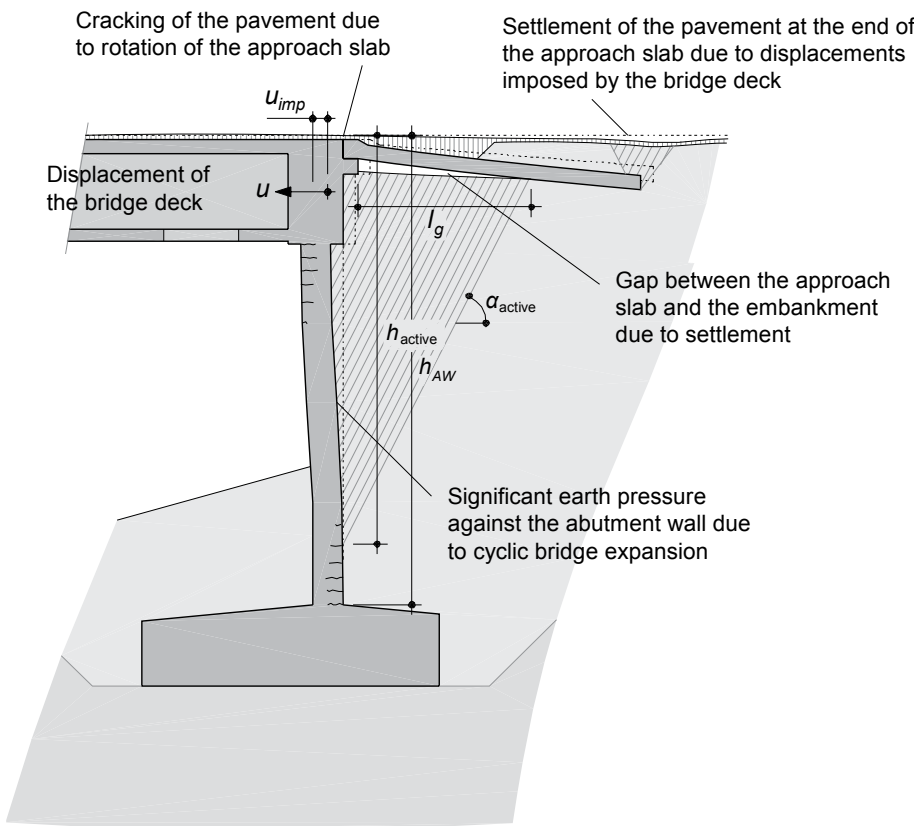
Fig. 114 Settlement Required Length for Approach Slab in Integral Abutment Bridge

As the abutments move back and forth due to fluctuating temperature, the backfill behind the abutments will be subjected to considerable deformations. Approach slabs are an important element for the long term performance and the serviceability

behavior of integral abutments. Especially for super-long integral abutment bridges, thermal induced displacements will be larger than normal bridges from the bridge deck, and are transferred to the abutment and the approach slab, which leads to a strong soil-structure interaction. The approach slab performance could be estimated through finite element method using a realistic stress-strain model for the approach fill and foundation soils, where the effects of various geometric and material parameters on the planarity of the road pavement at the end of the approach slab could be simulated to find out the beneficial design solutions (Arsoy et al., 1999; Dreier, 2010a).

7.3. Other Considerations on Design Details

Besides the approach slab of great importance to super-long integral abutment bridges, the other design and analysis considerations are necessary to discuss.

Creep and Shrinkage of Concrete

Generally, effects of creep and shrinkage will impose deformation on the bridge and displacement at ends of a continuous bridge (Fig. 115). In a long span bridge, this imposed displacement can add deflection or sag to the superstructure. For an integral abutment bridge, it means added rotation towards the center of the bridge and increased moments at the abutment-superstructure interface. However, because of shorter length for each span of jointless bridges, even super long integral abutment bridges, creep stresses are typically ignored. Only several recommendations stated that creep stresses are sometimes accounted for in prestressed concrete super-structures. In the case of Isola della Scala Bridge, due to the older girders before erected, the effects of the creep and shrinkage are neglected, because of the greater reduction in long-term abutment displacements.
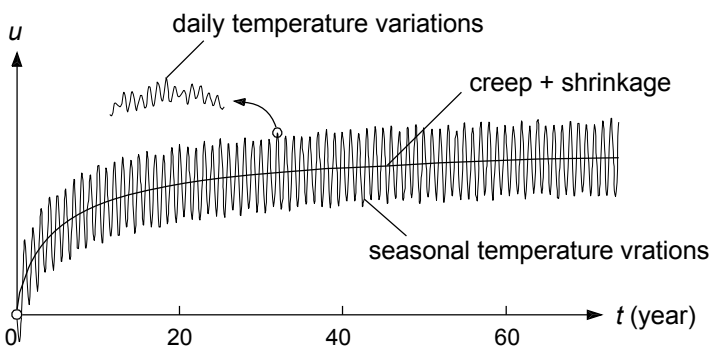
Fig. 115 Total Imposed Displacement over Time

Spread Footings

Because of moments and horizontal forces generated in jointless bridges, spread footings are not typically used. Spread footings (Fig. 114) do not allow the flexibility that is provided with a pile substructure so that spread footings are generally not recommended in super-long integral abutment bridges. However, regions based their decisions on several different factors such as soil conditions, depth to rock, anticipated scour and settlement, and thermal movement (Franco, 1999).

Wingwall Design

The wingwalls cantilever horizontally from the back of the abutment wall, and are designed to resist outward earth pressure. Typically wingwall designs are the same for non-integral bridges as for integral bridges. Almost all of the design manuals of states that required wingwalls limited them to 10 feet (3 m) in length if they are constructed integral with the abutment. If wingwalls are not integral with the abutment, they are designed separately to handle lateral loading of the approach and abutment. Both European countries and United States, survey respondents indicated that there are no restrictions on the use of U-wingwalls (wingwalls that are perpendicular to the abutment stem as shown in Fig. 116), flared wingwalls, and in-line wingwalls (White II, 2007). There are no established maximum lengths for the wingwalls that are required to be placed on an independent foundation, to allow the entire abutment to translate and rotate.

Fig. 116 Haavistonjoki Bridge, Finland, during Construction (Kerokoski & Laaksonen, 2005)

Backfill Details

In United States, 69% of the responding states require well-compacted granular backfill, while 15% require the backfill to be left loose in an effort to reduce forces

on the moving abutment stem. And 23% of the respondents use some sort of compressible material behind the abutment stem (Maruri & Petro, 2005). Some European countries require that the backfilling operations are conducted evenly on both sides of the structure to reduce any undue lateral forces on the structure. Other countries have no requirements at all for backfilling procedures. None of the countries require the use of an elastic "cushioning" material behind the abutments (White II et al., 2010). The weight of this backfill is calculated and is used in the earth pressure estimate. Therefore, it's of much importance for evaluating the long-term behaviors of the abutment and approach slab. For super-long integral abutment bridge, the detailed geotechnical studies and investigations, including soil-structure interactions, large displacements and cyclic movements, are needed to determine whether the backfill to be compacted or not.

Backwall Design

Commonly, backwalls shall be designed to resist passive earth pressure that will result from thermal movements. To reduce pressures, many kinds of materials, such as neoprene sponge, corrugated metal sheets, and flexible foam backing material, have been proposed by engineers and reseachers (Horvath, 2000; Kerokoski, 2006). In calculating earth pressure for backwall design, there was little agreement among the European countries; and in the United States, 59% of the states surveyed accounted for full passive pressure (White II, 2007). However, in conservative consideration, the pressure relieved by these materials is not recommended to account for in the design, and the full passive earth pressure on abutment is still suggested. Otherwise it necessary to reduce maximum spans and skews to accommodate earth pressures if backwall is designed to be weak.

Curved Beams

Some locations require curved beams to be used because of roadway geometry. Horizontally curved alignments are thought to be advantageous for integral abutment bridge. It is found that, through parametric analysis on 1200 ft (366 m) long curved integral abutment bridges, the bridge with the smaller radius has the less piles stress intensity and lateral displacement than the ones with larger radius (Thanasattayawibul, 2006). Constraints due to temperature and shrinkage can be considerably reduced by horizontal "relaxation" movement of the superstructure. In this way, complicated concrete technology and complicated on-site construction procedures can be avoided to decrease cracking and reduce overall cost. Additionally, the resulting slender structure offers an improved aesthetic for super-long continuous bridge. For example, the Sunniberg Bridge (Wikipedia, 2011b) in Switzerland is 526 m long and does not use any expansion joints or bearings. Another

example of the longest integral abutment bridge in United States is with curved deck (Fig. 8), where the maximum allowable degree of curvature ranges from 0° ~ 10° (Maruri & Petro, 2005).

Seismic Behaviour

Since the integral abutment bridge is directly restrained by earth, the bridge is expected to move together with the earth ground during most earthquakes, which would not cause much damage on the bridge. Considering resistance of the backfill, bridges up to 1000 ft (305 m) in length would experience no damage using both the current AASHTO and Expected Event (EE) design spectra. For the Maximum Considered Event (MCE) design spectrum, bridges less than 700 ft (213 m) in length would experience no damage and bridges between 700 and 1000 ft (213 ~ 305 m) in length would experience an acceptable level of damage (Talbott, 2008).

However, it's found that, from the strong-motion earthquake data and analytical studies, not the near-field but the far-field embankment response has a significant effect on the displacement demands of integral abutment bridges and the embankment-abutment-structure interaction (EASI) should not be ignored in design (Carvajal, 2011).
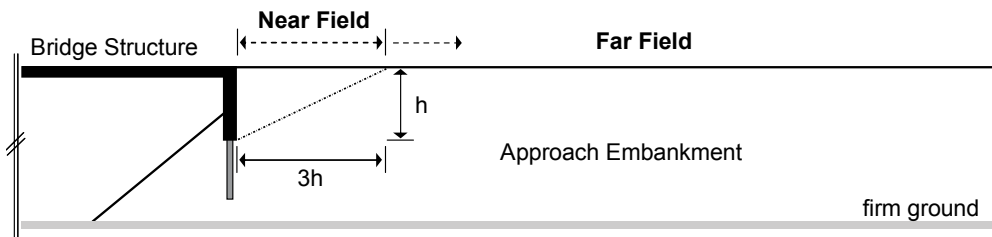
Fig. 117 Near and Far Field of an Approach Embankment (Carvajal, 2011)

To consider the seismic behaviour in design, a statistics was tried to be established in order to develop the LRFD (Load and Resistance Factor Design) on short and medium length integral abutment bridge (Kim, 2008). And, recent research on seismic design guidelines (Itani & Pekcan, 2011), based on analytical investigations and available experimental research, has shown that, in the longitudinal direction, a large percentage (72%) of the seismic force was resisted by the abutment-soil passive resistance. In the transverse direction, the overall response was governed by the soil-pile interaction. About 40% of the transverse seismic force was resisted by the soil-pile interaction for each abutment. This shows that the columns in integral

abutment bridges were subjected to low seismic forces, thus, limiting their damage during seismic events. Then the recommendations are presented on the sufficient embedment lengths that make the rigid girder-abutment connection assumption valid, and the procedure of evaluating the system damping accounting the soil-structure interaction and inelastic materials properties. A pile displacement capacity that produces 10% radian rotation is recommended based on the available experimental research. Moreover, for the super-long integral abutment, besides the complicated soil-structure interaction under big ground accelerations that needs to be evaluated, as well, the slender continuous deck should be considered, especially with high and slender piers, which would lead to large lateral displacements.

CONCLUSIONS

The research investigates the performance of the super-long integral abutment bridge, in order to maximize the benefits from integral abutment bridges. The complicated soil-structure interactions are the kernel factor for an effective design and satisfactory performance of integral abutment bridges. The literature survey on the applications of integral abutment bridges in worldwide, especially the current development of super-long integral abutment bridges was carried out firstly. Another literature review on soil-structure interaction was conducted to find out the most suitable methods in design. Involving the soil-structure interaction, thermal actions, non-linearity in materials and so on, structural study was performed structural study on an existing super-long integral abutment bridge. Based on that, length limit for this kind of bridge was evaluated and investigated in an analytical way. With this super length, the piles need to be designed with capacity of large lateral displacement. Therefore, an effective optimization approach, associating the finite element method with global optimization algorithm was presented for pile shape design.

Conclusions

On the basis of the findings of the literature reviews, analyses and derivations carried out, and the approaches presented, the conclusions are drawn as following:

- Arise in United States, integral abutment bridges have been widely applied in worldwide. They perform well with fewer maintenance problems than conventional bridges.

- There are different guidelines from state to state for designing integral abutment bridges in North America, while there is no specialty guideline in other countries and regions.

- The main reported problem with integral abutment bridges is that, due to temperature changes takes place at the abutments, the approach system requires special attention to the development of settlement caused problems like "bump at the end of the bridge", which could be avoided through applying approach slabs at the abutments.

- Maximum lengths or movements of integral abutment bridges are limited differently by different states; however, the bridges with lengths over 200 m have been built and have performed satisfactorily.

- Based on the classical theories and empirical experience, the lateral earth pressure on the abutment backwall could be generally presented by a universal relation between lateral pressure coefficient and generalized lateral displacement (ratio of abutment displacement to height). And the data provided by NCHRP is most used in engineering practice.

- For the pile embedded in soil, there are many empirical and analytical models to simulate the soil-pile interaction. Whereas, the design method recommended by API, concluding the studies on *p-y* curves, is most widely used in sophisticated nonlinear soil modelling and structural designs and analyses.

- Embedded piles can also be represented, using the equivalent cantilever method, as a column with a base fixed at some distant below the ground surface. This approach, however, may have difficulty in applying in the complicated soil configurations and could not reflect the real response in full piles.

- The temperature variations are the main horizontal loadings on the bridge, which is directly to impose movements on the abutments in integral abutment bridges. Therefore, the thermal induced displacement is the governing factor for integral abutment bridge, as reported in literatures, including its direct effects and possible fatigue strains on superstructure, abutment, and pile/foundation.

- Considering the critical issues in design and analysis of integral abutment bridge, a general finite element model is proposed, on the basis of current algorithm to account for soil-structure interaction, non-linear properties representing, and thermal loading capabilities.

- The layout of the studied integral abutment bridge, with its high concentration of stiffness at the abutments, is characterized by a remarkable presence of bending moment at the structure's ends. This aspect needs to be thoroughly investigated and represents one of the key factors influencing the structural response.

- According to the parametric analysis on the case of studied integral abutment bridge, the axial forces in the girders and piles are greatly influenced by positive and negative temperature variations, which are key parameters for assessing the bridge's response. The different soil conditions greatly affect the bending moment near abutments and axial force along the girder: this is more evident for negative temperature variations than for positive ones and is caused by the different reactions of the soil behind the abutment due to passive and active pressures and according to different load combinations.

- The response of the studied bridge in terms of internal force distribution, at abutments and in the end parts of the structure, is greatly influenced by significant temperature variations. Nevertheless these seem not to remarkably the other parts of the bridge, where a stable situation is recorded.

- Bridges characterized by slender and flexible piers respond more uniformly and predictably to temperature variations; flexible abutments or pin connections between girder and abutments should be considered as the preferred solution, even if these options were not applicable to the case presented for the reasons mentioned.

- Negative temperature variations need to be considered with the utmost attention, while passive pressures on abutment due to positive temperature variations are dominate the most design procedures.

- Dynamic tests have been carried out on the studied bridge. The operational modal analysis on the tests results has shown the good consistency of the bridge dynamic behavior with finite element analysis, through comparison of frequencies and mode shapes, where the finite element model is updated.

- The temperature variations caused displacements in the superstructure, through analytical formulations, are related by each span's parameters of span length, girder sections and pier stiffnesses. Based on conservatively assumption on the earth pressure on abutment, the reactions of pile head, then, the thermal induced displacements could be analytically expressed.

- Through comparison to finite element analysis, the formulations of thermal induced displacements could be corrected by coefficients on pier stiffnesses to consider the non-linearity in the specified bridge.

- Based on the modified formulations, considering the pier rotation and abutment capacities, the integral abutment bridge with length up to 540 m (30 m × 18 spans) could be built on the same conditions of studied bridge.

- With the same assumptions above, the length limit is 450 m (30 m × 15 spans), if considering the fatigue effects on the materials in the bridge.

- With the modified formulations, if considering the durability of approach slab with the maximum thermal induced bridge end displacement, the length of the bridge could be more than 430 m.

- The current design optimization on piles shows that lateral loaded pile could be optimized for better performance with less material; while the piles in integral abutment bridge are required a better behavior for accommodating the large lateral displacement. Therefore, an optimization procedure was proposed.

- The proposed optimization approach associates the finite element method with global optimization algorithm, which is implemented for pile design optimization procedure, which is verified through a lateral loaded pile optimization example comparison with a current approach.

- On the basis of proper optimization problem description on the objectives, constraints and design variables, the piles in different conditions could be optimized through the procedure proposed, including the pile profile with two varying sections and the profile with uniform section and pre-hole treatment.

- Through the design optimization procedure proposed, the piles could be designed with less materials and more capacity to displacement, while the stresses levels increase in absolutely reasonable and acceptable range considering the ultimate conditions.

- The two different optimized piles may reach nearly the same pile head flexibility to lateral displacements, stresses level in concrete and reinforcement.

Although the profile with varying sections has a higher reduction in volume, the construction technique for the continuous connection in the point of section change needs more attention in construction.

- The proposed design optimization shows the competitive approach and optimized solutions for pile design, which not only assures the pile displacement capacity for possible super-long integral abutment bridges, but also the application example of this design optimization procedure in general structural analysis and design.

- Converting from conventional bridges to integral abutment bridges, would bring benefits in performance and maintenance. It will be a good retrofitting solution for existing and old bridges.

- Approach system plays an important role in a super-long integral abutment bridge. The use of approach slab is necessary for the most situations, to avoid the possible problems caused by thermal induced bridge end displacements and settlements of the backfill and approach fill.

- Some design details are worth to be considered for super-long integral abutment bridge, including seismic resistance, although the short span integral abutment bridges are of good resistant to earthquakes.

Recommendations for Future Investigations

Although the present study preliminarily introduces performance of super-long abutment bridges mainly through parametric analysis and design optimization, to properly build a super-long abutment bridge there are still many factors and uncertainties in structural and non-structural considerations for analysis and design.

A more comprehensive analytical model of the bridge system that considers the inertia effect of the abutment soil must be developed. Also, further investigation through detailed finite element analysis of the connections, such as different embedment lengths and girder widths, is needed to verify the influence of the connection flexibility.

Besides theoretical analyses, experimental investigation on integral bridge abutment as a system should be established. Experiments of abutment-approach sys-

tem tests are needed for integral bridge abutments to better assess the subsystem cyclic response of integral abutments under large cyclic deformations.

It would be desirable to instrument abutments and supporting piles of integral abutment bridges to investigate the rotation behaviour of semi-integral abutments, and to investigate pile stresses under large bridge end displacement. Data from such tests would be very useful in validating the length limit for integral abutment bridges.

Research is recommended to investigate the dynamic soil-bridge interactions and seismic resistance for super-long integral abutment bridges.

Research is also recommended to evaluate semi-integral abutments for super-long integral abutment bridges.

BIBLIOGRAPHY

Ahn J.-H., Yoon J.-H., Kim J.-H. and Kim S.-H., (2011), *Evaluation on the Behavior of Abutment-Pile Connection in Integral Abutment Bridge*, Journal of Constructional Steel Research, 67, 7, 1134-1148.

Allemang R.J., (2003), *The Modal Assurance Criterion – Twenty Years of Use and Abuse*, Sound and Vibration, 37, 8, 14-23.

American Association of State Highway and Transportation Officials, (2002), *Standard Specifications for Highway Bridges, 17th Edition*, Washington DC, USA.

American Petroleum Institute, (2000), *Recommended Practice for Planning, Designing, and Constructing Fixed Offshore Platforms: Working Stress Design*, RP 2A-WSD, API Publishing Services, Washington D.C.

ANSYS Inc., (2007), *Release 11.0 Documentation for ANSYS [11.0]*, Canonsburg, Pennsylvania, USA.

Arnout S., Dooms D. and De Roeck G., (2008), *Shape and Size Optimization of Shell Structures with VariableThickness*. Proceedings of the 6th Conference on Computation of Shell and Spatial Structures IASS-IACM 2008, "Spanning Nano to Mega", Ithaca, NY, USA.

Arockiasamy M., Butrieng N. and Sivakumar M., (2004), *State-of-the-Art of Integral Abutment Bridges: Design and Practice*, Journal of Bridge Engineering, 9, 5, 497-506.

Arsoy S., (2000), *Experimental and Analytical Investigations of Piles and Abutments of Integral Bridges*, Thesis: Ph.D., Virginia Polytechnic Institute and State University.

Arsoy S., Barker R.M. and Duncan J.M., (1999), *The Behavior of Integral Abutment Bridges*, FHWA/VTRC 00-CR3, Virginia Transportation Research Council.

Arsoy S., Duncan J.M. and Barker R.M., (2004), *Behavior of a Semi-Integral Bridge Abutment under Static and Temperature-Induced Cyclic Loading*, Journal of Bridge Engineering, 9, 2, 193-199.

Bakeer R.M., Mattei N.J., Almalik B.K., Carr S.P. and Homes D., (2005), *Evaluation of DOTD Semi-Integral Bridge and Abutment System*, FHWA/LA.05/397, Department of Civil and Environmental Engineering, Tulane University, New Orleans, Louisiana, USA.

Baptiste K.T., Kim W. and Laman J.A., (2011), *Parametric Study and Length Limitations for Prestressed Concrete Girder Integral Abutment Bridges*, Structural Engineering International, 21, 2, 151-156.

Barker R.M., Duncan J.M.K., Rojiani K.B., Ooi P.S.K. and Kim S.G., (1991), *Manuals for the Design of Bridge Foundation*, NCHRP Rep.343, Transportation Research Board, National Research Council, Washington D.C.

Becker D.E. and Moore I.D., Eds, (2006), *Canadian Foundation Engineering Manual*. Richmond, Canada, Canadian Geotechincal Society.

Bettinger C., (2001), *Effects of Thermal Expansion on a Skewed Semi-Integral Bridge*, Thesis: Master of Science, Ohio University, Athens, Ohio, USA.

Bonczar C., Brena S.F., Civjan S.A., DeJong J. and Crovo D., (2005), *Integral Abutment Pile Behavior and Design - Field Data and FEM Studies*. Integral Abutment and Jointless Bridges (IAJB 2005), Baltimore, Maryland, 174-184.

Boulanger R.W., Curras C.J., Kutter B.L., Wilson D.W. and Abghari A., (1999), *Seismic Soil-Pile-Structure Interaction Experiments and Analyses*, Journal of Geotechnical and Geoenvironmental Engineering, 125, 9, 750-759.

Bowles J.E., (1996), *Foundation Analysis and Design*, McGraw-Hill, New York, USA.

Bozorgzadeh A., (2007), *Effect of Structure Backfill on Stiffness and Capacity of Bridge Abutments*, Thesis: PhD, University of California, San Diego, California, USA.

Briaud J.-L., James R.W. and Hoffman S.B., (1997), *Settlement of Bridge Approaches (the Bump at the End of the Bridge)*, NCHRP Synthesis 234, Transportation Research Board, National Research Council, Washington D.C., USA.

Brincker R., Ventura C. and Andersen P., (2001), *Damping Estimation by Frequency Domain Decomposition*. Proceedings of the 19th International Modal Analysis Conference (IMAC), Kissimmee, Florida, 698-703.

Brincker R., Zhang L. and Andersen P., (2000), *Modal Identification from Ambient Responses using Frequency Domain Decomposition*. Proceedings of the 18th International Modal Analysis Conference (IMAC), San Antonio, Texas, 625-630.

Briseghella B., Siviero E. and Zordan T., (2004), *A Composite Integral Bridge in Trento, Italy: Design and Analysis*. IABSE Symposium 'Metropolitan Habitats and Infrastructure', Shanghai, China, International Association for Bridge and Structural Engineering, 297-302.

Briseghella B. and Zordan T., (2004), *Adjustable Deck Solutions for "Veneto Strade" Flyovers*. IABSE Symposium 'Metropolitan Habitats and Infrastructure',

Shanghai, China, International Association for Bridge and Structural Engineering, 307-312.

Briseghella B. and Zordan T., (2007), *Integral Abutment Bridge Concept Applied to the Rehabilitation of a Simply Supported Concrete Structure*, Structural Concrete, 8, 1, 25-33.

Burke Jr M.P., (1993), *The Design of Integral Concrete Bridges*, Concrete International, 15, 6, 37–42.

Burke Jr M.P., (2009), *Integral and Semi-Integral Bridges*, Wiley-Blackwell, Oxford, UK.

Burke Jr M.P. and Bugler J.W., (2002), *The Long-Term Performance of Unsealed Jointed Concrete Pavements*. Transportation Research Board's 81st Annual Meeting, Washington, D.C.

Byrd R.H., Hribar M.E. and Nocedal J., (1999), *An Interior Point Algorithm for Large-Scale Nonlinear Programming*, SIAM Journal on Optimization, 9, 4, 877-900.

Carvajal J.C., (2011), *Seismic Embankment-Abutment-Structure Interaction of the Integral Abutment Bridges*, Thesis: PhD, The Universtity of British Columbia, Vancouver, Canada.

Chai Y.H., (2002), *Flexural Strength and Ductility of Extended Pile-Shafts - I: Analytical Model*, Journal of Structural Engineering, 128, 5, 586-594.

Chen Y., (1997), *Important Considerations, Guidelines, and Practical Details of Integral Bridges*, Journal of Engineering Technology, 14, 16-19.

Chiou J.S., Yang H.H. and Chen C.H., (2009), *Use of Plastic Hinge Model in Nonlinear Pushover Analysis of a Pile*, Journal of Geotechnical and Geoenvironmental Engineering, 135, 9, 1341-1346.

Civjan S.A., Bonczar C., Brena S.F., DeJong J. and Crovo D., (2007), *Integral Abutment Bridge Behavior: Parametric Analysis of a Massachusetts Bridge*, Journal of Bridge Engineering, 12, 1, 64-71.

Clough G. and Duncan J., (1991), *Foundation Engineering Handbook*, Van Nostrand Reinhold, New York.

Coduto D.P., (2001), *Foundation Design: Principles and Practices*, Prentice Hall, New Jersey.

Collin P., Veljkovic M. and Pètursson H., (2006), *International Workshop on the Bridges with Integral Abutments*, Luleå University of Technology, Luleå, Sweden.

Comisu C.C., (2005), *Integral Abutment and Jointless Bridges*, Bulletin of the Polytechnic Institute of Jassy, Constructions, Architechture Section, 51, 107-117.

Connal J., (2004), *Integral Abutment Bridges–Australian and US Practice*. Austroads 5th Bridge Conference, Hobart, Australia.

Cross H., (1930), *Analysis of Continuous Frames by Distributing Fixed-End Moments*, Proceedings of the American Society of Civil Engineers (ASCE), 919-928.

Dicleli M., (2000a), *A Rational Design Approach for Prestressed-Concrete-Girder Integral Bridges*, Engineering Structures, 22, 3, 230-245.

Dicleli M., (2000b), *Simplified Model for Computer-Aided Analysis of Integral Bridges*, Journal of Bridge Engineering, 5, 3, 240-248.

Dicleli M., (2004), *Effect of Cyclic Thermal Loading on the Performance of Steel H-Piles in Integral Bridges with Stub-Abutments*, Journal of Constructional Steel Research, 60, 2, 161-182.

Dicleli M., (2005), *Integral Abutment-Backfill Behavior on Sand Soil - Pushover Analysis Approach*, Journal of Bridge Engineering, 10, 354.

Dicleli M. and Albhaisi S.M., (2003), *Maximum Length of Integral Bridges Supported on Steel H-Piles Driven in Sand*, Engineering Structures, 25, 12, 1491-1504.

Dicleli M. and Albhaisi S.M., (2004a), *Estimation of Length Limits for Integral Bridges Built on Clay*, Journal of Bridge Engineering, 9, 6, 572-581.

Dicleli M. and Albhaisi S.M., (2004b), *Performance of Abutment-Backfill System under Thermal Variations in Integral Bridges Built on Clay*, Engineering Structures, 26, 7, 949-962.

Dicleli M. and Erhan S., (2011), *Effect of Foundation Soil Stiffness on the Seismic Performance of Integral Bridges*, Structural Engineering International, 21, 2, 162-168.

Douglas B.M. and Reid W.H., (1982), *Dynamic Tests and System Identification of Bridges*, Journal of the Structural Division, ASCE, 108, 10, 2295-2312.

Dreier D., (2008), *Influence of Soil-Structure Interaction on Structural Behaviour of Integral Bridge Piers*. Proceedings of the 7th International FIB PhD Symposium, Stuttgart, Germany, 11-20.

Dreier D., (2010a), *Interaction Sol-Structure dans le Domaine des Ponts Intégraux*, Thesis: PhD, École Polytechnique Fédérale de Lausanne, Lausanne, Switzerland. (in French)

Dreier D., (2010b), *Modified Geometry of Transition Slabs for Integral Bridges*. Proceedings of the 1st EPFL Doctoral Conference in Mechanics, Advances in Modern Aspects of Mechanics, Lausanne, Switzerland, 107-110.

Dreier D., Burdet O. and Muttoni A., (2011), *Transition Slabs of Integral Abutment Bridges*, Structural Engineering International, 21, 2, 144-150.

Dunker K.F., Klaiber F.W., Daoud F.K., Wiley W.E. and Sanders Jr. W.W., (1987), *Strengthening of Existing Continuous Composite Bridges*, Iowa DOT Project HR-287, Engineering Research Institute, Iowa State University, Ames, Iowa, USA.

England G.L., Tsang N.C.M. and Bush D.I., (2000), *Integral Bridges: A Fundamental Approach to the Time-Temperature Loading Problem*, Thomas Telford.

Erhan S. and Dicleli M., (2009), *Live Load Distribution Equations for Integral Bridge Substructures*, Engineering Structures, 31, 5, 1250-1264.

European Committee for Standardization (CEN), (2003a), *Eurocode 1: Actions on Structures*, *Part 1-5: General Actions – Thermal Actions*, EN 1991-1-5: 2003.

European Committee for Standardization (CEN), (2003b), *Eurocode 1: Actions on Structures*, *Part 2: Traffic Loads on Bridges*, EN 1991-2: 2003.

European Committee for Standardization (CEN), (2004a), *Eurocode 2: Design of Concrete Structures*, *Part 1-1: General Rules and Rules for Buildings*, EN 1992-1-1: 2004.

European Committee for Standardization (CEN), (2004b), *Eurocode 7: Geotechnical Design*, *Part 1: General Rules*, EN 1997-1: 2004.

European Committee for Standardization (CEN), (2005a), *Eurocode 8: Design of Structures for Earthquake Resistance*, *Part 2: Bridges*, EN 1998-2: 2005.

European Committee for Standardization (CEN), (2005b), *Eurocode 8: Design of Structures for Earthquake Resistance*, *Part 3: Assessment and Retrofitting of Buildings*, EN 1998-3: 2005.

Evangelista S., (2011, assessed), *200-Meter-Long Bridges without Expansion Joints: Is It Possible?*, Retrieved December 19, 2011, from EPFL: http://actu.epfl.ch/news/200-meter-long-bridges-without-expansion-joints-is/.

Evans L.T., (1982), *Simplified Analysis of Laterally Loaded Piles*, Thesis: PhD, University of California, Berkeley, California, USA.

Fan C.-C. and Long J.H., (2005), *Assessment of Existing Methods for Predicting Soil Response of Laterally Loaded Piles in Sand*, Computers and Geotechnics, 32, 4, 274-289.

Fang Y.-S., Chen T.-J. and Wu B.-F., (1994), *Passive Earth Pressures with Various Wall Movements*, ASCE Journal of Geotechnical Engineering, 120, 8, 1307-1323.

Faraji S., Ting J.M., Crovo D.S. and Ernst H., (2001), *Nonlinear Analysis of Integral Bridges: Finite-Element Model*, Journal of Geotechnical and Geoenvironmental Engineering, 127, 454.

Feldmann M., Naumes J., Pak D., Veljkovic M., Nilsson M., Eriksen J., Collin P., Kerokoski O., Petursson H., Verstraete M., Vroomen C., Haller M., Hechler O. and Popa N., (2010), *Economic and Durable Design of Composite Bridges with Integral Abutments*, RFSR-CT-2005-00041, European Commission, Research Fund for Coal and Steel, Luxembourg.

Fenu L., (2005), *On the Characteristics of Optimum Beams with Optimum Length Surrounded by a Winkler's Medium*, Structural and Multidisciplinary Optimization, 30, 3, 243-250.

Fenu L., (2010), *Fully Stressed Piles and Beams in a Winkler's Medium, End-loaded by an Orthogonal Force, and with Optimum Length*, Construction Technology, 39, 3, 110-115.

Fenu L. and Madama G., (2006), *Laterally Loaded R/C Bored Piles with Minimum Horizontal Top Displacement*. The 2nd fib Congress, Naples, Italy.

Fenu L. and Serra M., (1995), *Optimum Design of Beams Surrounded by a Winkler Medium*, Structural and Multidisciplinary Optimization, 9, 2, 132-135.

Flener E.B., (2004), *Soil-Structure Interaction for Integral Bridges and Culverts*, Thesis: PhD, Royal Institute of Technology, Stockholm, Sweden.

Franco J.M., (1999), *Design and Field Testing of Jointless Bridges*, Thesis: MSc, West Virginia University, Morgantown, West Virginia, USA.

Frosch R.J., Wenning M. and Chovichien V., (2005), *The In-Service Behavior of Integral Abutment Bridges: Abutment-Pile Response*. Integral Abutment and Jointless Bridges (IAJB 2005), Baltimore, Maryland, 30-40.

Gentile C., (2006), *Modal and Structural Indentification of a R.C. Arch Bridge*, Structural Engineering and Mechanics, 22, 1, 53-70.

Gill P.E., Murray W. and Saunders M.A., (2002), *SNOPT: An SQP Algorithm for Large-Scale Constrained Optimization*, SIAM Journal on Optimization, 12, 4, 979-1006.

Girton D.D., Hawkinson T.R., Greimann L.F., Bergenson K., Ndon U. and Abendroth R.E., (1989), *Validation of Design Recommendations for Integral Abutment Piles*, Iowa DOT Project HR-292, Engineering Research Institute, Iowa State University, Ames.

Greimann L., Phares B., Faris A. and Bigelow J., (2008), *Integral Bridge Abutment-to-Approach Slab Connection*, IHRB Project TR-530 & TR-539, Center for Transportation Research and Education, Iowa State University, Ames, IA, USA.

Greimann L.F., Abendroth R.E., Johnson D.E. and Ebner P.B., (1987), *Pile Design and Tests for Integral Abutment Bridges*, Iowa DOT Project HR-273, Department of Civil Engineering, Engineering Research Institute, Iowa State University, Ames.

Greimann L.F., Yang P.S., Edmunds S.K. and Wolde-Tinsae A.M., (1984), *Design of Piles for Integral Abutment Bridges*, Iowa DOT Project HR-252, Department of Civil Engineering, Engineering Research Institute, Iowa State University, Ames.

Greimann L.F., Yang P.S. and Wolde-Tinsae A.M., (1986), *Nonlinear Analysis of Integral Abutment Bridges*, Journal of Structural Engineering, 112, 10, 2263-2280.

Hällmark R., (2006), *Low-Cycle Fatigue of Steel Piles in Integral Abutment Bridges*, Thesis: MSc, Luleå University of Technology, Luleå, Sweden.

Hambly E.C., (1991), *Bridge Deck Behaviour*, Taylor & Francis, Abington, Oxon, UK.

Hambly E.C., (1997), *Integral Bridges*, Proceedings of the Institute Civil Engineers - Transport, 123, 1, 30-38.

Hassiotis S., Lopez J.A. and Bermudez R., (2005), *Full-Scale Testing of an Integral Abutment Bridge*. Integral Abutment and Jointless Bridges (IAJB 2005), Baltimore, Maryland, 199-210.

Highways Agency (1994). *BD 33/94: Expansion Joints for Use in Highway Bridge Decks*. Design Manual for Roads and Bridges, The Stationary Office Ltd., London, UK, Volume 2, Section 3, Part 6.

Highways Agency (2003). *BA 42/96: The Design of Integral Bridges*. Design Manual for Roads and Bridges, The Stationary Office Ltd., London, UK, Volume 1, Section 3, Part 12.

Hong J., (2006), *Research on Simplified Calculating Model and Loaded Behavior of Integral Abutment Bridges*, Thesis: PhD, Fuzhou University, Fuzhou, China. (in Chinese)

Hong J. and Peng D., (2004), *Design of Shangban Integral Abutment Bridge - Engineering Application of Jointless Bridge*, Fujian Architecture & Construction, 90, 5, 50-52. (in Chinese)

Horvath J.S., (2000), *Integral-Abutment Bridges: Problems and Innovative Solutions Using EPS Geofoam and Other Geosynthetics*, CE/GE-00-2, Civil Engineering Department, School of Engineering, Manhattan College, Bronx, New York, USA.

Horvath J.S., (2004), *Integral-Abutment Bridges: A Complex Soil-Structure Interaction Challenge*. Geotechnical Engineering for Transportation Projects : Proceedings of Geo-Trans, Los Angeles, California, USA, ASCE.

Huang J., (2004), *Behavior of Concrete Integral Abutment Bridges*, Thesis: Ph.D., University of Minnesota.

Huang J., Shield C. and French C., (2011), *Behavior of an Integral Abutment Bridge in Minnesota, US*, Structural Engineering International, 21, 3, 320-331.

Husain I., Huh B., Low J. and McCormick M., (2005), *Moose Creek Bridge - Case Study of a Prefabricated Integral Abutment Bridge in Canada*. Integral Abutment and Jointless Bridges (IAJB 2005), Baltimore, Maryland, 148-160.

Iles D.C., (2006), *Integral Bridges in the UK*. International Workshop on the Bridges with Integral Abutments, Luleå, Sweden, Luleå University of Technology.

Itani A.M. and Pekcan G., (2011), *Seismic Performance of Steel Plate Girder Bridges with Integral Abutments*, FHWA-HIF-11-043, Department of Civil and Environmental Engineering, University of Nevada, Reno, Nevada, USA.

Iwasaki N., Tenma S. and Kurita A., (2011), *Portal Frame Bridges in Japan: State of the Art Report*, Structural Engineering International, 21, 3, 290-296.

Jayakumaran S., Bergmann M., Ashraf S. and Norrish C., (2005), *Case Study: A Jointless Structure to Replace the Belt Parkway Bridge Over Ocean Parkway*. Integral Abutment and Jointless Bridges (IAJB 2005), Baltimore, Maryland, 73-83.

Jayaraman R. and Merz P., (2001), *Integral Bridge Concept Applied to Rehabilitate an Existing Bridge and Construct a Dual-use Bridge*. 26th Conference on Our World in Concrete & Structures, Singapore.

Jeremić B., (2001), *Development of Geotechnical Capabilities in OpenSees*, Pacific Earthquake Engineering Research Center, University of California, Berkeley, California, USA.

Jin X., (2007), *Design and Experimental Test for Innovative Jointless Bridges System*, Thesis: PhD, Hunan University, Changsha, China. (in Chinese)

Jin X., Shao X., Peng W. and Yan B., (2005), *A New Category of Semi-Integral Abutment in China*, Structural Engineering International, 15, 3, 186-188.

Kalayci E., Breña S.F. and Civjan S.A., (2009), *Curved Integral Abutment Bridges – Thermal Response Predictions through Finite Element Analysis*. Structures Congress 2009: Don't Mess with Structural Engineers – Expanding Our Role, Austin, Texas, USA, ASCE.

Kaufmann W. and Alvarez M., (2011), *Swiss Federal Roads Office Guidelines for Integral Bridges*, Structural Engineering International, 21, 2, 189-194.

Kerokoski O., (2006), *Soil-Structure Interaction of Long Jointless Bridges with Integral Abutments*, Thesis: PhD, Tampere University of Technology, Tampere, Finland.

Kerokoski O. and Laaksonen A., (2005), *Soil-Structure Interaction of Jointless Bridges*. Integral Abutment and Jointless Bridges (IAJB 2005), Baltimore, Maryland, 323-336.

Kim W.S., (2008), *Load and Resistance Factor Design for Integral Abutment Bridges*, Thesis: Ph.D., The Pennsylvania State University.

Kim W.S. and Laman J.A., (2010), *Numerical Analysis Method for Long-Term Behavior of Integral Abutment Bridges*, Engineering Structures, 32, 8, 2247-2257.

Krier D., (2009), *Modeling of Integral Abutment Bridges Considering Soil-Structure Interaction Effects*, Thesis: Ph.D., The University of Oklahoma.

Kunin J. and Alampalli S., (1999), *Integral Abutment Bridges: Current Practice in the United States and Canada*, Special Report 132, New York State Department of Transportation, Albany, New York.

Kunin J. and Alampalli S., (2000), *Integral Abutment Bridges: Current Practice in United States and Canada*, ASCE Journal of Performance of Constructed Facilities, 14, 3, 104-111.

Lehane B.M., Keogh D.L. and O'Brien E.J., (1999), *Simplified Elastic Model for Restraining Effects of Backfill Soil on Integral Bridges*, Computers & Structures, 73, 1-5, 303-313.

Lock R.J., (2002), *Integral Bridge Abutments*, CUED/D-SOILS/TR320, Department of Engineering, University of Cambridge, Cambridge, UK.

Ma J. and Jin X., (2002), *Design Philosophy of Guandong Qingyuan Sijiu Bridge - the First Integral Bridge without Expansion in China*, Central South Highway Engineering, 27, 2, 32-34. (in Chinese)

Malerba P.G. and Comaita G., (2011), *Twin Runway Integral Bridges at Milano Malpensa Airport, Italy*, Structural Engineering International, 21, 2, 206-209.

Maruri R.F. and Petro S.H., (2005), *Integral Abutments and Jointless Bridges (IAJB) 2004 Survey Summary*. Integral Abutment and Jointless Bridges (IAJB 2005), Baltimore, Maryland, 12-29.

Marx S. and Seidl G., (2011), *Integral Railway Bridges in Germany*, Structural Engineering International, 21, 3, 332-340.

Massachusetts Department of Transportation, (2007), *Bridge Manual 2005*, Highway Division, Massachusetts Department of Transportation, Boston, MA, USA.

MathWorks Inc., (2011), *MATLAB - Product Documentation [R2011a]*, Natick, Massachusetts, USA. http://www.mathworks.com/help/techdoc/

Matlock H., (1970), *Correlations for Design of Laterally Loaded Piles in Soft Clay. Second Annual Offshore Technology Conference*. Houston, Texas.

McGann C.R. and Arduino P., (2011, assessed 24 March 2011), *Laterally-Loaded Pile Foundation*, from OpenSeesWiki: http://opensees.berkeley.edu/wiki/index.php/Laterally-Loaded_Pile_Foundation.

McGann C.R., Arduino P. and Mackenzie-Helnwein P., (2011), *Applicability of Conventional p-y Relations to the Analysis of Piles in Laterally Spreading Soil*, Journal of Geotechnical and Geoenvironmental Engineering, 137, 6, 557-567.

Metzger A.T., (1995), *Measurement of the Abutment Forces of a Skewed Semi-Integral Bridge as a Result of Ambient Temperature Change*, Thesis: Master of Science, Ohio University, Athens, Ohio, USA.

MOHURD, (2010), *Code for Design of Concrete Structures*, GB 50010-2010, Ministry of Housing and Urban-Rural Development of the People's Republic of China. (in Chinese)

Naval Facilities Engineering Command, (1986), *Design Manual: Soil Mechanics, Foundations and Earth Structures*, Department of the Navy, Naval Facilities Engineering Command, Alexandria, Virginia, USA.

Nilsson A. and Torén K., (2001), *Foundation Methods for Small Span Bridges*, Thesis: MSc, Luleå University of Technology, Luleå, Sweden. (in Swedish)

Nilsson M., (2008), *Evaluation of In-situ Measurements of Composite Bridge with Integral Abutments*, Thesis: Licentiate, Luleå University of Technology, Luleå, Sweden.

Nippon Dohro Joint Association, (2010), *伸縮装置設計の手引き*, 日本道路ジョイント協会, Tokyo, Japan. (in Japanese)

O'Neill M.W. and Murchison J.M., (1983), *An Evaluation of p-y Relationships in Sands*, GT-DF02-83, University of Houston, Houston, Texas, USA.

Oesterle R.G. and Volz J.S., (2005), *Effective Temperature and Longitudinal Movement in Integral Abutment Bridges*. Integral Abutment and Jointless Bridges (IAJB 2005), Baltimore, Maryland, 302-311.

Ooi P.S.K., Lin X. and Hamada H.S., (2010), *Numerical Study of an Integral Abutment Bridge Supported on Drilled Shafts*, Journal of Bridge Engineering, 15, 1, 19-31.

OpenSees, (2011), *The Open System for Earthquake Engineering Simulation [2.3.2]*, Pacific Earthquake Engineering Research Center, University of California, Berkeley, California, USA. http://opensees.berkeley.edu

Paulay T. and Priestley M.J.N., (1992), *Seismic Design of Reinforced Concrete and Masonry Buildings*, John Wiley & Sons, Inc., New York, USA.

Peng D., (2001), *Development and Research of Bridges without Expansion Joints*, Journal of Fuzhou University, 29, 2, 70-75. (in Chinese)

Pétursson H. and Collin P., (2002), *Composite Bridges with Integral Abutments Minimizing Lifetime Cost*. IABSE Symposium, Melbourne.

Pétursson H. and Collin P., (2006), *Innovative Solutions for Integral Abutments*. International Workshop on the Bridges with Integral Abutments, Luleå, Sweden, Luleå University of Technology.

Pétursson H., Collin P., Veljkovic M. and Andersson J., (2011), *Monitoring of a Swedish Integral Abutment Bridge*, Structural Engineering International, 21, 2, 175-180.

Philipps D.P., (2010), *The Effect of Directionality of Groud Motion on Structural Response*, Thesis: MSc, University College London, London, UK.

Powell M.J.D., (1978), *A Fast Algorithm for Nonlinearly Constrained Optimization Calculations*, Lecture Notes in Mathematics, 630, 144-157.

Priestley M.J.N., Seible F. and Calvi G.M., (1996), *Seismic Design and Retrofit of Bridges*, John Wiley & Sons, New York, USA.

Pugasap K., Kim W. and Laman J.A., (2009), *Long-Term Response Prediction of Integral Abutment Bridges*, Journal of Bridge Engineering, 14, 2, 129-139.

Pugasap K. and Laman J.A., (2009), *Integral Abutment Bridge Hysteresis Model for Long Prediction*, Proceedings of the Institution of Civil Engineers - Bridge Engineering, 162, 1, 35-47.

Puppala A.J., Saride S., Archeewa E., Hoyos L.R. and Nazarian S., (2009), *Recommendations for Design, Construction, and Maintenance of Bridge Approach Slabs: Synthesis Report*, FHWA/TX-09/0-6022-1, Department of Civil Engineering, The University of Texas at Arlington, Arlington, Texas.

Reese L.C., Cox W.R. and Koop F.D., (1974), *Analysis of Laterally Loaded Piles in Sand*. Sixth Annual Offshore Technology Conference, Houston, Texas.

Reese L.C., Cox W.R. and Koop F.D., (1975), *Field Testing and Analysis of Laterally Loaded Piles in Stiff Clay*. The 7th Offshore Technology Conference, Houston, Texas, USA.

Road Management Technology Center, (1995), *即设桥梁のノージョイント工法设计施工引き（案）*, 道路保全技術センター, Tokyo, Japan. (in Japanese)

Rodriguez J., Martinez F. and Marti J., (2011), *Integral Bridge for High-Speed Railway*, Structural Engineering International, 21, 3, 297-303.

Roeder C.W., (2002), *Thermal Movement Design Procedure for Steel and Concrete Bridges*, NCHRP 20-07/106, Department of Civil Engineering, University of Washington, Seattle, WA, USA.

Rui-Wamba J., García-Acón C. and Estrada I., (2011), *A Spanish Perspective on Integral High-Speed Railway Viaducts*, Structural Engineering International, 21, 3, 341-345.

Russo G., Bergamo O. and Damiani L., (2009), *Retrofitting a Short Span Bridge with a Semi-Integral Abutment Bridge: The Treviso Bridge*, Structural Engineering International, 19, 2, 137-141.

Scott M.H. and Fenves G.L., (2006), *Plastic Hinge Integration Methods for Force-Based Beam-Column Elements*, Journal of Structural Engineering, 132, 2, 244-252.

Shah B.R., (2007), *3D Finite Element Analysis of Integral Abutment Bridges Subjected to Thermal Loading*, Thesis: Master of Science, Kansas State University, Manhattan, Kansas.

Shah B.R., Peric D. and Esmaeily A., (2008), *Effects of Ambient Temperature Changes on Integral Bridges*, K-TRAN: KSU-06-2, Kansas State University, Manhattan, Kansas.

Shamsabadi A., (2011), *Trenching and Shoring Manual*. Burkle K.J., Offices of Structure Construction, Department of Transportation, California.

Shehu J., (2009), *Evaluation of the Foundation and Wingwalls of Skewed Semi-Integral Bridges with Wall Abutments*, Thesis: Master of Science, Ohio University, Athens, Ohio, USA.

Shia H.-C., (2005), *A Study of the Effects of Slender Ratio on the Behavior of Piles in Sands under Cyclic Lateral Loading by Laboratory Model Test*, Thesis: Master of Science, Feng Chia University, Taichung, Taiwan, China. (in Chinese)

Snedeker K., White D. and Kahn L., (2011), *Evaluation of Performance and Maximum Length of Continuous Decks in Bridges – Part 1*, GDOT Research Project No. 09-07, School of Civil and Environmental Engineering, Georgia Institute of Technology, Atlanta, Georgia, USA.

Sullivan W.R., Reese L.C. and Fenske C.W., (1979), *Unified Method for Analysis of Laterally Loaded Piles in Clay*. Numerical Methods in Offshore Piling, London, 135-146.

Suykens J.A.K., Vandewalle J. and De Moor B., (2001), *Intelligence and Cooperative Search by Coupled Local Minimizers*, International Journal of Bifurcation and Chaos, 11, 8, 2133-2144.

Talbott A.M., (2008), *Earthquake Resistance of Integral Abutment Bridges*, Thesis: Ph.D., Purdue University.

Terzaghi K., (1943), *Theoretical Soil Mechanics*, John Wiley & Sons, Inc., New York, USA.

Teughels A., De Roeck G. and Suykens J.A.K., (2003), *Global Optimization by Coupled Local Minimizers and its Application to FE Model Updating*, Computers & Structures, 81, 24-25, 2337-2351.

Thanasattayawibul N., (2006), *Curved Integral Abutment Bridges*, Thesis: Ph.D., University of Maryland, College Park.

Thompson T.A., Jr., (1999), *Passive Earth Pressures behind Integral Bridge Abutments*, Thesis: Ph.D., University of Massachusetts, Amherst, Massachusetts, USA.

Tlustochowicz G., (2005), *Optimized Design of Integral Abutments for a Three Span Composite Bridge*, Thesis: Master, Luleå University of Technology, Luleå, Sweden.

Turner J.D. and Pretlove A.J., (1988), *A Study of the Spectrum of Traffic-Induced Bridge Vibration*, Journal of Sound and Vibration, 122, 1, 31-42.

Vägverket, (2002), *Vägverkets allmänna tekniska beskrivning för nybyggande och förbättring av broar*, ATB - Bro 2002, Vägverket, Swedish National Road Administration.

Venkataraman P., (2002), *Applied Optimization with MATLAB Programming*, John Wiley & Sons, Inc., New York, USA.

Waite C.A., Gemmiti T. and Capobianco D.R., (2010), *Thruway Structures Design Manual - 4th Edition*, New York State Thruway Authority, Albany, NY, USA.

Waltz R.A., Morales J.L., Nocedal J. and Orban D., (2006), *An Interior Algorithm for Nonlinear Optimization that Combines Line Search and Trust Region Steps*, Mathematical Programming, 107, 3, 391-408.

Wasserman E.P., (2007), *Integral Abutment Design (Practices in the United States)*. 1st U.S. - Italy Seismic Bridge Workshop, Pavia, Italy.

Wasserman E.P. and Walker J.H., (1996), *Integral Abutments for Steel Bridges*, American Iron and Steel Institute.

Weizenegger M., (2003), *Hybrid Frame Bridge, River Saale, Merseburg, Germany*, Structural Engineering International, 13, 3, 179-181.

White II H., (2007), *Integral Abutment Bridges: Comparison of Current Practice Between European Countries and the United States of America*, FHWA/NY/SR-

07/152, Transportation Research and Development Bureau, New York State Department of Transportation, Albany, New York, USA.

White II H., Pétursson H. and Collin P., (2010), *Integral Abutment Bridges: The European Way*, Practice Periodical on Structural Design and Construction, 15, 3, 201-208.

Wikipedia, (2011a, assessed 4 June 2011), *Lateral Earth Pressure*, from: http://en.wikipedia.org/wiki/Lateral_earth_pressure.

Wikipedia, (2011b, assessed 20 January 2012), *Sunniberg Bridge*, from: http://en.wikipedia.org/wiki/Sunniberg_Bridge.

Wolde-Tinsae A.M., Greimann L. and Yang P.-S., (1988a), *End-Bearing Piles in Jointless Bridges*, Journal of Structural Engineering, 114, 8, 1870-1884.

Wolde-Tinsae A.M., Klinger J.E. and White E.J., (1988b), *Performance of Jointless Bridges*, Journal of Performance of Constructed Facilities, 2, 2, 111-125.

Xu M., (2010), *Laboratory Study of the Behavior of Granular Soils behind Integral Bridge Abutments*, China Civil Engineering Journal, 43, 5, 136-140. (in Chinese)

Xu M., Bloodworth A.G. and Clayton C.R.I., (2007), *Behavior of a Stiff Clay behind Embedded Integral Abutments*, J. Geotech. and Geoenvir. Engrg., 133, 6, 721-730.

Xu M., Bloodworth A.G. and Lee M.M.K., (2003), *Numerical Analysis of the Embedded Abutments of Integral Bridges*. IABSE Symposium: Structures for High-Speed Railway Transportation, Antwerp, Belgium, International Association for Bridge and Structural Engineering, 57-62.

Yannotti A.P., Alampalli S. and White II H., (2005), *New York State Department of Transportation's Experience with Integral Abutment Bridges*. Integral Abutment and Jointless Bridges (IAJB 2005), Baltimore, Maryland, 41-49.

Zordan T. and Briseghella B., (2007), *Attainment of an Integral Abutment Bridge through the Refurbishment of a Simply Supported Structure*, Structural Engineering International, 17, 3, 228-234.

Zordan T., Briseghella B. and Lan C., (2010), *Parametric and Pushover Analyses on Integral Abutment Bridge*, Engineering Structures, 33, 2, 502-515.

Zordan T., Briseghella B. and Lan C., (2011), *Analytical Formulation for Limit Length of Integral Abutment Bridges*, Structural Engineering International, 21, 3, 304-310.

Zuk W., (1981), *Jointless Bridges*, Virginia Highway & Transportation Research Council, Charlottesville, Virginia, USA.